

**DEVELOPMENT OF A METHOD FOR THE  
DETERMINATION OF ANTIOXIDANTS AND TRACE  
HEAVY METALS BY ROBOTIC ELECTROCHEMISTRY  
IN MICROTITER PLATES**

**Sireerat Intarakamhang**

**A Thesis Submitted in Partial Fulfillment of the Requirements for the  
Degree of Doctor of Philosophy in Chemistry  
Suranaree University of Technology  
Academic Year 2012**

การพัฒนาเทคนิคสำหรับตรวจสอบสารต้านอนุมูลอิสระ  
และโลหะหนักปริมาณน้อย  
โดยเคมีไฟฟ้าโรบอดิกในไมโครไทดเตอร์เพลท

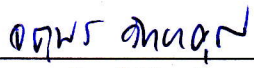
นางสาวสิริรัตน์ อินทรกำแหง

วิทยานิพนธ์นี้เป็นส่วนหนึ่งของการศึกษาตามหลักสูตรปริญญาวิทยาศาสตรดุษฎีบัณฑิต  
สาขาวิชาเคมี  
มหาวิทยาลัยเทคโนโลยีสุรนารี  
ปีการศึกษา 2555

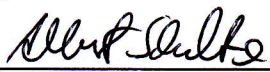
**DEVELOPMENT OF A METHOD FOR THE DETERMINATION  
OF ANTIOXIDANTS AND TRACE HEAVY METALS BY  
ROBOTIC ELECTROCHEMISTRY IN MICROTITER PLATES**

Suranaree University of Technology has approved this thesis submitted in partial fulfillment of the requirements for the Degree of Doctor of Philosophy.

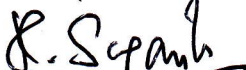
Thesis Examining Committee

  
(Assoc. Prof. Dr. Jatuporn Wittayakun)


Chairperson

  
(Assoc. Prof. Dr. Albert Schulte)

Member (Thesis Advisor)

  
(Prof. Dr. Kriksana Sagarik)

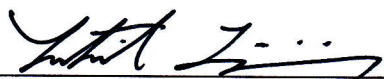
Member

  
(Prof. Dr. Orawon Chailapakul)


Member

  
(Asst. Prof. Dr. Sanchai Prayoonpokarach)

Member

  
(Prof. Dr. Sukit Limpijung)

Vice Rector for Academic Affairs

  
(Assoc. Prof. Dr. Prapun Manyum)

Dean of Institute of Science

สิริรัตน์ อินทรกำแหง : การพัฒนาเทคนิคสำหรับตรวจสอบสารต้านอนุมูลอิสระและโลหะหนักปริมาณน้อย โดยเคมีไฟฟ้าโรโบติกในไมโครไทดเตอร์เพลท (DEVELOPMENT OF A METHOD FOR THE DETERMINATION OF ANTIOXIDANTS AND TRACE HEAVY METALS BY ROBOTIC ELECTROCHEMISTRY IN MICROTITER PLATES) อาจารย์ที่ปรึกษา : รองศาสตราจารย์ ดร.อัลเบิร์ต ชูลเทอ, 226 หน้า.

วิทยานิพนธ์นี้มุ่งพัฒนา การวิเคราะห์เชิงปริมาณทางเคมีไฟฟ้าแบบอัตโนมัติเพื่อหาปริมาณสารต้านอนุมูลอิสระในอาหาร และโลหะหนักปริมาณน้อยในตัวอย่างทางสิ่งแวดล้อม ระบบนี้ประกอบด้วยไมโครไทดเตอร์เพลทขนาด 24 หลุม ขั้วไฟฟ้าทำงานเสถียรคือคาร์บอน ขั้วไฟฟ้าอ้างอิง Ag/AgCl และขั้วไฟฟ้าแคโทดเพลททินัม ทั้งหมดนี้ใช้คอมพิวเตอร์ในการควบคุมการเคลื่อนที่ของขั้วไฟฟ้าขึ้น-ลง (แกน z) ไมโครไทดเตอร์เพลท (แกน x y) และการทำงานของโพเทนชิโอสแตตควบคุมโดยโปรแกรมไปที่ไมโครไทดเตอร์เพลทขนาด 24 หลุม และเซนเซอร์ โดยมีการทำความสะอาดขั้วไฟฟ้า หรือใช้เทคนิคแอมเพอโรเมตรี/โวลแทมเมตรี ในการวิเคราะห์

ดิฟเฟอเรนเชียลพัลส์โวลแทมเมตรี (differential pulse voltammetry) ของกรดแอสคอบิกแบบอัตโนมัติในไมโครไทดเตอร์เพลทเมื่อใช้วิธีโวลแทมเมตรีแบบอัตโนมัติมีการตอบสนองความเป็นเส้นตรงที่ความเข้มข้น 0.1-8.0 มิลลิโมลาร์เซนซิวิตี  $1 \mu\text{AmM}^{-1}$  และความสามารถในการวัดที่น้อยที่สุด 50 ไมโครโมลาร์ ความเข้มข้นของตัวอย่างกรดแอสคอบิกที่ทราบค่าโดยวิธีสร้างกราฟมาตรฐาน (calibration curve method) และวิธีเพิ่มเติมความเข้มข้นสารมาตรฐาน (standard addition method) พบว่า ร้อยละการกลับคืน (recovery rate) ดี นอกจากนั้นยังได้ประยุกต์วิธีนี้ในการหาปริมาณกรดแอสคอบิก ในเมล็ดยาคิวตามินซี น้ำฝรั่ง และชาสมุนไพร

การใช้คอมพิวเตอร์ควบคุมไมโครไทดเตอร์เพลท ขนาด 24 หลุม และแอมเพอโรเมตรีแบบอัตโนมัติกับสารอนุมูลอิสระดีพีพีเอช (2,2-diphenyl-1-picrylhydrazyl radical (DPPH•)) เพื่อหาค่าสารต้านอนุมูลอิสระรวม พบว่าวิธีนี้ประสบความสำเร็จในการประยุกต์กับสารต้านอนุมูลอิสระมาตรฐานที่ทราบความเข้มข้น ชา น้ำผลไม้ และผักสด

ส่วนสุดท้ายเคมีไฟฟ้าโรโบติกในไมโครไทดเตอร์เพลทเพื่อการประยุกต์อย่างมีประสิทธิภาพโดยวิธี stripping ดิฟเฟอเรนเชียลพัลส์โวลแทมเมตรี (differential pulse stripping voltammetry) กับขั้วไฟฟ้าบิสมัท เพื่อหาตะกั่วและแคดเมียมปริมาณน้อย พบว่าปริมาณของโลหะหนักตะกั่วและแคดเมียมในตัวอย่างน้ำที่ใส่ตะกั่วและแคดเมียมลงไปมีร้อยละการกลับคืนที่ดีเมื่อประยุกต์กับสารตัวอย่างน้ำเสียที่มีใบรับรอง (certified waste water reference) ได้ค่าร้อยละการกลับคืนที่ดี ระหว่างร้อยละ 90-110 เช่นกัน โดยใช้วิธีเพิ่มเติมความเข้มข้นสารมาตรฐานกับเคมีไฟฟ้าโรโบติก การ



SIREERAT INTARAKAMHANG : DEVELOPMENT OF A METHOD FOR THE DETERMINATION OF ANTIOXIDANTS AND TRACE HEAVY METALS BY ROBOTIC ELECTROCHEMISTRY IN MICROTITER PLATES. THESIS ADVISOR : ASSOC. PROF. ALBERT SCHULTE, Ph.D. 226 PP.

ROBOTIC ELECTROCHEMISTRY/ELECTROANALYSIS/ ASCORBIC ACID/ TOTAL ANTIOXIDANT CAPACITY/ LEAD CADMIUM TRACE ANALYSIS/ CARBON PENCIL LEAD ELECTRODE/ MICRO TITERPLATE

This dissertation aimed on the development of a convenient automated electrochemical quantification of antioxidants in dietary and trace toxic heavy metals in environmental samples. The complete 24-well microtiter plate electrochemical assay uses a movable assembly of a carbon pencil lead working, an Ag/AgCl reference and a Pt counter electrode. A computer was in command of electrode assembly (z) and microtiter plate (x, y) positioning and timed potentiostat operation. Synchronization of these actions supported sequential approach of all 24 wells with the sensor device and subsequent execution of electrode treatment/cleaning procedures or amperometry/voltammetry by a programmed analytical platform.

Automated ascorbic acid (AA) differential pulse voltammetry (DPV) in microtiter plates offered a linear analytical response between 0.1 and 8.0 mM, a sensitivity of about  $1 \mu\text{A}\text{mM}^{-1}$  AA, and a detection limit of 50  $\mu\text{M}$ . When using with the calibration curve or standard addition method, automated AA voltammetry of samples with added known amounts of AA demonstrated good recovery rates. The assay also succeeded with the accurate determination of the AA content of vitamin C tablets, a fresh guava juice and a herbal tea extract.

The establishment of an accurate computer-controlled amperometric 2,2-diphenyl-1-picrylhydrazyl radical (DPPH·) assay was possible and allowed the determination of total antioxidant levels in 24-well microtiter plate format. The methodology was successfully applied to the assessment of the with synthetic antioxidants of known concentrations and tea infusions, fruit juices, and vegetable extracts.

Finally, trace Pb(II) and Cd(II) determination was effectively accomplished with robotic differential pulse stripping voltammetry (DPSV) in microtiter plates with bismuth-film electrode. The obtained heavy metal assay offered good recovery rates for trace Pb(II) and Cd(II) in spiked water samples. Applied to an analysis certified of waste water in the robotic stripping voltammetry standard addition mode delivered recovery rates between 90-110 % relation. In an application to real samples, the amount of Pb (II) in contaminated soil samples was determined, and the level compared well to the one determined in a measurement with robotic DPSV from inductively coupled plasma spectroscopy.

Microtiter plate-based robotic electroanalysis offers significant advantages over manual operation including convenience, time saving and minimization of manual errors. The methodology is certainly an attractive complementary option when the task is the screening large numbers of samples. Potential is thus for future applications in the laboratories of the food and pharmaceutical industry as well as for environmental monitoring and testing.

School of Chemistry

Academic Year 2012

Student's Signature

Advisor's Signature

Sincerat Intarakamhang

Albert Seulk

## ACKNOWLEDGEMENTS

This doctoral thesis would not have been accomplished without the help of many people. I would like to acknowledge all who were with me during this time.

First of all, I would like to express my appreciation to my thesis advisor, Assoc. Prof. Dr. Albert Schulte, for his great advice, kindness, encouragements, and fruitful instructions throughout my Ph.D. thesis work.

Prof. Dr. Wolfgang Schuhmann is acknowledged for his kindness in accepting me to join for a total of nine months the Analytische Chemie Electroanalytik&Sensorik, Department of Chemistry and Biochemistry, Ruhr University Bochum, Germany as an associate researcher. I had a worthy time, gained a lot of for my thesis and got the chance to additional knowledge about electrochemistry. In addition, I would like to thank Dr. Thomas Erichsen and Christian Leson for their support with the instrumentation and scientific discussions. And all “ELAN” group members especially, Minling Sao, Dr. Michaela Nebel, Dr. Yvonne Ackermann, Lutz Stratmann, Dr. Xingxing Chen, Bettina Stetzka, Dr. Magdalena Gebala and Piyanut Pinyou. The lovely Thai friends are thanked for their friendships during my visit in Germany.

I wish to thank all the lecturers of the School of Chemistry, Suranaree University of Technology for their good attitude and useful advice during the seven years of my M.Sc. and Ph.D. studies. And, thanks to all the lecturers in the Department of Chemistry, Khon Kaen University for guiding my first steps into chemistry and for useful suggestions throughout my bachelor study.

.



I am thankful to the Biochemistry-Electrochemistry Research Unit, for principle investigators Assoc. Prof. Dr. Wipa Suginta, Assoc. Prof. Dr. Albert Schulte, Dr. Panida Khunkaewla and Dr. Chutima Talabnin for their provision of a professional laboratory of instrument standard, valuable scientific discussion and many social celebrations in warm atmosphere. In addition, I am grateful to the graduate students in the unit, especially, Jiyapa Sripirom, Piyanuch Kullawong and Somjai Teanponklang, for kindness, smile, and entertainment during work on top of the scientific discussion.

I am grateful to the Rajamangala University of Technology Isan (RMUTI), Nakhon Ratchasima for the first year scholarship and, to the Office of the Higher Education Commission for a grant of the “Strategic Scholarships for Frontier Research Network” (Sandwich program) which allowed me to complete my thesis. Moreover, the National Research Council of Thailand (NRCT) is thanked for thesis support through the “High-throughput screening/analysis: Tool for drug discovery, disease diagnosis and health safety” project.

Last but not least, I would like to express my grateful admiration to my beloved parents and my brother for support, believe, understanding and encouragement all though the time of the part few years. Not to forgot, my husband, Dr.Nithi Lisnund when I got married during my doctoral time for sharing happiness and sadness, for his understanding and standing beside me all time. Without all of them, I may not have been able to accomplish the degree, thanks all of you very much.

Sireerat Intarakamhang

# CONTENTS

	<b>Page</b>
ABSTRACT IN THAI.....	I
ABSTRACT IN ENGLISH.....	III
ACKNOWLEDGEMENTS.....	V
CONTENTS.....	VII
LIST OF TABLES.....	XVI
LIST OF FIGURES.....	XIX
LIST OF ABBREVIATIONS.....	XXXI
<b>CHAPTER</b>	
<b>I INTRODUCTION.....</b>	<b>1</b>
<b>II LITERATURE REVIEWS.....</b>	<b>5</b>
2.1 The concept of normal electroanalysis.....	5
2.2 Normal manual electroanalysis experiments.....	10
2.3 Robotic electrochemistry.....	15
2.3.1 General remarks.....	15
2.3.2 Hard- and software design of a device for robotic electrochemistry in microtiter plate.....	18
2.3.3 Published applications of the electrochemical robotic system in microtiter plate format.....	23
2.4 Ascorbic acid (AA).....	26
2.4.1 AA background.....	26

## CONTENTS (Continued)

	<b>Page</b>
2.4.2 AA electrochemical measurement .....	27
2.4.3 Literature review of electrochemical ascorbic acid determination .....	29
2.5 Total antioxidant capacity (TAC) .....	32
2.5.1 The principle of free radicals and antioxidants .....	32
2.5.2 Known methods for total antioxidant measurements .....	35
2.5.3 Electrochemical determination of total antioxidant capacity .....	38
2.5.4 High TAC in Thai plants, tea infusion and fresh fruit sample .....	39
2.5.4.1 Antioxidants in Thai plants .....	39
2.5.4.2 Antioxidants content in tea and herbal infusion .....	40
2.5.4.3 Antioxidants content in tropical fruits .....	43
2.6 Heavy metals analysis .....	43
2.6.1 Heavy metal in general .....	43
2.6.2 The analytical method for the quantitative determination of heavy metal .....	46
2.6.3 Introduction to bismuth-film electrode, an alternative to mercury-film electrode .....	48
2.6.4 The principle of anodic stripping voltammetry at bismuth-film electrode (BFE) .....	51
2.6.5 Applications of bismuth electrodes .....	53

## CONTENTS (Continued)

	<b>Page</b>
2.7 Pencil leads graphite electrode	55
2.7.1 Concept of pencil leads graphite electrode.....	55
2.7.2 Application of pencil leads graphite electrode in electroanalysis.....	57
<b>III EXPERIMENTAL PART</b> .....	59
3.1 Materials and Reagents.....	59
3.1.1 List of chemicals in alphabetical order.....	59
3.1.2 Supporting electrolyte.....	60
3.2 Samples screened for their AA and antioxidant contents.....	61
3.2.1 AA determination.....	61
3.2.2 TAC determination.....	61
3.3 Environmental sample for lead and cadmium heavy metals analysis.....	63
3.4 Instrumentation.....	63
3.5 Consumables.....	64
3.6 Working (WE), reference (RE) and counter electrodes preparation.....	65
3.6.1 Miniaturized working electrode (WE).....	65
3.6.2 Miniaturized reference electrode (RE).....	65
3.6.3 Miniaturized Counter electrode (CE).....	68
3.7 The robotic electrochemical workstation.....	68
3.8 Ascorbic acid analysis.....	70

## CONTENTS (Continued)

	<b>Page</b>
3.8.1 Pretreatment of the PLE working electrode .....	70
3.8.2 Cyclic voltammograms of AA.....	71
3.8.3 Response stability of the working electrode and degradation resistance of the analyte AA.....	71
3.8.4 Linear range and sensitivity of AA.....	71
3.8.5 AA quantification via normal calibration method.....	72
3.8.6 AA quantification via standard addition method.....	74
3.8.7 AA quantification in real samples.....	75
3.8.8 Titrimetric AA measurements in real sample as reference.....	77
3.9 Robotic electrochemical DPPH free radical amperometry for evaluation the total antioxidant capacity.....	81
3.9.1 CV of the DPPH free radical.....	81
3.9.2 The reaction of DPPH free radical with Trolox via conventional beaker type amperometry.....	82
3.9.3 The reaction of DPPH free radical with Trolox assessed Via automated amperometry in 24-well microtiter plate format.....	83
3.9.4 A reproducibility test for Trolox quantification via automated amperometry in microtiter plate format.....	85

## CONTENTS (Continued)

	<b>Page</b>
3.9.5 Automated assessment of the antioxidant activity of standard antioxidants.....	85
3.9.6 Automated assessment of the antioxidant activity of real samples.....	87
3.9.6.1 The preparation fresh fruit juice.....	87
3.9.6.2 The preparation herbal tea infusion.....	87
3.9.6.3 Standard spectroscopic reference measurements	88
3.9.7 The process of plant antioxidant extraction.....	89
3.10 Robotic stripping voltammetry for the determination of lead (II) and cadmium (II) at bismuth modified pencil-lead electrode.....	90
3.10.1 The effect of Bi solution concentration on Pb (II) and Cd (II) robotic stripping voltammetry.....	91
3.10.2 The effect of the deposition time on the quality of Pb (II) and Cd (II) robotic stripping voltammetry.....	93
3.10.3 The robotic calibration curve acquisition for Pb (II) and Cd (II) via robotic differential pulse anodic stripping voltammetry in 24-well microtiter plate format.....	94
3.10.4 The application of robotic differential pulse stripping voltammetry for Pb (II), and Cd (II) measurements in real samples.....	96
3.10.4.1 Soil sample extraction.....	96

## CONTENTS (Continued)

		<b>Page</b>
	3.10.4.2 The loading of the various real samples into 24-well micro titer plates.....	98
<b>IV</b>	<b>RESULTS AND DISCUSSIONS</b> .....	102
	4.1 Robotic electroanalysis in microtiter plate .....	102
	4.1.1 Hardware components of electrochemical robotic system.....	102
	4.1.2 Robotic electroanalysis: General comments on system operation.....	106
	4.2 Ascorbic acid analysis (AA).....	107
	4.2.1 Cyclic voltammograms of AA.....	108
	4.2.2 Signal stability of AA voltammetry.....	110
	4.2.3 Linear range and sensitivity of AA voltammetry.....	112
	4.2.4 Robotic AA quantification via normal calibration method .....	115
	4.2.5 Robotic AA quantification via standard addition method .....	117
	4.2.6 AA quantification in real samples.....	121
	4.2.7 Comparison of robotic AA electroanalysis with conventional AA titration.....	123
	4.3 Robotic electrochemical DPPH free radical amperometry for total antioxidant capacity determination in fruit and vegetable sample.....	125

## CONTENTS (Continued)

	<b>Page</b>
4.3.1 Electrochemical basis of the proposed amperometric method for antioxidant screening.....	125
4.3.2 Cyclic voltammetry of the DPPH free radical molecule	128
4.3.3 The reaction of DPPH free radical with Trolox in conventional beaker type amperometric trial.....	131
4.3.4 The concept of automated antioxidant capacity measurement via DPPH free radical amperometry in microtiter plate format.....	134
4.3.5 Automated assessment of DPPH•/Trolox calibration curves in microtiter plate.....	137
4.3.6 Reproducibility of automated DPPH•/Trolox amperometry in microtiter plate format.....	139
4.3.7 The radical screening of standard antioxidants.....	139
4.3.8 Trolox equivalent from spectroscopic measurement (reference measurement).....	143
4.3.9 Robotic electrochemical assessment of Trolox equivalent of standard (model) antioxidants : comparison of amperometric and spectroscopic data.....	144
4.3.10 The antioxidant activity in real samples.....	146



## CONTENTS (Continued)

	<b>Page</b>
4.4 Determination of trace lead (II) and cadmium (II) by robotic anodic stripping voltammetry at bismuth modified pencil-lead electrodes.....	150
4.4.1 Optimization of the measuring procedure for robotic anodic heavy metal stripping voltammetry using Bi(III) film modified pencil lead electrode (BF-PLE).....	151
4.4.2 Pb(II) and Cd(II) calibration trials via robotic differential pulse anodic stripping in 24-well microtiter plate.....	156
4.4.3 The application of robotic differential pulse stripping voltammetry for Pb(II) and Cd(II) measurements in real samples .....	160
4.4.3.1 The analysis Pb(II) and Cd(II) in bottled mineral drinking and tap water.....	161
4.4.3.2 Analysis of Pb(II) and Cd(II) in wastewater certified reference material (CRM713).....	167
4.4.3.3 The evaluation of Pb(II) and Cd(II) contamination in a soil sample from an industrial zone.....	170
<b>V CONCLUSION AND OUTLOOK</b> .....	174
REFERENCES.....	179
APPENDICES.....	198

## CONTENTS (Continued)

	<b>Page</b>
APPENDIX A DESIGN OF SOFTWARE SCRIPT FOR THE EXECUTION OF ROBOTIC ELECTROCHEMICAL ANALYSIS IN 24-WELL MICROTITER PLATES.....	199
APPENDIX B ASCORBIC ACID ANALYSIS.....	203
APPENDIX C ROBOTIC ELECTROCHEMICAL DPPH RADICAL METHOD: APPLICATION FOR TOTAL ANTIOXIDANT CAPACITY MEASUREMENT.....	211
APPENDIX D ROBOTIC STRIPPING VOLTAMMETRY AS APPLIED FOR THE DETERMINATION OF LEAD AND CADMIUM WITH A PENCIL-LEAD BISMUTH-FILM ELECTRODE.....	220
CURRICULUM VITAE.....	227

## LIST OF TABLES

Table		Page
2.1	Software modules and parameter list which are transferred from a software script file to the robotic program for the execution of different experimental sequences.....	22
2.2	Some examples of free radicals.....	34
2.3	DPPH radical-scavenging activity and total phenolic content of Thai plant extracts.....	40
2.4	Permissible limits and health effects of various toxic heavy metals.....	45
2.5	Selected applications of stripping analysis on Bismuth film electrodes..	53
3.1	Microtiter plate load for determining the Trolox equivalents of three synthetic antioxidants via robotic DPPH• amperometry.....	86
3.2	The preparation of Pb (II), Cd (II) and Bi (II) 10.0 mg/L from standard stock solution.....	90
3.3	The preparation of Pb (II), Cd (II) and Bi (III) solutions as used for the 24-well microtiter plate analysis via stripping voltammetry.....	92
3.4	The load of a 24-well microtiter plate used for the inspection of the effect of the accumulation time on the quality of the Pb/Cd stripping voltammetry.....	94
3.5	Microtiter plate layout for robotic Pb (II) and Cd (II) stripping voltammetry.....	95
3.6	Microtiter plate layout for robotic Pb (II) and Cd (II) DPSV analysis..	99

## LIST OF TABLES (Continued)

Table	Page
3.7	Microtiter plate layout for percent recovery determination of Pb (II) and Cd(II) measurements in a robotic DPSV trial on water sample ..... 100
3.8	The 24 well microtiter plate load for robotic Pb (II) and Cd (II) voltammetry in certified waste water..... 101
3.9	Microtiter plate load for robotic Pb (II) and Cd (II) voltammetry analysis of aqueous soil extracts ..... 101
4.1	Determination of AA in guava juice by standard addition method (n=3) 123
4.2	Ascorbic acid quantities in a vitamin C tablet, fresh guava juice, and a herbal tea a comparison of levels from robotic voltammetric screening in microtiter plates with those from manual titrations..... 125
4.3	Stability of DPPH• voltammetry at pencil lead electrode..... 131
4.4	Free radical scavenging capacity of a set of three synthetic model antioxidant samples as obtained by automated DPPH• amperometry and a spectroscopic method..... 145
4.5	Names and photos of real sample that are rich in antioxidants..... 146
4.6	Trolox equivalents obtained by robotic amperometric and spectrophotometric measurement in a varying of food samples..... 150
4.7	Robotic Pb (II) and Cd (II) anodic stripping voltammetry in microtiter plate: summary of calibration trials..... 160
4.8	The loads solution into 24-well microtiter plate for analysis Pb (II) and Cd (II) in bottle mineral drinking water using robotic DPSV..... 162

## LIST OF TABLES (Continued)

<b>Table</b>	<b>Page</b>	
4.9	Robotic stripping voltammetry on spiked bottled mineral drinking water and tap water; summary of the determined Pb/Cd contents and the corresponding % recovery rates .....	166
4.10	The elements content in certified reference material (CRM) BCR® – 713.....	167
4.11	Automated stripping voltammetry determination of Pb/Cd in certified waste water reference material: Summary of measure Pb/Cd analyte and of recovery rate (n=6).....	170
4.12	Robotic stripping voltammetry of Pb (II), and Cd (II) in a soil sample by the standard addition method comparison between the electrochemically to a spectroscopic measurement.....	173

## LIST OF FIGURES

Figure		Page
2.1	Potential wave forms and voltammograms for a) normal pulse voltammetry (NPV), b) differential voltammetry (DPV) and c) square wave voltammetry (SWV).....	9
2.2	Schematic diagram of a conventional cell for voltammetric measurements: WE-working electrode; RE-reference electrode; CE-counter electrode.....	11
2.3	Steps of manual electrochemical measurement .....	12
2.4	A representative example of a sequential injection anodic stripping voltammetric system.....	14
2.5	Schematic of a microtiter plate well with a notification of its diameter related to the well plate number.....	17
2.6	Schematic representation of an electrochemical robotic system.....	19
2.7	Schematic representation of the hardware architecture and structure of the control software for microtiter plate-based electrochemistry.....	20
2.8	Photograph of the electrochemical robotic system with a 96-well gold microtiter plate in a chamber for controlling the atmosphere as used for antibiotic biosensor fabrication and characterization.....	24

## LIST OF FIGURES (Continued)

Figure	Page	
2.9	a) Photographic view of a robotic instrument for automated electro-synthesis, b) assembly of electrodes, from left to right: counter, electrolysis working, CV microdisk, reference electrode and c) typical charging of a 96-well microtiter plate for reaction wells.....	25
2.10	Electrochemical oxidation of ascorbic acid.....	28
2.11	Cyclic voltammograms of $4 \times 10^{-4}$ M ascorbic acid in (a) acetate buffer at pH 3.05 and (b–d) phosphate buffer at pH (b) 2, (c) 2.95, and (d) 7. Scan rate, 100 mV/s.....	30
2.12	Schematic cartoon of chemical attack of a healthy cell by a free radical a) and the protective action of a free radical scavenger by antioxidant b).....	32
2.13	Chemical structures of some common antioxidants.....	35
2.14	Reaction of DPPH radical with an antioxidant (AH).....	36
2.15	a) Moringa tree, b) Dried moringa tea and c) Dried moringa capsule...	41
2.16	Rose tea a) and a rose tea infusion b).....	42
2.17	Stripping voltammograms of lead, cadmium, and zinc at glassy-carbon A) and carbon-fiber B) electrodes coated with bismuth a) and mercury b)films.....	50
2.18	Schematic of representation of the principle of anodic stripping voltammetry at bismuth-film electrodes for the determination Pb(II), Cd(II) and Zn (II).....	52

## LIST OF FIGURES (Continued)

Figure		Page
2.19	Photograph of a pencil and a boxed pencil leads as used for working electrode preparation.....	55
2.20	Cyclic voltammograms obtained at a scan rate of 500 mV s <sup>-1</sup> for oxidation of K <sub>4</sub> Fe(CN) <sub>6</sub> in 2 M H <sub>2</sub> SO <sub>4</sub> at a pencil electrode. K <sub>4</sub> Fe(CN) <sub>6</sub> concentrations are (a) 1, (b) 1.43, (c) 1.83, (d) 2.20 and (e) 2.53 mM.....	56
2.21	Cyclic voltammograms for oxidation of 2.53 mM K <sub>4</sub> Fe(CN) <sub>6</sub> in 2M H <sub>2</sub> SO <sub>4</sub> at (a) 0.5 mm diameter 3H renewable pencil electrode, (b) bare 3H pencil lead (length 20 mm, diameter 0.5 mm) and (c) 3 mm diameter glassy carbon electrode.....	57
3.1	Photos of samples used for antioxidant capacity screening a) Teaw, b) Phak Paew, c) Kri-Leck, d) Horse radish tea, e) Rose tea, f) Green tea, g) Guava, h) Papaya, and i) Kumquat or small seedless orange.....	62
3.2	Preparation of miniaturized working electrode for the robotic voltammetric analyzer: a) Pencil lead, b) Heat shrinking tubes, c) Heat gun applying a hot air steam to the carbon pencil lead that was inserted in a heat shrinking tube, and d) The completed carbon pencil lead working electrode.....	65



## LIST OF FIGURES (Continued)

<b>Figure</b>	<b>Page</b>
3.3 Preparation of a miniaturized Ag/AgCl reference electrode, a) The electrolysis setup, b) The reaction of Ag wire and Ag/AgCl formation at anode(+) and hydrogen gas evolution at the cathode (-), c) tip of electrode with sealed with ceramic frit, d) The completed miniaturized Ag/AgCl reference electrode .....	67
3.4 The fabrication of a Pt wire counter electrode. a) coiled Pt wire soldered to a copper cable wire b) heat shrinking tube used to seal the junction Pt/Cu, and c) Photo of the complete counter electrode.....	68
3.5 Photo of Robotic electrochemical system: a) i) z-positioning for Vertical movement, ii) electrode holder with working electrode, counter electrode, reference electrode; iii) 24-well microtiter plate base, iv) x-, y-positioning for container movement, and v) vibration dampening table. Of note: this instrument was used during a research stay at Ruhr University Bochum, Bochum, Germany for AA and Pb/cd analysis, and b) Three-electrodes fixed to the holders and dipped in a container of the 24-well microtiter plate.....	69
3.6 SEM image of a pencil lead electrode before a), and after b) voltammetric pretreatment with 0.5 M H <sub>2</sub> SO <sub>4</sub> .....	70
3.7 The microtiter plate load for the robotic voltammetric AA calibration trial.....	72
3.8 The 24-well microtiter plate load for a AA quantification via the calibration method.....	73

## LIST OF FIGURES (Continued)

Figure		Page
3.9	The 24-well microtiter plate load for robotic AA differential pulse voltammetry and analysis via the standard addition method four samples were automatically assessable in one run.....	75
3.10	Photos of a Guava fruit, pharmaceutical vitamin C tablet, (Ja Zink+ VitaminC, 120 mg/tablet) and a Thai herbal tea, (Horse radish tree ( <i>Moringa oleifera</i> )).....	75
3.11	The reaction of AA with DCIP as used for titrimetric measurements for AA analyte.....	78
3.12	Simple drawing of DCPI-based titration of AA standards a), and for evaluated AA in real sample b).....	78
3.13	Schematic for, a) Standardization of the Iodine solution, and b) Determination of AA by Iodometry back titration.....	81
3.14	Drawing of the amperometry of DPPH• and its reaction with Trolox, Conditions: PLE working electrode; potential +100 mV vs Ag/AgCl in 0.1 M EPBS.....	83
3.15	a) Assignment of well number for the 24-well microtiter plate used for Trolox calibration trial. b) Details of the plate load in the layout for Trolox calibration measurements.....	84
3.16	A schematic of the plant extraction for the evaluation of antioxidant capacity in crude extract.....	89

## LIST OF FIGURES (Continued)

Figure		Page
3.17	The 24-well microtiter plate labeling for all Pb(II) and Cd(II) robotic stripping voltammetry trial of this study. AC is 0.1 M acetate buffer pH 4.5, Ac+Bi is Bismuth containing buffer.....	93
3.18	a) 425 $\mu\text{m}$ stainless steel mesh sieve, b) dried soil before and c) after sieving .....	97
3.19	The 24 well microtiter plate layout for automated voltammetric measurement of Pb(II) and Cd(II) in water and soil samples using the standard addition method.....	98
4.1	Schematic of a 24-well microtiter-plate.....	103
4.2	Schematic of the electrode holder forming a three-electrode assembly of a reference electrode (RE), working electrode (WE), and counter electrode (CE).....	104
4.3	a) Schematic representation of the electrochemical robotic system employed in this thesis; b) Photograph of instrumentation.....	105
4.4	Schematic representation of the robotic electrochemical system; a) a typical microtiter plate load; b) flowchart of a measurement cycle; c) communication between software and hardware execution....	107
4.5	Cyclic voltammogram of 1 mM AA 0.1 M KCl. Condition; 0 to 1.0 V scan rate 50 mV/s; RE:Ag/AgCl; CE: Pt wire; WE: Carbon pencil lead in a beaker type electrochemical cell .....	109
4.6	Suggested oxidation mechanism of AA: a) electrode reaction, b) chemical reaction.....	109

## LIST OF FIGURES (Continued)

<b>Figure</b>	<b>Page</b>	
4.7	Cyclic a) and differential pulse b) ascorbic acid voltammetry in one trough of a 24-well microtiter plate.....	111
4.8	a) The load of the 24-well microtiter plate for AA calibration; the number in each well is AA concentration in mM, b), and c) automatically recorded differential pulse voltammogram in 16 wells of the microtiter plate that were filled with analyte solutions of 0.05-1 mM b), and 2-100 mM c); parameter DPV: step height of 10 mV, pulse time of 0.5 s and pulse height of 50 mV.	113
4.9	a) Plots of the peak height, $I_p$ , of the AA differential pulse robotic voltammograms in Figure 4.8 b), and as a function of the analyte concentration with 0.05 mM-100 mM AA.....	114
4.10	Robotic voltammetric quantification of ascorbic acid in microtiter plate wells by the precalibration method.....	116
4.11	Example of an analyte quantification via method of standard additions. The signal is plotted versus the concentration of the added standard after dilution.....	118
4.12	Robotic voltammetric quantification of ascorbic acid in microtiter plate wells by means of the standard addition method.....	120
4.13	a) Robotic voltammetric quantification of the ascorbic acid level of freshly prepared guava juice. b) standard addition plot.....	122

## LIST OF FIGURES (Continued)

Figure	Page	
4.14	a) Antioxidant molecule, AH, (analyte) react with the DPPH• free radical producing the non-residue DPPH-H; b) Scheme of the amperometric measurement, a DPPH• reduction current is adjusted by cathodic working electrode potential and a suitable fixed DPPH• supplement of the measuring solution.....	127
4.15	The structure of 6-hydroxy-2,5,7,8-tetramethylchroman-2-carboxylic acid, Trolox.....	128
4.16	Repetitive cyclic voltammogram of the DPPH• as recorded in ethanolic phosphate buffer (EPBS) with a beaker assembly of a pencil lead Working Ag/AgCl pseudo-reference and Pt spiral counter electrode.....	130
4.17	a) Typical amperometric current response of an assembly of a pencil lead working, Ag/AgCl pseudo-reference and Pt spiral counter electrode that was kept at +100 mV and exposed in a beaker type experiment to multiple additions of DPPH• and then Trolox solutions. b) and c) are the calibration graphs for DPPH• and Trolox, respectively.....	133
4.18	a) Details of the exact plate layout for automated Trolox calibration measurements and reproducibility tests. b) 24-well microtiter plate with well number running in a). c) Schematic presentation of the sequence of automated analytical run through a preloaded microtiter plate in b).....	136

## LIST OF FIGURES (Continued)

Figure	Page
4.19 a) Representative collection of the twelve current recordings as obtained in the even-numbered wells of a microtiter plate that was charged as shown in Figure 4.18 a) during a calibration run b) A zoom into the traces in a) at times between 80 and 100 s. c) The Trolox calibration curve, which is the plot of the current magnitude as extracted from graph b) versus the actual Trolox level in the measuring buffer of the sample well .....	138
4.20 a) Details of the exact microtiter plate layout for DPPH•/Trolox reproducibility tests. b) 24-well microtiter plate with well number running in a). c) Twelve amperograms of 250 μM DPPH• and 25 μM Trolox.....	141
4.21 a) Microtiter plate filling for determining the Trolox equivalents of three synthetic antioxidants (Ascorbic acid, AA; Gallic acid, GA; αTocopherol, TP) via robotic DPPH•/Trolox amperometry. b) A representative set of amperograms from an automated antioxidant power scaling for gallic acid.....	142
4.22 Calibration graph used for TE calculation data was determined by spectrophotometry. Experimental condition: 100 μM DPPH• (initial concentration), each point corresponds to addition of 1mM Trolox 10 μL, $\lambda_{\max} = 519 \text{ nm}$ .....	144

## LIST OF FIGURES (Continued)

<b>Figure</b>	<b>Page</b>	
4.23	a) The microtiter plate load for measuring triple values of the antioxidant capacity of the same freshly squeezed orange juice via robotic DPPH• amperometry in tropical runing. b) Amperograms from an automated antioxidant power scaling for orange juice. ....	149
4.24	a) Robotic differential pulse stripping voltammetry. The measuring buffer (0.1M acetate buffer pH 4.5 (0.1 M KCl)) had 20 µg/L Pb(II), Cd(II) and Bi(III) levels that varies from 100-2000 µg/L.; a deposition time of 120 s (stirred) and a deposition potential of -1.4 V were used for analyte accumulation onto working electrode, WE: PLE, CE: Pt spiral and RE: Ag/AgCl b) Peak height and c) Peak area of Pb(II) and Cd(II) as a function of Bi(III) concentration, the curve is associated with the voltammograms shown in a).....	154
4.25	a) Robotic Differential pulse stripping voltammetry of 40 µg/L Pb(II) And Cd(II) under the condition of different deposition (accumulation) time. b) Peak heights increase with increasing deposition time. Experimental condition; Bi(III) 500 µg/L, 0.1 M acetate buffer pH 4.5 (0.1M KCl),under stirring solution, deposition potential -1.4 V, WE: PLE, CE: Pt spiral and RE: Ag/AgCl.....	155

## LIST OF FIGURES (Continued)

Figure	Page
4.26 a) Schematic of the robotic electrochemical instrument for automated heavy metal anodic stripping voltammetry, b) Numbering of the 24-well microtiter plate; AC is 0.1 M acetate buffer, Bi is Bi(III), c) Drawing of three electrodes assembly consist of a PLE working (WE), pseudo Ag/AgCl reference (RE) and platinum spiral counter electrode (CE). d) The design of the microtiter plate for automated Pb(II) and Cd(II) calibration measurement.....	157
4.27 a) Robotic differential pulse stripping voltammetry of Pb(II) and Cd(II) with increasing analyte concentrations from 0 to 200 µg/L from a). Experimental condition; Bi(III) 500 µg/L, 0.1 M acetate buffer pH 4.5 (0.1M KCl), under stirring solution, Deposition potential -1.4 V for 600 s, WE: PLE, CE: Pt spiral and RE: Ag/AgC.....	159
4.28 Robotic differential pulse stripping voltammetry of bottled mineral drinking water without and with spike Pb(II), and Cd(II) supplement of 20, 30, 40, and 50 µg/L. The experimental conditions for measurement are the same as Figure 4.27 .....	162
4.29 Robotic differential pulse stripping voltammetry of tap water without and with spike Pb(II), and Cd(II) supplement of 20, 30, 40 and 50 µg/L. The experimental conditions for measurement are the same as Figure 4.27.....	163



## LIST OF FIGURES (Continued)

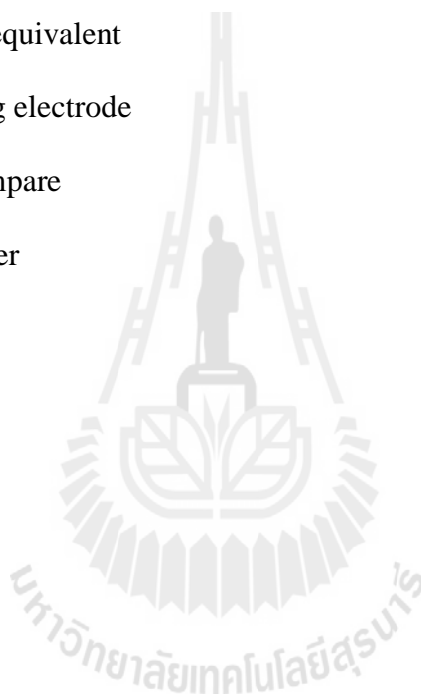
<b>Figure</b>	<b>Page</b>
4.30 a) Robotic differential pulse stripping voltammetry of bottled mineral drinking water that with a 20 $\mu\text{g/L}$ supplementation of Pb/Cd. b) Standard addition plot used for the determination of Pb(II), and Cd(II) content in the spike bottled mineral drinking water sample. The experimental conditions for the measurement were the same as Figure 4.27 .....	165
4.31 a) Robotic differential pulse stripping voltammetry for certified wastewater reference material, (CRM 713). Show the sample trace and the trace heavy metal after addition of Pb/Cd dolution. b) Standard addition plot for the determination Pb(II). The experimental conditions for the measurement were the same as Figure 4.27 .....	169
4.32 a) Robotic differential pulse stripping voltammetry for a contaminated soil sample. Shown the current traces reveals for the soil sample together with the one for the sample that was spiked with increasing levels of Pb/Cd standard, b) Standard addition plot for the determination of Pb(II). The experimental conditions for the measurement were the same as Figure 4.27 .....	172

## LIST OF ABBREVIATIONS

AA	Ascorbic acid
AAS	Atomic absorption spectroscopy
AdS	Adsorptive stripping
AH	Antioxidant
ASV	Anodic stripping voltammetry
BFE	Bismuth film electrode
BF-PLE	Bi(III) film modified pencil lead electrode
CE	Counter electrode
CSV	Cathodic stripping voltammetry
CV	Cyclic voltammetry
DCIP	2,6-dichloroindophenol
DHAA	Dehydro ascorbic acid
DPPH	2,2-diphenyl-1-picrylhydrazyl
DPSV	Differential pulse stripping voltammetry
DPV	Differential pulse voltammetry
ICP-AES	Inductively coupled plasma atomic emission spectroscopy
ICP-OES	Inductively coupled plasma optical emission spectrometry
$I_p$	Peak current
mM	millimolar
NPV	Normal pulse voltammetry
PLE	Pencil lead electrode

**LIST OF ABBREVIATIONS (Continued)**

RE	Reference electrode
Std	Standard solution
SWV	Square wave voltammetry
TAC	Total antioxidant capacity
TE	Trolox equivalent
WE	Working electrode
$\mu\text{A}$	microampere
$\mu\text{L}$	microliter



# CHAPTER I

## INTRODUCTION

As central theme of this Ph.D. thesis was chosen the development of a convenient since automated electrochemical quantification of antioxidants in dietary and toxic heavy metals in environmental samples. Knowledge of food antioxidant levels is of great significance since this class of compounds can act in the human body as scavenger of reactive free radicals that, at internal concentration out of control, are known to damage cells and cellular tissue and thus badly affect human health up to cancer disease triggering. In food industry, on the other hand, antioxidants are used as beneficial supplements that protect products against oxidative degradation via free radicals. Good sources of antioxidants are edible plants and compounds with a confirmed antioxidant activity may include species such as polyphenols, flavonoids, carotenoids, tocopherols, glutathione, ascorbic acid and even various enzymes. The antioxidants play an important for human health and food technology. Their quantification in plant extracts or synthetic (dietary) products is important. Exact knowledge of antioxidant levels provides a useful guideline for responsible food producers and consumers who want to offer and consume antioxidant-rich foodstuff, respectively. Many methods for the determination of total antioxidant capacities (TAC) of food samples have been proposed in the past. Common for antioxidant measurements are schemes with an optical (spectroscopic) or electrochemical detection. Because of the enormous variety of relevant fruits, vegetables, and herbal

plants on the market and the related high number of samples, an efficient quality control on the food market depends on the availability of convenient and accurate antioxidants assays. The only chance to increase the economics of the analysis in terms of time and costs per sample screen, release laboratory staff from the monotonous labor-intensive duties for other activity and cut back on the risk for human error is the move to a non-manual analysis. Some semi- or fully automated flow-based antioxidant assays with optical or electrochemical detections have been proposed as strategies for handling larger collections of food and pharmaceutical samples to be screened for the target content. In this context a first objective of this work was to take advantage of comparatively cheap electrochemical equipment and simple 6x4 standard microtiter plates for establishing robotic electrochemical antioxidant screening as a convenient and cost-effective alternative assay to the existing more complex fluidic device and explore its analytical performance level in terms of e.g. reproducibility, accuracy, and time consumption.

Another area where large numbers of samples are likely to be faced is the trace analysis of heavy metal and organic environmental pollutants. In use for a routine quantification of toxic heavy metals such as lead (Pb) and cadmium (Cd) are atomic adsorption, atomic emission, ion couple plasma, and mass spectrometry as well as the electrochemical scheme of stripping voltammetry. With respect to their sensitivity the spectrometric and voltammetric methods are about equally good and remarkable sub-ppb detection limits have been reported in either case. As already mentioned advanced electrochemical workstations are favorably priced, but also compact in design and thus in contrast to spectroscopic trace metal analyzers potentially portable and associated with low running costs. It made therefore good sense to define as a second objective of

this thesis work the implementation of a heavy metal trace analysis via stripping voltammetry into the robotic electrochemical device that was already targeted for the plant antioxidant measurements and extend the scope of the application of the novel non-manual electroanalysis in microtiter plates from food to environmental screening

In more detail, the research objectives of this Ph.D. thesis are mainly three topics.

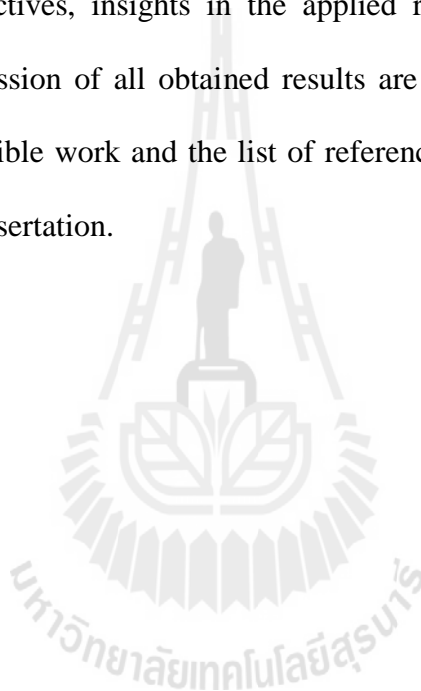
(1) The establishment of automated ascorbic acid voltammetry in the 24-well microtiter plate format. Completed has to be the adaptation of a purchased robotic electrochemical device for voltammetric ascorbic acid quantification. Addressed will be the sensitivity, linear range, reproducibility, detection limit, stability and recovery rate of the methodology. Also considered was the application of the differential pulse robotic voltammetry for measurements of ascorbic acid levels in a variety of food (e.g. fruits and Thai herbal tea) and pharmaceutical formulations (e.g. buyable vitamin C tablet).

(2) The establishment of an amperometric Total Antioxidant Capacity (TAC) measurement in the microtiter plate format. Task was the implementation of a DPPH-based amperometry into the robotic electrochemical device. The sensitivity, linear range, stability, reproducibility of the automated DPPH-based amperometry was assessed. In addition, an application of the established methodology for the determination of TAC values of a selection of Thai herbs, edible plants, fruits and beverages was carried out.

(3) Trace toxic heavy metal voltammetry (here; lead (Pb) and cadmium (Cd)) was implemented into the robotic electrochemical device that was initially established for antioxidant measurements. An automated screening of heavy metal levels in

environmental wastewater and soil sample nearby industrial zone were applications of the established robotic stripping voltammetry scheme.

In the following sections, a comprehensive literature review will first be presented on the relevance and the analysis of antioxidants and heavy metals. Then literature-known work on the development of a microtiter plate-compatible workstation for electrochemical measurements will be summarized. The exact definition of the objectives, insights in the applied research methodologies and a presentation and discussion of all obtained results are next before a conclusion and outlook on future possible work and the list of references will complete the essential parts of this written dissertation.



## **CHAPTER II**

### **LITERATURE REVIEWS**

#### **2.1 The concept of electroanalysis**

Electroanalytical techniques take advantage of the interplay between electricity and chemistry, and use the measurements of electrical quantities, such as current, potential, or charge, to create a relation to identify and concentration of species. Such use of electrical measurements for analytical purposes has found a vast range of applications, including environmental monitoring, industrial quality control, and biomedical analysis. The two most prominent types of electroanalytical measurements are potentiometry and voltammetry.

Potentiometry (Monk, 2001; Bagotsky, 2005) is a static (zero-current) technique in which the information about the sample composition is obtained from measurement of the potential established at electrode/electrolyte or membrane/electrolyte interface. Different types of various membrane materials incorporating types of ion-selective species, have been developed to impart high selectivity. Potentiometric probes also known as ion-selective electrode have been widely used for several decades to directly monitor ionic species such as protons or calcium, fluoride, and potassium ions in complex samples.

A well-known example of a potentiometric device is the pH glass electrode which is a valuable in almost every laboratory for routine measurements of the pH of (buffer) solutions.



Voltammetry is a controlled-potential (potentiostatic) technique that deals with charge transfer processes at the electrode–solution interface. It is based on a dynamic (non-zero-current) situation. Here, the electrode potential is being used to force an electron transfer reaction to take place and the resultant current is measured. The role of the potential is analogous in terms of system application to that of the wavelength in optical measurements. The electrically easy to control parameter can be viewed as induced “electron pressure,” which forces dissolved chemical species that come in physical contact to the electrode surface to gain or lose an electron (reduction or oxidation, respectively). Accordingly, the resulting current reflects the rate at which electrons move across the electrode–solution interface. Potentiostatic techniques (voltammetric) can thus measure any chemical species that is electroactive and can be reduced or oxidized. The advantages of controlled-potential techniques include high sensitivity, selectivity toward electroactive species, a wide linear range, portable and low-cost instrumentation, speciation capability, and a wide range of electrodes that facilitate assays for unusual environments. The specific types voltammetric electrochemical analysis are reviewed by Monk (2011) and Wang (2001).

- **Chronoamperometry:** Applied is a constant potential and measured current.
- **Voltammetry:** The general groups of techniques that work with potential ramps or steps and use current vs time or potential plot for analysis.
- **Linear sweep voltammetry:** The potential of the working electrode is ramped with a given scan rate from an initial potential to a final potential. The current is plotted as function of the time potential.
- **Cyclic voltammetry:** The potential is similarly ramped from an initial potential but at the end of the first linear sweep, the direction of the potential scan is

reversed, plots of current (I) versus potential (E) are called cyclic voltammograms. This technique is probably the most commonly encountered technique for studying dynamic electrochemistry, discerning kinetics, rates and mechanism, in addition to thermodynamic parameter.

- **Pulse voltammetry:** The analytical sensitivity of classical polarographic or voltammetric method is usually good at about  $5 \times 10^{-5}$  molar. The benefit of the pulse technique is the elimination of capacitive currents (unwanted flow of charge to establish the electrical double layer of cathode or anode) and detection of faraday currents (relevant signal, flow of charge in response to interfacial redox reactions or electron transfer at the surface of anode and cathodes). Therefore pulse method improves the sensitivity and lower the detection limit of the measurements. The difference between the various pulse voltammetric and polarographic technique is the excitation waveform and the current sampling regime.

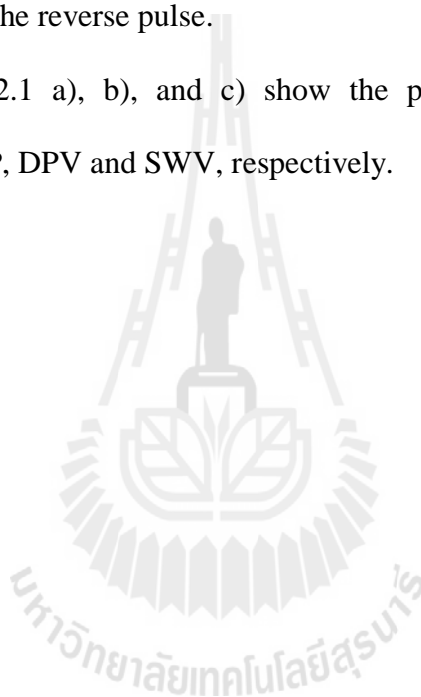
· *Normal pulse voltammetry* (NPV) consists of a series of pulses of increasing amplitude applied to the working electrode. The resulting voltammograms has a sigmoidal shape.

· *Differential pulse voltammetry* (DPV) is an extremely useful technique for measuring trace levels of organic and inorganic compound species. A fixed magnitude pulse, superimposed on a linear potential ramp, is applied to working electrode. The current is sampled twice, just before the pulse application and again late in the pulse life. Then the first current is subtracted from the second and this computed current difference is plotted against the applied potential. The resulting differential pulse voltammograms consists of current peaks, the height of which is directly

proportion to the concentration of corresponding analytes. The peak potential is a characteristic feature of the related compound.

· *Square wave voltammetry* (SWV) is a large-amplitude differential technique in which a waveform composed of a symmetric square wave, superimposed on a base staircase potential, is applied to the working electrode. The current is sampled twice during each square-wave cycle, once at the end of the forward pulse and once at the end of the reverse pulse.

Figure 2.1 a), b), and c) show the potential waveform and pulse voltammogram of NVP, DPV and SWV, respectively.



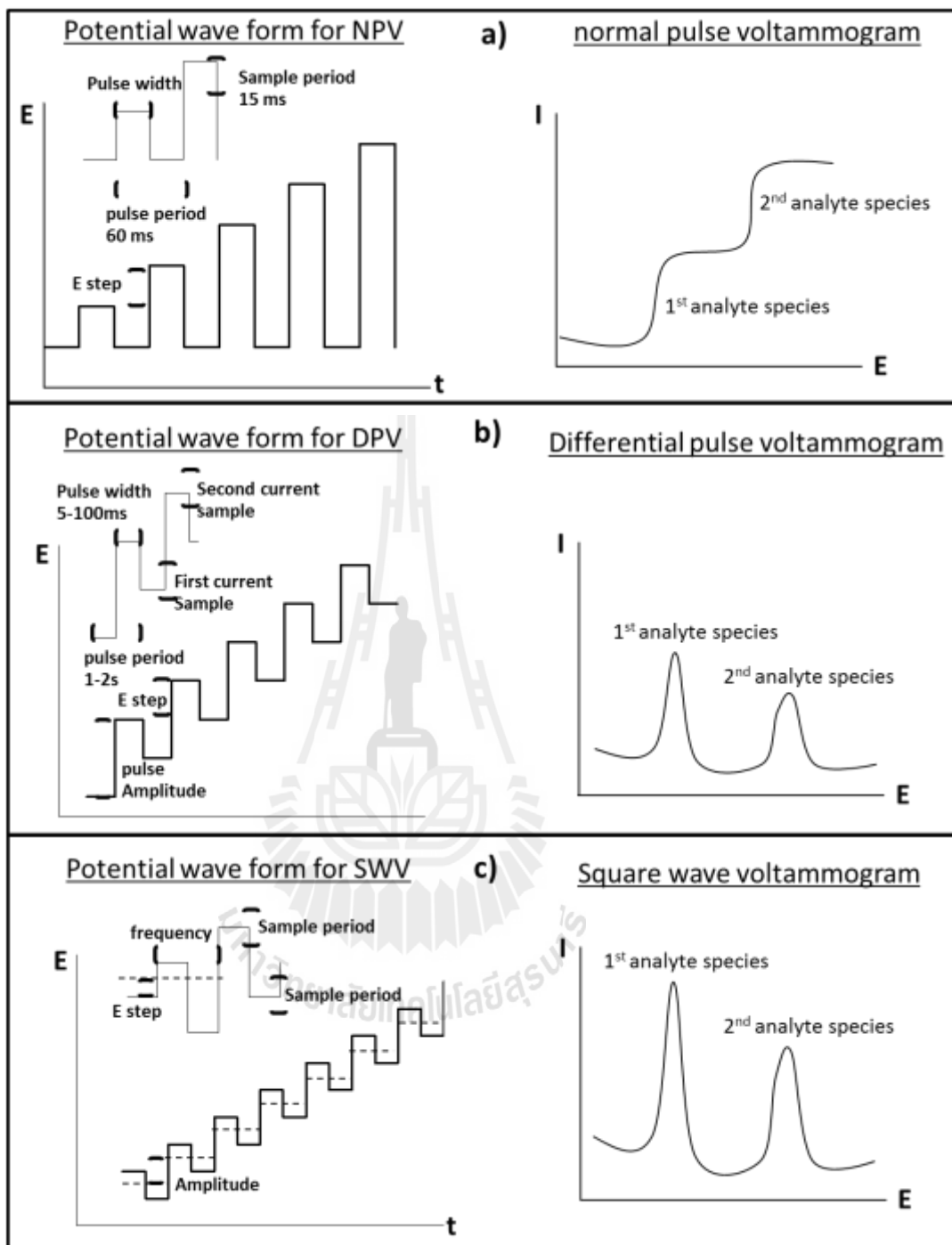


**Figure 2.1** Potential wave forms and voltammograms for a) normal pulse voltammetry (NPV), b) differential voltammetry (DPV) and c) square wave voltammetry (SWV).

- **Stripping voltammetry:** is an extremely sensitive method for measuring trace metals at concentration levels down to  $10^{-10}$  M. Essentially, stripping analysis is a two-step technique. The first, or deposition step, involves the electrolytic deposition of a small portion of the metal ions in solution onto the working electrode with the aim to preconcentrate the metal. Accumulation is followed by the stripping step (the measurement step), which involves the dissolution (stripping) of the deposit. Different versions of stripping analysis can be employed, depending on the nature of the deposition and the measurement steps.

- **Polarography:** A subclass of voltammetry in which the working electrode is dropping or hanging mercury. Because of the special properties of this electrode, particularly its renewable surface and wide cathodic potential range polarography has been widely used for the determination of many important reducible species.

## 2.2 Normal manual electroanalysis experiments

The electrochemical cell, where the voltammetric experiment is carried out, consists of a working (indicator) electrode, a reference electrode, and a counter (auxiliary) electrode. Three-electrode cells (see Figure 2.2) as commonly used in controlled potential experiments are usually a covered beaker of 5–50mL volume, and have the three electrodes immersed in the sample solution. While the working electrode is the electrode at which the reaction of interest occurs, the reference electrode serves a stable and reproducible potential (independent of the sample composition), against which the potential of the working electrode can be controlled. The plate or coiled wire made of an inert conducting material, such as platinum or graphite, is usually employed as the current-carrying counter electrode. Glass is commonly used as the cell material, due to its low cost, transparency, chemical

inertness, and impermeability. Teflon and quartz represent other possible cell materials. (Wang, 2001; Zoski, 2007)

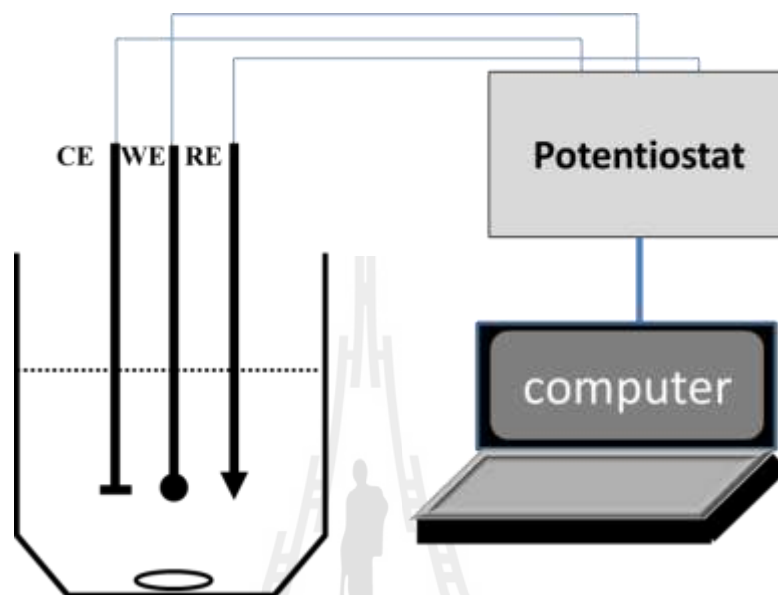


**Figure 2.2** Schematic diagram of a conventional cell for voltammetric measurements:

WE-working electrode; RE-reference electrode; CE-counter electrode.

Steps in the typical manual are; (1) Electrode pretreatment, modification and cleaning, (2) immersion electrode in solution, connection with potentiostat, (3) execution of the actual electrochemical measurement via computer control, and (4) removed of electrode and repeating of step (1) to (4). Figure 2.3 is a schematic representation of the manual voltammetric procedure. For the acquisition of a calibration curve or to complete a stripping voltammetry experiment with standard addition in charge of analyte quantification, the cycle of steps in Figure 2.3 may have to be repeated multiple times.

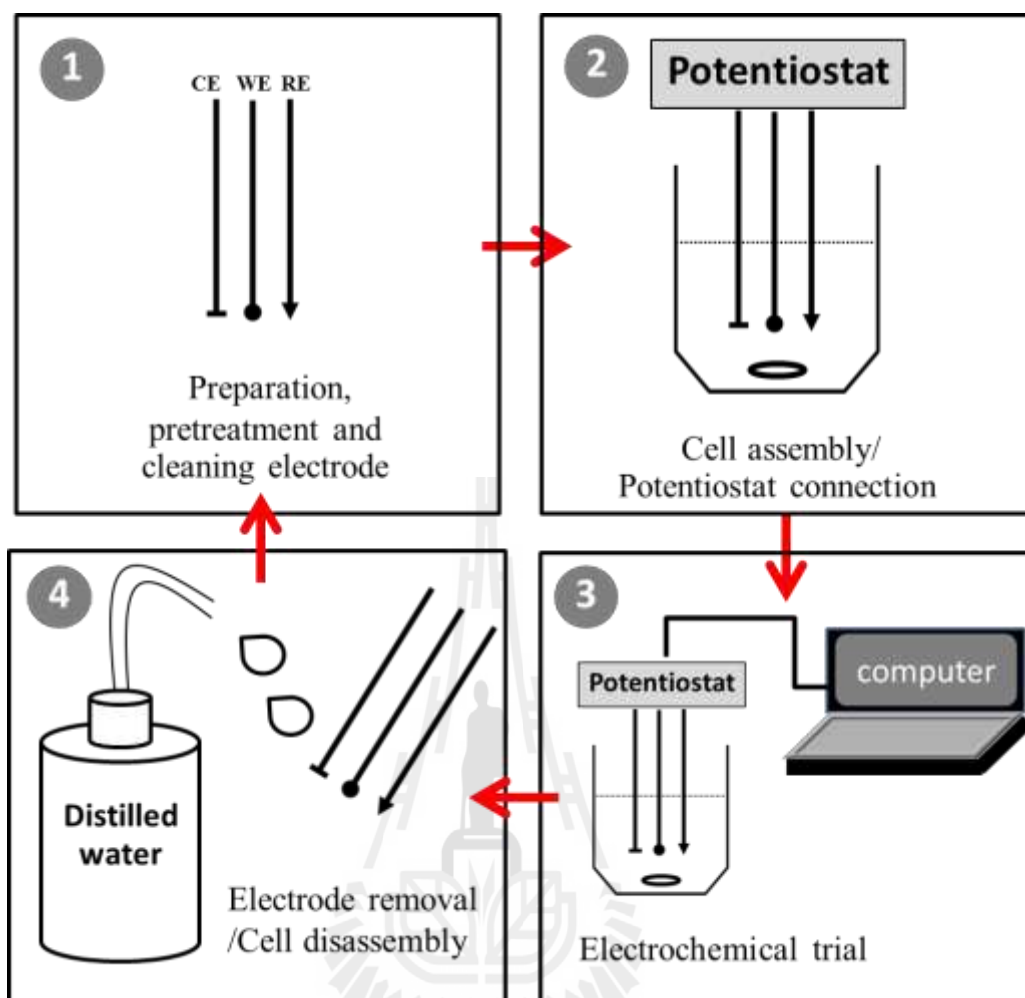


**Figure 2.3** Steps of manual electrochemical measurement.

Beaker type of electrochemistry works very well with few samples, but obviously the method becomes tedious, time-consuming and awkward when dealing with libraries of larger number of samples. In addition, manual operator errors may occur and badly influence the accuracy and reproducibility of measurements more drastic with increasing number of measurements.

Desirable for a more convenient and more efficient analysis would be an automatic execution with a voltammetric system with high-throughput capability. In

the past, several strategies for automated voltammetry have been developed and applied to the routine analysis of trace heavy metal ion such as cadmium, nickel, cobalt (Ensafi, and Zarei, 2000), copper, zinc, and manganese (Achterberg, and Braungardt, 1999; Tercier, Buffle, and Graziottin, 1998). Regardless of the variety of studied samples and preferred approaches to automation, the developed systems had the common goal to increase the speed and throughput of routine voltammetric analysis while maintaining or possibly improving the quality of measurements over the manual process. In the earlier reported attempts, automatic voltammetric analyzers have been realized by means of flow injection analysis (FIA) systems with a programmed stream of analyte and reagent solution into electrochemical flow-through cells. Siriangkhawut, Pencharee, Grudpana, and Jakmune, (2009), for instance, established the flow voltammetry determination of cadmium and lead using a bismuth film working electrode in a flow system. The approach (see Figure 2.4) provided sensitive and reproducible determinations of Cd(II) and Pb(II) and performed well for analysis of water samples collected from a draining pond of a zinc mining, with semiautomatic analysis and low chemical consumption.



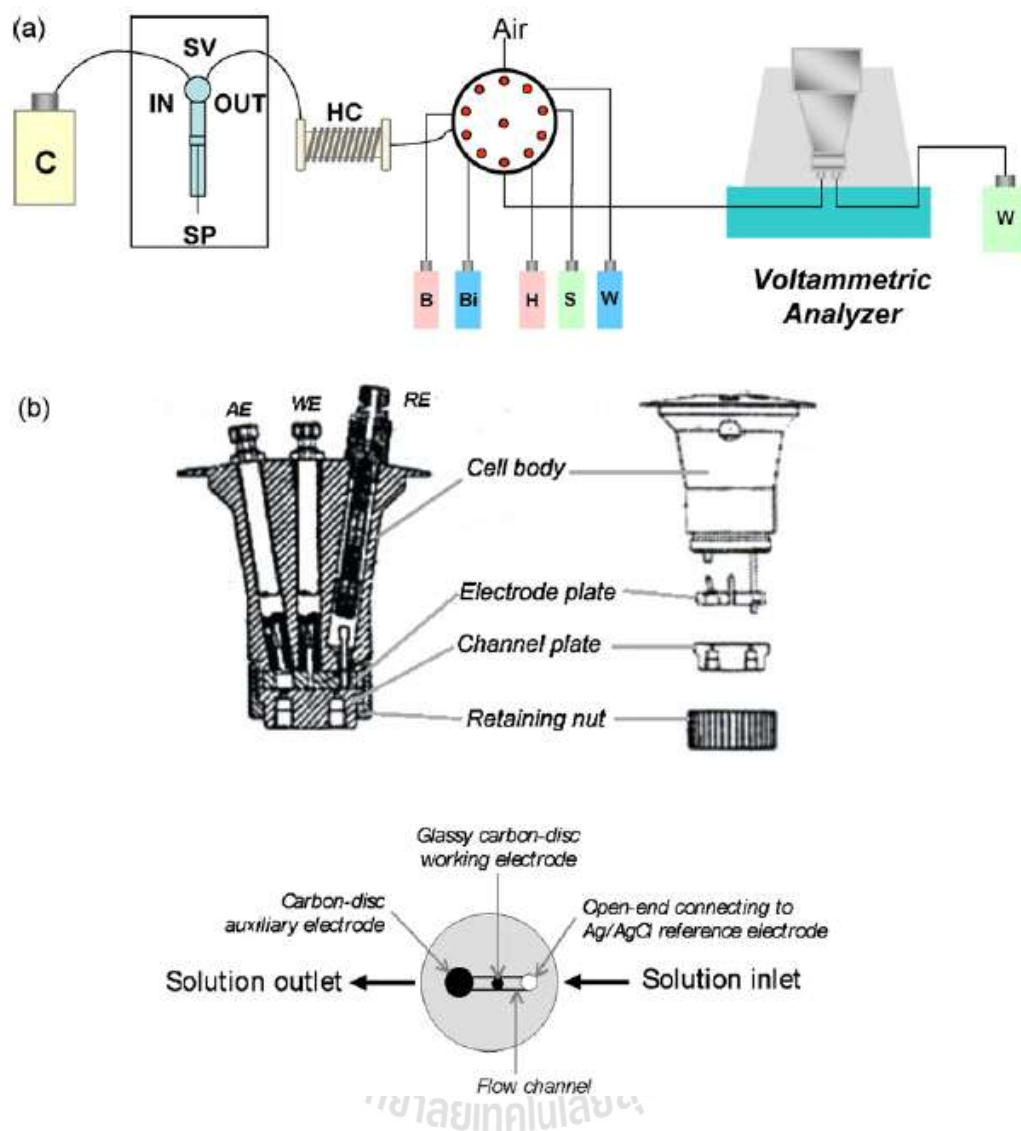


**Figure 2.4** A representative example of a sequential injection anodic stripping voltammetric system. (a) Schematic diagram of the system, C: carrier (deionized water), SP: syringe pump, SV: switching valve, HC: holding coil, B: 0.2 M acetate buffer, Bi: 40 mg L<sup>-1</sup> Bi(III) in 3M acetate buffer, H: cleaning solution (0.1 M HNO<sub>3</sub>), S: mixed metals standard/sample and W: waste. (b) A thin layer electrochemical flow-cell and the flow channel, AE: auxiliary electrode, WE: working electrode and RE: reference electrode. (Siriangkawut et al., 2009)

Further advances of automatic electrochemistry could be expected from the involvement of which multipotentiostats which support voltammetric measurements however carried out with multichannel electrode arrays. Parallelization of the electrochemical trials using eight electrode bundles and analysis in eight electrochemical cell simultaneously was seen as a chance for automation and advancement in term of speed and convenient (Hintsche, Albers, Bernt, and Eder, 2000).

In a methodological rather different approach, the work in this dissertation proposes the integration of conventional voltammetry and amperometry into an electrochemical robotic device that was specially designed for automated electrochemical measurements in the 24-well microtiter plate format. In the following the state of the art for electrochemistry in the microtiter plate format was reviewed and the basic principle explained.

## **2.3 Robotic electrochemistry**

### **2.3.1 General remarks**

The concepts of robotic electrochemistry were introduced for studies with large sample libraries and then an adaptation for high-throughput applications with respect to organic polymer synthesis, biosensor fabrication and characterization and electroanalysis took place. One particular strategy that is commonly employed when dealing with large compound libraries is the use of microtiter plates, which are commercially available in several formats containing 24, 96, 384, or 1536 wells. Concurrently with the handling of large compound libraries in microtiter plates, there is a need for automation and parallelization of the individual well assessments which led

to the development of robotic systems for non-manual liquid management and execution of the analytical sequences.

An early design of electrochemistry in microtiter plate format was established with a multielectrode sequential analyzer (MESA) (Reiter, Eckhard, Blöchl, and Schuhmann, 2001) which allows to show up to 16 cyclic voltammograms or differential pulse voltammograms in a “sequential-parallel” mode at 16 individual three electrode bundles in 16 wells. Redox proteins with Ru-complexes were evaluated with respect to the coordinative labeling by 16 three electrode sets, which were sequentially connected to a potentiostat. In another variant, a multichannel electrochemical detector (MED) consisting of eight sets of electrodes guided into eight wells of a microtiter plate was explored for sequential amperometric immunoassays (Tang, Deng, and Huang, 2002).

A really convenient electrochemical robotic system was developed and applied with a movable 3-electrode assembly moving in center way from well to well of a microtiter plate. This robotic electrochemistry approach has been first realized by Schuhmann, Speiser and coworker (Reiter, Ruhlig, Ngounou, Neugebauer, Janiak, Vilkanauskyte, Erichsen, Schuhmann, and Macromol, 2004) who successfully designed and constructed the instrumentation and tailored the device for non-manual electrochemical trials on large compound collection.

An electrochemical robotic assay in the microtiter plate format should offer the following features:

- (1) The system should be functional in common microtiter plates with defined number of wells made of different materials (glass, Teflon®, polyethylene, polystyrene etc.) and with additional features such as transparent bottom,

combined wells, deep wells etc. So far robotic electrochemistry work has been established for the 24 and 96-well plates of wells. The system apparently gets more difficult in the operation, with increasing well number per plate since the size of the individual well into which the counter, reference and working electrode have to fit is decreasing (see Figure 2.5).

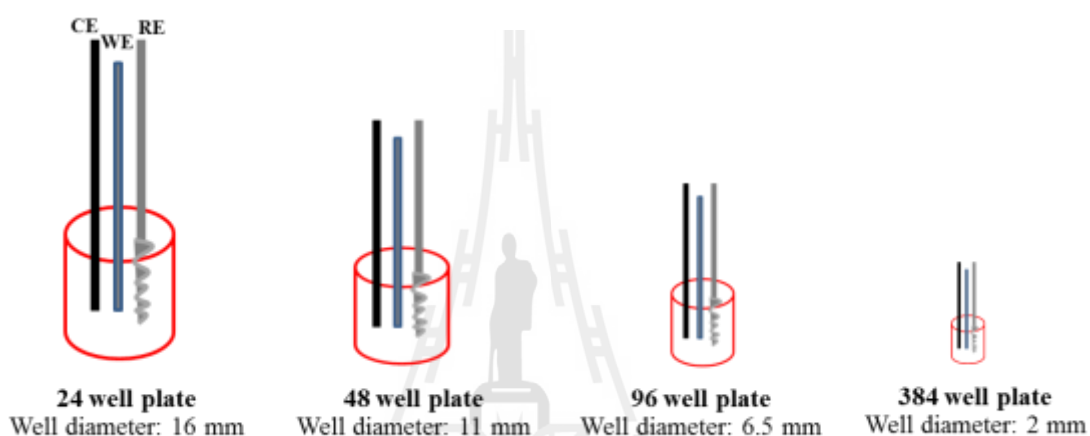


**Figure 2.5** Schematic of a microtiter plate well with a notification of its diameter related to the well plate number.

- (2) A three-electrode assembly is needed that can be moved through the wells for either cleaning, pretreatment or measuring/synthesis electrochemistry. As smaller the well (a larger the number of wells per plate is) as smaller (more miniaturized) the 3-electrode assembly has to be (Figure 2.5).
- (3) Automation of all steps that are involved in the electrochemical procedures carried out in the microtiter plate: the system should allow sequential electrochemical experiments and flexible variation of parameters.

Furthermore, the operation of microtiter plate based robotic electrochemistry should support time effectiveness of the analytical or synthetic procedures, and an easy data management. Desired may also be on automatic addition of chemicals using suitable pumps for delivery, a control of the temperature within the wells, and the integration of a microtiter plate shaker to join some kind of a stirring in the plate wells.

### **2.3.2 Hard- and software design of a device for robotic electrochemistry in microtiter plate**

A micro-positioning system consisting of three stepper motor-driven positioning stages with a nominal positioning accuracy of 1.25  $\mu\text{m}$  per half step, a maximum speed of 8  $\text{mm s}^{-1}$ , and a repositioning accuracy of better than 2  $\mu\text{m}$  is used as the heart of the instrument for the up-and down movement of the 3-electrode assembly and an x, y movement of the microtiter plate. The independent microcontroller on the stepper motor card provides the precise time base for the stepper motor movements ensuring an accurate positioning. The x- and y-positioning tables are used to position the standard microtiter plate under the electrode holder which is moved up and down using the z-motor stage. The maximum traveling range of the stepper motors are 13 cm for x, 9 cm for y, and at least 5 cm for z. The microtiter plate itself may be placed in a chamber with a lid that has a hole in it for the insertion of the electrode assemble. As long as the hole and the tip of the 3-electrode assembly are aligned above each other up and down movement can bring the electrode into the wells, at least after proper plate x, y alignment. The chamber may be purged with inert gas, if the electrochemistry is desired to be carried out in oxygen free

environment. Figure 2.6 shows a prototype of the designed electrochemical robotic device.

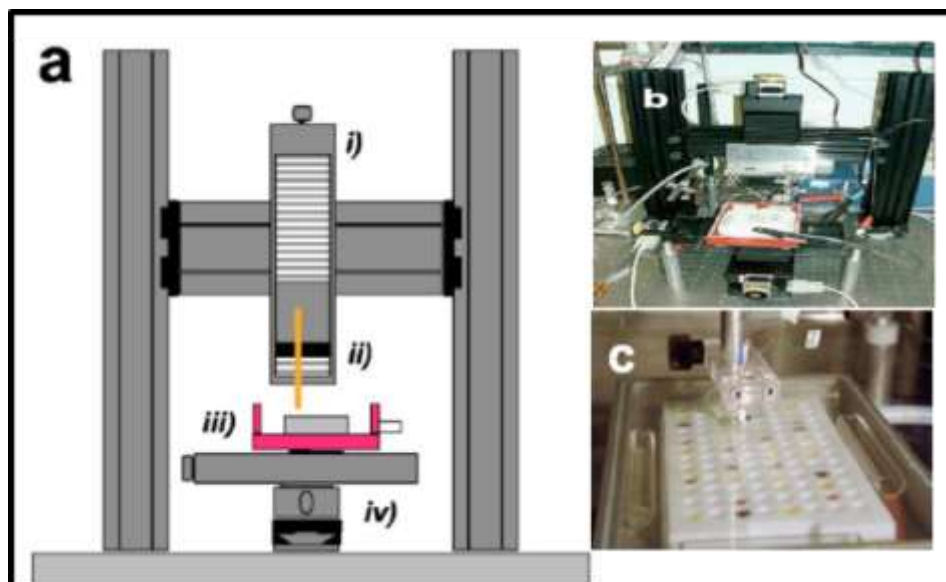


**Figure 2.6** Schematic representation of an electrochemical robotic system (a). (i) z-positioning table; (ii) electrode holder with working electrode, counter electrode, reference electrode; (iii) chamber with option of argon supply; and (iv) x-, y- positioning tables. Photographs of instrumentation (b) and the lid-covered microtiter plate. (Erichsen et al., 2005)

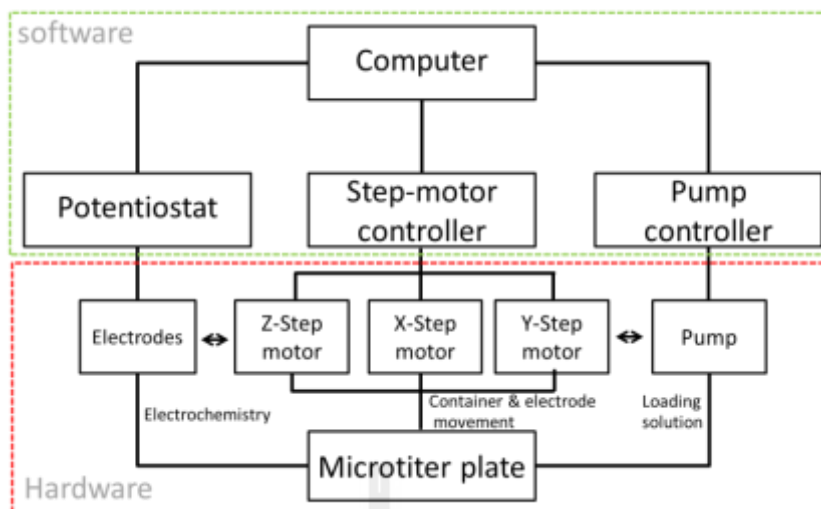


**Figure 2.7** Schematic representation of the hardware architecture and structure of the control software for microtiter plate-based electrochemistry.

The controlled movement of the stepper motor stages is induced with specifically designed software written in Visual Basic 6.0. Requirements for the software include the option to run complex analytical procedures, the provision of a high accuracy of the performed measurements, and the software should have an easy adaptability to design new experiments and incorporate a variety of electroanalytical and/or electrosynthetic methods for execution.

A sample user interface is the platform to set the all choices for a specific experiment, e.g. the distances between the center of wells of used microtiter plate (e.g., 2 cm for a 24-well plate and 9 mm for a 96-well plate) can be countered, the number of lines and rows defined, the insertion depth of the electrode bundle chosen, and the z-displacement during movement of the microtiter plate can be set. The electrochemistry actions (such as, cyclic voltammetry, differential pulse voltammetry,

amperometry) have to be programmed in a script written in Notepad and the conditions and parameters such as the scan rate, potential range, starting and ending potential, conditioning time for cyclic voltammetry or differential pulse voltammetry have to be entered. The up and down movement of the electrodes within the well may be programmed to establish mixing or electrode cleaning. The independent software module can be executed in series with the x, y with positioning of the electrodes. Some examples of electrochemistry actions that may run on the electrochemical robotic device are listed in Table 2.1.

The obtained data set for each individual position (a given well) is saved in files with automatically generated file names, including a combination of well number, measuring method, and a serial number. This leads to a fast allocation of the obtained data files to the positions in the microtiter plate, which is essential for later (optional automated) data management.

Apart from the hard-and software, a suitable electrode bundles that in terms of size fits into the well of a selected microtiter plate of crucial importance for the utilization of the robotic system. The three electrode bundle typically consists of a choice of a working, reference and counter electrode. A previous study (Erichsen et al., 2005) used miniaturized three-electrode system consisting of a Pt disk working electrode with 10 to 250  $\mu\text{M}$  diameter, a Pt disk or wire counter electrode and a miniaturized Ag/AgCl reference electrode implemented in a special polymer holder. In certain circumstance also a chloridized Ag wire can be used as a pseudo-reference electrode. However, chloride should then be in the measuring buffer to ensure stable reference potential.



**Table 2.1** Software modules and parameter list which are transferred from a software script file to the robotic program for the execution of different experimental sequences.

<b>Action modules</b>	<b>Transferred parameters</b>
amperometry	position, electrochemical technique (amp), measuring time (s), applied potential (mV)
cyclic voltammetry	position, electrochemical technique (cv), number of cycles, scan rate (mV/s), start (vertex 1, vertex 2 and end) potential (mV)
differential pulse voltammetry	position, electrochemical technique sdpvd, measuring time ssd, applied base potential (mV), pulse height (mV), pulse time (ms), time between pulses (ms), scan rate (mV/s), start (vertex 1, vertex 2 and end) potential (mV)
z-approach	position, command (approach), applied potential (mV), stop case
SECM	(% change of bulk current signal), maximum driving way ( $\mu\text{m}$ ),
feedback control	driving speed ( $\mu\text{m/s}$ )
pumping	position, command (pump), pumped volume ( $\mu\text{l}$ ), speed of pump ( $\mu\text{l/s}$ ), pump direction (1, 0), valve number (0, 1)
Dip coating	position, command (dip), times of dip (s), time to dry (s)
Mixing	position, command (mix), number of times,
(moving electrodes up and down)	driving way ( $\mu\text{m}$ )
stop	position, command (stop)

### 2.3.3 Published applications of the electrochemical robotic system in microtiter plate format

The adaptability of the robotic system to the specific needs of an experiment together with the versatility of the system to perform electrosynthesis and electroanalysis in a variety of solvents and under control of a number of experimental parameters permits a broad applicability. There are two groups in Germany who first established in joined effort the robotic electrochemical system one of which is Prof. Wolfgang Schuhmann's group at Ruhr-Universität in Bochum and the other Prof. Bernd Speiser is group at the Universität of Tübingen in Tübingen. For example, the optimization and fabrication of amperometric glucose biosensors based on a library of 148 cathodic electrodeposition paints was carried out via combined electroanalysis/electrosynthesis in microtiter plates; biosensor fabrication and property evaluation of sensors were activated automatically studied (Reiter et al., 2004). Then, the measurement of nitric oxide was established with high sensitivity and selectivity within 96-well microtiter plates by automatic detection of analyte that was released by human umbilical vein endothelial cells (T-HUVEC) upon stimulation with vascular endothelial growth factor E (VEGF-E). The NO sensors were obtained by electrochemically induced deposition of Ni<sup>II</sup> tetrakis (*p*-nitrophenylporphyrin) on a 50- $\mu$ M diameter platinum disk electrode (Borgmann et al., 2006). Automatic cathodic adsorptive stripping voltammetry with high sensitivity and selectivity was used in the robotic device for quantification of the Ni<sup>2+</sup> ion release from electropolished surface of NiTi shape memory alloys during active corrosion in NaCl. The 24-well microtiter plate format worked with a bismuth film-modified glassy carbon electrode working used as the basic for the robotic Ni release voltammetry (Ruhlig et al., 2006).

Guschin et al. (2009) described the adaption of the early version of the microtiter plate of the robotic electrochemical device that was better suited for the automatic biosensor fabrication and instant characterization. The system is shown in Figure 2. 8 and had implemented a 96-well gold microtiter plate in a chamber that would be atmosphere controlled; e.g. flushed with inert gas and held at desired humidity. Also implemented was the option of stirring of the well solution, which actually was achieved by the microtiter plate shaking with a shaker device attached to the plate platform. Glass vial were placed in the surrounding of the microtiter plate and could be reach by the electrode assembly via micropositioning for cleaning or calibration.

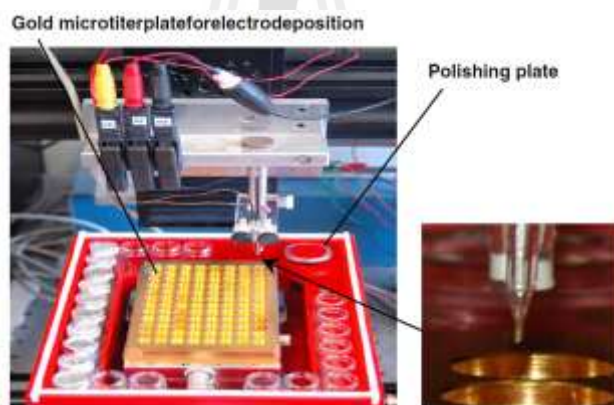


**Figure 2.9** Photograph of the electrochemical robotic system with a 96-well gold microtiter plate in a chamber for controlling the atmosphere as used for antibiotic biosensor fabrication and characterization (Guschin et al., 2009).

Other than direct sensor applications of the robotic electrochemical system have been approached by Prof. Bernd Speiser's group and co-worker (Märkle, Speiser,

Titel, and Vollmer, 2004). They reported automatic combinatorial electroynthesis of benzaldehydes and phenylhydrazones, which were oxidized at the working electrode in the microtiter plate wells. Thus, a collection of 36 different [1,2,4]triazolo [4,3-*a*]pyridinium perchlorates was generated non-manually within only a few hours by automated electroynthesis in a computer controlled instrument as shown in Figure 2.8.

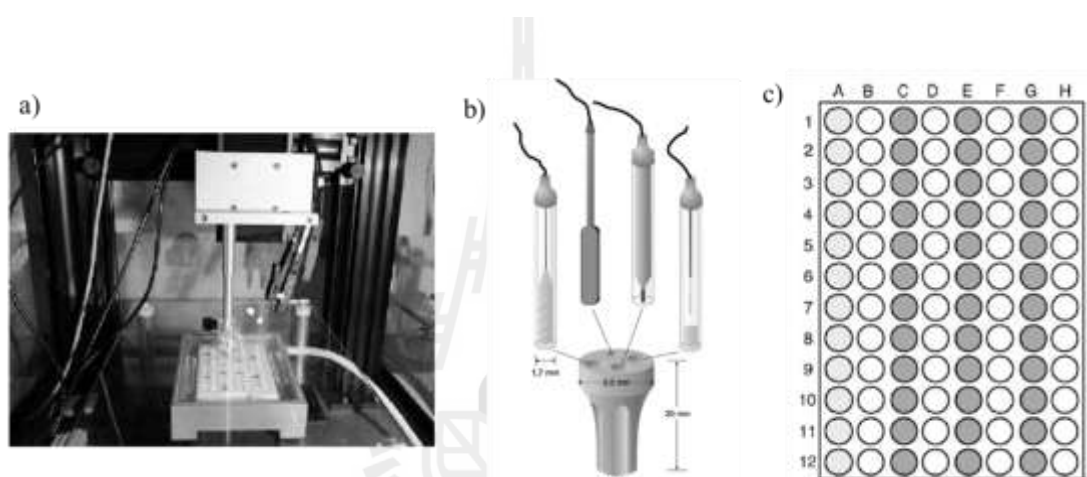


**Figure 2.9** a) Photographic view of a robotic instrument for automated electroynthesis, b) assembly of electrodes, from left to right: counter, electrolysis working, CV microdisk, reference electrode, and c) typical charging of a 96-well microtiter plate for reaction wells. (Märkle et al., 2004)

Lindner, Lu, Mayer, Speiser, Titel, and Warad, 2005 reported on the rapid determination of the redox properties of electroactive diamine (phosphine) ruthenium (II) complexes by repetitive automated cyclic voltammetry in 96-microtiter plates. The execution of the multiple voltammetry cycles by the computer controlled instrument

was very fast as compared to the classical way of manual one-by-one measurements. Thus suitability for high-throughput CV screening of compound libraries was suggested.

Until now, the electrochemical robotic approach in the microtiter plate format has not yet been applied for electroanalysis, in particular not for the assessment of dietary sample or contents in pharmaceutical compounds and environmental screening. Application of robotic voltammetry in a microtiter plate to food analysis was thus made the first task of this thesis. In extension, environmental heavy metals pollutant monitoring was defined as second target to be realized by the robotic electrochemical microtiter plate assay.

## **2.4 Ascorbic acid (AA)**

### **2.4.1 AA Background**

L-Ascorbic acid (AA, vitamin C) is a six-carbon water-soluble lactone that is not synthesized in humans and has a recognized essential function in living organism. It is for instance one of the major biological antioxidants in the human body fluid. As potent antioxidant AA is an actor against oxidative cell stress as it helps controlling the level of cell damaging reactive oxygen species. It is also known to take part in several physiological and metabolic reactions and it presents a chemical modulator in the mammalian brain. Too low physiological AA sooner or later will causes illness and, in severe ongoing cases, response can be scurvy with symptoms as bad as vessel fragility, connective tissue damage, swollen gums, unfastened teeth, bone deformity, extreme fatigue and, without medication, death. Accordingly, AA is used clinically in the treatment and prevention of scurvy. As human cannot create and store AA in their body, the vitamin thus has to be gained daily from a diet rich in

natural AA or via solid or liquid formulations of synthetic AA. However, AA is not only good for the health but also applied in the food and cosmetics industry to protect product against degradation and goods such as butters and margarines, vegetable oils, skincare creams and lotion etc. and all protected by an AA supplementation. Due to the broad use of AA, the health care and the food processing, cosmetic and pharmaceutical industry are all in the need of analytical schemes for an accurate, straightforward and economical screening of the multifunctional compound, special for evaluations of dietary plant extracts and pharmaceutical dosage forms. Obviously, many samples will pile up in the application and have to be systematically worked off while exploring new natural AA sources or studying the effect of botanical plant diversity, climate, soil condition, parameters on the actual AA levels in products from edible vegetables, fruits or herbs. The call for an AA analysis with reasonable sample throughput at a minimum labor is therefore a plausible issue in the AA business.

#### **2.4.2 AA electrochemical measurement**

A variety of methods have been reported for the ascorbic acid detection in aqueous sample solutions derived from, for instance, plant extracts, fruit drinks, teas or dissolved pharmaceuticals such as vitamin C tablets. Common strategies consist of acid-base and redox titration, (Marsh, Jacobs, and Veeninget, 1973; Suntornsuk, Gritsanapun, Nikamhank, and Paochom, 2002; Melo, 2006) fluorometry, spectrophotometry and chromatography (Burini, 2007; Güçlü, Sözgen, Tütem, Özyürek, and Apak, 2005; Özyürek, Güçlü, Bektaşoğlu, and Apak, 2007). Non-manual, AA measurement have been established by automatic detection which is flow injection analysis coupled with optical spectroscopy or electrochemical detection (Chergi, and Danet, 1997).

An electrochemical determination of AA profits from the ease of the anodic oxidation of the AA molecules to dehydroascorbic acid (DHAA). The reaction happens at positively polarized working electrodes either by means of constant potential amperometry, cyclic voltammetry or pulse voltammetry. Actually, the electrode-induced AA oxidation leads to a current proportional to the concentration of the substance in the electrolyte solution, like schematically shown in Figure 2.10. Cyclic (CV), differential pulse (DPV) and square wave (SWV) voltammetry, in particular, are sensitive electroanalytical schemes that work very well for the quantification of ascorbic acid and better sensitivity, little or no sample preparation. And the low cost and ease of operation of the involved instrumentation are generally acknowledged as advantages over their optical spectroscopy and titrimetric counterparts.

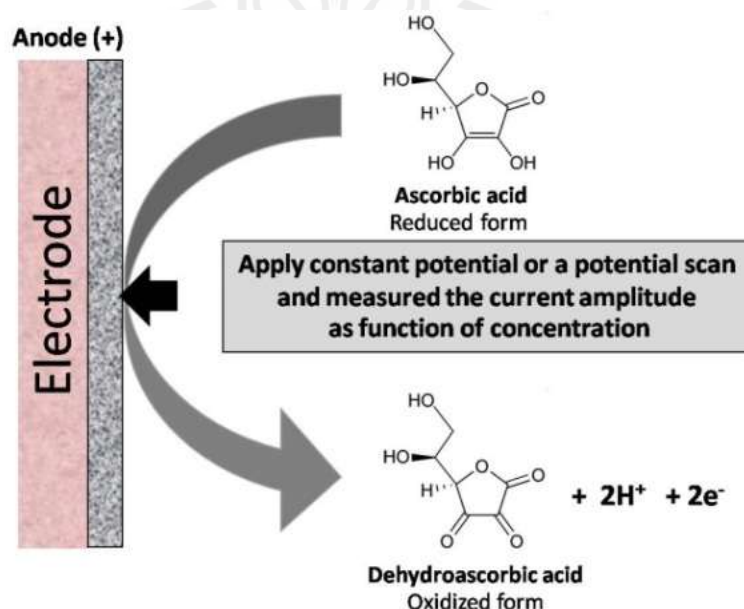


**Figure 2.10** Electrochemical oxidation of ascorbic acid

### 2.4.3 Literature review of electrochemical ascorbic acid determination

Voltammetry is an increasingly popular method for the determination of ascorbic acid in real samples because it offers low detection limits. Neither it requires complicated, expensive equipment nor well-qualified personnel. And voltammetry has the potential to be used even in turbid solution, which are difficult or not at all to measure with spectroscopy.

As said, electrochemical methods allow nicely to evaluate ascorbic acid levels and different materials have been proposed in recent times for the working electrode. Rueda, Aldaz<sup>1</sup>, and Sanchez-Burgos<sup>and</sup> (1978), for instance, proposed the oxidation of L-ascorbic acid on a gold electrodes which in the CV mode showed the existence of two oxidation waves but no reduction wave. The electrochemical oxidation of AA was also investigated by cyclic, linear sweep, differential pulse (DPV) and square wave (SWV) voltammetry at a bare glassy carbon working electrode. Here, a very well defined voltammetric peak was obtained in acetate buffer at pH 3.5 (see Figure 2.11), and AA detection at a GC surface was developed into an assay for the determination of AA in pharmaceutical dosage forms and *Rosa* species.



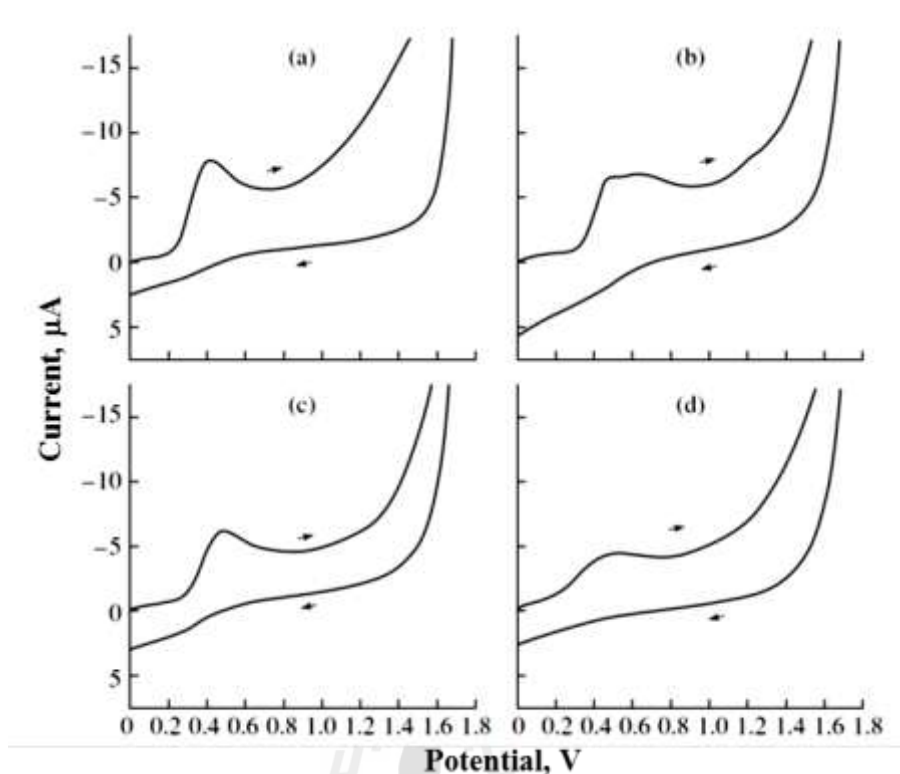


**Figure 2.11** Cyclic voltammograms of  $4 \times 10^{-4}$  M ascorbic acid in (a) acetate buffer at pH 3.05 and (b–d) phosphate buffer at pH (b) 2, (c) 2.95, and (d) 7. Scan rate, 100 mV/s. (Erdurak-Kilic, Uslu, Dogan, Ozkan, and Coskun, 2006)

In another case with non-modified working electrode, a glassy carbon electrode together with square wave anodic stripping voltammetry measured accurately the known commercial drink (Ly, Chae, Jung, Jung, Lee, and Lee, 2004). A Pt bare electrode was used for assessing AA concentration in commercial fruit juice by cyclic voltammetry (Pisoschi, Danet, and Kalinowski, 2008). The fabrication of a platinum microelectrode and its application as amperometric sensor for mapping AA profiles in slices of an orange was reported (Thiago, Denise, Lowinsohn, and Bertotti, 2006). And finally, the use of pencil lead as a working electrode for AA with cyclic voltammetry

and the determination of vitamin C in commercial orange juice was successful (King, Friend, and Kariuki, 2010).

A variety of working electrodes with a chemical modification has been reported for sensitive AA quantification. An example is the amperometric determination of ascorbic acid in fresh fruit juice, vegetable extracts and dissolved pharmaceutical preparations using nickel hexacyanoferrate (NiHCNF) film modified aluminum electrode (Pournaghi-Azar, Razmi-Nerbin, and Hafezi, 2001). Gold nanoparticles embedded in a layer of polymer on the surface of glassy carbon electrode and were used for joint determination of dopamine and AA in human blood serum samples (Gopalan, Lee, Manesh, Santhosh, Kima, and Kang, 2007). Ferritin protein molecules immobilized on a single-walled carbon nanotubes electrode were reported as catalytic for the electrochemical oxidation of AA (Dechakiatkrai, Chen, Lynam, Shin, Phanichphant, and Wallace, 2008). The fixation of multi-walled carbon nanotubes on to a basal plane pyrolytic electrode gave sensors that determined AA in tablets and fruit juice (Goh, Tan, Lim, and Maamon, 2008). In addition, an amperometric AA determination was reported which used the modification of the conductive surface of screen-printed carbon electrodes with *o*-aminophenol films as electrocatalyst modification (Civit, Nassef, Fragoso, and Sullivan, 2008). The modified electrode showed an increased detection sensitivity.

## 2.5 Total antioxidant capacity (TAC)

### 2.5.1 The principle of free radicals and antioxidants

Free radicals are atoms or groups of atoms with an odd (unpaired) number of electrons and can be formed when, for instance, oxygen interacts with certain molecules. Reactive free radicals play an important role in food and chemical material degradation and contribute also to many disorders in humans. Free radicals can induce oxidative damage to biomolecules. This damage (oxidative stress) has been associated with ageing and several human pathologies such as cancer, atherosclerosis, rheumatoid arthritis and other diseases (Mahadik, and Mukherjee, 1996; Mehlhorn, and Cole, 1985). Inside the body, free radicals can appear as side product of normal metabolic processes and they may be formed by white blood cells, which use them as a weapon to kill disease-causing infection elements in the body. They can also be generated by oxidation of unsaturated fats such as those found in the brain and other parts of the body.

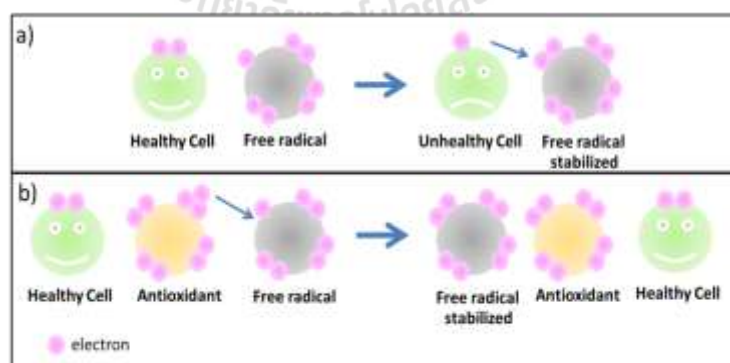


**Figure 2.12** Schematic cartoon of chemical attack of a healthy cell by a free radical a) and the protective action of a free radical scavenger by antioxidant b).

Free radicals are lacking an electron and because of their unpaired electron they are very unstable and thus extremely reactive. Free radical want to uptake an electron from another molecule to stabilize itself, and in doing so, create a new free radical. This new unstable molecule starts the search all over again for another target to get an electron from. A chain reaction develops causing repeated damage to healthy cells, if there were the partner for the oxidative electron exchange (Figure 2.12 a). First attacked may be the cell membrane and its protein and lipid and then the DNA of the cell. When there is an antioxidant molecule available (Figure 2.12 b) the free radical will bypass the damaging reaction with cellular tissue and take the missing electron from the antioxidant to become neutralized. Presence of antioxidant in the body thus helps to avoid damage to a healthy cell.

Some of the environmental risks of exposure to free radicals are hard x-rays, strong ultraviolet light, chemical toxins in the air and water and nuclear radiation. Cigarette smoking and crack able dietary fats and oils are other common sources of free radicals. Table 2.2 shows some example of free radical that has been formed in the human body fluid.

Antioxidants significantly delay or prevent the oxidation of easily oxidizable substrates and thus are beneficial and should be ingredients of the daily diet. Plants contain high concentrations of numerous redox-active antioxidants, such as polyphenols, carotenoids, tocopherols, glutathione, ascorbic acid and enzymes with antioxidant activity. After uptake into the body action of all these antioxidants helps to fight against hazardous oxidative cell and tissue damage (Birlouez-Aragon, and Tessier, 2003). The intake of food rich in  $\alpha$ -tocopherols,  $\beta$ -carotene and ascorbic acid has thus been associated with reduced oxidative-stress related diseases (Correa,

Malcom, Schmidt, Fontham, Ruiz, Bravo, Bravo, Zarama, and Realpe, 1998). Phenolic acids, polyphenols and flavonoids scavenge free radicals such as peroxide, hydroperoxide or lipid peroxy, thus inhibiting the oxidative mechanism that lead to degenerative diseases. Figure 2.13 shows the structure of some antioxidants (Kilmartin, Honglei, and Waterhouse, 2001 and Maisuthisakul, Pongsawatmanit, and Gordon, 2007).

**Table 2.2** Some examples of free radicals.

Free radical name	Abbreviation
Hydroxyl radical	$\text{OH}\cdot$
Hydroperoxyl radical	$\text{HOO}\cdot$
Alkyl radical	$\text{R}\cdot$
Alkoxy radical	$\text{RO}\cdot$
Alkylperoxy radical	$\text{ROO}\cdot$
Glutathyl radical	$\text{GS}\cdot$
Methyl radical	$\cdot\text{CH}_3$
Nitric oxide radical	$\cdot\text{NO}$
Nitrogen dioxide radical	$\cdot\text{NO}_2$

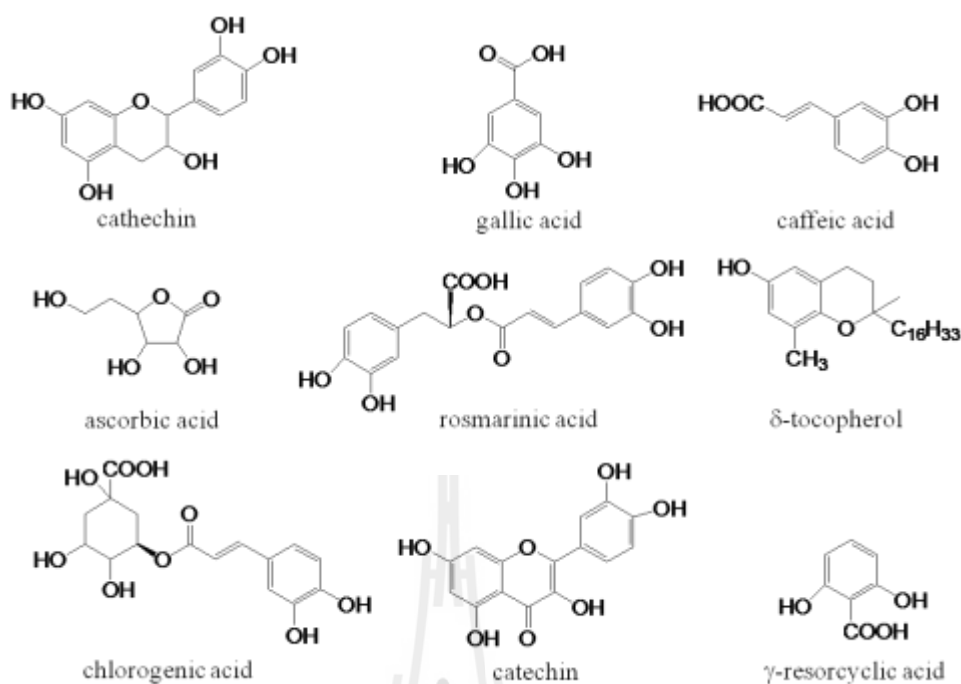


**Figure 2.13** Chemical structures of some common antioxidants.

### 2.5.2 Known methods for total antioxidant measurements

The role of antioxidant as beneficial food ingredient is prominent and many methods for the determination of antioxidant activity in food samples and biological fluids have been proposed during the past decade. Most commonly because of their ease, speed and sensitivity are those involving chromogen compounds of a radical oxygen and nitrogen species. After, chromogen-antioxidant reaction, the residual concentration of chromogen compound is determined by spectrophotometry or colorimetry and the value related to the antioxidant level. The most often used chromogen compounds include 2,2-Vazino-bis(3-ethylbenzthiazoline)-6-sulfonic acid (ABTS), 2,2-diphenyl-1-picrylhydrazyl (DPPH), ferric reducing antioxidant power (FRAP) and oxygen radical absorption capacity (ORAC). The DPPH molecule is

popular because it reacts directly and rapidly with antioxidant compounds. The DPPH free radical reaction with an antioxidant (AH) follows the schematic in Figure 2.14.

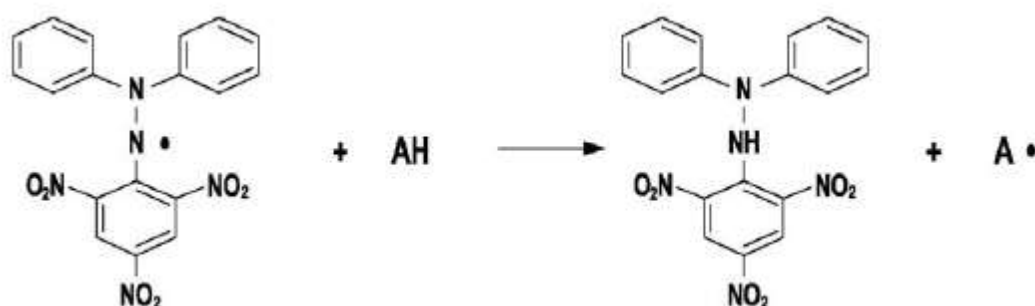


**Figure 2.14** Reaction of DPPH radical with an antioxidant (AH). (Pisoschi, Cheregi, and Danet, 2009).

As clear from Figure 2.14, any substance that can donate a hydrogen atom to dissolved DPPH• can act as antioxidant and reduce the free radical concentration and change the color of solution from violet (DPPH•) to pale yellow (DPPH). The remaining radical form of DPPH absorbs in the visible range and spectroscopic analysis is possible via measurements of the color intensity at a wave length of 517 nm. The basis of this method was introduced more than 50 years ago by Marsden Blois, working at Stanford University (Blois, 1958).

The original Blois method has been modified, optimized and applied by several successors. Brand-Williams, Curerlier, and Berset (1994) for instance, used the spectroscopic method and checked the mechanism of twenty antioxidant compounds with the DPPH radical. Ascorbic acid, isoascorbic acid and isoeugenol reacted quickly with the DPPH radical. Rosmarinic acid and s-

tocopherol reacted a little slower and reached at steady state within 30 min. Caffeic acid, gentisic acid and gallic acid showed the highest antioxidant activity with a stoichiometry of 4 to 6 for reduced DPPH· molecules per antioxidant. Molyneux, (2003) suggested that an analysis of the antioxidant efficiency of samples with DPPH· assay should consider the properties of the reaction vessel, the solvent and pH, reagent concentration, and reaction time when analyzing the calibration curves. Sanchez-Moreno, (2002) introduced two methods, which they called the “TRAP” (Total Radical-Trapping Antioxidant Parameter) and the “ORAC” (Oxygen-Radical Absorbance Capacity) method and used to evaluate the free radical scavenging activity in foods and biological system. Total antioxidant capacity measurement using the DPPH radical together with spectrophotometry at an absorbance of about 517 nm were applied for screening and evaluation of solutions of in several pure compounds and more complex matrices such as plants, herbals, fruits, beverages and pharmaceutical drugs. For example: Krings, and Berger, (2001) evaluated the antioxidant activity of roasted wheat germ and roasted press cake and the antioxidant capacity of 27 fruit pulps from Singapore markets were investigated by Leong and Shui (2002). An automatic method for AA quantification based on multi-syringe flow injection analysis was developed for the determination of the total antioxidant capacity expressed as vitamin C equivalent antioxidant capacity of wines, juices and tea which (Magalhaes, Segundo, Reis and Lima, 2006). In Thailand, recently the “Flow Innovation- Research for Science and Technology” (FIRST) group at Mahidol University in Bangkok (Chan-Eama, Teerasong, Damwan, Nacapricha, and Chaisuksant, 2011; Amatongchai, Laosing, Chailapakul, and Nacapricha, 2012) used a microfluidic system as automatic system for high throughput screening of total antioxidant capacity



and total phenolic compound contents. The method was actually applied to the analysis of Thai vegetables, herbs, and fruits.

### **2.5.3 Electrochemical determination of total antioxidant capacity**

Electrochemical estimation of total antioxidant capacity has been reported by Chevion and colleague as suitable for human plasma and blood sample (Chevion, Berry, Kitrossky, and Kohen, 1997). Milardovic, Iveković, Rumenjak, and Grabarić (2005) used a biamperometric scheme for measuring antioxidant activity of artificial and real samples that contained either non-phenolic (ascorbic acid, uric acid, gallic acid and N-acetyl-L-cysteine and L-glutathione) or phenolic (caffeic acid, ferulic acid, sinapic acid catechin hydrate and quercetin) antioxidant. They also studied real samples in form of beverage, and related them to Trolox equivalent (TE) that were measured using amperometric (Milardovic et al., 2005). Cosio, Buratti, Mannino, and Benedetti (2006) suggested the antioxidant activity measurements of herb methanolic extracts such as rose-mary, sage, oregano, brasil and peppermint via a flow injection (FI) system with an electrochemical detector, which was a glassy carbon working electrode were operated amperometrically at a potential of 0.5 V for analyzing the DPPH·/DPPH redox couple. Recently, Pisoschi and colleagues assessed the total antioxidant capacity by a biamperometry method, using DPPH·/DPPH and Trolox as an indicator and reference artificial antioxidant, respectively. Real samples such as mature fruit juice and soft drink were analyzed via biamperometry and obtained results were in good agreement with spectrophotometric data (Pisoschi et al., 2009).

If not used in combination with complex flow-through systems, CV, DPV and SWV analysis of electroactive species is manually carried out in beaker-type electrochemical cells, which in repetitive, time-consuming and mind-numbing manner

have to be cleaned and refilled with fresh supporting electrolyte in between individual antioxidant measurements. The principle drawbacks of manual analysis are avoidable by using a non-manual automated approach for electroanalysis. This objective was approached by development of automated (robotic) quantitative voltammetry for detection and quantification of antioxidant species. Thus the first part of this work was a focus of this work with an eye on easy and convenient for total antioxidant capacity measurement.

#### **2.5.4 High TAC in Thai plants, tea infusion and fresh fruit sample**

##### **2.5.4.1 Antioxidants in Thai plants**

Plants are a major source of phenolic compounds, which are synthesized as secondary metabolites during normal development in response to stress conditions, such as wounding and UV radiation. The phenolic compounds and their antioxidant properties present in no fewer than 3000 plant species including some Thai plants have been studied (Chanwitheesuk, Teerawutgulrag and Rakariyatham, 2005; Maisuthisakul, Pasuk, and Ritthiruangdej, 2008; Nanasombat, and Teckchuen, 2009; Maisuthisakul et al., 2007). Thai plant sources have been studied as sources of phenolic compounds which may be useful because of their antioxidant potential. Table 2.3 present antioxidant contents as measured by the optical DPPH method with wavelength maximum 515 nm in spectrophotometry of some phenolic contents in Thai edible plant extracts and *P. odoratum* (Pak-Paew in common Thai name) has the strongest antioxidant activity. A balance diet with vegetable containing some high phenolic contents will have beneficial health effects. In addition, identified plants with high antioxidant content could be used as a source of drug or could be beneficial as supplement for food.

**Table 2.3** DPPH radical-scavenging activity and total phenolic content of Thai plant extracts. (Nanasombat, and Teckchuen, 2009)

Plant species	common name/Thai name	EC50 (mg extract / mg DPPH) <sup>a</sup> ± SD	Antiradical efficiency (x10 <sup>-5</sup> ) <sup>a</sup> ± SD	Total phenolic content (mg Gallic Acid Equivalents (GAE)/mg dry extract) <sup>a</sup> ± SD	
Acacia	pennata	Thorny tree/ Cha-Om	3,565.70 ± 41.5	28.1 ± 0.3	45.3 ± 5.8
Anethum	graveolens	ดี/ Phak-Chee-Lao	2,297.80 ± 80.4	43.6 ± 1.5	12 ± 0
Cassia	siamea	Cassod Tree/ Khi-Leck	349.9 ± 5.7	285.8 ± 4.7	35.3 ± 5.8
Centella	asiatica	Asiatic pennywort/ Boa-Bok	6080 ± 80.5	16.4 ± 0.2	7.8 ± 1.9
Coccinia	grandis	Ivy gourd/ Tum-Lueng	6,640.20 ± 52.4	15.1 ± 0.1	14.4 ± 1.9
Coriandrum	spp.	Hom-Yae Leaves	1,868.80 ± 62.3	53.6 ± 1.8	13.3 ± 0
Diplazium	esculentum	Paco/ Phak-Good	3,353.20 ± 50.6	29.8 ± 0.04	3.7 ± 2.9
Eryngium	foetidum	Garden parsley/ Phak-Chee-Farang	4,739.70 ± 61.3	21.1 ± 0.3	3.7 ± 2.9
Garcinia	cowa	Cha-Muang	1597.5 ± 99.3	62.7 ± 4	2 ± 0
Lasia	spinosa	Phak-Nam	3,105.60 ± 45.9	32.2 ± 0.5	2 ± 0
Limnophila	aromatica	Rice paddy herb/ Phak- Ka-Yeang	550.5 ± 12.2	181.7 ± 4	42 ± 0
Momordica	charantia	Noni, Indian Mulberry/ Yau	4,230.80 ± 33.8	23.6 ± 0.2	3.7 ± 2.9
Morinda	citrifolia	Bitter cucumber/ Ma-Ra-Khi-Nok	990.5 ± 26.1	101 ± 2.8	0.3 ± 2.9
Ocimum	americanum	Lemon basil/ Meang-Luck Leaves	1,817.30 ± 61.3	55.1 ± 1.8	25.3 ± 5.8
Ocimum	gratissimum	Tree basil, Shrubby basil / Yee-Ra	3,321.90 ± 54.9	30 ± 0.5	14.4 ± 1.9
Polygonum	odoratum	Vietnamese coriander/ Phak-Paew	315.4 ± 18.8	317.9 ± 19.5	52 ± 0
Sesbania	grandiflora	Vegetable Humming Bird/ Kae	13,425.90 ± 97	7.4 ± 0.1	12 ± 0
Sesbania	javanica	Sesbania flower/ Sa-No	2,265.60 ± 83	49 ± 1.9	2 ± 0
Spilanthes	acmella	Para cress/ Phak-Krad Leaves	4,963.70 ± 79.9	20.2 ± 0.3	18.7 ± 2.9
Tillacora	triandra	Bamboo grass/ Ya-Nang	3,903.90 ± 32.9	25.6 ± 0.2	13.3 ± 0
α-tocopherol	vitamin E		322.4 ± 0.6	310.9 ± 0.4	b

<sup>a</sup>Data are mean of three replications <sup>b</sup>not determined

#### 2.5.4.2 Antioxidants content in tea and herbal infusion

Tea is one of the most consumed beverage in the world and it has been popular over 4000 years. Tea leaves are considered to be important sources of polyphenols. More than 35% of their dry weight may be polyphenol (Liebert, Licht, and BÖhm, 1999). Green tea contains predominantly flavanols, flavandiols and phenolic acid like gallic acid, cumaric acid or caffeic acid. Several studies report for the presence and the activity of antioxidants in green tea with prepared under different conditions. (Atoui, Mansouri, Boskou, and Kefalas, 2005; Henning, Fajardo-Lira, Lee and Youssefian, 2003; Bancirava, 2010).

*Moringa oleifera* Lam. (drumstick tree, horseradish tree) is an original plant in Thailand and often cultivated in hedges and home yards. The tree is valued mainly for the tender pods, which are esteemed as a vegetable. Flowers and young leaves are also eaten as vegetables or used as tea infusion and the blending dried leaves

pharmaceutical capsules. Figure 2.15 shows the Moringa tree and illustrate selected applications. A paste of the leaves is used as an external application for wounds. Moreover, the leaves are a rich source of several classes of flavonoids which is common antioxidant and essential amino acids such as methionine, cystine, tryptophan, and lysine with a high content of proteins (Siddhuraju, and Becker, 2003) (Sreelatha, and Padma, 2009).



**Figure 2.15** a) Moringa tree, b) Dried moringa tea, and c) Dried moringa capsule.

The other fascinating herb containing high antioxidant are roses which are used as edible flowers for centuries, either in the fresh form or in processed products, such as confectionary and beverages (Vinokur, Rodov, Reznick, Goldman, Horev, Umiel, and Friedman, 2006). In particular, the tea of rose flowers (*Rosa damascene*)

was reported to the strongest antioxidant activity among the 30 medicinal plant teas tested (VanderJagt, Ghattas, VanderJagt, Crossey, and Glew, 2002). The antioxidant activity of water extracts of rose flowers were reported to contain a lot of phenolic compounds. (Youwei, Jinlian, Zhao, and Yonghong, 2008). Figure 2.16 shown rose tea: a) and their infusion for drinking: b).

It is one of aims of this Ph.D. thesis to measure the total antioxidant capacity in herbal tea; both (Moringa) and flowers tea (Rose) by an assessment in the robotic electrochemical system.



**Figure 2.16** Rose tea a) and a rose tea infusion b)

#### **2.5.4.3 Antioxidants content in tropical fruits**

Fruits are known to be rich antioxidants such as polyphenols and Vitamin C, Vitamin A, B, and E and carotenoids. Several studies have been conducted to confirm the presence and the activity of antioxidants in tropical fruits in

e.g. China, Singapore and Malaysia (Leong, and Shui, 2002; Yan, Teng, and Jhi, 2006 and Lim, Lim, and Tee, 2007).

Guava (*Psidium guajava* L.) Papaya (*Carica Papaya* L.) and Kumquat or small orange seedless (*Citrus Japonica* Thunb) fruits have been investigated in this study because of their rich content of antioxidants. Reference studies are available on individual basis using different analytical methods based on spectroscopy. In a comparison study, guava and papaya had higher primary antioxidant potential than orange (Lim et al., 2007).

## **2.6 Heavy metals analysis**

### **2.6.1 Heavy metal in general**

Heavy metals are elements having atomic weights between 63.5 and 200.6 g/mole, and a specific gravity greater than 5.0. With the rapid development of industrial activities such as metal plating, mining, fertilizer production, tanneries, batteries fabrication and recycling, paper making and pesticide synthesis etc., heavy metals wastewaters are intentionally or unwanted discharged into the environment at a critical rate, especially in developing countries. Unlike a lot of organic contaminants, heavy metals are not biodegradable and tend to accumulate in living organisms. Many heavy metal ions, on the other hand, are known to be toxic or carcinogenic. Toxic heavy metals of particular concern of industrial wastewaters include zinc, copper, nickel, mercury, cadmium, lead and chromium. (Fu, and Wang, 2011)

Zinc is a trace element that corrected level is essential for human health. It is important for the physiological functions of living tissue and regulates many biochemical processes. However, too much zinc can cause eminent health problems,

such as stomach cramps, skin irritations, vomiting, nausea and anemia. (Lai, Moxey, Nowak, Vashum, Bailey, and McEvoy, 2012)

Copper does essential work in animal metabolism. But the excessive ingestion of copper brings about serious toxicological concerns, such as vomiting, cramps, convulsions, or even death. (Long, Peng, and Bradshaw, 2012)

Nickel exceeding its critical level might bring about serious lung and kidney problems aside from gastrointestinal distress, pulmonary fibrosis and skin dermatitis. And it is known that nickel is human carcinogen. (Forgacs, Massányi, Lukac, and Somozy, 2012)

Mercury is a neurotoxin that can cause damage to the central nervous system. High concentrations of mercury cause impairment of pulmonary and kidney function, chest pain and dyspnea. The classic example of mercury poisoning is Minamata Bay. (Bernhoft, 2012)

Cadmium has been classified by U.S. Environmental Protection Agency as a probable human carcinogen. Cadmium exposes human health to severe risks. Chronic exposure of cadmium results in kidney dysfunction and high levels of exposure will result in death. (Lalor, 2008)

Lead can cause central nervous system damage. Lead can also damage the kidney, liver and reproductive system, basic cellular processes and brain functions. The toxic symptoms are anemia, insomnia, headache, dizziness, irritability, weakness of muscles, hallucination and renal damages. (Landrigan, Boffetta, and Apostoli, 2000)

Chromium exists in the aquatic environment mainly in two states: Cr (III) and Cr (VI). In general, Cr (VI) is more toxic than Cr (III). Cr( VI) affects human

physiology, accumulates in the food chain and causes severe health problems ranging from simple skin irritation to lung carcinoma. (Dayan, and Paine, 2001)

**Table 2.4** Permissible limits and health effects of various toxic heavy metals (Sud, Mahajan, and Kaur, 2008).

Metal contaminant	Permissible limits by international bodies ( $\mu\text{g/l}$ )		Health hazards
	WHO	USEPA	
Arsenic	10	50	Carcinogenic, producing liver tumors, skin and gastrointestinal effects
Mercury	01	02	Corrosive to skin, eyes and muscle membrane, dermatitis, anorexia, kidney damage and severe muscle pain
Cadmium	03	05	Carcinogenic, cause lung fibrosis, dyspnea and weight loss
Lead	10	05	Suspected carcinogen, loss of appetite, anemia, muscle and joint pains, diminishing IQ, cause sterility, kidney problem and high blood pressure
Chromium	50	100	Suspected human carcinogen, producing lung tumors, allergic dermatitis
Nickel	-	-	Causes chronic bronchitis, reduced lung function, cancer of lungs and nasal sinus
Zinc	-	-	Causes short-term illness called "metal fume fever" and restlessness
Copper	-	1300	Long term exposure causes irritation of nose, mouth, eyes, headache, stomachache, dizziness, diarrhea

WHO is World Health Organization and USEPA is United States Environmental Protection Agency.

### 2.6.2 The analytical method for the quantitative determination of heavy metal

The widely used analytical methods for the quantitative determination of heavy metals in environmental, pharmaceuticals, foods, agricultural and biological sample are X-ray analysis, inductively coupled plasma atomic emission spectroscopy



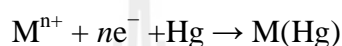
(ICP-AES), atomic absorption spectroscopy (AAS), and also electrochemical methods such as adsorptive stripping voltammetry, and anodic or cathodic stripping voltammetry.

The AAS technique has been accepted as the standard technique for metal determination since it offers satisfactory sensitivity and fairly low acquisition cost. However, a limitation of AAS is that it can measure only one element at a time. Inductively coupled plasma optical emission spectrometry (ICP-OES), on the other hand, offers multi-element analysis, but this technique is not yet extensively used in under developed countries due to their high implementation and maintenance costs. These constraints justify the search for improved methods and suggest that the potential of electrochemical analytical method for metal ions may be worth to be explored.

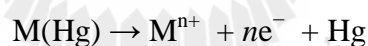
A commonly accepted advantages of electroanalytical methods do the combination of a high sensitivity and selectivity with the chance to simultaneously determined multiple heavy metals with comparatively simple and low cost equipment. Indeed, the electroanalytical technique of stripping voltammetry with adsorptive accumulation has acquired a lot attention for metal ion determination due to outstanding sensitivity and selectivity. (Eshaghi, Khalili, Khazaeifar, and Rounaghi, 2011)

Stripping analysis has two steps that are, a pre-concentration step followed by combined with a stripping or measurement step. During the pre-concentration step, the metal of interest is accumulated onto the working electrode and during the stripping step the collected metal is stripped out into solution. Brief description of the possible modes of stripping voltammetry follow:

- *Anodic stripping voltammetry* (ASV) is the most widely used form of stripping analysis. Usually, the metals are being preconcentrated by cathodic electrodeposition onto the working electrode, which could be a thin mercury or a hanging mercury drop electrode. The preconcentration is done by cathodic reduction of the dissolved metal ion at a controlled time and potential. The deposition potential is usually 0.3–0.5 V more negative than  $E^\circ$  for the least easily reduced metal ion to be determined and the related reaction is:



Assuming amalgam formation of the deposited metal and mercury following the deposition step, and the potential is scanned anodically, linearly, or in a more sensitive way with pulsed waveform, usually square-wave or differential-pulse ramps. During this anodic scan, the amalgamated metals are reoxidized, stripped off of the electrode (in an order that is a function of each metal standard potential):



Usually, the voltammetric peak is proportional to the concentration of the metal in the solution and the peak potential can be used to identify the metal in the sample.

- *Cathodic stripping voltammetry* (CSV) is used to measure a wide range of organic and inorganic compounds, various thiols or penicillins, as well as halide ions, cyanide, and sulfide that are capable of forming insoluble salts with mercury. CSV actually is the mirror image of ASV. In contrast, it involves anodic deposition of the analyte, followed by cathodic stripping in a negative-going potential scan.

- *Adsorptive stripping* (AdS) analysis greatly enhances the scope of stripping measurements toward numerous trace elements and organic compounds (including

cardiac or anticancer drugs, nucleic acids, vitamins, or pesticides). The strategy involves the adsorptive accumulation of the analyte species and then reduction or oxidation of adsorbed material surface. The related current caused by the surface-confined species is directly related to its surface concentration, and this proportion can be used for sensitive quantification. Example of Ads schemes for measuring trace Ni with dimethylglyoxime used as complexing agent or chelating agent. (Wang, 2006)

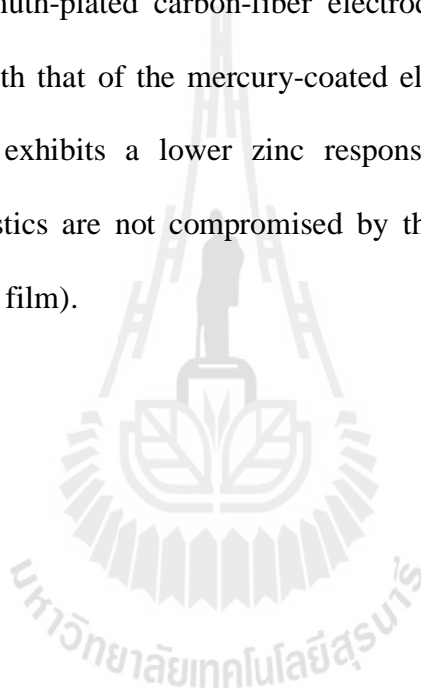
### **2.6.3 Introduction to Bismuth-film electrode, an alternative way to mercury-film electrode**

Historically, the mercury drop electrode was used for stripping voltammetry analysis (Economou, 1997). In the past then, mercury-film electrodes, prepared by coating a suitable substrate with a thin “film” of metallic mercury, replaced the drop electrode and proved to be valuable tools for electroanalysis in the reductive potential regime, especially for anodic stripping analysis and adsorptive stripping analysis. The greatest drawback of mercury-film electrodes, which is becoming increasingly significant in our environmentally conscious world, is the extreme toxicity of mercury and the mercury salts employed for the preparation of mercury-film electrodes. As a result, electrode materials that can replace mercury were continually sought.

In about 2000, a new type of electrode, the Bismuth-film electrode (BFE), was proposed as an alternative to mercury-film electrodes. Bismuth-film electrode are prepared by plating a thin bismuth, rather than mercury, film on a suitable substrate material. The most significant advantage of BFEs is that they are more environmentally friendly, since the toxicity of bismuth and its salts is negligible. At the same time, the advantageous analytical properties of Bismuth-film electrode in voltammetric analysis are roughly comparable to those of mercury-film electrodes.

They are attribute to the property of bismuth to form fused alloys with heavy metals and the high overpotential for hydrogen evolution since their introduction, Bismuth-film electrode have attracted the attention of the electroanalytical community and several groups are conducting research in this area. (Economou, 2005; Wang, 2005)

Wang, Farias, and Hocevar (2000) reviewed a good example of the attractive stripping performance of the bismuth-film electrode as shown in Figure 2.17. The sensitivity of the bismuth-plated carbon-fiber electrode toward lead and cadmium compares favorably with that of the mercury-coated electrode although the bismuth-based microelectrode exhibits a lower zinc response. In addition the signal-to-background characteristics are not compromised by the use of the bismuth coating (instead of the mercury film).



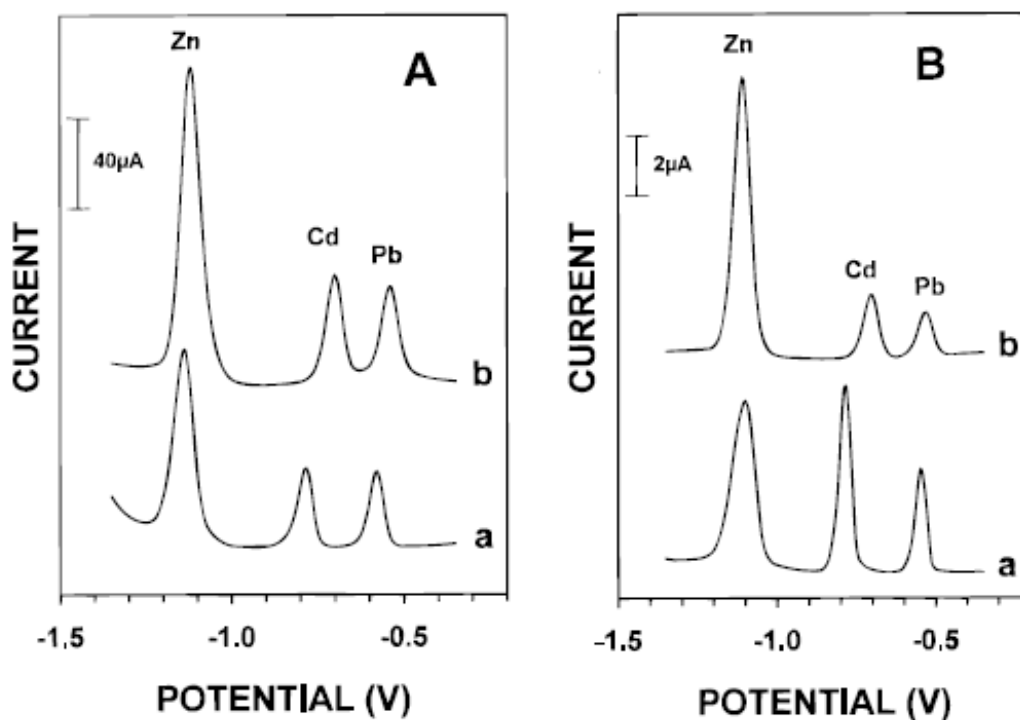
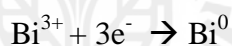


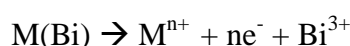
**Figure 2.17** Stripping voltammograms of lead, cadmium, and zinc at glassy-carbon (A), and carbon-fiber (B) electrodes coated with bismuth (a), and mercury (b) films. Solutions, 0.1 M acetate buffer (pH 4.5) containing 50  $\mu\text{g/L}$  lead (II), cadmium (II), and zinc (II), along with 400  $\mu\text{g/L}$  bismuth (a), or 10 mg/L mercury (b). Deposition for 120 s at -1.4 V; “cleaning” for 30 s at +0.3 V. Square-wave voltammetric stripping scan with a frequency of 20 Hz, potential step of 5 mV, and amplitude of 25 mV (Wang et al., 2000).

#### 2.6.4 The principle of anodic stripping voltammetry at bismuth-film electrode (BiFE)

Anodic stripping voltammetry is a voltammetric method for quantitative determination of specific ionic species and usually incorporates these steps. The first step is a cleaning step or conditional step; in this step, the potential is held for a period of time at a more oxidizing potential than the reduction potential of the analyte of interest in order to fully remove it from the electrode (Wang, 2001) (Figure 2.18 a)). In the second step, the deposition step; the Bi film is prepared ex situ (preplate) or in situ (by adding 0.25-1.0 ppm bismuth(III) directly to the sample solution) and keep the potential at a low value (such as -1.4 volt) for about 30 to 900 second. The cathodic potential provides the driving force reduce the analyte and the Bi simultaneously and deposit it on the electrode following this equation (Figure 2.18 b)):



The third and last step involves raising the working electrode potential to a higher values, and carry out stripping (oxidizing) of the analyte (Figure 2.18 c)). As the analyte is oxidized, it gives off electrons which are measured as a current following equation:



As already mentioned, the stripping step can be either linear, staircase, squarewave, or differential pulse voltammetry. More than one ion in sample solution can be analyzed for by stripping technique because of the specification of standard redox potential ( $E^0$ ) of each metal on the potential scale (x-axes). When the applied working electrode

potential at stripping step reaches the metal-metal ion redox potential the metal is stripped from the bismuth-film, and current peaks are observed for the analytes, e.g. zinc (II), cadmium (II) and lead (II), respectively in Figure 2.17 d). The peak potential is a characteristic of the analyte and can be used to identify the metal.

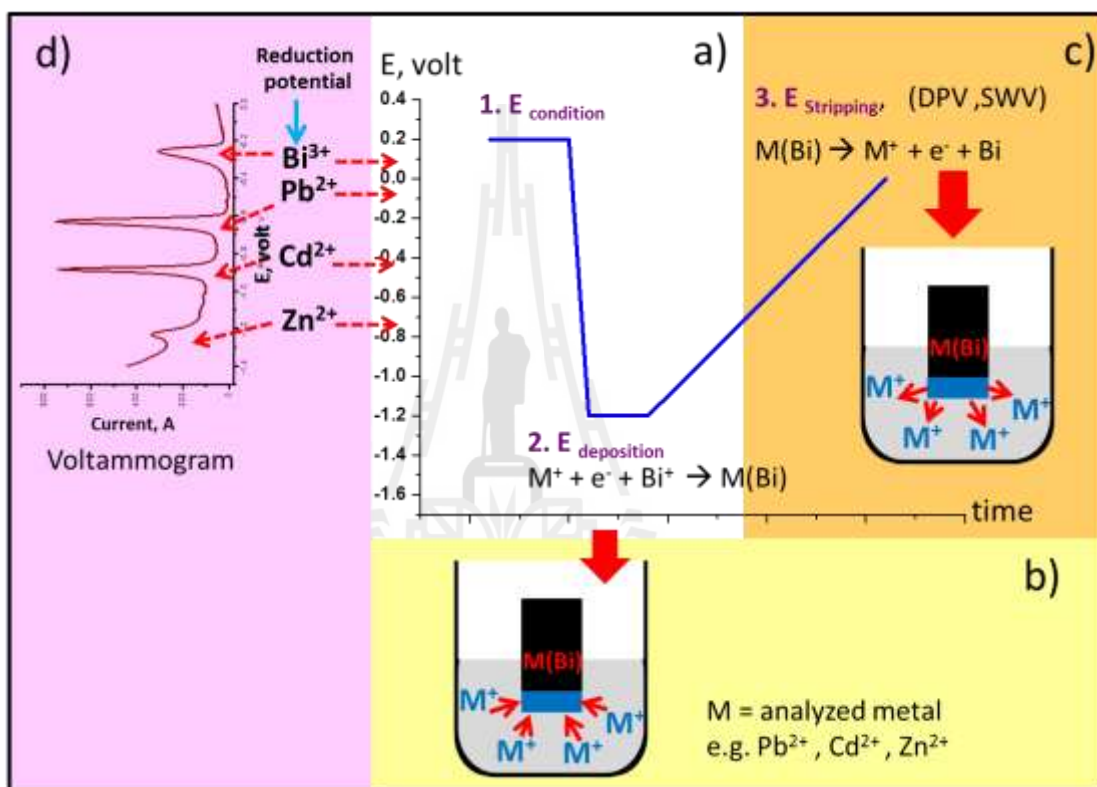


**Figure 2.18** Schematic of representation of the principle of anodic stripping voltammetry at bismuth-film electrodes for the determination  $\text{Pb}(\text{II})$ ,  $\text{Cd}(\text{II})$ , and  $\text{Zn}(\text{II})$ .

### 2.6.5 Applications of bismuth electrodes

Although bismuth electrodes were introduced only 12 years ago, they have already found a wide range of environmental, clinical and food applications. The metal ions so far detected by stripping analysis at Bi electrode include Cd, Pb, Zn, Tl, In and Cu by anodic stripping analysis and Ni, Co and Cr by adsorptive stripping analysis (Table 2.5). In most cases, the methodology of detection is adopted from similar procedures on mercury-film electrodes.

Zn, Cd and Pb have been determined by anodic stripping analysis at trace levels in a variety of environmental samples (e.g., tap water, drinking water and soils), biological fluids (e.g. oral fluid) and food product (Thai herb and vegetable).

**Table 2.5** Selected applications of stripping analysis on Bismuth film electrodes.

Element	Matrix	Technique	Substrate	Reference
Pb, Zn	Tap water	DPASV	Modified Screen-printed carbon	Serrano, Díaz-Cruz Ariño, and Esteban, 2010
Cd, Pb	Soil	SWASV	Modified Carbon paste	Ping, Wu, Ying, Wang, Liu, and Zhang, 2011
Cd, Pb	Soil, wastewater	CCSCP	Screen-printed carbon	Kadara, and Tothill, 2004
Pb, Cd, Zn	Drinking water	SWASV	Modified Screen-printed carbon	Chuanuwatanakul, Dungchai, Chailapakul, and Motomizu, 2008



**Table 2.5** Selected applications of stripping analysis on Bismuth film electrodes

(Continued)

<b>Element</b>	<b>Matrix</b>	<b>Technique</b>	<b>substrate</b>	<b>Reference</b>
Cd, Pb	Certificated river water	SWASV	Silicon	Kokkinos, Economou, Raptis, and Efstathiou, 2008
Cd, Pb	Soil and water sample	CCSCP	Modified screen-printed carbon	Kadara, and Tohill, 2008
Pb, Cd, Zn	Thai herb	SIA-ASV	Screen printed carbon nanotubes	Injang, Noyrod, Siangproh, Duangchai, Motomizu, and Chailapakul, 2010
Pb	Tap-water, Urine, Wine	SWASV	Nafion coated glassy carbon	Kadara, and Tohill, 2004
Cd	Oral (saliva) fluid	SWASV	Modified screen-printed carbon	Khairy, Economou, and Voulgaropoulos, 2010
Cd, Pb	Soil	DPASV	Carbon paste	Cao, Jia, and Wang, 2008
Pb, Cd, Zn	Tap water	SWASV	Carbon pencil rod	Demetrides, Economou, and Voulgaropoulos, 2004
Pb	Soil	CCSCP	Screen printed carbon	Kadara, and Tohill, 2005
Pb, Cd, Zn	vegetables	DPASV	Nafion coated glassy carbon	Xu, Zeng, Huang Xian, and Jin, 2008

Constant Current Stripping Chronopotentiometry: CCSCP

Sequential Injection Analysis Anodic Stripping Voltammetry: SIA-ASV

## 2.7 Pencil leads graphite electrode

### 2.7.1 Concept of pencil leads graphite electrode

Pencil leads or carbon rods (Figure 2.19) can be seen as important electrode materials for the electroanalytical applications due to their availability high electrochemical reactivity, good mechanical rigidity, low cost, simple technology, and ease of modification, renewal and miniaturization. Electrodes made of pencil lead have already been used in many voltammetry studies (Bond, Mahon, Schiewe, and Vicente-Beckett, 1997; Wang, and Kaede, 2001; Gao, Song, and Wu, 2005; Özan, and Şahin, 2010; Ensafi, Rezaei, Amini, and Heydari-Bafrooei, 2012; Dilgin, Kızılkaya Ertek1, Işık, and Dilgin, 2012) and their electrochemical properties were found to be similar to other carbon electrode.



**Figure 2.19** Photograph of a pencil and a boxed pencil leads as used for working electrode preparation.

Figure 2.20, for instance, shows cyclic voltammograms in 2 M  $\text{H}_2\text{SO}_4$  for the oxidation of hexacyanoferrate (II) at five different concentrations using the pencil electrode as working electrode. The peak current is well proportional to the concentration of redox mediator. Though the peak separation is deviating slightly from

the theoretical than 59 mV, the wave shape supports the idea that pencil lead electrode can be analytical for voltammetric application.

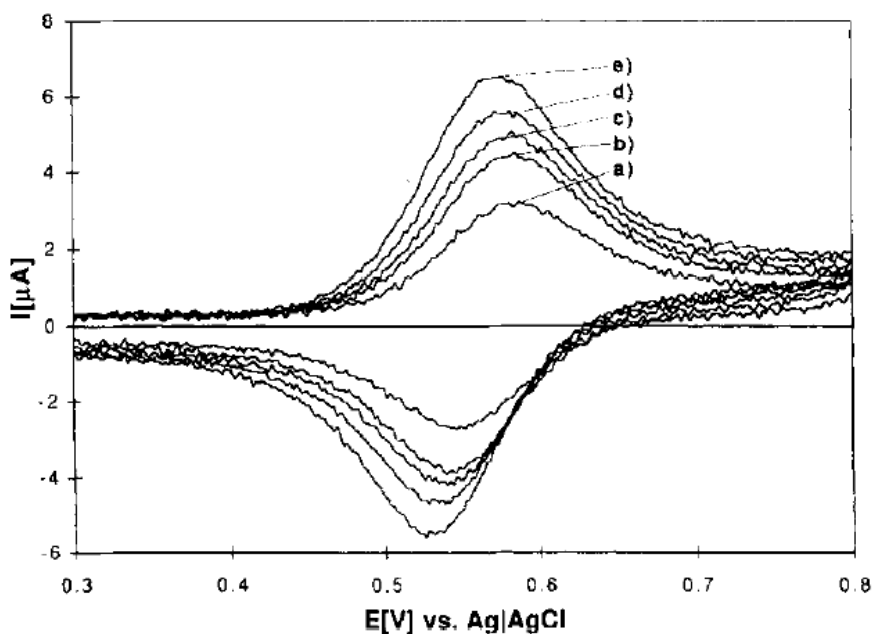


**Figure 2.20** Cyclic voltammograms obtained at a scan rate of  $500 \text{ mV s}^{-1}$  for oxidation of  $\text{K}_4\text{Fe}(\text{CN})_6$  in  $2 \text{ M H}_2\text{SO}_4$  at a pencil electrode.  $\text{K}_4\text{Fe}(\text{CN})_6$  concentrations are (a) 1, (b) 1.43, (c) 1.83, (d) 2.20 and (e) 2.53 mM. (Bond et. al., 1997)

This is further supported by Figure 2.21, which compares cyclic voltammograms for the oxidation of hexacyanoferrate(II) at lead pencil electrode, with the one from a 3 mm diameter glassy carbon electrode, both immersed into the mediator solution. The pencil lead electrode gave about the same result as observed with the glassy carbon electrode. The pencil electrode apparently can be a good choice when compared with for instances high cost electrode for electroanalysis.

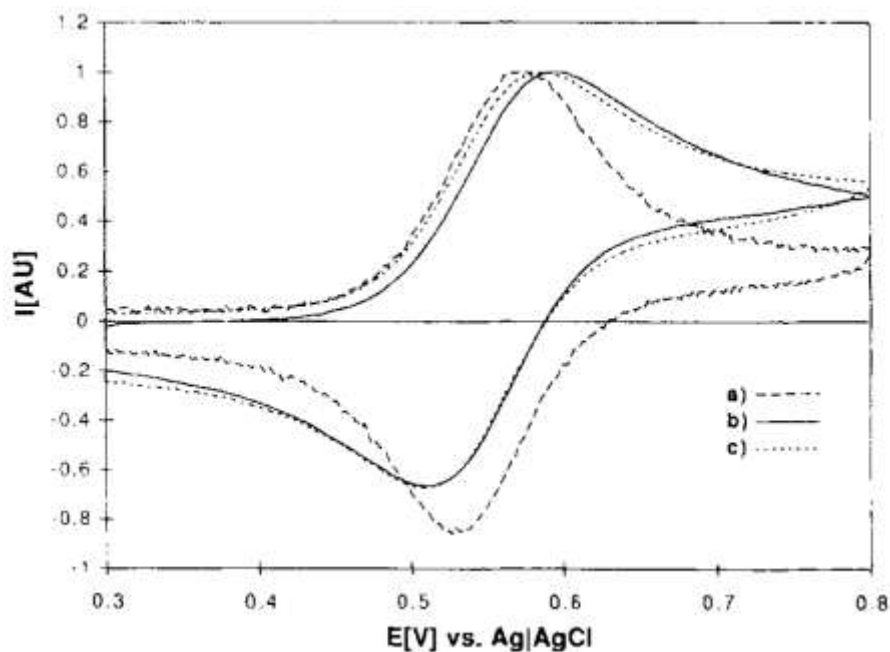


**Figure 2.21** Cyclic voltammograms for oxidation of 2.53 mM  $K_4Fe(CN)_6$  in 2 M  $H_2SO_4$  at (a) 0.5 mm diameter 3H renewable pencil electrode, (b) bare 3H pencil lead (length 20 mm, diameter 0.5 mm) and (c) 3 mm diameter glassy carbon electrode (current values are normalized) (Bond et. al., 1997).

### 2.7.2 Application of pencil leads graphite electrode in electroanalysis

The main positive features of pencil electrode are its good electrical conductivity, functionality, fast and easy pretreatment, low-cost, wide availability and low background current. Accordingly, many researchers used nowadays pencil leads as working electrode for their electrochemical studies. For instance, a pencil lead electrode has been applied to cathodic or anodic stripping voltammetry for the detection of the trace metals Hg, Cd, and Pb in the ng/ml range, (Bond et al., 1997), for DNA hybridization sensing (Wang, and Kaede, 2001), for trace detection of

muscle relaxant drug, Trebibtone (Gao et al., 2004) for the determination of uric acid in urine and blood serum (Özan, and Şahin, 2010), for paracetamol drug analysis in body fluids (Özan, and Şahin, 2011), for DNA-biosensing for detection of a carcinogen, Sudan II (Ensafi et al., 2012) and more recently in 2012, for the investigation of the electrocatalytic oxidation of sulphide (Dilgin et al., 201).

Apparently, the carbon pencil rod electrode works well and is successful when combined with highly sensitive and accurate voltammetric technique such as cyclic, square-wave or differential pulse voltammetry or with the amperometric technique. In the context of this study pencil lead electrodes were thus chosen as sensors for the electroanalysis in the robotic electrochemical device and were meant to be applied for automated ascorbic acid, total antioxidant and trace heavy metals in food, drug and environmental sample, respectively.



# CHAPTER III

## EXPERIMENTAL PART

### 3.1 Materials and Reagents

#### 3.1.1 List of chemicals in alphabetical order

- Acetic acid ( $\text{CH}_3\text{COOH}$ ) (Carlo Erba Réactifs-SdS, Val de Reuil, France),
- Ascorbic acid ( $\text{C}_6\text{H}_8\text{O}_6$ , vitamin C, AA) (Sigma-Aldrich, A.C.S. reagent),
- Bismuth (Bi) standard solution AAS grade 1000 mg/L  $\pm$ 4 mg/L in 5% w/w  $\text{HNO}_3$  (Sigma-Aldrich, Fluka Analytical),
- Cadmium (Cd) standard solution ICP/DCP grade 10147 ppm in 1-2%  $\text{HNO}_3$  (Sigma-Aldrich, Fluka Analytical),
- 1,1-diphenyl-2-picrylhydrazyl (DPPH•) (Sigma-Aldrich),
- Disodium phosphate ( $\text{Na}_2\text{HPO}_4$ ) (Sigma-Aldrich, reagent grade),
- Gallic acid (Acros Organics, New Jersey, USA, 98%),
- Hydrochloric acid (HCl) (Carlo Erba Réactifs-SdS, Val de Reuil, France),
- Lead (Pb) standard solution ICP/DCP grade 10019 ppm in  $\leq$  2%  $\text{HNO}_3$  (Sigma-Aldrich, Fluka Analytical),
- Monosodium phosphate ( $\text{NaH}_2\text{PO}_4$ ) (Sigma-Aldrich, A.C.S. reagent),
- Nitric acid ( $\text{HNO}_3$ ) (Carlo Erba Réactifs-SdS, Val de Reuil, France),
- Potassium chloride (KCl) (Sigma-Aldrich, Steinheim, Germany, laboratory, grade)

- Potassium hexacyanoferrate (III)  $K_3[Fe(CN)_6]$  (Sigma-Aldrich, Steinheim, Germany, laboratory grade),
- Sodium acetate ( $CH_3COONa$ ) (Sigma-Aldrich, Steinheim, Germany, laboratory grade),
- Sulfuric acid ( $H_2SO_4$ ) (Sigma-Aldrich, Steinheim, Germany, 95-97 %, extra pure),
- Trolox (Acros Organics, New Jersey, USA, 97 %), and
- Tocopherol (Sigma-Aldrich, Steinheim, Germany, > 97.0% ( HPLC))

### 3.1.2 Supporting electrolyte

- 0.1 M KCl, for AA measurement,
- 0.1 M Ethanolic phosphate buffer (EPBS) pH 7.4, for TAC measurement, and

For the phosphate buffer solution of pH= 7.4, 1 M stock solutions of  $Na_2HPO_4$  and  $NaH_2PO_4$  were prepared in DI water. To obtain the buffer solution of the desired pH both stock solutions were later mixed in an appropriate ratio. 40% by volume in ethanol were adjusted by the addition of absolute ethanol. Subsequently, KCl was added at a concentration of 0.1 M.

- 0.1 M acetate buffer pH 4.5 containing 0.1 M KCl for heavy metal analysis

Stock solutions of 0.1 mM  $CH_3COOH$  and  $CH_3COONa$  were prepared in Milli-Q water. To obtain the desired pH value both stock solutions were mixed in an appropriate ratio.

### 3.2 Samples screened for their AA and antioxidant contents

#### 3.2.1 AA determination

- Synthetic vitamin C formulation was pharmaceutical vitamin C tablet (Ja Zink+ Vitamin C, 120 mg/tablet, Germany),
- Fresh fruit juice was prepared from the guava fruit (*Psidium guajava* L.). (Local market, Nakhon Ratchasima, Thailand), and
- Thai herbal tea that was inspected was dried Horse radish tree (*Moringa oleifera*) Maroom in Thai language name. (Healthy Snack, Balanzer, Bankanomdee, Nakhon Ratchasima, Thailand)

#### 3.2.2 TAC determination

- Fresh leave of the local Thai vegetable plate; Teaw (*Cratoxylum formosum Dyer*), (Local market, Mukdaharn, Thailand),
- Fresh leave of the local Thai vegetable plate; Phak Paew (*Polygonum odoratum Lour.*) (Local market, Nakhon Ratchasima, Thailand),
- Fresh leave of the local Thai vegetable plate; Kri-Leck (*Cassia siamea*) (Local market, Nakhon Ratchasima, Thailand),
- The Thai herbal tea; Horse radish tree (*Moringa oleifera*) (Healthy Snack, Balanzer Bankanomdee, Nakhon Ratchasima, Thailand); dried in form of tea bag,
- The Thai herbal tea; Rose (*Rosa damascene*) (Changrai, Thailand) ); dried in form of tea bag,
- The Thai herbal tea; Green tea (*Camellia sinensis*). (The Mall department store, Nakhon Ratchasima, Thailand) ); dried in form of tea bag,



- Fresh juice of guava (*Psidium guajava* L.) (Local market, Nakhon Ratchasima, Thailand),
- Fresh juice of papaya (*Carica Papaya* L.) (Local market, Nakhon Ratchasima, Thailand), and
- Fresh juice of kumquat or small seedless orange (*Citrus Japonica* Thunb) (Local market, Nakhon Ratchasima, Thailand).



**Figure 3.1** Photos of samples used for antioxidant capacity screening a) Teaw, b) Phak Paew, c) Kri-Leck, d) Horse radish tea, e) Rose tea, f) Green tea, g) Guava, h) Papaya, and i) Kumquat or small seedless orange.

### **3.3 Environmental sample for lead and cadmium heavy metals analysis**

- Bottled mineral drinking water
- Tap water (NC04 laboratory building, Ruhr University Bochum, Germany)
- Certified wastewater reference material BCR-713 (European Commission, Institute for Reference Material and Measurements (IRRM), Geel, Belgium)
- Soil sample collection (close to battery factory, Suranaree industrial, Nakhon Ratchasima, Thailand)

### **3.4 Instrumentation**

- A commercial robotic electrochemical device (Sensolytics GmbH, Bochum, Germany).

This electrochemical workstation included a potentiostat (PalmSENS, Palm instruments BV, BZ Houten, The Netherlands) and three computer-controlled positioning devices (Linear Measuring Stage, Limes 90, Owis, Staufen, Germany). The whole system was operated via adapted software and a usual personal computer (PC)

- UV-VIS Spectrophotometer (PG Instrument ,T80+),
- Inductively Couple Plasma Mass Spectrometer (ICP-MS, 7500CE, Agilent Technologies, Agilent Technologies (Thailand) Ltd.), The center of scientific and Technological Equipment, Suranaree University of Technology, Nakhon Ratchasima, Thailand,
- Heat gun (1600 W, 60-590 °C, CT-3A, Wahlun electric tools Co., Ltd, China),
- Freezer dry (LABCONCO, Becthai Bangkok Equipment, chemical Co., Ltd.),

- Rotary evaporator (Heating bath B-490, Buchi, Becthai Bangkok Equipment, chemical Co., Ltd.),
- Vacuum pump, (Vac<sup>®</sup> V-500, Buchi Becthai Bangkok Equipment, chemical Co., Ltd.),
- Refrigerator -80 °C (Model 8696, ThermoScientific, Becthai Bangkok Equipment, chemical Co., Ltd.),
- Shaker (MRC, LM-510-2/5, LM-530-2/5, Israel),
- Microwave-assisted proteomic sample preparation (CEM Discover model, CEM, GmbH, Germany),
- DI Water (SG Ultra clear UV, SG water Treatment and regeneration station GmbH, Germany),
- Power supply,
- Micropipet set,
- Blender (Moulinex), and
- Oven (UFB 400, MEMMERT, Becthai Bangkok Equipment, chemical Co., Ltd.).

### **3.5 Consumables**

- 24-well microtiter plates, polystyrene (SPL life science)
- Thin 6-cm-long pencil leads (Pentel High Polymer, 0.9 mm, HB)
- Poly-olefin-based heat shrinking tubes (Salipt S-901 Normal Wall Halogen-Free Flame-Retardant Heat-Shrinkable Tubing, 1 and 0.5 mm diameter before and after heat application, Dongguan Salipt Co., Ltd., Dongguan, China)
- Pipette tips (2 - 1000 µL), polypropylene, (Labcon, Petaluma, CA. U.S.A.)
- Pasteur pipettes (L = 230 mm, glass) (VWR, Darmstadt, Germany)

- 15, 50 mL centrifuge tube (Runlab, Labware Manufacturing, Co., Ltd, China)

### 3.6 Working (WE), Reference (RE) and Counter Electrodes preparation

#### 3.6.1 Miniaturized Working Electrode (WE)

Cylindrical carbon working electrodes was constructed from thin pencil leads 6 cm length. The rod was firmly sealed into thin polymeric heat shrinking tubes so that only 3 mm of the conductive black carbon leads protruded at the bottom to provide the active electrode surface. About 1 cm was left exposed at the top to allow a miniature crocodile clamp to make electrical connection to the potentiostat WE line.

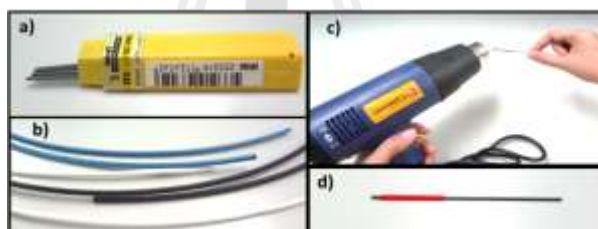


**Figure 3.2** Preparation of miniaturized working electrode for the robotic voltammetric analyzer: a) Pencil lead, b) Heat shrinking tubes, c) Heat gun applying a hot air steam to the carbon pencil lead that was inserted in a heat shrinking tube, and d) The completed carbon pencil lead working electrode.

#### 3.6.2 Miniaturized Reference Electrode (RE)

In order to fabricate a miniaturized Ag/AgCl/3M KCl reference electrode the following materials have been used

- Ag wire (0.5 mm  $\varnothing$ ) (Goodfellow, Cambridge Limited Huntingdon, England),
- Borosilicate Pasteur pipettes,
- Ceramic frit, (Metrohm, Filderstadt, Germany), and
- A mixture of 3 M KCl and 0.1 M HCl (5 mL).

The pasteur pipette was cut at both ends to the desired length approximately 10 cm of the tip and reservoir. A porous ceramic frit was cut to produce a 3-4 mm long cylinder, and then inserted into the narrow end of the pasteur pipette. Heating with a mini-burner torch was used to melt the glass and tightly seal the frit into the pipette.

The Ag wire was coiled to obtain a spiral that could fit into the reservoir of the pasteur pipet. Chloridization of the Ag wire was achieved in an electrolytic setup by immersing the Ag wire spiral together with a Pt wire counter electrode in a mixture of 3 M KCl and 0.1 M HCl. The electrodes were connected to a power supply with the Pt wire acting as the cathode (-) and the Ag wire as the anode (+). The electroprecipitation of AgCl on the Ag wire was initiated by applying a potential of 5 V for about 1 min followed by applying a potential of 10 V for 10 min. During the electrolysis a grey-black deposit formed on the silver wire while H<sub>2</sub> gas appeared at the cathode. After the AgCl formation, the chloridized Ag wire was thoroughly rinsed with deionized water and placed in the pipette which was then filled in 3 M KCl. At the end of the procedure the Ag wire was fixed to the glass cylinder of the pasture pipet by using a modify clay and parafilm.

After fabrication, the miniaturized reference electrode was checked for connection by measuring the potential difference to a commercial Ag/AgCl/ 3 M KCl

reference electrode (Metrohm) using a multimeter. Reference electrodes were only used when the potential difference was insignificant.

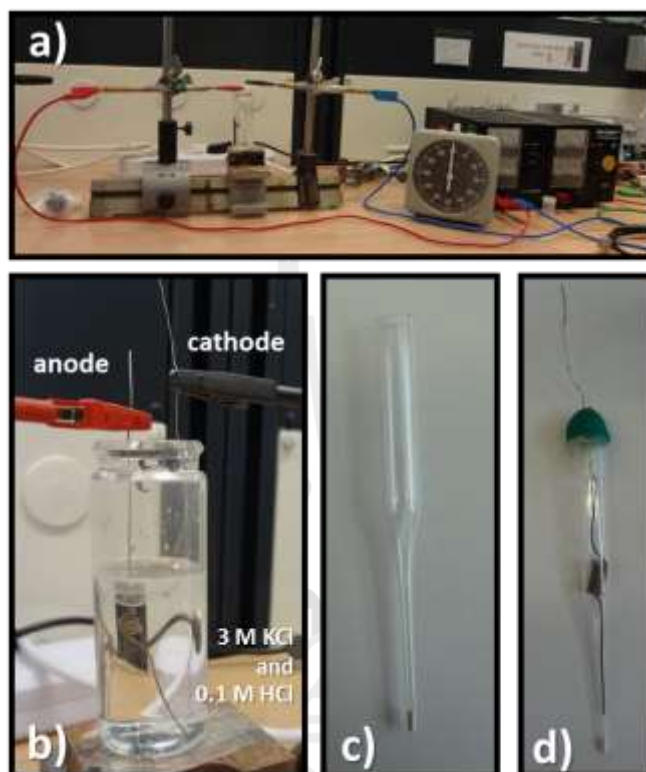


**Figure 3.3** Preparation of a miniaturized Ag/AgCl reference electrode, a) The electrolysis setup, b) The reaction of Ag wire and Ag/AgCl formation at anode (+) and hydrogen gas evolution at the cathode (-), c) tip of electrode with sealed with ceramic frit, d) The completed miniaturized Ag/AgCl reference electrode.

### 3.6.3 Miniaturized Counter Electrode (CE)

A Pt wire (10 cm in length, 0.25 mm  $\varnothing$ , GoodFellow, Cambridge Science Park, England) was coiled to a spiral and soldered to a copper cable wire. Afterward the Pt and cable connection was sealed into a heat shrinking tube.

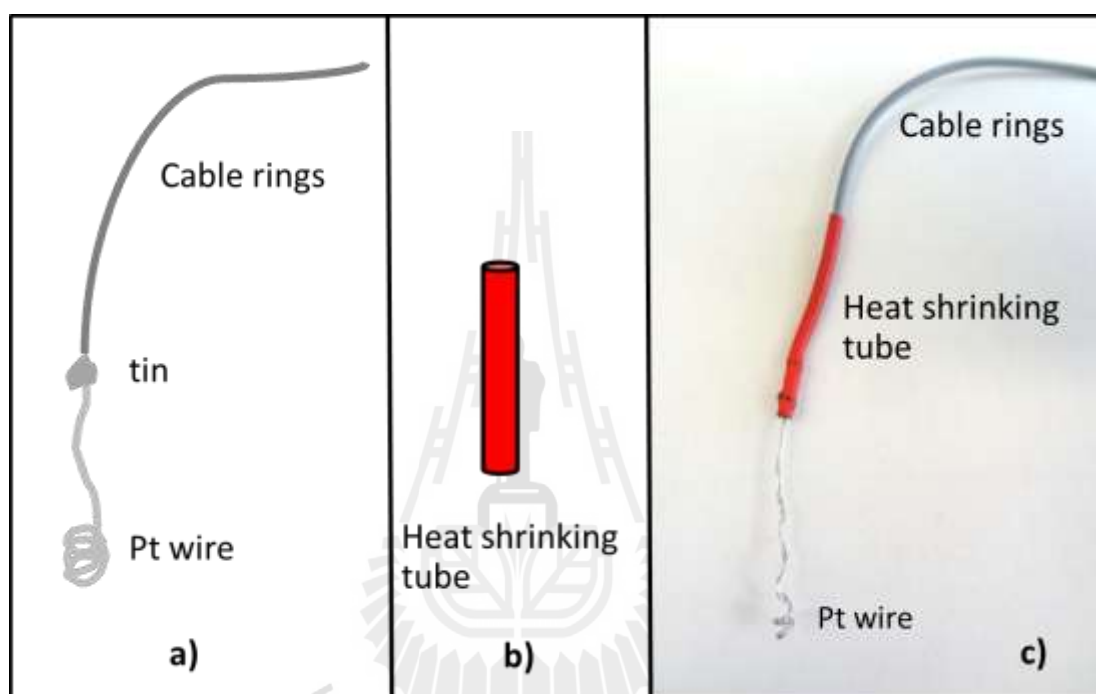


**Figure 3.4** The fabrication of a Pt wire counter electrode. a) coiled Pt wire soldered to a copper cable wire b) heat shrinking tube used to seal the junction Pt/Cu, and c) Photo of the complete counter electrode.

## 3.7 The robotic electrochemical workstation

The hardware and software of the robotic device were purchased from Sensolytics, Bochum, Germany. Three computer-controlled positioning devices enabled precise vertical (z) positioning of an assembly of the WE, CE and RE and horizontal (x/y) movements of a standard 24-well microtiter plate. All electrochemical

experiments were carried out through the operation of a three-electrode electrochemical sensor assembly small enough to be immersed into the microtiter plate well without damage. A PC in combination with tailored Sensolytics software controlled the automatically performed positioning and electrochemical procedures and was used for data acquisition and analysis. Figure 3.5 a) shows the robotic electrochemical system in a photo. The three-electrode assembly with a working, counter, reference electrode incorporated in special holders as shown in Figure 3.5 b). The volume of the analyzed sample depends on the type of the microtiter plate. For the 24-well plate version the sample volumes was about 2.5 mL.

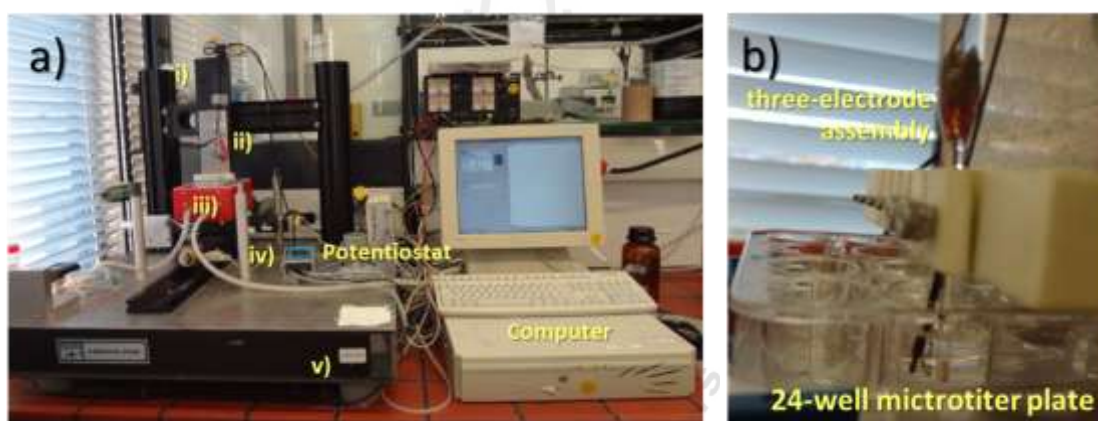


**Figure 3.5** Photo of Robotic electrochemical system: a) i) z-positioning for vertical movement, ii) electrode holder with working electrode, counter electrode, reference electrode; iii) 24-well microtiter plate base, iv) x-, y-positioning for container movement, and v) vibration dampening table. Of note: This instrument was used during a research stay at Ruhr University Bochum, Bochum, Germany for AA and Pb/cd analysis, and b) Three-electrodes fixed to the holders and dipped in a container of the 24-well microtiter plate.



### 3.8 Ascorbic acid analysis

For voltammetric measurements in the robotic device, a three-electrode assembly was used with the above mentioned working, counter, reference electrode incorporated in a solid plastic holder. The volume of the analyzed sample was 2.5 mL for the employed 24-well microtiter plate. All measurements were performed at room temperature using aerated 0.1 M KCl solutions as supporting electrolyte.

#### 3.8.1 Pretreatment of the PLE working electrode

Before each measurement, the pencil lead working electrode was electrochemically pretreated in 0.5 M H<sub>2</sub>SO<sub>4</sub> by applying repetitive CVs within the range 0 to 800 mV and at a scan rate of 100 mV/s, for a total of 50 cycles. The SEM image in Figure 3.6 is showing the surface of pencil lead electrode before a), and after b) pretreatment with sulfuric acid.

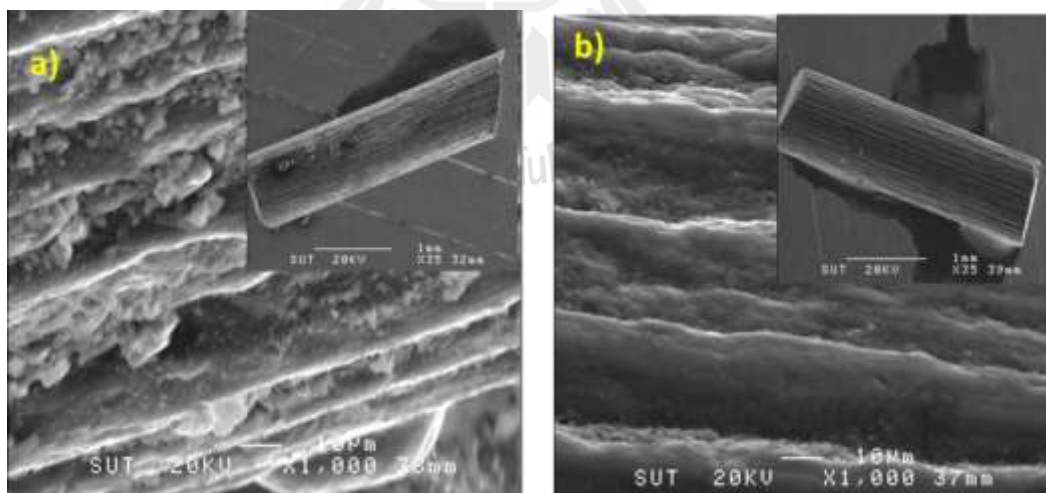


**Figure 3.6** SEM image of a pencil lead electrode before a), and after b) voltammetric pretreatment with 0.5 M H<sub>2</sub>SO<sub>4</sub>.

### **3.8.2 Cyclic voltammograms of AA**

Cyclic voltammetry measurements were conducted with the carbon pencil lead electrode using 1 mM solution of AA in 0.1 M KCl buffer solution and a potential scan from 0 to 1.0 Volt, scan rate 50 mV/s, RE:Ag/AgCl, CE: Pt wire. The experiment was usually carried in a beaker type electrochemical cell.

### **3.8.3 Response stability of the working electrode and degradation resistance of the analyte AA**

Three hour long measurements in 1 mM AA solutions were performed in the DPV and CV mode in a well of a microtiter plate. Both DPV and CV were executed and stored every 15 minutes and the resulting traces compared for judgments on electrode and analyte stability.

### **3.8.4 Linear range and sensitivity of AA**

Robotic differential pulse voltammetry of AA was executed for solutions of increasing AA levels. Calibration curves were constructed by plotting the obtained voltammetric peak current against the adjusted sample concentration in the range 0.2-100 mM AA in 0.1 M KCl buffer solutions. The microtiter plate lead for the calibration trial is shown in Figure 3.7. The robotic run started in 0.5 M H<sub>2</sub>SO<sub>4</sub> with an electrode pretreatment and continue with DI water immersion for rinsing. The software script supported pretreatment of electrodes and rinsing with water in wells A1 to D1 then triggered DPV in the 0.1 M KCl buffer following by another electrode, cleaning in water. This sequence was repeated to address all sample wells with 0.05 mM to 100 mM AA.

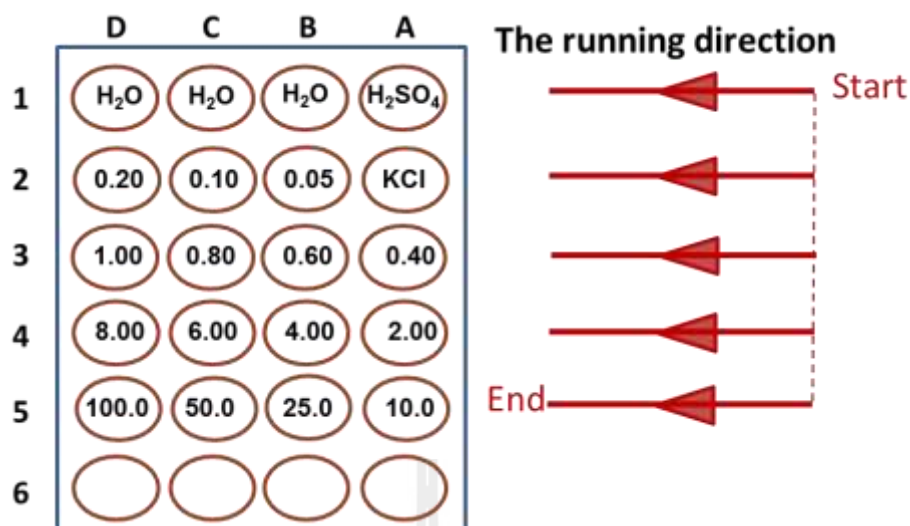


**Figure 3.7** The microtiter plate load for the robotic voltammetric AA calibration trial.

The number in each well is the adjusted AA concentration in mM.

### 3.8.5 AA quantification via normal calibration method

Ascorbic acid solution was prepared in nine different concentrations within the linear range and the volume ranged from 0.2 mM to 5.0 mM DPV measurements were carried out in the calibration solution to get the data for the calibration curve. Then the ten model samples, all equally adjusted to 4 mM, were worked off automatically. The microtiter plate used for run is shown in Figure 3.8. In between DPV measurements always a rinsing treatment via immerse in one of the water wells was carried out.

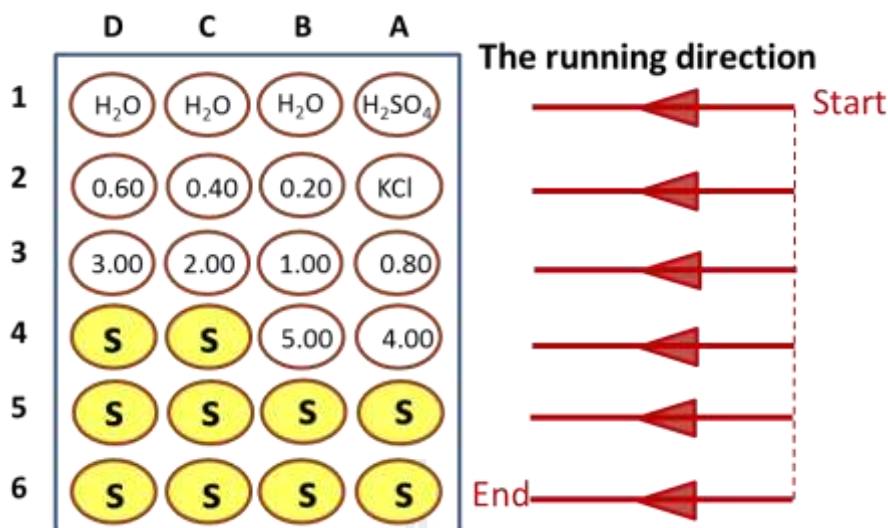


**Figure 3.8** The 24-well microtiter plate load for a AA quantification via the calibration method. Electrolyte buffer was KCl,(A2) 0.02- 5mM AA concentration (B2 to D3), and model standard AA solution, “S”, (A5 to D6) was 4.00 mM AA.

A linear regression line was constructed for a plot of the DPV peak currents as a function of AA concentration. The linear equation of this regression curve was used for the quantification of the analyte. The performance of the procedure could then be assessed by the analysis of synthetic (or 'spiked') model samples. In the latter method, the recovery of a known amount of analyte added to an actual sample matrix is checked. The recovery rates for a determination of AA by the normal calibration method were computed as the following:

$$\text{percent of recovery} = \frac{(\text{experiment values})}{(\text{adjusted values})} \times 100$$

### 3.8.6 AA quantification via standard addition method

For this trial, the AA sample solution “S” was adjusted to 1.00 mM. The model sample was spiked with additions of AA standard solution to raise the concentration by 1, 2 and 3 mM. This allowed the assessment via the standard addition method. The microtiter plate loaded for robotic AA assessments by the triple standard addition method is shown in Figure 3.9 and was as follows: A1, 0.5 M H<sub>2</sub>SO<sub>4</sub> for electrode pretreatment; B1, C,1 and D1, water for electrode rinsing; A2, A3, A4 and A5 (“S”) kept four sample solutions; B2 (C2, D2), B3 (C3, D3), B4 (C4, C5), and B5 (C5, D5), had sample plus 1<sup>st</sup> (2<sup>nd</sup>, 3<sup>rd</sup>) addition of AA stock solution. In one 24-well microtiter plate, one could thus measure a set of four unknown “S” solution via the standard addition method. From plots of the background-corrected peak currents as a function of added AA the sample concentrations were computed as usual for the standard calibration method. To check on the accuracy of the developed assay, recovery rate experiments were performed on sample with a known amount of pure ascorbic acid. The recovery of the added AA was calculated by comparing the concentration obtained from spiked samples with the actual added concentration.

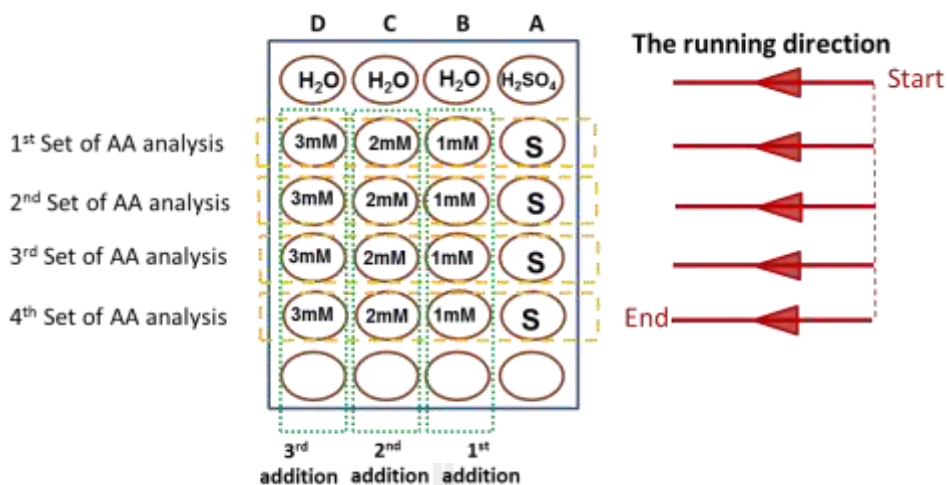


**Figure 3.9** The 24-well microtiter plate load for robotic AA differential pulse voltammetry and analysis via the standard addition method four samples were automatically assessable in one run.

### 3.8.7 AA quantification in real samples

Guava juice, Thai plants tea and a pharmaceutical vitamin C tablet were used in first place as real samples. Their photos of real samples are shown in Figure 3.10.

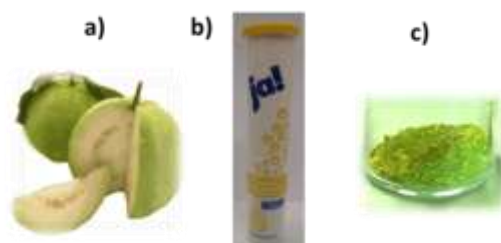


**Figure 3.10** Photos of a Guava fruit, pharmaceutical vitamin C tablet, (Ja Zink+ VitaminC, 120 mg/tablet) and a Thai herbal tea, (Horse radish tree (*Moringa oleifera*)).

*Guava juice:* For this non-juicy fruit, a weighed amount of the edible portion of the fruit was minced and blended with 100 mL water. Then the blend was churned by a mechanical machine for approximately 2 minute. The homogenized sample was filtered through a fine-porous piece of white cloth. The filtrate was kept in a dark bottle and always used at the day of preparation used for measurements.

*Vitamin C tablet (Ja):* An accurately weighed portion of a finely powdered tablet, typically 0.200 g, was dissolved in 100 mL 0.1 M KCl in a volumetric flask. The amount of ascorbic acid was determined by mean of the standard addition method. The value on the label of the commercial product indicated a constant of 120 mg AA per tablet.

*Thai herbal tea:* The water extract of the herbal tea was made by adding 50 mL of hot water (80°C) to 2 g of the plant material and allowing the mixture to stand for 10 min. The mixture was then filtered through filter paper (Whatman, no.1) to remove solid matter and separate the clear tea for the subsequent measurement.

For all the named samples the amount of AA was evaluated by the common standard addition method and a 24-well microtiter plate as shown in Figure 3.9 for robotic differential pulse voltammetry. The AA content was calculated by extracting the peak current from the voltammograms and using the standard addition method for determining the interception at x axes. For each sample, the amount added AA was determined and the degree of recovery was calculated as follows:

$$\text{percent of recovery} = \frac{(\text{experiment values})}{(\text{adjusted values})} \times 100$$

### 3.8.8 Titrimetric AA measurements in real sample as reference

In the chemical titration estimation of AA in various biological materials the two reagents most commonly employed are 2,6 dichloroindophenol (DCIP) and iodine:

#### *2,6 dichloroindophenol (DCIP) titration method (AOAC, 2000)*

The moles of DCIP are equal to the moles of ascorbic acid as shown reaction equation in Figure 3.11. The indophenol solution was standardized by titration with 5 mL of 0.1000 g ascorbic acid in 250 mL water and 2 mL 3 M H<sub>2</sub>SO<sub>4</sub> to the end point (a persistent rosy-pink color had to show up for about 30 seconds). For the sample titration, a certain known volume of the juice was mixed with the 3 M H<sub>2</sub>SO<sub>4</sub> and 20 mL water. Then, it was titrated with the DCIP solution until a pink color appeared that stayed for at least about 30 seconds. Figure 3.11 displays the simple reaction shown behind the AA quantification. Figure 3.12, on the other hand, is a graphic representation of the standard AA a) and sample b) titration with DCIP. All titration experiment were carried out as triplicate measurements, three times. The calculation of the sample content is explained in the Appendix chapter.



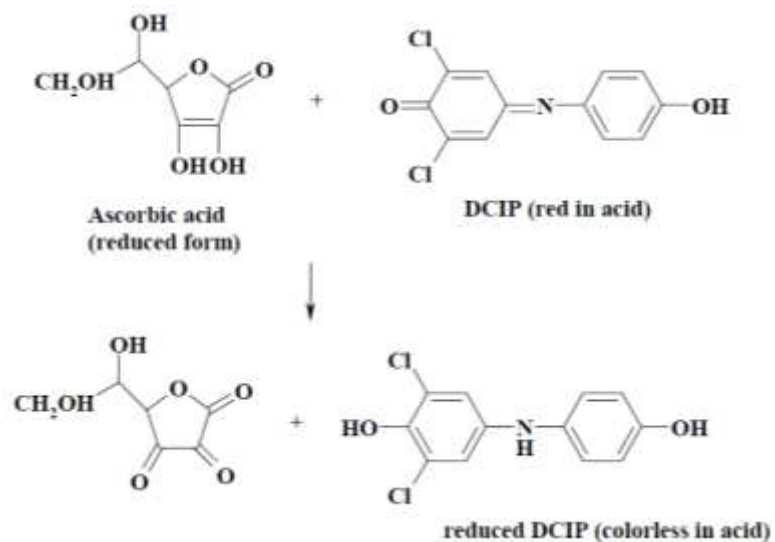


**Figure 3.11** The reaction of AA with DCIP as used for titrimetric measurements for AA analyte. The color change from colorless to light pink indicates complete AA consumption and end pointed establishment.

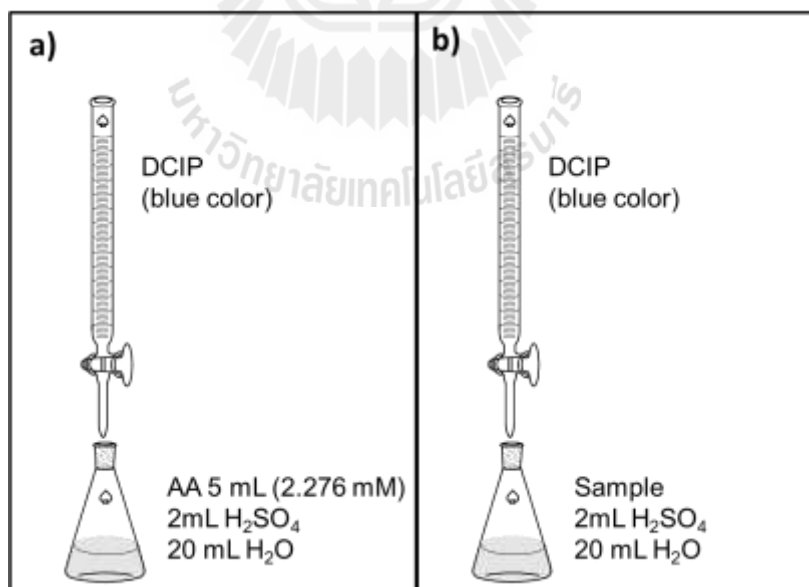


**Figure 3.12** Simple drawing of DCPI-based titration of AA standards a), and for evaluated AA in real sample b).

*Iodometry method (Silva, Simoni, Collins and Volpe, 1999)*

The calibration of the iodine solution was carried out with standardized 0.2 M Na<sub>2</sub>S<sub>2</sub>O<sub>3</sub> solution Figure 3.13 a) is a simple schematic of the back titration and the Iodometry procedure involved the following steps.

1. 10 mL KIO<sub>3</sub> 0.0500 M are pipetted into each of the three 125 mL erlenmeyer flasks used for the triplicate titration.
2. Add 2 g of KI and 10 mL of 0.5 M H<sub>2</sub>SO<sub>4</sub> to the flask and immediately begin the titration with the Na<sub>2</sub>S<sub>2</sub>O<sub>3</sub> solution in the burette.
3. When the titration solution has lost almost all of its color (only a pale yellow remains), add 2 mL of 0.5% w/v starch indicator solution.
4. Continue titration until the blue color of the indicator disappears (colorless endpoint). Repeat for the other 2 flask then calculate the molar concentration of the Na<sub>2</sub>S<sub>2</sub>O<sub>3</sub> following:

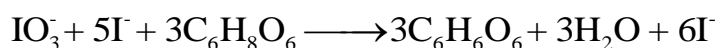


$$\frac{\text{mole S}_2\text{O}_3^{2-}}{\text{mole IO}_3^-} = \frac{6}{1}$$

$$M_{\text{S}_2\text{O}_3^{2-}} = \frac{6M_{\text{IO}_3^-} V_{\text{IO}_3^-}}{V_{\text{S}_2\text{O}_3^{2-}}}$$

### *Determination of ascorbic acid*

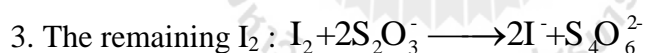
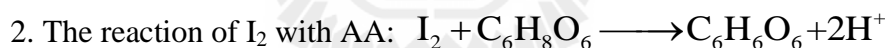
The Iodometry involves an AA redox titration with iodine solution using starch as an indicator. Titrate sample with the thiosulfate solution as done for the calibration of the thiosulfate solution. The overall reaction can be written as



For AA quantification via back titration, consider the reaction of  $\text{IO}_3^-$  with excess  $\text{I}^-$  in acid condition.  $\text{I}_2$  was produced after AA was finished and would not react anymore with  $\text{I}_2$ . Next, the remaining  $\text{I}_2$  in solution was titrated with  $\text{Na}_2\text{S}_2\text{O}_3$  using starch as indicator. At the end point a change from blue to colorless took place. The AA was calculated as follows:



The overall  $\text{I}_2$  production = 3x mole  $\text{KIO}_3$



The remaining  $\text{I}_2 = \frac{1}{2} \times \text{mole Na}_2\text{S}_2\text{O}_3$

Thus, the reaction of  $\text{I}_2$  with AA are (The overall  $\text{I}_2$  production) – (The remaining  $\text{I}_2$ )

The mole of  $\text{I}_2$  reacted with AA are mole of AA. The meaning are (The overall  $\text{I}_2$  production) – (The remaining  $\text{I}_2$ ).

Therefore; Mole AA =  $(3M_{\text{IO}_3^-} V_{\text{IO}_3^-}) - (\frac{1}{2} M_{\text{S}_2\text{O}_3^{2-}} V_{\text{S}_2\text{O}_3^{2-}})$

The simple procedure of iodometry titration method was shown in Figure 3.13 b)

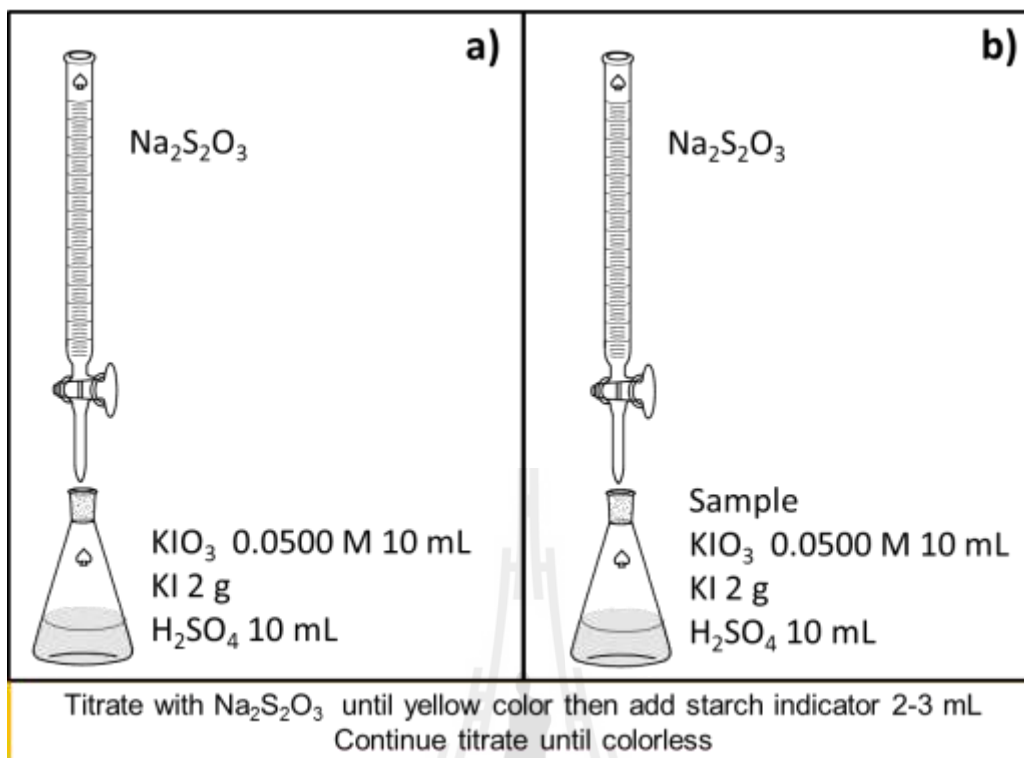


**Figure 3.13** Schematic for, a) Standardization of the Iodine solution, and b) Determination of AA by Iodometry back titration.

### 3.9 Robotic electrochemical DPPH free radical amperometry for evaluation the total antioxidant capacity

#### 3.9.1 CV of the DPPH free radical

The electrochemical characteristics of the DPPH/DPPH• redox couple was gained from CV measurements. The three electrode held together as a assembly were identical in design to the one used for AA analysis in the earlier part. 2.5 mM

in 0.1 M EPBS pH 7.4 was used as electrolyte for the acquisition of the CV in a conventional beaker-type cell. The parameter for the CV measurements were scan range of -100 mV to 600 mV and scan speed of 50 mV/s. The reversible reduction/oxidation of the two species led to nicely symmetrical anodic and cathodic peaks. The cathodic DPPH radical peak potentials and current were used to decide on the working potential for amperometric antioxidant measurement.

### **3.9.2 The reaction of DPPH free radical with Trolox via conventional beaker type amperometry**

From the cyclic voltammetry study, a cathodic working potential of 100 mV was identified as suitable to reduce DPPH• at diffusion-limitation conditions. The current response at this potential was measured for a blank 0.1 M EPBS buffer solution for two minute (current data points sampled every 0.1 second) and for the buffer after sequential additions of 5 mM DPPH• stock solution. The additions brought the level of DPPH• in 10 equal increment from 10  $\mu$ M to 100  $\mu$ M. The amperometric current was recorded and used to construct a calibration curve. After the 10 DPPH• addition, 2.5  $\mu$ M Trolox was added repetitively as model antioxidant to the obtained DPPH• solution. Trolox as antioxidant reacted of course with the DPPH• and reduced its concentration in step-like fashion until the current back to the starting point of 0.1M EPBS buffer. A drawing of the expected (and also experimentally verified) amperometry of DPPH• and its reaction with Trolox is presented in Figure 3.14. It clear that the current for DPPH• reduction decrease with the concentration of added Trolox. Calibration graphs can be plotted as the current response of the working electrode vs concentration of Trolox. Of note, analysis of the raw I/t recording were

processed with Origin software and subjected to a FFT filter smoothing with a point number of 50 before readout.

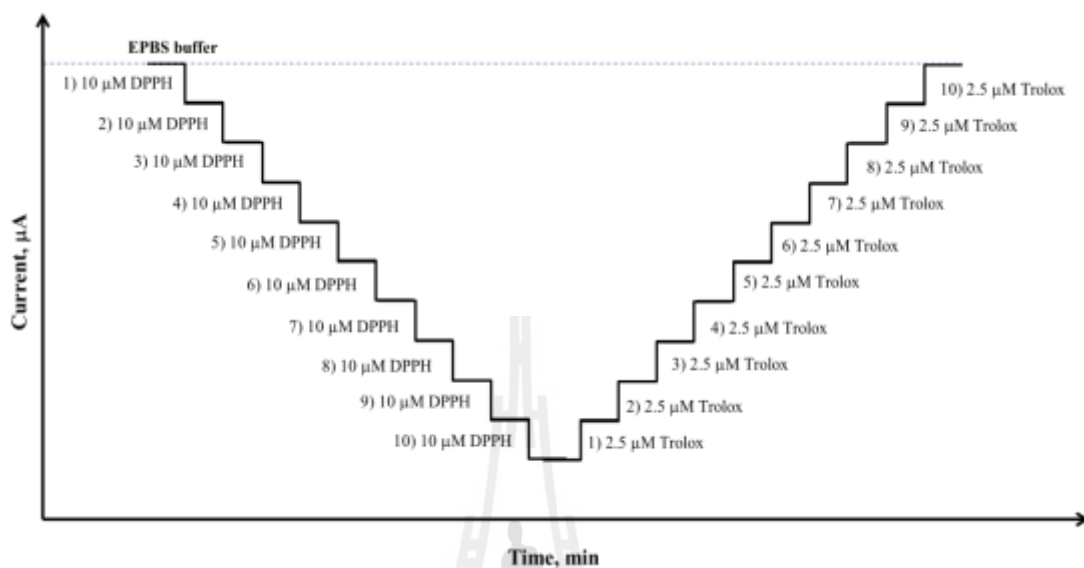


**Figure 3.14** Drawing of the amperometry of DPPH• and its reaction with Trolox, Conditions: PLE working electrode; potential +100 mV vs Ag/AgCl in 0.1 M EPBS.

### 3.9.3 The reaction of DPPH free radical with Trolox assessed via automated amperometry in 24-well microtiter plate format

Figure 3.15 a) is a schematic of the valid 24-well microtiter plate load and the code that have been defined for translation: wells A1-A6 → 1-6, B1-B6 → 7-12, C1-C6 → 13-18, and D1-D6 → 19-24, Figure 6.15 b) informs on the load of the well of the microtiter plate with EPBS, 5 mM DPPH•, and 1 mM Trolox. With this plate layout, the verified DPPH• Trolox amperometry was carried out in robotic manner for automated total antioxidant assessments. Water for periodic electrode dip cleaning was actually in all wells with an odd number. Well #2 was filled with 2 mL of pure EPBS for baseline current recording, well #4 contained 2 mL EPBS spiked

with 100  $\mu\text{L}$  5 mM DPPH• stock solution for the establishment of the initial DPPH• reduction current and the other 10 wells with even numbers had a filling as well #4 but additionally carried Trolox at incrementally increasing concentrations within the range suitable for linearly scaling the Trolox radical scavenging. A freshly loaded microtiter plate was placed on the x, y movable horizontal stage of the robotic device and the electrode assembly was fixed on the designated platform on the z-positioning element; then the system was ready for an automated analytical run. The electrochemical trials used PLE working electrode at an applied potential of + 100 mV vs. Ag/AgCl in 0.1M EPBS with 10 current data points sampled per seconds. The software script for robotic DPPH•/Trolox amperometry is available in the Appendix chapter. Again, for analysis the raw I/t data was processed with Origin software and subjected to a FFT filter smoothing with a point number of 50 before readout and computation of sample levels.

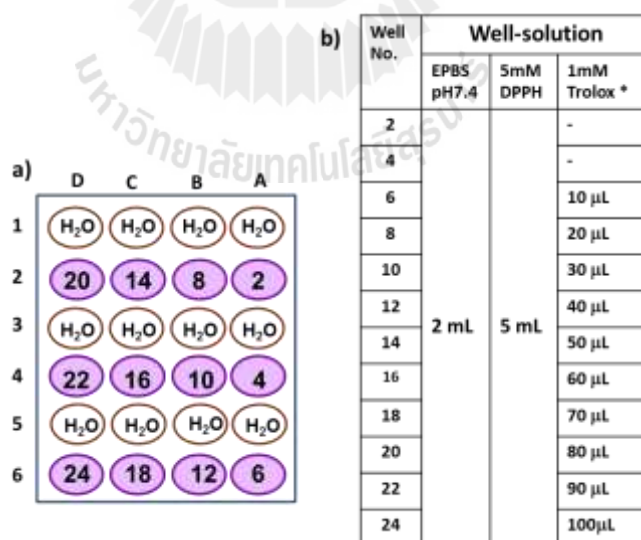


**Figure 3.15** a) Assignment of well number for the 24-well microtiter plate used for Trolox calibration trial, and b) Details of the plate load in the layout for Trolox calibration measurements.

### **3.9.4 A reproducibility test for Trolox quantification via automated amperometry in microtiter plate format**

In the reproducibility test the sample wells #6, #8, #10, #12, #14, #16, #18, #20, #22 and #24 (see Figure 3.15 a)) were all spiked with 250  $\mu\text{M}$  DPPH $\bullet$  and 25  $\mu\text{M}$  Trolox, the quenching reaction allowed to occur and the remaining DPPH $\bullet$  reduction current in the 10 wells was determined in an automated amperometric measuring run. The load of the 24-well microtiter plate is shown in Figure 4.20 b). The experimental conditions and the robotic script commands were listed in section 3.9.3.

### **3.9.5 Automated assessment of the antioxidant activity of standard antioxidants**

1 mM ascorbic acid and gallic acid were dissolved in DI water to get their stock solutions.  $\alpha$ -tocopherol however, was dissolved in absolute ethanol to get the standard solution for antioxidant capacity measurements. The microtiter plate load for Trolox equivalent measurements with the three model antioxidant is detailed in Table 3.1 and was as the following, well #1,3 water fill and well #2 0.5 M  $\text{H}_2\text{SO}_4$  while the wells #4-10, #11-17 and #18-24 were set for the characterization of ascorbic acid, gallic acid and  $\alpha$ -tocopherol, respectively. For the antioxidant capacity determination, the 1<sup>st</sup> (well #4) of the seven available wells for a particular antioxidant kept 2 mL of pure EPBS, the 2<sup>nd</sup> (well #5) was filled with the same solution 2 mL EPBS added 100  $\mu\text{L}$  5 mM DPPH $\bullet$  standard solution, the 3<sup>rd</sup> (well #6), 4<sup>th</sup> (well #7), and 5<sup>th</sup> (well #8) had the same solution the 2<sup>nd</sup> well but supplementation with 1 mM standard solution of the antioxidant (10 (3<sup>rd</sup>), 20 (4<sup>th</sup>) or 30 (5<sup>th</sup>)  $\mu\text{L}$  for the specific wells). The last two wells of each set were further spiked with 10 (6<sup>th</sup> or well #9)) and 20 (7<sup>th</sup> or well #10)  $\mu\text{L}$  of 1 mM Trolox standard solution to evaluate the scavenging



capacity of the model antioxidant in terms of Trolox equivalents. Table 3.1 shows the microtiter plate load for determining the Trolox equivalents of three synthetic antioxidants via robotic DPPH• amperometry. The experimental conditions, robotic script command and analysis raw data were the same as listed in section 3.9.3. All three antioxidants were measured three trial and the average value compared with the literature and/or spectroscopic data.

**Table 3.1** Microtiter plate load for determining the Trolox equivalents of three synthetic antioxidants via robotic DPPH• amperometry

Well-No.			Well-Solution					
			EPBS (mL)	5mM DPPH (μL)	Model Antioxidant			1 mM Trolox (μL)
Well 4-10 1 mM AA (μL)	Well 11-17 1 mM GA (μL)	Well 18-24 1 mM TP (μL)						
4	11	18	2	-	-	-	-	-
5	12	19	2	100	-	-	-	-
6	13	20	2	100	10	10	10	-
7	14	21	2	100	20	20	20	-
8	15	22	2	100	30	30	30	-
9	16	23	2	100	30	30	30	10
10	17	24	2	100	30	30	30	20

### **3.9.6 Automated assessment of the antioxidant activity of real samples.**

#### **3.9.6.1 The preparation fresh fruit juice**

Local kumquats (*Citrus japonica* (Thunb.)), the cherry tomato version of ordinary oranges, were cut into half and squeezed by hand to get the liquid out. Freshly collected juice was kept cold in the fridge in a dark bottle and at the day of preparation used for antioxidant assessments.

Weighed amounts of the edible portions of ripe local guava (*Psidium guajava*) and papaya (*Carica papaya*) fruits were well minced and the resulting puree merged with 100 mL water. The fruit/water blend was then vigorously stirred for 2 minutes before a white cloth filtration of the homogenized pulp separated the solid from the liquid content. The filtrates with the water-soluble antioxidants were kept in a dark bottle in the fridge before and after sample aliquot withdrawal. The juice was used at the day of preparation for measurement.

#### **3.9.6.2 The preparation herbal tea infusion**

To prepare herbal tea extracts for the electrochemical test trials, 1 g of Drumstick (*Moringa oleifera*), Rose tea leaves (*Rosa damascene*) or Green tea leaves (*Camellia sinensis*) were exposed to 50 mL of water that had at first a temperature of 80 °C but cooled throughout the steeping process. After 10 min of brewing the solids were filtered off and the clear teas allowed to reach room temperature. Brews with the water-soluble antioxidants were kept in a dark bottle in the fridge before and after sample aliquot withdrawal. The tea extracts were measured at the day of preparation.

### 3.9.6.3 The process of plant antioxidant extraction

The studied vegetable species were the popular Thai plants Teaw (*Cratoxylum formosum Dyer*), Phak Paew (*Polygonum odoratum Lour.*) and Kri-Leck (*Cassia siamea*). On arrival in the laboratory the leaves of fresh lots from local markets in the north-east, Thailand region were collected and in a safe place air-dried at 30°C over a period of a few days. The obtained dried leaf material was crushed and finely powdered through the impact of the fast rotating blade of a mechanical blender. The final product was kept in sealed plastic bags at room temperature until further processing. For the ethanolic antioxidant extraction, 50 g of an individual plant powder was placed in 1 L 95% ethanol and the mixture shivered for 24 h at ambient temperature. Next, a common vacuum filtration using a Buchner funnel produced a filtrate that was treated in a vacuum rotary evaporator at 40°C for ethanol removal. The crude ethanolic plant extract was freeze-dried with a common laboratory Freeze-dryer and the obtained samples stored at -30 °C until used for analytical trials. A schematic representation of the process of plants antioxidant extraction is shown in Figure 3.16. The percent yield of crude extract from dry leaves was about 7-10% (see Appendix chapter).

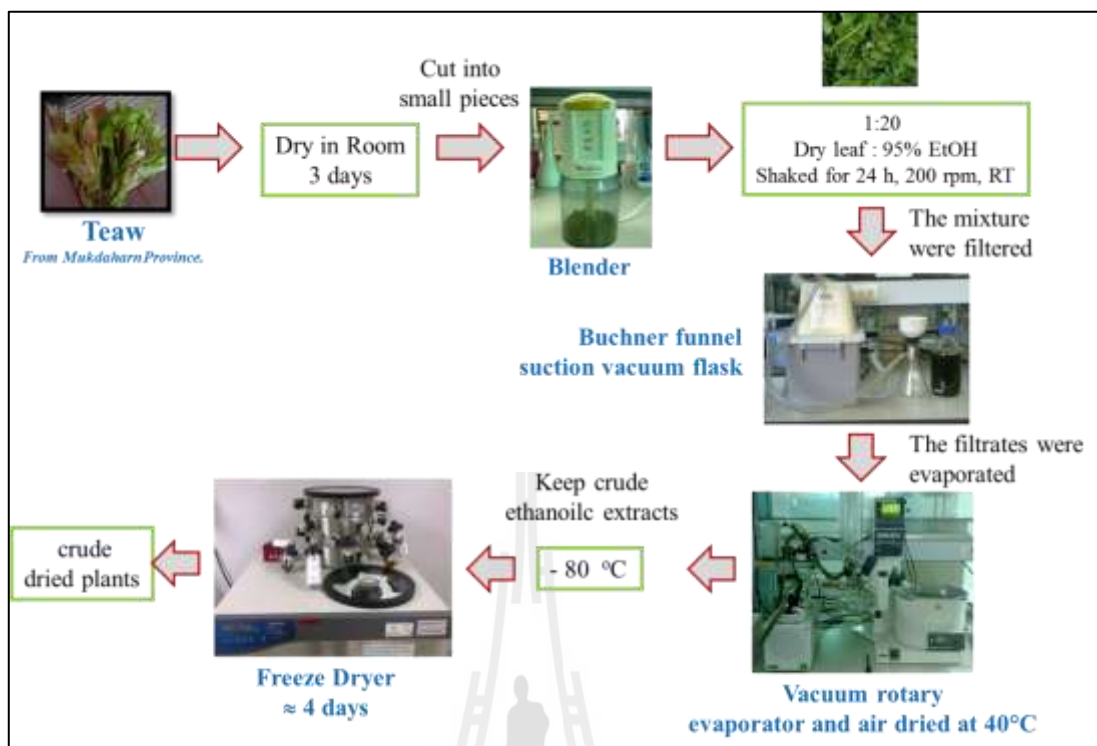


**Figure 3.16** A schematic of the plant extraction for the evaluation of antioxidant capacity in crude extract.

### 3.9.7 Standard spectroscopic reference measurements

DPPH• absorbance (A) measurements were carried out with a UV spectrometer (PG Instrument, T80+), standard 1-cm path length optical cuvettes and a working wavelength of 519 nm, which corresponds to the analytically practical absorbance maximum of the radical antioxidant marker. For the purpose of calibration, plots of particular  $A_{519}$  values as a function of [DPPH•] and [Trolox]) were constructed with the data from measurements on solutions with increasing levels of DPPH•, and a fixed DPPH• level but sequential Trolox model antioxidant additions,

respectively. The antioxidant activity of the studied model and real samples in terms of spectroscopic Trolox equivalents were measured by using solutions with pre-set DPPH• levels as starting point and then by following the decrease in the  $A_{519}$  signal due to radical scavenging in course of additions of small aliquots of the sample and Trolox standards.

### 3.10 Robotic stripping voltammetry for the determination of lead (II) and cadmium (II) at bismuth modified pencil-lead electrode

This part of the thesis was carried out under the guidance of Professor Dr. Wolfgang Schuhmann in Analytische Chemie Electroanalytik & Sensorik, Department of Chemistry and Biochemistry, Ruhr-University Bochum, Bochum, Germany. A standard  $Pb^{2+}/Cd^{2+}$  solution with a concentration 10 mg/L was prepared from commercial stock solutions of the two metal ions by dilution with an appropriate volume of 1%  $HNO_3$ . Table 3.2 shows a chart for the preparation of 10 mg/L Pb (II) and Cd(II) for further analysis.

**Table 3.2** The preparation of Pb (II), Cd(II) and Bi (II) 10.0 mg/L from standard stock solution.

Standard solution	Stock concentration mg/L	Desired concentration mg/L	Desired volume mL	Pipet stock solution, volume $\mu$ L
Bi(III)	1000	10.0	10.0	100
Pb (II)	10019	10.0	5.0	4.99
Cd(II)	10147	10.0	5.0	4.93

### **3.10.1 The effect of Bi solution concentration on Pb (II) and Cd(II) robotic stripping voltammetry**

Wells with different Bi(III) concentration were designed for studying the effect of dissolved Bi(III) levels on stripping voltammetry of Pb(II) and Cd(II). The 24-well microtiter plate load is showing in Table 3.3. The labeling of the 24-well microtiter plate setting is displayed in Figure 3.17, and the sequence of for electrode movement was follow:

1. At A1 well: Electrode rinsing with DI water by 20 times dipping.
2. At A2 well: Electrode was cleaned with 1% HNO<sub>3</sub> via a constant potential at 300 mV for 2 min to remove any remaining analyte metals and bismuth film.
3. At A3 well: Another electrode rinsing with DI water by 20 times dipping.

The parameters for the acquisition of stripping differential pulse voltammograms were as follows: deposition time 120 s deposition under stirring force; deposition potential, -1.4 V; starting potential, -1200 mV; stop potential, 0 mV; pulse height, 25 mV; pulse time, 10 ms; potential step, 5mV and pretreatment potential, -350 mV for 30 s. The working, counter and reference electrode were similar to Section 3.8 and 3.9. The robotic script responsible for the execution of the electrochemical microtiter plate run meant to reveal the effect of the Bi concentration in the measuring buffer on the quality of the Pb/Cd stripping peak. The details of the used data analysis is available in the Appendix chapter.

**Table 3.3** The preparation of Pb(II), Cd(II) and Bi(III) solutions as used for the 24-well microtiter plate analysis via stripping voltammetry.

Well	Volume of	[Bi]	Volume for	[Pb] and	Volume for
	0.1M acetate buffer pH4.5		pipet Bi(III) 10 mg/L	[Cd]	pipet 1 mg/L [Pb] and [Cd]
	$\mu\text{L}$	$\mu\text{g/L}$	$\mu\text{L}$	$\mu\text{g/L}$	$\mu\text{L}$
1, B1	1980	100	20	-	-
2, B2	1950	250	50	-	-
3, B3	1900	500	100	-	-
4, B4	1850	750	150	-	-
5, B5	1800	1000	200	-	-
6, C1	1700	1500	300	-	-
7, C2	1600	2000	400	-	-
8, C3	1900	100	20	20	40, 40
9, C4	1870	250	50	20	40, 40
10, C5	1820	500	100	20	40, 40
11, D1	1770	750	150	20	40, 40
12, D2	1720	1000	200	20	40, 40
13, D3	1620	1500	300	20	40, 40
14, D4	1520	2000	400	20	40, 40

	D	C	B	A
1	11	6	1	H <sub>2</sub> O
2	12	7	2	HNO <sub>3</sub>
3	13	8	3	H <sub>2</sub> O
4	14	9	4	AC
5	15	10	5	AC+Bi
6				

**Figure 3.17** The 24-well microtiter plate labeling for all Pb(II) and Cd(II) robotic stripping voltammetry trial of this study. AC is 0.1 M acetate buffer pH 4.5, Ac+Bi is Bismuth containing buffer.

### 3.10.2 The effect of the deposition time on the quality of Pb(II) and Cd(II) robotic stripping voltammetry

The effect of the deposition time on the quality of the voltammetric Pb/Cd peaks was checked for solution with 20 µg/L Pb(II) and Cd(II) and preconcentration (accumulation) times of 60, 120, 300, 600 and 900 s. The other parameters for the stripping differential pulse voltammetry were similar to the one listed in 3.10.1 p. Table 3.4 presents the details of plate load with the Pb(II), Cd(II) and Bi(III) solution. The script for the robotic DPSVrun is displayed in the Appendix D.



**Table 3.4** The load of a 24-well microtiter plate used for the inspection of the effect of the accumulation time on the quality of the Pb/Cd stripping voltammetry.

Well	Volume of 0.1M acetate buffer pH4.5 $\mu\text{L}$	[Bi] $\mu\text{g/L}$	Volume for pipet Bi(III) 10 $\text{mg/L}$ $\mu\text{L}$	[Pb] and [Cd] $\mu\text{g/L}$	Volume for pipet 1mg/L [Pb] and [Cd] $\mu\text{L}$	<b>Note Deposition time s</b>
1, B1	1740	500	100	40	80, 80	60
2, B2	1740	500	100	40	80, 80	120
3, B3	1740	500	100	40	80, 80	300
4, B4	1740	500	100	40	80, 80	600
5, B5	1740	500	100	40	80, 80	900

### 3.10.3 The robotic calibration curve acquisition for Pb(II) and Cd(II) via robotic differential pulse anodic stripping voltammetry in 24-well microtiter plate format

The calibration curves for the simultaneous determination of Pb(II) and Cd(II) were obtained via robotic DPSV in the 24-well microtiter plate format using in situ Bi film modified PLE for stripping analysis. The parameters used for the calibration trial were: Bi(III) solution concentration, 500  $\mu\text{g/L}$ ; deposition time, 600 s; deposition potential, -1.4 V and 0.1M acetate buffer pH 4.5 as a supporting electrolyte. The load of a microtiter plate with metal ion solution of concentration ranging from 0-200  $\mu\text{g/L}$  is illustrated in Table 3.5. The script for the employed robotic DPSV was provided in the Appendix D.

**Table 3.5** The microtiter plate load for calibration measurements Pb(II) and Cd(II) via robotic stripping voltammetry.

Well	Volume of 0.1 M acetate buffer pH 4.5	[Bi]	Volume of 10 mg/L Bi	[Pb]	Volume of 1 mg/L [Pb]	[Cd]	Volume of 1 mg/L [Cd]
	$\mu\text{L}$	$\mu\text{g/L}$	$\mu\text{L}$	$\mu\text{g/L}$	$\mu\text{L}$	$\mu\text{g/L}$	$\mu\text{L}$
1, B1	1900	500	100	0.25	0.5	0.25	0.5
2, B2	1900	500	100	0.5	1	0.5	1
3, B3	1900	500	100	1	2	1	2
4, B4	1900	500	100	2	4	2	4
5, B5	1900	500	100	4	8	4	8
6, C1	1900	500	100	6	12	6	12
7, C2	1900	500	100	8	16	8	16
8, C3	1900	500	100	10	20	10	20
				[Pb]	Volume of 10 mg/L [Pb]	[Cd]	Volume of 10 mg/L [Cd]
				$\mu\text{g/L}$	$\mu\text{L}$	$\mu\text{g/L}$	$\mu\text{L}$
9, C4	1900	500	100	20	4	20	4
10, C5	1900	500	100	40	8	40	8
11, D1	1900	500	100	60	12	60	12
12, D2	1900	500	100	80	16	80	16
13, D3	1900	500	100	100	20	100	20
14, D4	1900	500	100	150	30	150	30
15, D5	1900	500	100	200	40	200	40

### **3.10.4 The application of robotic differential pulse stripping voltammetry for Pb(II), and Cd(II) measurements in real samples**

Robotic DPSV was used to carry out Pb(II) and Cd(II) measurements in real samples including bottled mineral drinking water, tap water, wastewater certified reference material (CRM713), and soil collected close to an industrial zone. The bottled, tap and waste water were used without any purification, filtration or preconcentration before analysis. However, the collected soil from industrial area was treated with an extraction process.

#### **3.10.4.1 Soil sample extraction**

-Soil collection & physical treatment: the contaminated soil sample was collected at a nearby battery factory in the Suranaree Industrial Zone, Nakhon Ratchasima, Thailand. The soil sample was obtained with a spade from an area about 10-15 cm deep into the ground. The collected soil, actually about 50-100 g, was kept in a plastic box at room temperature before further treatment. 10-20 g of soil was heated in laboratory oven at 80 °C for one hour to remove the residual humidity. Finally, the dried soil was passed through a sieve with a 425  $\mu\text{m}$  stainless steel mesh. Figure 3.18 shows the 425  $\mu\text{m}$  stainless steel mesh sieve and the photos of soil before and after sieving.

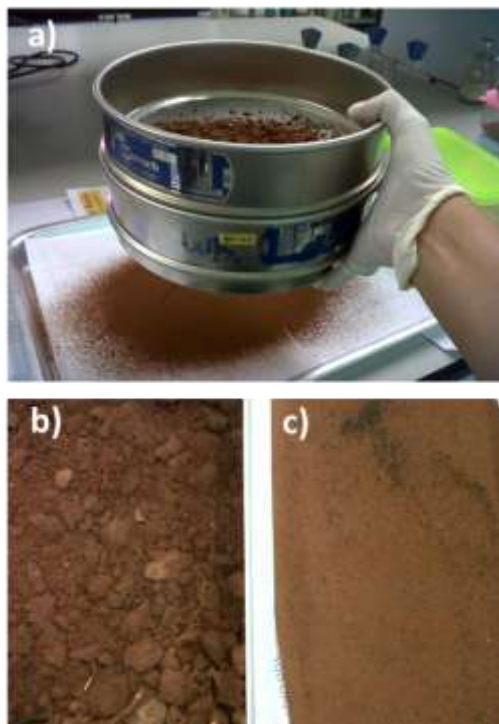


**Figure 3.18** a) 425  $\mu\text{m}$  stainless steel mesh sieve, b) dried soil before sieving and c) dried soil after sieving.

-Soil microwave extraction: the soil sample was treated following EPA Method 3051A by a microwave assisted acid digestion as typically applied to sediments, sludge, soils and oils. The microwave digestion was performed in a CEM microwave oven. In the procedure, the sample to be analyzed needs to be randomly drawn from the well-mix sample of 0.500 g and weighed into a 10 mL microwave digestion vessel. Then 5 mL of freshly prepared  $\text{HNO}_3:\text{HCl}$  (9:3) was added. The samples were digested at 175  $^{\circ}\text{C}$  for 5 min and the solution allowed to cool down to room temperature. After filtration through a Whatman filter paper the filtrate was transferred to a 50 mL volumetric flask and brought to correct volume with deionized water. The

soil extract was stored in a refrigerator until used for robotic DPSV or ICP/MS analysis.

### 3.10.4.2 The loading of the various real samples into 24-well micro titer plates

The standard addition method was chosen for the quantification of Pb(II) and Cd(II) in the 24-well microtiter plate. In a 24 well microtiter plate a set three samples had place in the #1 well of the B, C and D columns. Four additions of standard solution of Pb(II) and Cd(II) could be added into 2<sup>nd</sup>, 3<sup>rd</sup>, 4<sup>th</sup> and 5<sup>th</sup> row of the B, C and D columns of microtiter plate. The corresponding plate layout is illustrated in Figure 3.19.

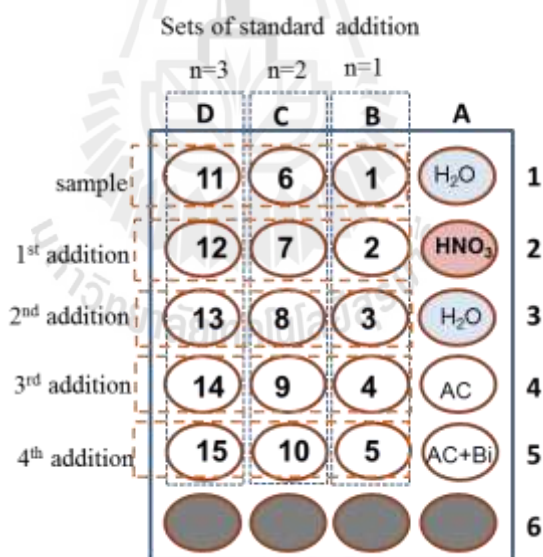


**Figure 3.19** The 24 well microtiter plate layout for automated voltammetric measurement of Pb(II) and Cd(II) in water and soil samples using the standard addition method.

- *Bottled mineral drinking water and tap water*

The well solutions for the analysis of Pb(II) and Cd(II) in bottled mineral drinking water are depicted in Table 3.6. In case of tap water, the plate layout copied the one for the bottled water analysis in Table 3.6. The software script for robotic DPSV in the water samples is provides in the Appendix chapter.

**Table 3.6** Microtiter plate layout for robotic Pb(II) and Cd(II) DPSV analysis.

Well	Volume of 0.1 M acetate buffer pH 4.5	Volume Bi(III) 10 mg/L	[Pb]	Volume of 1 mg/L [Pb]	[Cd]	Volume of 1mg/L [Cd]	Bottled mineral drinking water*
	$\mu\text{L}$	$\mu\text{L}$	$\mu\text{g/L}$	$\mu\text{L}$	$\mu\text{g/L}$	$\mu\text{L}$	$\mu\text{L}$
B1, C1, D1	900	100	-	-	-	-	1000
B2, C2, D2	900	100	20	4	20	4	1000
B3, C3, D3	900	100	30	6	30	6	1000
B4, C4, D4	900	100	40	8	40	8	1000
B5, C5, D5	900	100	50	10	50	10	1000

\* Otherwise by tap water

The microtiter plate layout for the recovery rate inspection with spiked mineral drinking and tap water is shown in Table 3.7.

**Table 3.7** Microtiter plate layout for percent recovery determination of Pb(II) and Cd(II) measurements in a robotic DPSV trial on water sample.

Well	Volume of 0.1 M acetate buffer pH 4.5	Volume Bi(III) 10 mg/L	[Pb]	Volume of 1 mg/L [Pb]	[Cd]	Volume of 1 mg/L [Cd]	Bottled mineral drinking water*
	$\mu\text{L}$	$\mu\text{L}$	$\mu\text{g/L}$	$\mu\text{L}$	$\mu\text{g/L}$	$\mu\text{L}$	$\mu\text{L}$
B1, C1, D1	900	100	20	4	20	4	1000
B2, C2, D2	900	100	30	6	30	6	1000
B3, C3, D3	900	100	40	8	40	8	1000
B4, C4, D4	900	100	50	10	50	10	1000

\*tap water

- Waste water certificated reference material (CRM713)

The microtiter plate load for the measurement of Pb(II) and Cd(II) in certified waste water is illustrated in Table 3.8. The software script for this automated DPSV in this sample is displayed in the Appendix chapter.

- Contaminated soil sample

After treatment of the soil microwave extraction, the soil extract was diluted 20 fold before loading it into the 24 well microtiter plate. Table 3.9 shows the microtiter plate layout for the measurement of Pb(II) and Cd(II) in the soil sample that was expected to be contaminated with at least Pb(II). The software script for robotic DPSV is displayed in the Appendix chapter.

**Table 3.8** The 24 well microtiter plate load for robotic Pb(II) and Cd(II) voltammetry in certified waste water.

Well	Volume of 0.1 M acetate buffer pH 4.5 $\mu\text{L}$	500 $\mu\text{g/L}$ [Bi] Volume of Bi(III) 10 mg/L $\mu\text{L}$	[Pb] $\mu\text{g/L}$	Volume of 1 mg/L [Pb] $\mu\text{L}$	[Cd] $\mu\text{g/L}$	Volume of 1 mg/L [Cd] $\mu\text{L}$	Waste-water CRM $\mu\text{L}$
B1, C1, D1	1500	100	-	-	-	-	400
B2, C2, D2	1492	100	20	4	20	4	400
B3, C3, D3	1488	100	30	6	30	6	400
B4, C4, D4	1484	100	40	8	40	8	400
B5, C5, D5	1480	100	50	10	50	10	400

**Table 3.9** Microtiter plate load for robotic Pb(II) and Cd(II) voltammetry analysis of aqueous soil extracts.

Well	Volume of 0.1 M acetate buffer pH 4.5 $\mu\text{L}$	500 $\mu\text{g/L}$ [Bi] Volume of Bi(III) 10 mg/L $\mu\text{L}$	[Pb] $\mu\text{g/L}$	Volume of 1 mg/L [Pb] $\mu\text{L}$	[Cd] $\mu\text{g/L}$	Volume of 1 mg/L [Cd] $\mu\text{L}$	Volume of soil extract $\mu\text{L}$
B1, C1, D1	1800	100	-	-	-	-	100
B2, C2, D2	1792	100	20	4	20	4	100
B3, C3, D3	1788	100	30	6	30	6	100
B4, C4, D4	1784	100	40	8	40	8	100
B5, C5, D5	1780	100	50	10	50	10	100



## **CHAPTER IV**

### **RESULTS AND DISCUSSIONS**

#### **4.1 Robotic electroanalysis in microtiter plate**

In the problem and identification chapter III, it has been specified that the routine chemical analysis in both industrial and academic laboratories gets problematic when large number of samples have to be solved. The automation of the analytical task was proposed on opportunity to reduce both the cost and the number of tedious manual operations. Presented in this thesis is the integration of conventional difference pulse voltammetry for ascorbic acid analysis, amperometry for total antioxidant capacity measurement and anodic stripping voltammetry for lead and cadmium determination into an electrochemical robotic device that was specially designed for electroanalysis measurements in the microtiter plate format. Details of the instrument, the arrangement of the electrodes and the software for sequential measurement and data storage will be provide and the suitability of the system demonstrated with assessment of model and real sample.

##### **4.1.1 Hardware component of electrochemical robotic system**

The electrochemical robotic system was designed for automatically performing voltammetry in individual compartments of 24-well microtiter plates.

The device is schematically shown in Figure 4.1. Each well of the plate contains solution of 2.0 to 2.5 mL. The user can freely design the outline of the change of the microtiter plate. Well solutions may include DI water for electrode cleaning,  $\text{H}_2\text{SO}_4$  for electrochemical pretreatment of electrodes, then the sample and/or standard solutions in the other wells. The loading of the microtiter plate wells is variable and depends on whether the standard addition method or sensor precalibration is used with voltammetry for analyte quantification.

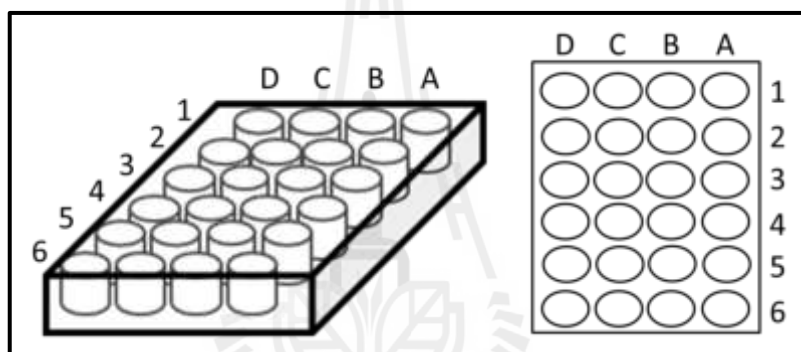


**Figure 4.1** Schematic of a 24-well microtiter-plate.

An assembly of working, counter and reference electrodes had to be used that could easily be positioned in the wells of the microtiter plate for performing automated differential pulse voltammetry, amperometry and anodic stripping voltammetry. Figure 4.2 is a schematic illustration of the holder for the three electrodes with these components already in place. A centered aluminum rod worked as the connector to the Z-positioning device, which had the corresponding adapter available. The counter electrode that was implemented was simply a coiled platinum wire, the reference a

Ag/AgCl wire and the working was a 2 mm long cylindrically carbon pencil lead electrode.

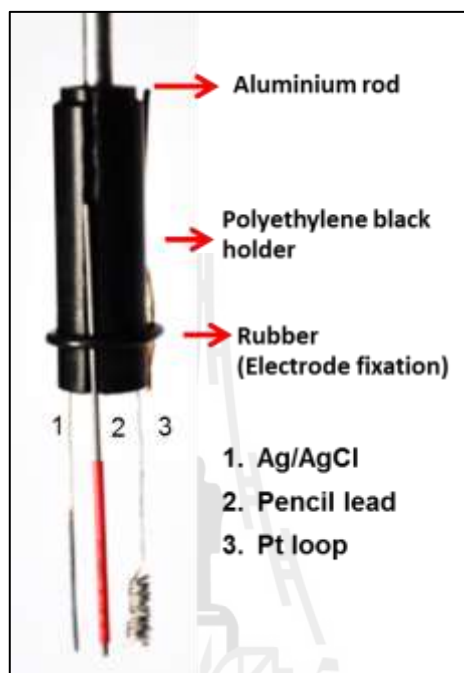


**Figure 4.2** Schematic of the electrode holder forming a three-electrode assembly of a reference electrode (RE), working electrode (WE), and counter electrode (CE): RE is a Ag/AgCl, WE is a carbon pencil rod electrode, and CE is a coiled platinum wire.

The microtiter plate as the solution container, the special electrode holder, the potentiostat and the computer for system are the main components of robotic electrochemical device. A schematic representation and a photograph of the robotic system of this thesis are shown in Figure 4.3.

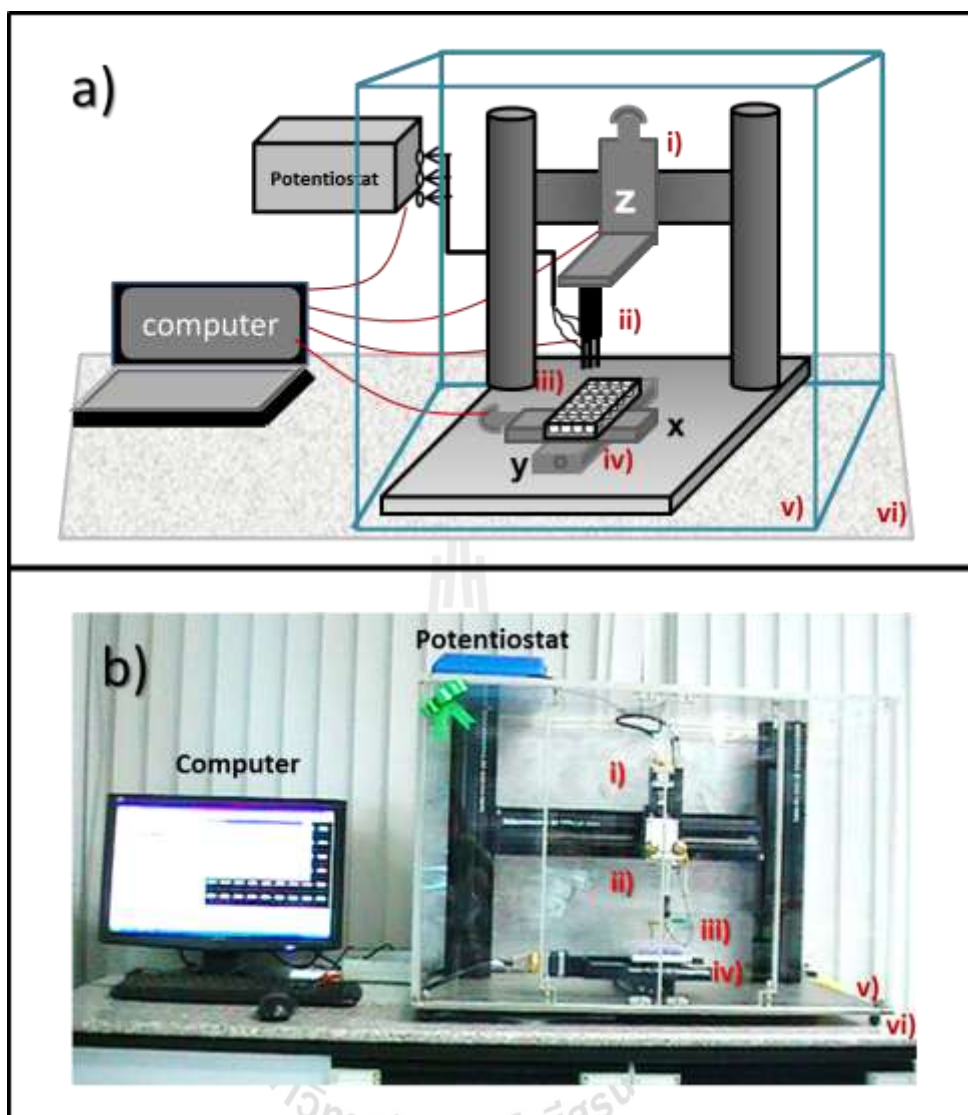


**Figure 4.3** a) Schematic representation of the electrochemical robotic system employed in this thesis: i) z-positioning for vertical movement, ii) electrode holder with working electrode, counter electrode, reference electrode; iii) 24-well microtiter plate format for solution containing, iv) x-, y-positioning for microtiter plate movement, v) faraday cage for electrical noise elimination, and vi) marble vibration dampening table; b) Photograph of instrumentation.

#### 4.1.2 Robotic electroanalysis: General comments on system operation

Key components of the system for robotic electroanalysis are the movable WE/CE/RE assembly that fits into the approximately 2 mL containers of standard 24-well microtiter plates and the three high precision linear stages for the independent movement of the microtiter plate in x and y and the electrodes in the z directions. Software-controlled communication between a personal computer, the positioning devices and the potentiostat was used for sequentially addressing the individual wells of the microtiter plate with the tip of the electrode assembly and, through an appropriate trigger, for timed execution of CV, DPV, SWV or amperometry. Finally, automatic data storage modules save freshly acquired measurement in individual wells in a .dat file that were compatible to software such as MS office or Origin for visualization and analysis. The script of the command interface to the hardware for electrode positioning (z axial), microtiter plate (x, y axial) movement and electrochemical processing was written in a Notepad .txt file, examples of which are added in the Appendix chapter. A brief flowchart of the robotic system operation is represented in Figure 4.4. Firstly, the microtiter plate load had to be defined and the sequence of electrode movement thought out. Then, the script had to be written in a way, that the wells of the microtiter plate was approached with the electrode assembly in right way. Start of a measuring sequence was usually a pretreatment of the working electrode via cyclic voltammetry. The script orders immersing of the electrode assembly into well A1 for pretreatment in H<sub>2</sub>SO<sub>4</sub> via CV. Next, the electrode assembly was move up, and repositioning into well A2. Here, activation of several up and down movements allowed the electrode assembly to be cleaned from H<sub>2</sub>SO<sub>4</sub>, the pretreatment solution. Cleaning in water was followed by

immersion into well A3 with subsequent initiation of e.g. voltammetric or amperometric trace. The sequence of pretreatment, cleaning and measurement was repeated until all sample wells were worked off by voltammetry and amperometry.

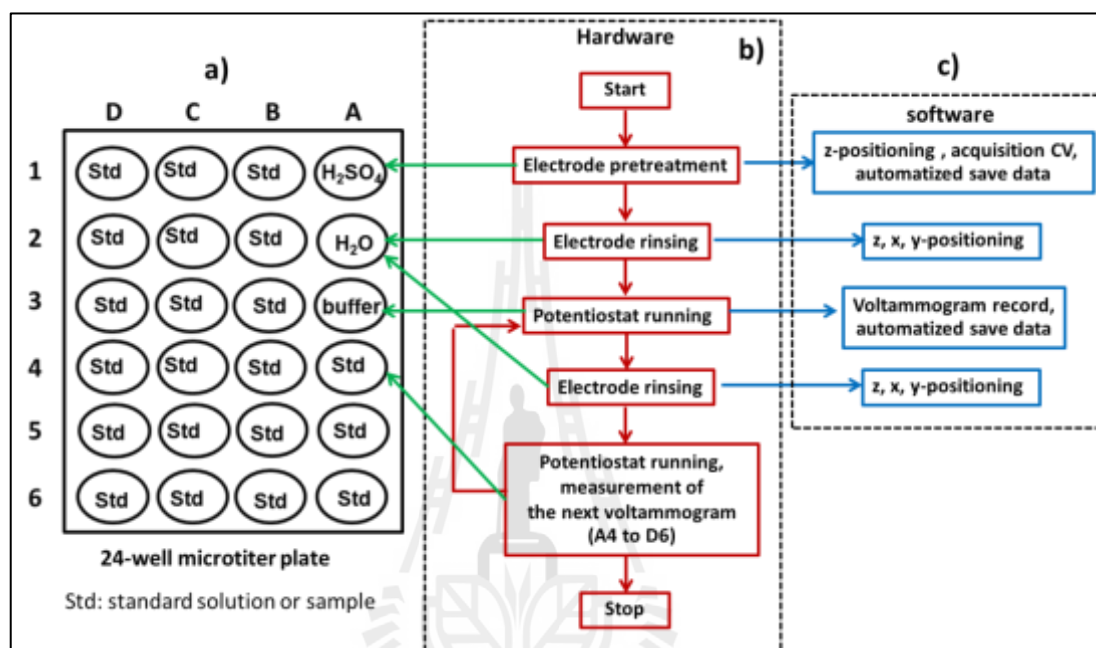


**Figure 4.4** Schematic representation of the robotic electrochemical system; a) a typical microtiter plate load; b) flowchart of a measurement cycle; c) communication between software and hardware execution.

## 4.2 Ascorbic acid analysis (AA)

AA is an electroactive biomolecule that can be oxidized on metal polarized electrodes for instance gold, platinum, glassy carbon disks electrode or carbon fiber and pencil rod electrodes. Before AA was established in the robotic electrochemical system, the electrochemistry in terms of cyclic voltammetry was inspected in

conventional beaker type to gain information about the redox behavior of the employed analyte at the carbon pencil lead working electrode.

#### 4.2.1 Cyclic voltammograms of AA

In terms of voltammetric performance in sequential determinations, ease of access, preparation and use and cost of the starting material, sensors derived from conventional graphite pencil leads were best, and these were used as the standard working electrode throughout a thesis part of this AA robotic voltammetric analysis. Cyclic voltammetric measurements were conducted at the carbon pencil lead using 1 mM solution of AA in 0.1 M KCl. As shown in Figure 4.5 in the positive potential scan direction, a single oxidation peak was observed. The scan actually started at 0 V vs Ag/AgCl, moved into the positive direction to 1.0 V and went back to starting point. The peak of anodic oxidation came up about 0.6 V, but no reduction wave or peak corresponding to the anodic wave was observed on the cathodic range. This can be explained by changes in the protonation of the acid–base functions in the molecule. The oxidation of AA involves two electrons and two protons to produce dehydroascorbic acid (DHAA), which is followed by an irreversible solvation reaction. The irreversibility of the AA oxidation is known in literature (Erdurak-Kilic et al., 2006). The results have confirmed the irreversible and character of the oxidation of AA at a pencil carbon rod electrode and obtained CVs were in full agreement with the literature (Erdurak-Kilic et al., 2006; Ernst and Knoll, 2001; Rueda et al., 1978; Roy et al., 2004).

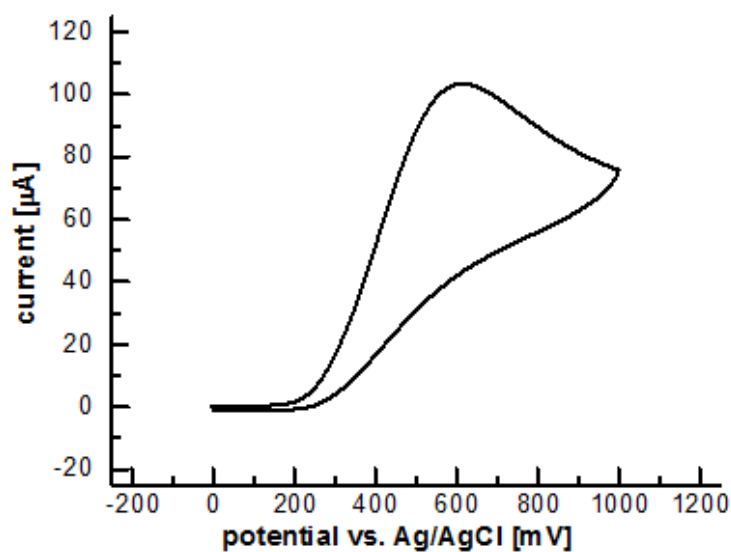


**Figure 4.5** Cyclic voltammogram of 1 mM AA 0.1 M KCl. Condition; 0 to 1.0 V scan rate 50 mV/s; RE:Ag/AgCl; CE: Pt wire; WE: Carbon pencil lead in a beaker type electrochemical cell.

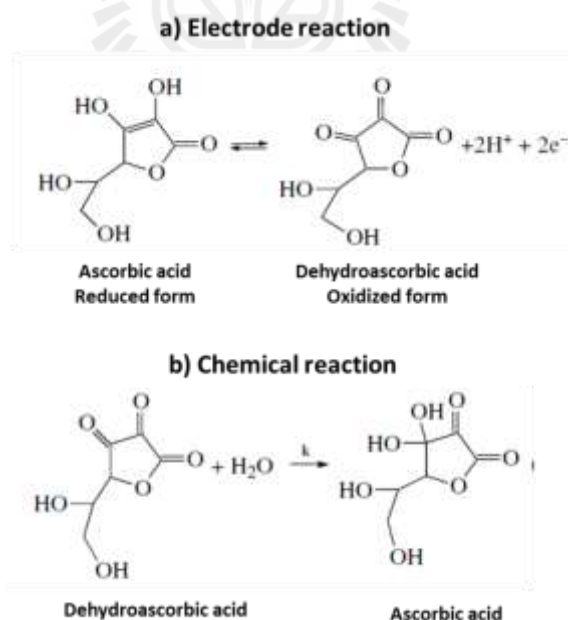


**Figure 4.6** Suggested oxidation mechanism of AA: a) electrode reaction, b) chemical reaction (Erdurak-Kilic et al., 2006).



#### 4.2.2 Signal stability of AA voltammetry

A complete analytical run through a loaded microtiter plate was expected to take time in the order of about 3 hour, depending on the type of trial. It had to be ensured that during this time the response of the pencil lead electrode (PLE) working electrode did not decay in terms of the peak current for the analyte AA. Tests have been performed to inspect the appropriateness of this boundary condition with respect to the stable of the sensor. In Figure 4.7 collections of CVs and DPVs are shown that were recorded with a 3 mm long pencil lead electrode during a 3 h voltammetric trial in a microtiter plate well containing 1 mM AA at intervals of 15 min. Before the first AA measurement took place, the working electrode was pretreated by means of repetitive anodic potential scans in sulfuric acid and subsequently rinsed with water. In the CVs the expected well-expressed maximum at about +0.6V proved the diffusion-controlled oxidation of AA to DHAA while the absence of a clear reduction peak confirmed the known irreversibility of the reaction. The DPVs, on the other hand, produced typical bell-shaped I/E curves with a symmetrical current peak at about 0.4V relative to the reference electrode (Figure 4.7 b). The shapes of the 12 consecutive sets of CVs and DPVs in the AA-containing well were as they should be, and the peak heights for the repeated measurements of the same AA concentration did not vary significantly over a period of 3 h. Thus the obligatory condition for successful robotic voltammetric quantification of AA in the microtiter plate format was fulfilled, since a complete analytical run through the individual wells would not be badly affected by analyte degradation or electrode fouling. Apparently, degradation of the labile analyte and a detrimental coverage of

the working electrode surface with DHAA, the product of the reaction, are not a problem, at least over the 3 h time span investigated.

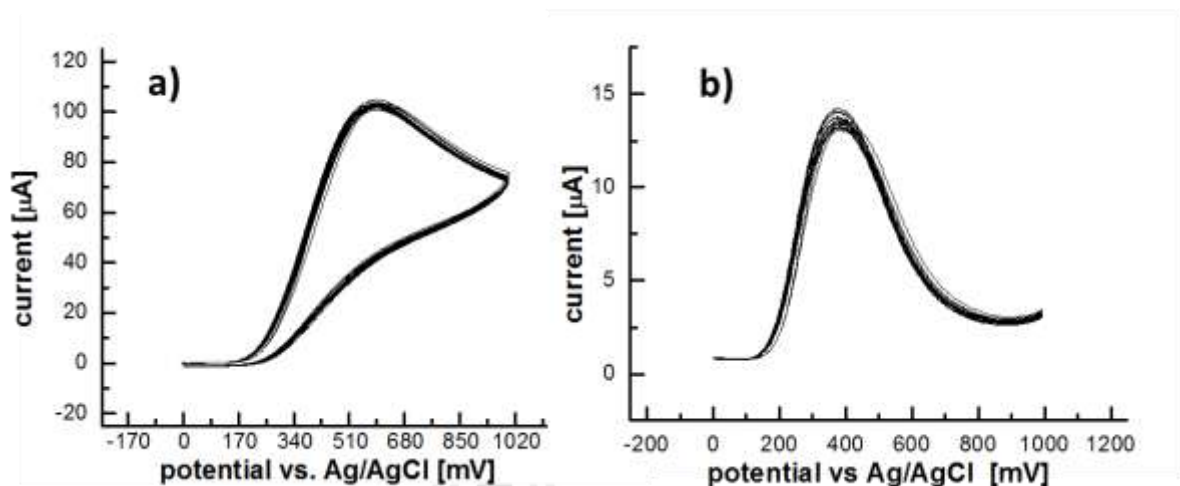


**Figure 4.7** Cyclic a) and differential pulse b) ascorbic acid voltammetry in one trough of a 24-well microtiter plate. The electrochemical detection of 1 mM of the analyte used an electrode assembly with a PLE, an Ag/AgCl reference and a Pt-wire counter electrode. Supporting electrolyte was 0.1 M KCl. The scan speed for the cyclic voltammograms (CVs) was  $50 \text{ mVs}^{-1}$  and differential pulse voltammograms (DPVs) involved a step height of 10 mV, pulse time of 0.5 s and pulse height of 50 mV. A pair of a CV and a DPV was measured every 15 min for a period of 3 h. The individual recordings are overlaid in the corresponding graphs A and B and the excellent superimposition of the traces indicates the stability of the analyte throughout the extended period of measurement.

### 4.2.3 Linear range and sensitivity of AA voltammetry

As it is associated with an elimination of capacitive charging currents, differential pulse voltammetry was used instead of cyclic voltammetry to quantitatively evaluate the response of the PLE to 15 AA concentrations in the range 0.05–100 mM. The load of the 24-well microtiter plate with the involved electrolyte solution is shown in Figure 4.8 included are 0.5 M H<sub>2</sub>SO<sub>4</sub> for electrode pretreatment, and DI water for rinsing. The arrays of DPV curves that are the result of a typical automated run through the wells are shown in Figure 4.8 a) and b). As expected, the values of the DPV peak height,  $I_p$ , and the corresponding peak area increased progressively with increased AA concentration. The programmed software moved the electrode from well to well and executed at defined electrode pretreatment, rinsing and DPV measurements in wells with KCl buffer solution or AA.



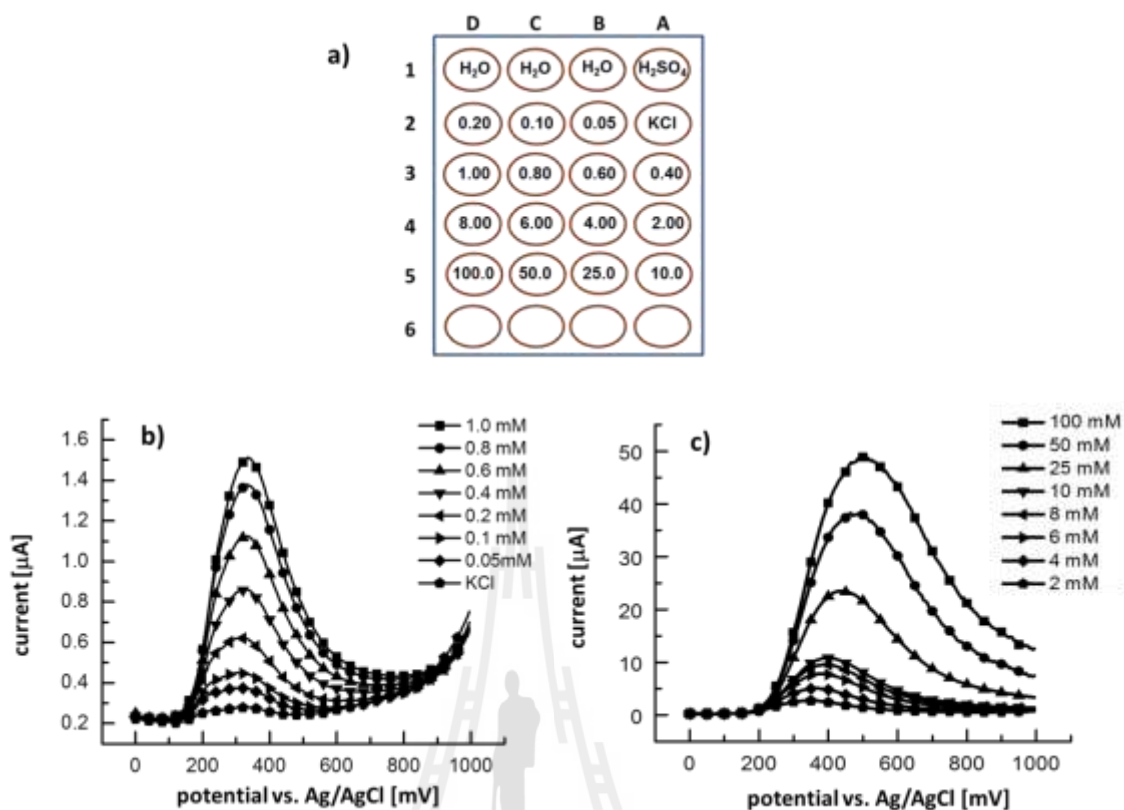


**Figure 4.8** a) The load of the 24-well microtiter plate for AA calibration; the number in each well is AA concentration in mM, b), and c) Automatically recorded differential pulse voltammogram in 16 wells of the microtiter plate that were filled with analyte solutions of 0.05-1 mM b), and 2-100 mM c); parameter DPV: step height of 10 mV, pulse time of 0.5 s and pulse height of 50 mV.

The calibration plots of  $I_p$  versus AA concentration, [AA] (see Figure 4.9) were linear up to about 8 mM. The corresponding linear equation followed the algorithm;  $y = 0.450 + 1.110x$ , with an  $R^2$  value of 0.998 (Figure 4.9 b). At higher AA levels a deviation from linearity started to occur, probably indicating electrode fouling

(see Figure 4.9 a). The limitation of linearity was not critical for the targeted fruit juice and vegetable tea analysis since it took place at low concentrations within the linear range. From three independent robotic microtiter plate assessments of the 15 AA concentrations, the average sensitivity of the assay was determined as  $1.1 \pm 0.2 \mu\text{A mM}^{-1}$  AA and the range of AA concentrations that could be reliably determined was 0.1–8.0 mM.

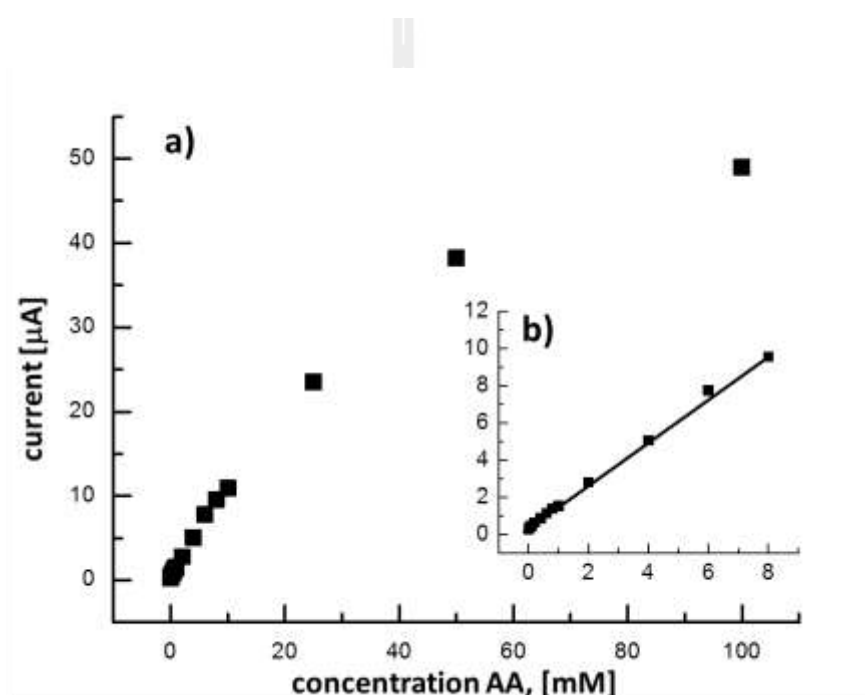


**Figure 4.9** a) Plots of the peak height,  $I_p$ , of the AA differential pulse robotic voltammograms in Figure 4.8 b) and as a function of the analyte concentration with 0.05 mM–100 mM AA. b), Linearity of the voltammetric response is observed only up to 8.0 mM.

#### 4.2.4 Robotic AA quantification via normal calibration method

In analytical chemistry, the construction and utilization of a calibration curve is a routine strategy for determining the concentration of a substance in an unknown sample. Compared of the unknown to a set of standard samples with known concentration. The calibration curve is a plot of how the instrumental response, the so-called analytical signal, in this study the current magnitude of a DPV trace, changes with the adjusted concentration of the analyte. The preparation of a series of standard across a range of concentrations near the expected concentration of analyte in the unknown is needed. For analyses, a plot of the instrument response, here the peak high  $I_p$ , vs. analyte concentration should offer a linear relationship. The signal ( $I_p$ ) for the sample with the unknown concentration is measured and, using the calibration curve, the concentration of analyte is computed. The analyte concentration ( $x$ ) of the unknown sample may also be calculated from the equation of the linear regression of the calculation plot or graphically obtained from the calibration plot (Harvey, 1956).

To test the suitability of the precalibration strategy, a microtiter plate was loaded with (i) 0.5 M  $H_2SO_4$  in well A1 for the pretreatment, (ii) water in wells B1, C1 and D1 for the electrode cleaning, (iii) bare measuring electrolyte (0.1 M KCl) in well A2 for base line recording, (iv) nine calibration solutions of known AA concentrations (0.1, 0.2, 0.4, 0.6, 0.8, 1.0, 2.0, 3.0 and 5.0 mM) in wells B2–D2 for construction of the calibration curve, and (v) ten AA samples in the wells C3–D6 as shown the loading solution (see Figure 4.10 a). Figure 4.10 b)) is the representative calibration plot, constructed from the DPVs in wells B2–D2, while Figure 4.10 c) is a typical AA sample DPV with a test concentration of 4 mM. Based on the linear calibration plot ( $r^2 = 0.993$ ), the  $I_p$  value of 15.6  $\mu A$  observed for the sample converted to an AA

concentration of 4.13 mM. The apparent recovery rate was thus 103.3% . When all AA sample wells were filled with a 4 mM test solution for repeated evaluations, robotic AA voltammetry in combination with the calibration method revealed an average assay recovery rate of  $105.6 \pm 4.8\%$  ( $n = 10$ ) for the microtiter plate run.

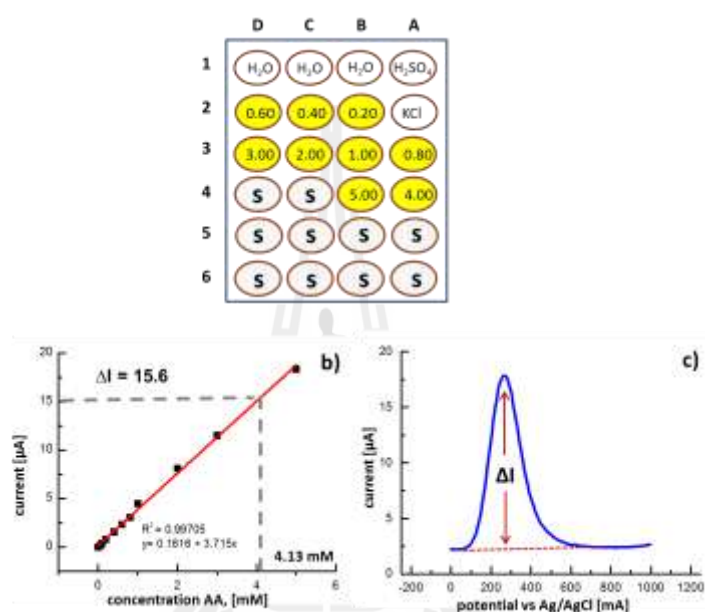


**Figure 4.10** Robotic voltammetric quantification of ascorbic acid in microtiter plate wells by the precalibration method: a) the 24-well microtiter plate loading electrolyte buffer, KCl, (A2) 0.02-5 mM AA concentration (B2 to B4), and model sample AA solution, “S”, (A5 to D6), b) The calibration plot for adjusted ascorbic acid concentrations of 0–5 mM, and c) one of the ten sample ascorbic acid differential pulse voltammograms acquired in an automated run through a loaded microtiter plate. The adjusted standard sample concentration was 4 mM, while the value obtained from the measured peak current was 4.13 mM.

#### 4.2.5 Robotic AA quantification via standard addition method

The standard addition method is a second quantification strategy commonly used to determine the concentration of an analyte that is in a complex matrix such as biological fluids, soil extracts, wastewater etc. The reason for using the standard additions method is that matrix component possibly interfering with the analyte signal are eliminated. The principle is to add analyte of known concentration to the sample and monitor the change in instrument response. The change in instrument response between the sample and the addition of standard analyte solution is assumed only due to change in analyte concentration. The procedure for an application of the standard addition method to the robotic AA analysis is to split the sample into several even aliquots in separate container of the same volume. The first container is then diluted to volume with the selected diluent. A standard containing the analyte is then added in increasing volumes to the other containers and each container is then diluted to volume with the selected diluent. The optimal size of each addition is that which gives a signal 1.5 to 3 times that of the sample. For the robotic measurement of AA the containers are the wells of standard microtiter plate and the filling is worked and according to the description. A plot of the signal intensities in term of peak high (or peak area) of the solutions vs. the added known concentration of analyte yields a straight line. As shown in Figure 4.11, plots of the instrument response vs. added analyte level are constructed subsequent to the robotic analytical run. The concentration of the analyte is determined from the point at which the extrapolated line regression through the data plot crosses the concentration axis at zero signal.



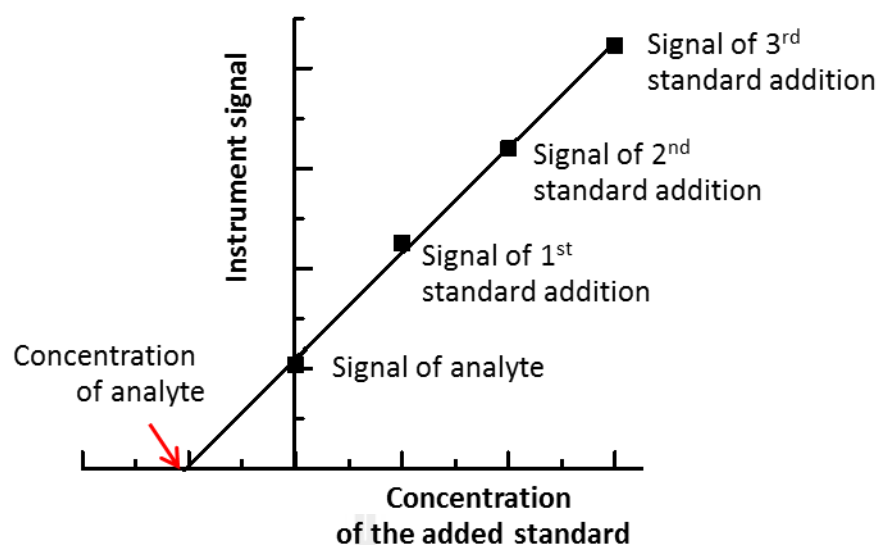


**Figure 4.11** Example of an analyte quantification via method of standard additions.

The signal is plotted versus the concentration of the added standard after dilution. A line is drawn through the data points and extrapolated towards the x-axis. The point of interception with the x-axis provides the concentration of analyte in the sample.

The load of a microtiter plate for robotic AA assessments by the standard addition method is shown in Figure 4.12 a). Actually, the filling was A1, 0.5 M H<sub>2</sub>SO<sub>4</sub> for electrode pretreatment; B1, C1, and D1, water for electrode rinsing; A2, A3, A4 and A5, four sample solutions; B2 (C2, D2), B3 (C3, D3), B4 (C4, C5), and B5 (C5, D5), sample plus 1<sup>st</sup> (2<sup>nd</sup>, 3<sup>rd</sup>) addition of AA stock solution Figure 4.12 b) shows the four DPVs that were recorded sequentially in a test trial with the robotic device handling first a 1mM AA model sample and then the sample with 1 mM, 2 mM and 3 mM standard additions of AA, respectively. The analysis of the experiment is shown in Figure 4.12 c) as a plot of  $I_p$  vs. [added AA]. The original AA concentration in the sample was then obtained from the intersection of the extrapolation of the linear

fit ( $r^2 = 0.998$ ) with the x-axes. For the specific test shown the measured AA level was estimated to be 1.03 mM, corresponding to an apparent recovery rate of 102.6%. In multiple trials, the average assay recovery rate for the joint between the robotic DPV AA analysis and the triple standard addition method was  $105.2 \pm 6.1\%$  ( $n = 20$ ), %RSD 5.80%, average [AA] 1.05 mM.

The recovery rate from the calibration method (external standard) and standard addition method for model AA sample was similar and close to 100%. This means both methods are functional and a good choice and suitable for robotic differential pulse voltammetric AA analysis. In real sample, when matrix effects are to be expected and matrix-matched calibration samples are not available, the standard addition method is probably better accurate for quantification than the calibration method.

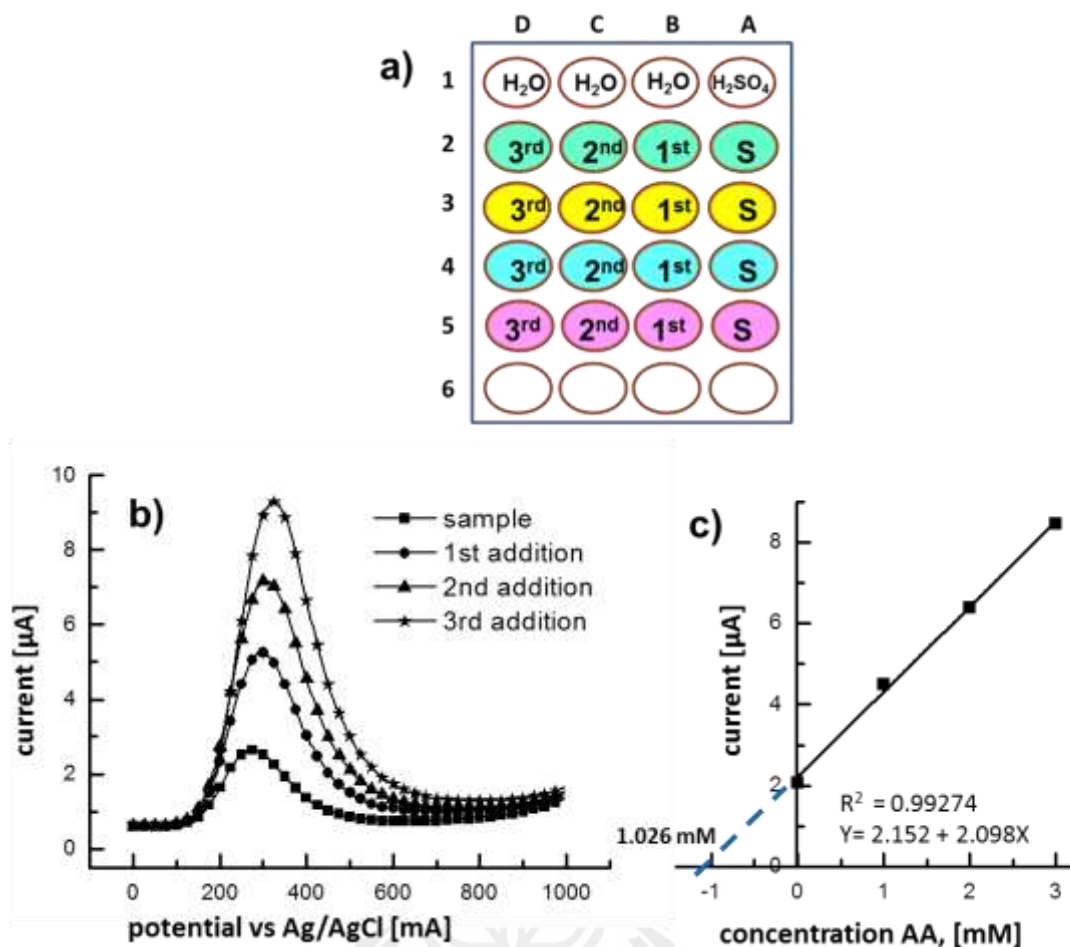


**Figure 4.12** Robotic voltammetric quantification of ascorbic acid in microtiter plate wells by means of the standard addition method: a) the 24-well microtiter plate for triplicate run of the standard addition method (A2 to D2, A3 to D3 and A4 to D4 for each set). b) Representation set of AA differential pulse voltammograms (step height: 10mV; pulse time: 0.5 s; pulse height: 50 mV) for bare sample and the sample plus 1, 2, and 3 mM additions of analyte, and c) Standard addition plot and the regression graph analysis.

#### 4.2.6 AA quantification in real samples

The novel robotic AA voltammetry procedure was applied to real samples and measurements were made with solutions of a commercial AA tablet, fresh juice from guava fruits obtained from a local market, and tea brewed from the leaves of the popular Thai medical/herbal plant called “Maroom” in Thai, “Horse radish tree” in English or *M. oleifera*. Figure 4.13 shows the DPV recordings of a typical standard addition voltammetry test with a guava juice sample in a microtiter plate well and, indicating AA as the main contributor to the electrochemical signal, a peak occurred at about 0.35 V vs. reference that increased linearly with the three equal additions of the AA stock solution. The analysis of plots of the peak currents (determined as the vertical distance between the top of the peak and a virtual base line drawn by the potentiostat software between the cathodic and anodic side of the peak) vs. the concentration of added AA allowed the calculation of the AA level in the fresh juice as  $1.7 \pm 0.1$  mM ( $n=3$ ). The AA determination in fresh guava juice and spiked AA in guava juice sample is shown in Table 4.1, when the juice sample was supplemented with 1 and then 2 mM AA, the detected values increased from 1.7 to  $2.7 \pm 0.1$  mM ( $n = 3$ ) and  $3.7 \pm 0.1$  mM ( $n=3$ ), indicating apparent recovery rates of 100.7 and 99.9% for the two additions, respectively.

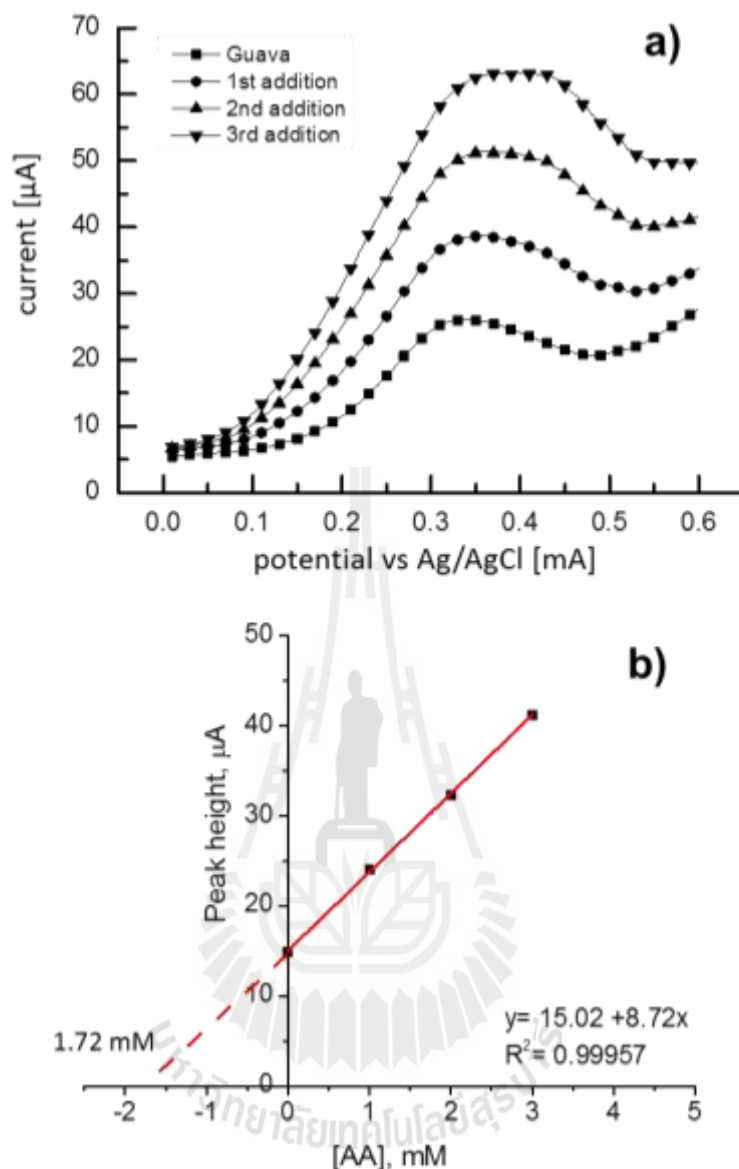


**Figure 4.13** a) Robotic voltammetric quantification of the ascorbic acid level of freshly prepared guava juice. A representative example of a set of four differential pulse voltammograms (step height: 10mV; pulse time: 0.5 s; pulse height: 50 mV) is shown for a pure sample and then for the sample plus successive additions of analyte. b) standard addition plot.

**Table 4.1** Determination of AA in guava juice by standard addition method (n=3).

sample	Added (mM)	Found (mM)	% Recovery
Guava	0	1.73±0.12	-
	1	2.75±0.11	100.73
	2	3.72±0.09	99.95

#### 4.2.7 Comparison of robotic AA electroanalysis with conventional AA titration

Since the proposed robotic differential pulse voltammetry is convenient, automatic and sensitive for the AA determination, the standard addition method is a promising option for evaluation of AA in sample. Table 4.2 compares the results determined with the robotic voltammetric assessment with the ones from a manual titrimetric trial on the AA tablet, the guava juice and the tea sample. For all three samples the AA contents obtained through the robotic electrochemical approach were in good agreement with values obtained from the conventional titration procedure that used either DCIP titration method (recognized as official method for the determination of vitamin C (AOAC, 2000)) and Iodometric titration (Silva et., al., 1999). Also, the measured AA content of the commercial AA tablet (128 mg per tablet) agreed reasonably well with the 120 mg per tablet (the calculation see appendix chapter) claimed on the product label. For the guava juice and the *M. oleifera* extracts,

the AA content revealed in this study compared favorably to reported values. In comparison to the 59 mg per 100 g of guava fruit reported here, Okiei, Ogunlesi, Azeez, Obakachi, Osunsanmi, and Nkenchor (2009) found 51 mg AA per 100 g fruit in an African guava, and 89 and 49mg per 100 g fruit were reported in two independent studies by Melo (2006), and Ferreira, Bandeira, Lemos, Santos, Costa and Jesus (1997) for guava sold in different regions of Brazil. The modest deviations between the above stated levels are likely to be explicable by geographic, genetic, and seasonal divergences. About 4.4 mgAAg<sup>-1</sup> of leaves were found in tea from the *M. oleifera* tree, about 70% of the value recently reported by Sreelatha and Padma (2009) who dealt with the antioxidants in leaf extracts from the same type of tree and found AA levels of 6.6 and 5.8 mgg<sup>-1</sup> of substance for samples prepared with dried and fresh leaves, respectively. The leaves in the present study were obtained as a commercial herbal tea that had probably been stored for some time while in the cited reference study fresh leaves were assessed just after the completion of the dehumidifying process. Degradation during storage could thus be the cause of the lower AA levels in our commercial Moringa tea.

In conclusion, the developed new methodology produced an accurate assessment of the AA content of commercial vitamin C tablets, fruit juices and herbal tea extracts. The good performance level of the robotic electrochemical AA assay was validated by its agreement both with data from classical volumetric chemical analysis and data found in the literature.

**Table 4.2** Ascorbic acid quantities in a vitamin C tablet, fresh guava juice, and a herbal tea a comparison of levels from robotic voltammetric screening in microtiter plates with those from manual titrations.

Sample	Voltammetry	Titration
Ja tablet, mg/tablet	128.04±5.07	129.7±1.82 <sup>b</sup>
Guava juice, mg/100 g fruit	58.71±4.00	51.93±0.24 <sup>b</sup>
Moringa tea, mg/1g tea	4.37±0.51	4.17±1.32 <sup>c</sup>

Standard deviation came from measurements for at least 3 times.

<sup>b</sup> DCIP method

<sup>c</sup> Iodometry method

### 4.3 Robotic electrochemical DPPH free radical amperometry for total antioxidant capacity determination in fruit and vegetable sample

#### 4.3.1 Electrochemical basis of the proposed amperometric method for antioxidant screening

For determination of antioxidant activity in food samples and biological fluids, methods are mainly based on reaction between a free radical, DPPH•, with the target antioxidant molecule “AH”. With the two standard electrochemical techniques, the cathodic current for scanned (voltammetry) or constant potential (amperometry)



reduction of the electroactive DPPH• radical at properly polarized carbon or metal working electrode is unaffected by solution turbidity and coloring and its magnitude is proportional to the actual DPPH• concentration in the measuring buffer. The amperometric determination of antioxidant activity takes advantage of the reaction between DPPH• with AH according to Figure 4.14 a) and the detection of the residual concentration of nonreacted free radical (<sup>\*</sup>DPPH•, in Figure 4.14 b)) by the electrode. The resulting current on a carbon pencil lead electrode polarized to DPPH• reducing potential is then proportional to the concentration of unreacted DPPH•.

The difference current,  $\Delta I$ , between the currents before adding antioxidant (unquenched condition) and after (quenched condition) addition of a small sample aliquot with antioxidant molecule provides the measure of the capacity of antioxidants in the supplement. Obviously, the larger the observed  $\Delta I$  value is the more antioxidant molecules got via sample addition into the measuring buffer to consume DPPH. Typically, calibration measurements with standards of synthetic antioxidants such as Trolox, vitamin E or vitamin C, are used to derive comparable measures of the total antioxidant capacity of sets of samples.

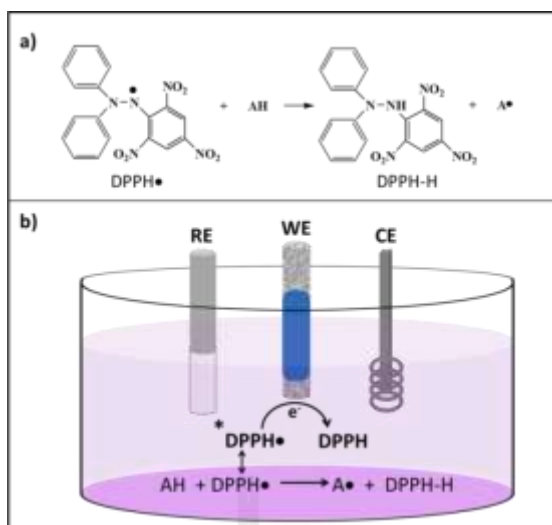


**Figure 4.14** a) Antioxidant molecule, AH, (analyte) react with the DPPH• free radical producing the non-residue DPPH-H; b) Scheme of the amperometric measurement, a DPPH• reduction current is adjusted by cathodic working electrode potential and a suitable fixed DPPH• supplement of the measuring solution. Food sample addition the DPPH• consuming antioxidant (AH) is introduced to the electrolyte and drop in DPPH• concentration and accordingly in the cathodic current ( $\Delta I$ ) is observed. The magnitude of  $\Delta I$  is proportional to AH molecules in artificial antioxidant or real food sample. \*DPPH• is nonreacted free radical.

In this dissertation, total antioxidant capacities in samples were expressed as the Trolox equivalent obtained by dividing the values of the current difference, actually an average  $\Delta I$ , measured in DPPH• ethanoic buffer solution after multiple times addition of an antioxidant by the values induced by a known duplications of Trolox addition. Trolox is a synthetic water-soluble compound, and vitamin E derivative (Figure 4.15 shown the Trolox structure). It became attractive for use as an

indicator compound for screening the free-radical scavenging capacity of food samples. A Trolox equivalent antioxidant capacity value can be assigned to all antioxidants compounds in real sample which are able to scavenge the free radical (DPPH•) by comparing their scavenging power. Many studies were reported on Trolox base antioxidant capacity screening in samples of foods, beverages and, plants extracted units of the measurements are mM Trolox/kg of sample or  $\mu\text{g}$  Trolox/1L of juice, and then Trolox equivalencies are commonly used as a benchmark for the antioxidant capacity of sample from the food science and technology.

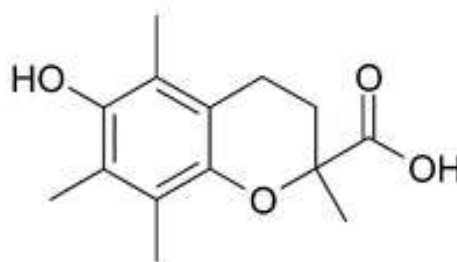


**Figure 4.15** The structure of 6-hydroxy-2,5,7,8-tetramethylchroman-2-carboxylic acid, Trolox.

#### 4.3.2 Cyclic voltammetry of the DPPH free radical molecule

The optimum working electrode potential for the surface-induced electrochemical reduction of the DPPH• indicator molecule at the pencil lead WE of the robotic electrode device had to be identified. The used carbon pencil WE were similar to the part for the ascorbic acid electroanalysis. Shown in Figure 4.16 is a cyclic voltammogram (CV) that was recorded by subjecting the three-electrode

assembly in a conventional beaker-type electrochemical cell to a solution of 2.5 mM DPPH• in ethanolic phosphate buffer pH 7.4 in 0.1 M KCl and a potential scan from +0.6 to -0.2 V and back. Consistent with literature (Milardovic et al., 2006; Milardovic et al., 2005, and Pisoschi et al., 2009), the typical CV of the DPPH• /DPPH redox couple should show the existence of an anodic and a cathodic current peak. Usually, a difference between peak potential of 59 mV implicates good reversibility of the redox couple. In the present study, the two expected current peaks for the DPPH• reduction and oxidation were clearly, however, the separation of maxima between the anodic peak corresponding to DPPH oxidation and cathodic peak corresponding to DPPH• reduction was much more 59 mV. This pointed towards a rather slow electron transfer kinetics of the involved carbonaceous pencil lead WE surface for the particular interfacial redox reaction. Nevertheless, a DPPH• reduction current suitable for analytical determinations turned up at potential of +150 mV to +100 mV and the latter more cathodic value was selected as the constant working potential for the amperometric assessment of the solution concentration of dissolved DPPH• in the robotic operation. A robotic analytical trial in the 24-well microtiter plate is related to an electrode operation up to three hours.

CVs were therefore recorded one after another in the same solution of the radical compound but at 10 minute intervals for a total time of 3 hours. As Table 4.3 indicates, the standard deviation of the observed cathodic and anodic peak currents was only  $\pm 0.1 \mu\text{A}$ . At least on the time scale of the experiment the dissolved DPPH• thus proved to be stable in the measuring buffer and the electrode response was stable too. This was an important principle asset for success with the planned robotic antioxidant electroanalysis with DPPH• based redox indication considering that the

completion of an analytical run through all 24 wells of a microtiter plate is a time consuming action.

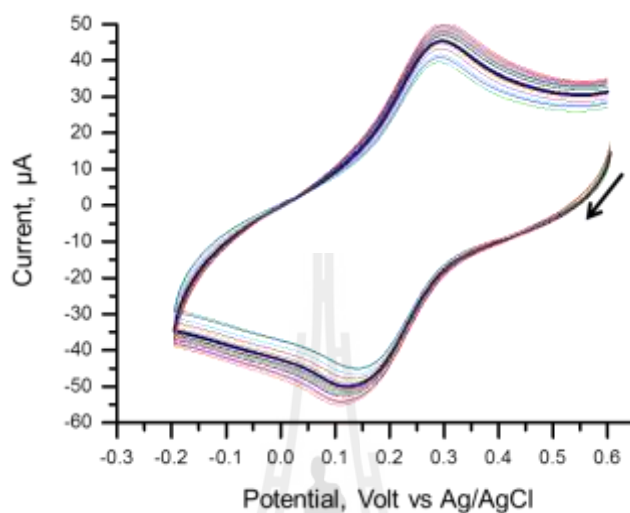


**Figure 4.16** Repetitive cyclic voltammogram of the DPPH• as recorded in ethanolic phosphate buffer (EPBS) with a beaker assembly of a pencil lead working, Ag/AgCl pseudo-reference and Pt spiral counter electrode. The 2.5 mM DPPH• had a pH of 7.4 in 0.1 M KCl. Starting point for the potential scan was + 0.6 V vs. Ag/AgCl and the scan rate 50 mV/s.

**Table 4.3** Stability of DPPH• voltammetry at pencil lead electrode (data from Figure 4.16)

	Cathodic peak	Anodic peak
Average peak height*, $\mu\text{A}$	28.7	28.6
Standard deviation*	0.095	0.099
%RSD*	3.30	3.47

\* n= 18, running 10 minute interval for total time of 3 hours

#### 4.3.3 The reaction of DPPH free radical with Trolox in conventional beaker type amperometric trial

The amperometric method proposed for the determination of antioxidant activity of food sample in microtiter plate wells is based on the electrochemical reduction in DPPH• at pencil lead carbon electrodes. To avoid possible electrochemical interference and the highest potential for DPPH• reduction, actually 100 mV, was selected based on the previous CV as the amperometric working potential.

The current-time diagram (Figure 4.17 a)) is a representative amperometric recording with a pencil lead WE that was together with the other two electrodes of the sensor assembly immersed into pure EPBS brought to working potential and then challenged with sequential additions of small aliquots of a DPPH• stock solutions. Each current step on the left side of amperogram belongs to the addition of one aliquot of DPPH• into the measuring cell. The concentration of the DPPH• in the beaker was

increased in increments of 10  $\mu\text{M}$  through individual addition. As expected, the DPPH $\bullet$  supplementation in quanta of 10  $\mu\text{M}$  raised the cathodic current through the cell in step like fashion. Each current step on the right side of amperogram corresponds to the addition of Trolox 2.5  $\mu\text{M}$  to the solution that now had DPPH $\bullet$  at 100  $\mu\text{M}$  level as exemplary radical scavenger. After 14 additions of Trolox the spiked DPPH $\bullet$  content was completely reduced and the current response settled back to the initial residual level.

As evidenced by the calibration curve in Figure 4.17 b), the incremental decay of the WE current in the DPPH $\bullet$  quenching part of the test appeared to be directly proportional to the amount of added Trolox up to 25  $\mu\text{M}$  or 10 additions. Another 4 additions of 2.5  $\mu\text{M}$  Trolox were then needed to fully suppress the remaining DPPH $\bullet$  reduction and set the current flow through the cell back to the initial baseline level according to Figure 4.17 on the right side which represents the start of the experiment. As commonly known the stoichiometry for the DPPH $\bullet$  Trolox reaction was not exactly 1:1. But the radical quenching power of Trolox observed in this study was actually about the same as the one that was earlier reported by Milardovic et al. for the same type of DPPH $\bullet$  amperometry, however, carried out with a glassy carbon working electrode. The same equivalent concentration of DPPH in radical form determined electrochemically implicated that the active DPPH $\bullet$  concentration was affected by the used solvent, which is in agreement with the literature (Molyneux, 2004). Based on the good agreement with the published DPPH $\bullet$  assay the method of an amperometric indicator detection at + 100 mV with a pencil lead electrode should be practical and had the quality required for the purpose of an antioxidant valuation of real sample in the robotic electrochemical mode.

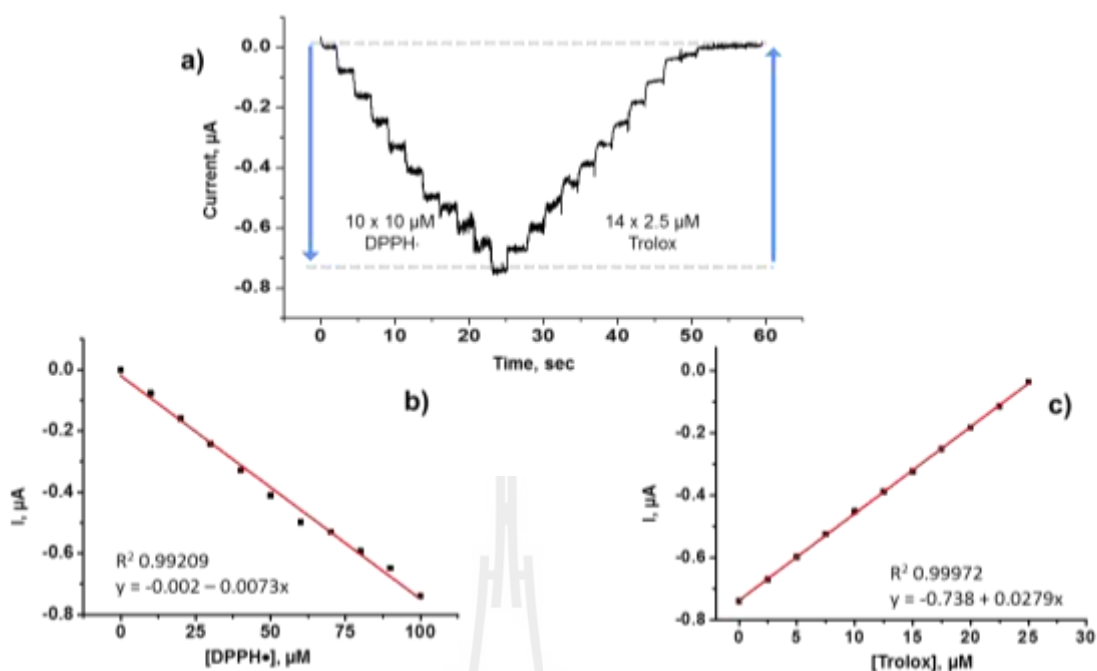


**Figure 4.17** a) Typical amperometric current response of an assembly of a pencil lead working, Ag/AgCl pseudo-reference and Pt spiral counter electrode that was kept at +100 mV and exposed in a beaker type experiment to multiple additions of DPPH• and then Trolox solutions. Down steps in the left part of the amperogram stand for sequential 10  $\mu\text{M}$  raises in DPPH• while rising steps in the right part indicate successive 2.5  $\mu\text{M}$  increases in level of the synthetic antioxidant Trolox. Electrolyte was pH 7.4 ethanolic phosphate buffer spiked with 0.1 M KCl. b) and c) are the calibration graphs for DPPH• and Trolox, respectively. They were selected from the original data shown in a) by determine the step height and plot then as a function of concentration.

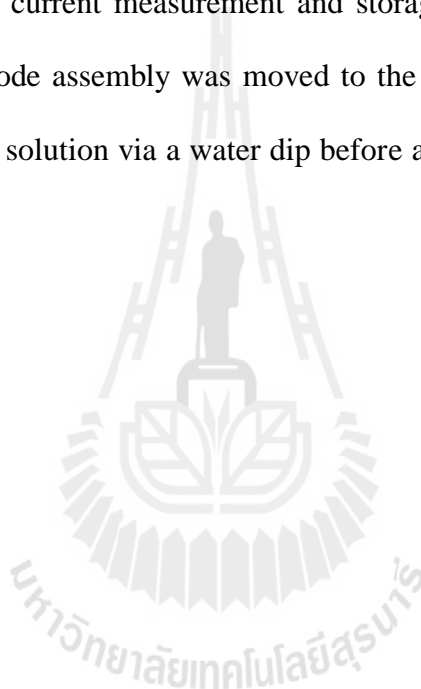


#### **4.3.4 The concept of automated antioxidant capacity measurement via DPPH• free radical amperometry in microtiter plate format**

As mentioned earlier, the reaction of Trolox as represented antioxidant with DPPH• was followed using amperometry in common beaker type electrochemical cell. Next was the transfer of the methodology into the robotic electrochemical device. The instrument and the basic of its operation was available from the earlier work on robotic ascorbic acid DPV. What had to be done was the processing of a new software script that suited the DPPH• amperometry and the design of the microtiter plate well load.

Figure 4.18 shows how the already establish DPPH• /Trolox amperometry was organized in the robotic device for automated electrochemical antioxidant assessments in the microtiter plate format. The plate layout for the robotic acquisition of, for instance, the data for Trolox calibration curves is shown as an example in Figure 4.18 a) and b). Water for periodic electrode dip cleaning was in all wells with an odd number. Well #2 was filled with 2 mL of pure EPBS for baseline current recording, well #4 contained 2 mL EPBS spiked with 100  $\mu$ L 5 mM DPPH• stock solution for the establishment of the initial DPPH• reduction current and the other 10 wells with even numbers had a filling as well #4 but additionally carried Trolox at incrementally increasing concentrations within the range suitable for linearly scaling the Trolox radical scavenging capacity according to Figure 4.18 a). Freshly loaded microtiter plate were placed on the x, y movable horizontal stage of the robotic device and the electrode assembly was fixed to the designated holder on the z-positioning element; then the system was ready for an automated analytical run as sketched in

Figure 4.18 c). Starting at a position just above the surface of the solution in well #1, the electrode set was enforced to travel from well to well and automatically record 2-min-long amperograms (I vs. t curves at the constant WE potential of + 100 mV vs. RE) in all containers with even numbers, one after another addressed with the computer-controlled stepper motors and an adapted software script in charge of the necessary electrode and plate movements for sequential immersions, electrode polarization and timed current measurement and storage. After measuring a DPPH• amperogram the electrode assembly was moved to the following odd-numbered well to remove any dragged solution via a water dip before approaching the next plate well with sample.



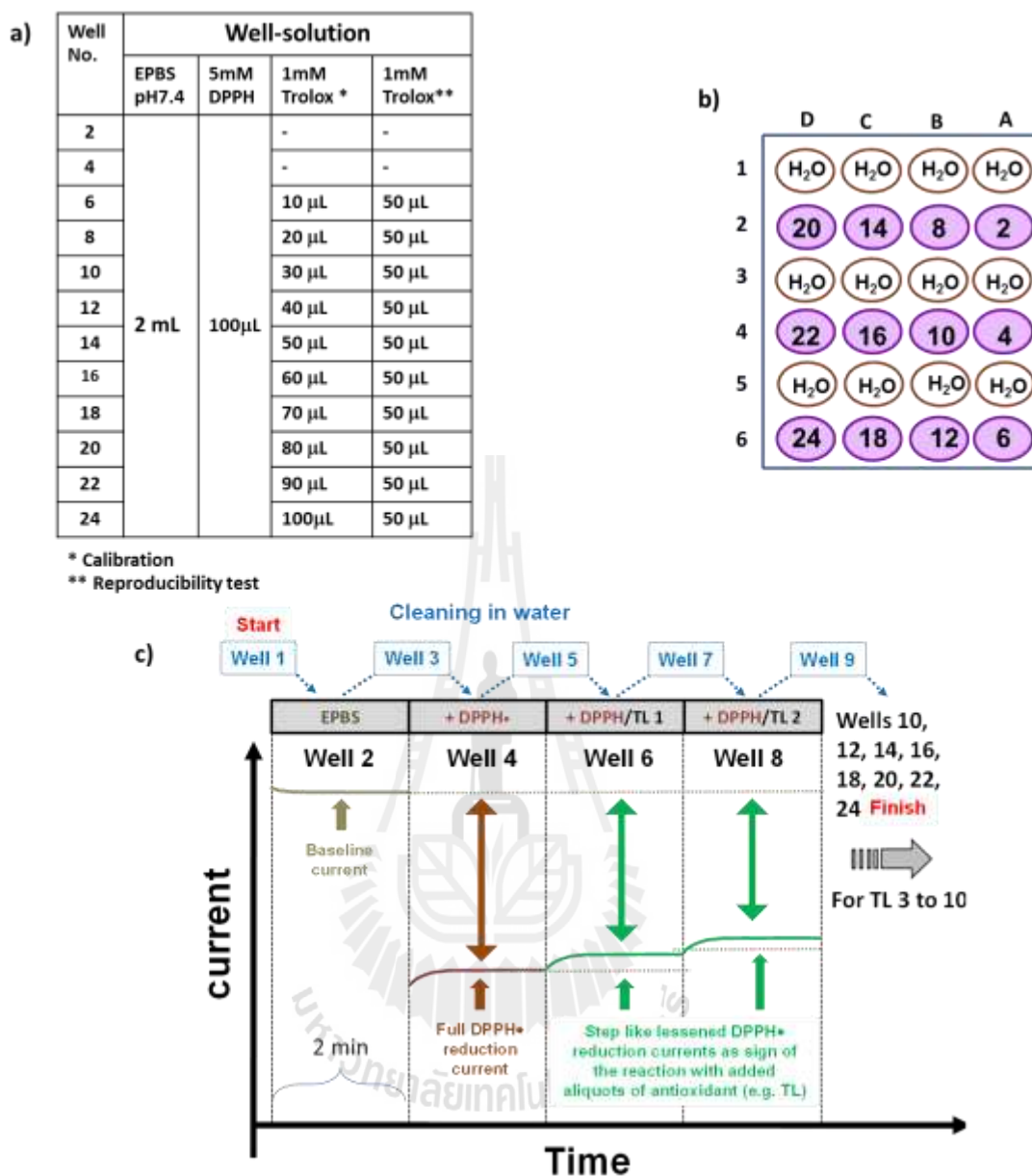


**Figure 4.18** a) Details of the exact plate layout for automated Trolox calibration measurements and reproducibility tests. b) 24-well microtiter plate with well number running in a). c) Schematic presentation of the sequence of an automated analytical run through a preloaded microtiter plate in b).

#### **4.3.5 Automated assessment of DPPH•/Trolox calibration curves in microtiter plate**

Figure 4.18 displays the design of the experiments for the acquisition of DPPH•/Trolox calibration curves in the automatic microtiter plates. Figure 4.19 is the outcome of a plate run and display of the analytical signals achieved in wells. Unsurprisingly the stable cathodic current was highest in well #4 with its pre-adjusted, unaffected DPPH• level and decreased in visible increments when Trolox was made additionally present as radical scavenger at increasing concentration in the wells #6, #8, #10, #12, #14, #16, #18, #20, #22 and #24. Figure 4.19 a) is the original set of data for twelve amperograms in the even numbered plate wells. Figure 4.19 b) is a zoom into the plateau region of the amperometric trace shown in Figure 4.19 a). Considering in I-E curve the plateau region at times between 80 and 100 s after initiation of the amperograms in the specific wells (see Figure 4.19 b) the average current during the 20 seconds piece of this section of the trace is computed and used for the construction of Trolox calibration curves. Plots of the DPPH• reducing current as function of Trolox concentration were linear up to 50  $\mu\text{M}$  levels of the radical quencher as presented in Figure 4.19 c).

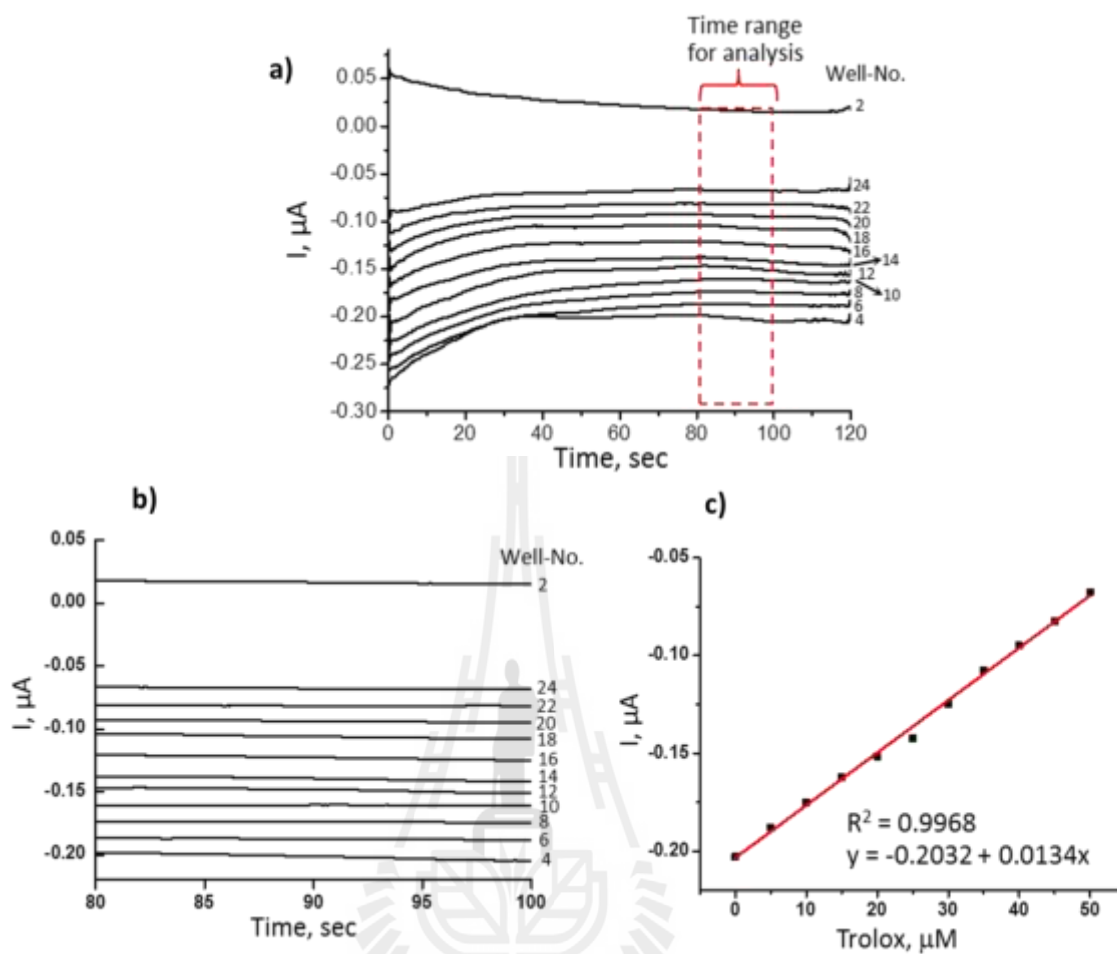


**Figure 4.19** a) Representative collection of the twelve current recordings as obtained in the even-numbered wells of a microtiter plate that was charged as shown in Figure 4.18 a) during a calibration run. b) A zoom into the traces in a) at times between 80 and 100 s. c) The Trolox calibration curve, which is the plot of the current magnitude as extracted from graph b) versus the actual Trolox level in the measuring buffer of the sample well.

#### **4.3.6 Reproducibility of automated DPPH•/Trolox amperometry in microtiter plate format**

In a reproducibility test the sample wells #6, #8, #10, #12, #14, #16, #18, #20, #22 and #24 were all spiked with 250  $\mu\text{M}$  DPPH• and 25  $\mu\text{M}$  Trolox (Figure 4.20 a,b)), the quenching reaction allowed to occur and the remaining DPPH• reduction current in the 10 wells was determined in an automated amperometric measuring run. Figure 4.20 c) shows the good overlay of the 10 current plateaus of the experiment. The average current was 0.132  $\mu\text{A}$ , % RSD was with 8.7% which below 10 % which confirms the response repeatability of the robotic screening mode and a reasonably reproducibility.

#### **4.3.7 The antioxidant activity of standard antioxidants**

Robotic electrochemical determination of antioxidant activity was performed under the same experimental conditions as for the calibration and reproducibility test. The model standard antioxidants, ascorbic acid, gallic acid and  $\alpha$ -tocopherol were used to study their capacity for a DPPH• scavenging in term of Trolox equivalent. Figure 4.21 a) shows the microtiter plate load designed for measuring the Trolox equivalents of the three model standard antioxidant radical scavengers in one microtiter plate run. Well#1, 3 had water fill and well#2 0.5 M  $\text{H}_2\text{SO}_4$  while the wells #4-10, #11-17 and #18-24 were set for the characterization of ascorbic acid, gallic acid and  $\alpha$ -tocopherol, respectively. For the loading solution of antioxidant capacity determination, the 1<sup>st</sup> (well #4 for) of the seven available wells kept 2 mL of bare EPBS, the 2<sup>nd</sup> (well #5 for AA) was filled with same solution 2 mL EPBS plus 100  $\mu\text{L}$  5 mM DPPH• standard solution, the 3<sup>rd</sup> (well #6 for AA), 4<sup>th</sup> (well #7 for AA), and 5<sup>th</sup> (well #8 for AA) had the solution of the 2<sup>nd</sup> well and a supplementation with 1 mM

antioxidant standard solution 10 (3<sup>rd</sup>), 20 (4<sup>th</sup>) or 30 (5<sup>th</sup>)  $\mu\text{L}$  in volumn. The last two wells of each set were further spiked with 10 (6<sup>th</sup> or well #9 for AA)) and 20 (7<sup>th</sup> or well #10 for AA)  $\mu\text{L}$  of 1 mM Trolox standard solution to evaluate the scavenging capacity of the model antioxidant in terms of Trolox equivalents. An example the amperometric current response in the 80 to 100 second time frame of the three-electrode assembly at 100 mV vs. RE in the wells for the gallic acid scaling was shown in Figure 4.21 b). The Trolox equivalent, TE, was derived from the set of amperograms and the observed levels of the model antioxidant as a ratio with Trolox scavenging DPPH•. The trolox equivalent was computed using the following equations adapted by Pisoschi et al. (2009) and Milardovic et al. (2006). Here, written for the gallic acid example, the equation applied to the two other examples, AA and TP, accordingly:

$$\begin{aligned}
 1) \quad \Delta I_{\text{Gallic acid}} &= \frac{[(I_{\text{well \#12}} - I_{\text{well \#13}}) + (I_{\text{well \#13}} - I_{\text{well \#14}}) + (I_{\text{well \#14}} - I_{\text{well \#15}})]}{3} \\
 2) \quad \Delta I_{\text{Trolox}} &= \frac{[(I_{\text{well \#15}} - I_{\text{well \#16}}) + (I_{\text{well \#16}} - I_{\text{well \#17}})]}{2} \\
 3) \quad \text{TE}_{\text{Gallic Acid}} &= \frac{\Delta I_{\text{Gallic acid}}}{\Delta I_{\text{Trolox}}}
 \end{aligned}$$

The particular calculation is supplied in the Appendix C.

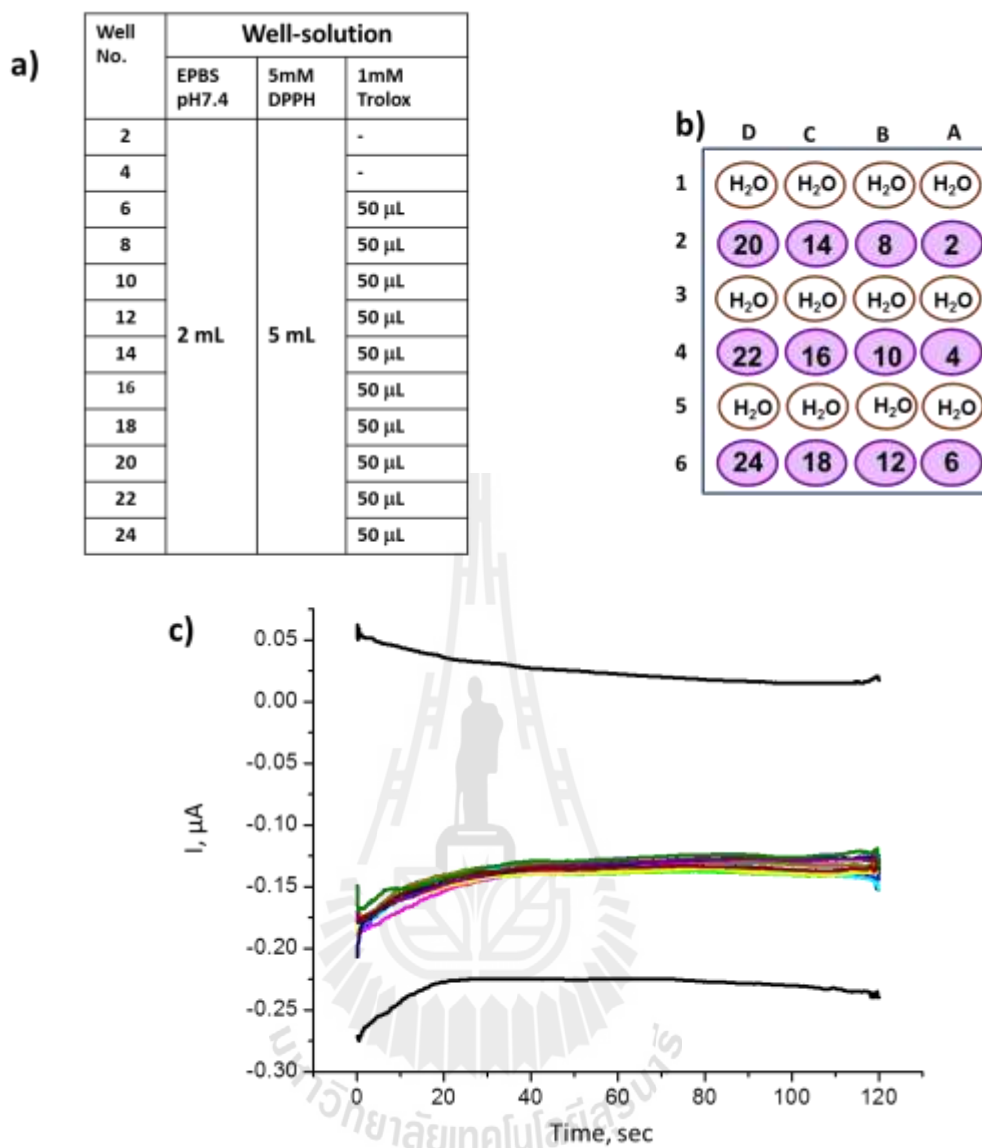


**Figure 4.20** a) Details of the exact microtiter plate layout for DPPH•/Trolox reproducibility tests. b) 24-well microtiter plate with well number running in a). c) Twelve amperograms of 250  $\mu$ M DPPH• and 25  $\mu$ M Trolox.



a)

Well-No.			Well-Solution					
Well-No.			EPBS (mL)	5mM DPPH ( $\mu$ L)	Model Antioxidant			1 mM Trolox ( $\mu$ L)
Well-No.					1 mM AA ( $\mu$ L)	1 mM GA ( $\mu$ L)	1 mM TP ( $\mu$ L)	
4	11	18	2	-	-	-	-	-
5	12	19	2	100	-	-	-	-
6	13	20	2	100	10	10	10	-
7	14	21	2	100	20	20	20	-
8	15	22	2	100	30	30	30	-
9	16	23	2	100	30	30	30	10
10	17	24	2	100	30	30	30	20

b)

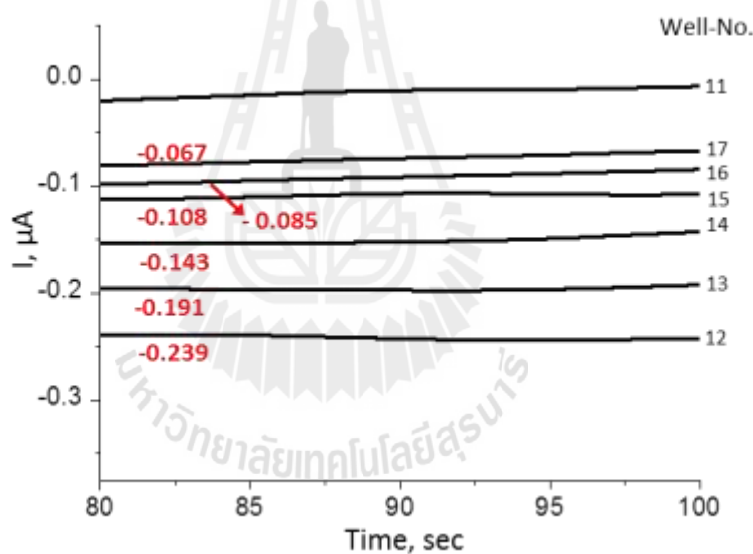


**Figure 4.21** a) Microtiter plate filling for determining the Trolox equivalents of three synthetic antioxidants (Ascorbic acid, AA; Gallic acid, GA;  $\alpha$ Tocopherol, TP) via robotic DPPH $\cdot$ /Trolox amperometry. b) A representative set of amperograms from an automated antioxidant power scaling for gallic acid.

#### 4.3.8 Trolox equivalent from spectroscopic measurement (reference measurement)

The spectrophotometric method of total antioxidant capacity screening is widely used assays for antioxidant capacity determination employing the scavenging of the stable radical DPPH• that is a chromogen species. The determination is based on the color disappearance due to the scavenging of DPPH• by antioxidant compounds monitored spectrophotometrically at 519 nm.

Spectroscopic measurements were carried out with solution having 100 μM DPPH• solution in EPBS plus addition of stock solutions 1 mM Trolox 10 to 80 μL in volumn. The data allows of the construction of calibration curves as displayed in Figure 4.22.

The calculation of Trolox itself and of model standard antioxidant samples based on the calibration plot and worked out the Trolox equivalent, TE,

$$TE = \frac{\text{volume Trolox at Abs Trolox}}{\text{volume Trolox at Abs Gallic}}$$

Example calculation are included in the Appendix C. TE levels from electrochemical determinations would then be compared with the one from spectroscopic measurements and the overlap used for judgments on the quality of the robotic amperometry.

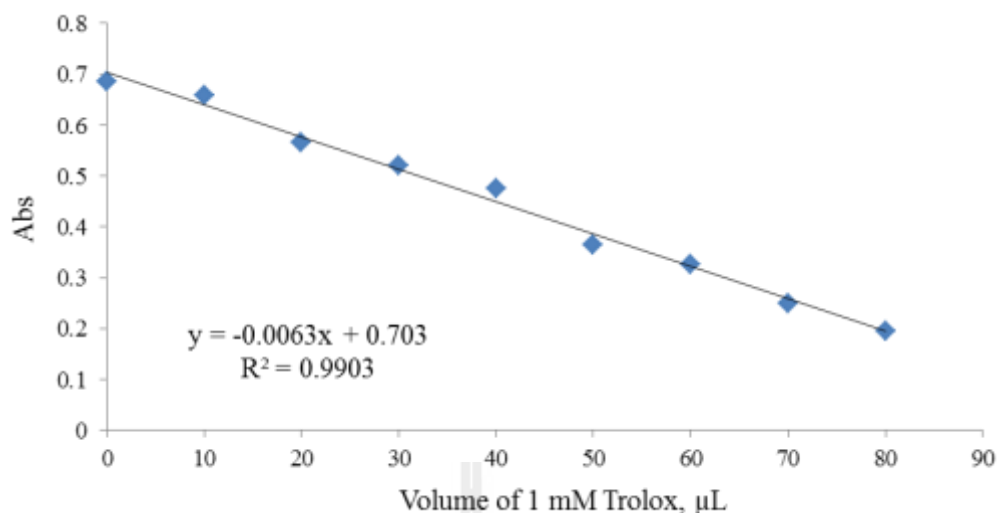


**Figure 4.22** Calibration graph used for TE calculation data was determined by spectrophotometry. Experimental condition: 100  $\mu\text{M}$  DPPH $\cdot$  (initial concentration), each point corresponds to addition of 1mM Trolox 10  $\mu\text{L}$ ,  $\lambda_{\text{max}} = 519 \text{ nm}$ .

#### 4.3.9 Robotic electrochemical assessment of Trolox equivalent of standard (model) antioxidants: comparison by the amperometric and spectroscopic data

For three synthetic model antioxidants (pure compound) the Trolox equivalent was determined spectroscopically and via robotic amperometry. The data is summarized in Table 4.4. In general, the robotic electrochemical and the manual optical colorimetric assay showed a good agreement between the results from triplicate trials. Also, the Trolox equivalents from robotic DPPH $\cdot$  amperometry and spectroscopy had a good overlap, and for ascorbic and gallic acid the value had a good agreement with published data from traditional beaker-type amperometric DPPH $\cdot$

assay. The expected Trolox equivalent of standard antioxidant “Trolox” was assessed as 1.0 by both robotic electrochemistry and spectrophotometry.

**Table 4.4** Free radical scavenging capacity of a set of three synthetic model antioxidant samples as obtained by automated DPPH• amperometry and a spectroscopic method

Standard antioxidant	Total Antioxidants Capacity (Trolox equivalent)	
	Robotic Amperometry	Spectrometry
Trolox	1.06 ± 0.01	1.03 ± 0.04
α- Tocopherol	0.9 ± 0.0	0.8 ± 0.1 (0.98 <sup>a</sup> )
Gallic acid	2.2 ± 0.2 (2.33 <sup>b</sup> )	2.4 ± 0.2
Ascorbic acid	0.9 ± 0.1 (0.89 <sup>b</sup> )	0.8 ± 0.0

<sup>a</sup> Tang and Liu (2007)










<sup>b</sup> Milardovic et al. (2006)

In summary it can be said that the DPPH•/Trolox based total antioxidant capacity assay was successfully implemented in the amperometric mode into a robotic electrochemical device. Trolox equivalents of model antioxidants were reliably and accurately measured in a convenient non-manual manner. In the next sub-section the novel assay has been used for the antioxidant capacity screening in real samples.

#### 4.3.10 The antioxidant activity in real samples

As previous mention, the robotic amperometry was successful used for evaluation of the antioxidant activity of model antioxidants. Next in this study was the application of this novel automated assay for actually herbal tea infusions, tropical fruit juices, and Thai herbal extracts. In the “State of the art” chapter the high total antioxidant activity of some Thai plants, tea infusion and fresh fruit sample were reported as samples with outstanding value and thus used for “the real sample” antioxidant study were Teaw, Phak Paew, Kri-Leck, Horse radish tree, Rose tea, Green tea, Guava, Papaya and Orange (see Table 4.5).

**Table 4.5** Names and photos of real sample that are rich in antioxidants. For these examples TE were evaluated using robotic DPPH• amperometry.

Herbal tea infusions		Tropical fruit juices		Thai herbal extracts	
Photo	Name	Photo	Name	Photo	Name
	Moringa		Guava		Teaw ( <i>Cratoxylum formosum Dyer</i> )
	Rose		Papaya		Phak Paew ( <i>Polygonum odoratum Lour.</i> )
	Green tea		Orange		Kri-Leck ( <i>Cassia siamea</i> )

For the representative case of automated orange juice electroanalysis the microtiter plate load and the set of corresponding amperograms are shown in Figure 4.23. The microtiter plate actually measuring triple values of the antioxidant capacity of the same freshly squeezed orange juice via robotic DPPH• amperometry. Wells #1-3 were water-filled while the wells #4-10, #11-17 and #18-24 were reserved for triplicate juice analysis, respectively. For a certain sample, all related wells had the measuring buffer, but either bare (1<sup>st</sup>) or spiked with 100  $\mu$ L 5 mM DPPH• stock solution (2<sup>nd</sup>) or 100  $\mu$ L 5 mM DPPH• stock plus 10 (3<sup>rd</sup>), 20 (4<sup>th</sup>) or 30 (5<sup>th</sup>)  $\mu$ L of orange juice. The 6<sup>th</sup> and 7<sup>th</sup> wells of each set were further spiked with 10 and 20  $\mu$ L of a 1 mM Trolox standard to enable calculating the scavenging capacity of the antioxidant in terms of  $\mu$ mole Trolox units, as following equation.

$$1) \quad \Delta I_{\text{sample}} = \frac{[(I_{\text{Well \#5}} - I_{\text{Well \#6}}) + (I_{\text{Well \#6}} - I_{\text{Well \#7}}) + (I_{\text{Well \#7}} - I_{\text{Well \#8}})]}{3}$$

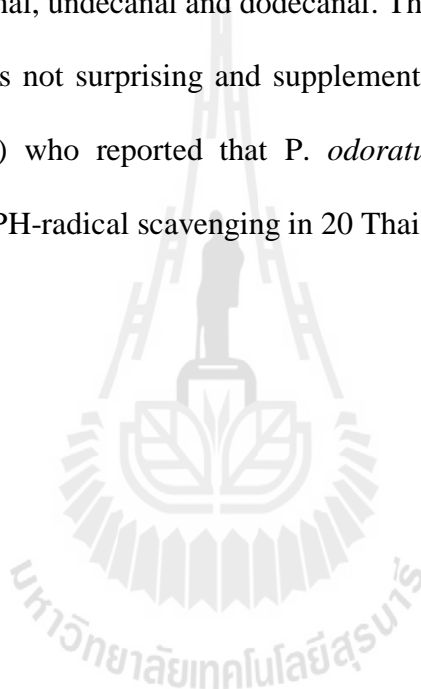
$$2) \quad \Delta I_{\text{Trolox}} = \frac{[(I_{\text{Well \#8}} - I_{\text{Well \#9}}) + (I_{\text{Well \#9}} - I_{\text{Well \#10}})]}{2}$$

$$3) \quad \text{TE} = \frac{\Delta I_{\text{sample}}}{\Delta I_{\text{Trolox}}}$$

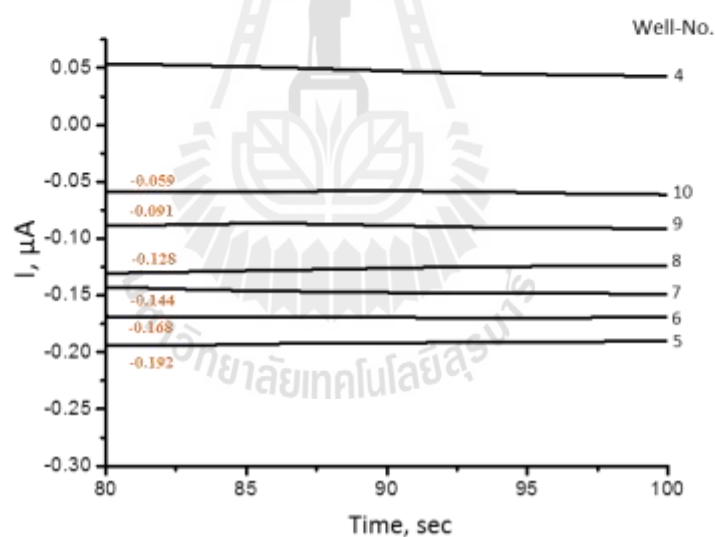
An example calculation is provided in the Appendix C.

Table 4.6, summarizes the TE contents for all nine samples and reports the total antioxidant capacities as the average of triplicate electrochemical assessments together with the average of triplicate spectroscopic measures in the unit  $\mu$ Mole Trolox equivalents. It is obvious that the relative standard deviation for the replicate determinations (n=3) was well below the 10% barrier for all tea, fruit and plant samples, regardless of the applied principle of detection. Besides throughout the sample collection the Trolox equivalents from the proposed robotic electrochemical screening were in good agreement with the ones obtained from the routine

spectrophotometry. Also well indicated in the results of the automated DPPH• amperometry assay was the common observation that green tea and guava are usually in the top ranks among tea infusions or fruits as indeed both showed up with highest Trolox equivalents in their category. In addition, among three Thai herbal plant extracts, Pak Paew (*P. odoratum*) had the highest total antioxidant activity because these plant extracts are known to have many organic phenol compounds such as hexenal, hexenol, decanal, undecanal and dodecanal. The prominent content of the Pak Paew samples was thus not surprising and supplement was reported by Nanasombat and Teckchuen (2009) who reported that *P. odoratum* had a highest antioxidant capacity in term of DPPH-radical scavenging in 20 Thai local vegetables.



Well-No.	Well-Solution			
	EPBS (mL)	5mM DPPH ( $\mu$ L)	Orange juice ( $\mu$ L)	1 mM Trolox ( $\mu$ L)
4,11,18	2	-	-	-
5,12,19	2	100	-	-
6,13,20	2	100	10	-
7,14,21	2	100	20	-
8,15,22	2	100	30	-
9,16,23	2	100	30	10
10,17,24	2	100	30	20



**Figure 4.23** a) The microtiter plate load for measuring triple values of the antioxidant capacity of the same freshly squeezed orange juice via robotic DPPH• amperometry in tropical runing. b) Amperograms from an automated antioxidant power scaling for orange juice.



**Table 4.6** Trolox equivalents obtained by robotic amperometric and spectrophotometric measurement in a varying of food samples.

Type	Sample	Total Antioxidants Capacity ( $\mu$ mole Trolox equivalent)	
		Robotic Amperometry	Spectrometry
Tea (1g)	Moringa	37.9 $\pm$ 3.4	38.1 $\pm$ 1.0
	Rose	41.3 $\pm$ 6.9	47.0 $\pm$ 4.4
	Green tea	466 $\pm$ 42	433 $\pm$ 25
Fruit	Guava	35.9 $\pm$ 1.4	33.9 $\pm$ 1.6
	Papaya	18.8 $\pm$ 1.4	16.7 $\pm$ 2.5
	Orange	0.62 $\pm$ 0.09	0.50 $\pm$ 0.05
plants extract (1g)	Teaw <i>(Cratoxylum formosum Dyer)</i>	491 $\pm$ 8.6	482 $\pm$ 46
	Phak Paew <i>(Polygonum odoratum Lour.)</i>	661 $\pm$ 11.1	670 $\pm$ 7.7
	Kri-Leck <i>(Cassia siamea)</i>	155 $\pm$ 14.4	166.5 $\pm$ 2.5

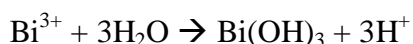
#### 4.4 Determination of trace lead(II) and cadmium(II) by robotic anodic stripping voltammetry at pencil-lead bismuth-film electrodes

Based on literature, bismuth-film electrode (BFE) obtained during the analysis via *in situ* plating of dissolved Bi(III) ions in the measuring were chosen as the working electrode for lead and cadmium voltammetry. *In situ* plating of the electrode modifier simplifies and shortens the experimental procedure as no separate bismuth-plating step is required. The substrate electrode were again pencil lead electrode that already worked well as sensor for robotic AA and AH electroanalysis. After good success was achieved with robotic AA differential pulse voltammetry and robotic total antioxidant amperometry, after that was to extend the methodology of

robotic electroanalysis to the anodic stripping voltammetry of heavy metals, in particular lead (II) and cadmium (II) in aqueous solution. Part of the conditions of the designed robotic differential pulse anodic stripping voltammetry (DPASV) using Bi(III) modified pencil lead electrode were chosen based on available literature e.g. the deposition potential, cleaning potential and supporting electrolyte. The concentration of dissolved bismuth (III) in the measuring buffer and deposition time was optimized for the procedure in this thesis. The quantity of bismuth deposition depends on type of substrate material and the sensor size. And surely the sensitivity and detection limit will be influenced by the deposition time. In the following the optimization of Bi(III) in the measuring buffer and the deposition time will be studied and discussed.

#### **4.4.1 Optimization of the measuring procedure for robotic anodic heavy metal stripping voltammetry using Bi(III) film modified pencil lead electrode (BF-PLE)**

The need for dissolved Bi(III) in the measuring buffer is associated with some limitations in the possible pH range of the sample solution. Bi(III) ions are, for instance very susceptible to hydrolysis in neutral and alkaline media according to the reaction (Economou, 2005):



Accordingly, the *in situ* plating is best performed in fairly acidic samples. Pb/Cd anodic stripping was test with varies supporting electrolytes such as phosphate buffer, HCl, acetate buffer and HClO<sub>4</sub> and in accordance with published procedures, the best stripping performance of PLE was gained in acetate buffer (Ping et al., 2011). The useful potential window was also strongly affected by the pH of solution. Based

on the positive earlier finding from others an acetate buffer of pH 4.5 with 0.1 M KCl was chosen as the measuring media for robotic Pb/Cd stripping voltammetry (Economou, 2005; Hočevár, Ogorevc, Wang, and Pihlar, 2002; Cao et al., 2008).

The deposition/preconcentration step is done by anodic deposition at a controlled time and potential. The deposition potential is usually 0.3 - 0.5 V more negative than the apparent  $E^0$  for the least easily reduced metal ion to be determined. The influence of the deposition potential on the stripping peak of Pb(II) and Cd(II) was examined at value of -1.3, -1.4, and -1.5 V vs Ag/AgCl by Chuanuwatanakul et al. (2008). A deposition potential of -1.4 V vs Ag/AgCl produced the highest stripping peak current and best results in terms of Pb(II) and Cd(II) trace analysis. When the deposition was more negative, the reproducibility of stripping current of Cd(II) and Pb(II) become poor, most likely because of the onset of mild hydrogen evolution. Again, based on recommendation from literature, -1.4V was adopted for the robotic stripping voltammetry of Pb/Cd with the expectation of good sensitivity and reproducibility.

In anodic stripping voltammetry, the surface of the working electrode must be cleaned after a particular stripping step by polarization to a potential facilitating oxidation of any remaining species. The step involves a potential positive enough for the oxidation of the metals on electrode surface, normally, for times about several tens of second. Here, with the *in situ* plated BF-PLE, the Bi film is stripped off electrochemically after each measurement at a potential of +0.3 V vs Ag/AgCl and amperometric cleaning of the electrode is then applied in 1% HNO<sub>3</sub> (+0.3 V for 120 s) to remove and strip off any metal ions from the sensor surface. After that a new Bi film is re-plated as part of the next analysis cycle.

The level of spiked Bi(III) in the measuring buffer for the *in situ* formation of the functional Bi film affects the sensitivity of the target metal determination. Tests were thus carried out with the robotic stripping voltammetry in 24-well microtiter plate format with solution that contained 20 ppb of Pb(II) and Cd(II) and different concentration of Bi(III) 100, 500, 750, 1000, 1500, 2000 ppb in 0.1 M acetate buffer pH 4.5 with 0.1 M KCl (the plate load is mentioned in the Experimental chapter). In the trial, a deposition potential of  $-1.40$  V versus Ag/AgCl electrode for 120 s was applied to the working electrode and the stripping or measurement was performed in the differential pulse mode by scanning the potential from  $-1.10$  to  $0.0$  V. Figure 2.25 a) shows the obtained results of the robotic differential pulse stripping voltammetry of Pb(II) and Cd(II) at 20 ppb but with different Bi(III) level in the measuring solution. The observed peak potential of the Bi(III), Pb(II) and Cd(II) peak were about  $-200$ ,  $-550$  and  $-800$  mV vs Ag/AgCl, respectively. The effect of the Bi(III) concentration in the buffer on the peak height and peak area of the analyte metals is illustrated in Figure 4.24 b) and c). It was found that the magnitude of the Pb(II) peak sharply increased with the increase of Bi(III) concentration and reached a maximum at about  $500$   $\mu\text{g/L}$  Bi(III). For the Cd(II) peak the effect was less pronounced and the increase observed was followed by a current plateau at higher active Bi(III) levels. Higher Bi(III) concentration would favor increase in the thickness of the Bi film that acts as support for the better deposition of the analyte metals. Initially, an increase in Bi(III) may thus support the deposition of analyte and accordingly the peak current due to a large area for their co-deposition. When the Bi(III) became higher than the expected/adjusted Pb/Cd levels, the competition of the ions for a chair on the voltammetric reduction current may be at the disadvantage of the heavy metals and the

peak current stopped increasing (for Cd(II)) or decreases (for Pb(II)). As the, peak current for Pb(II) and Cd(II) was highest at a spiked Bi(III) level of 500 ppb, this Bi(III) concentration was chosen as the one for all following stripping analysis in the robotic system.

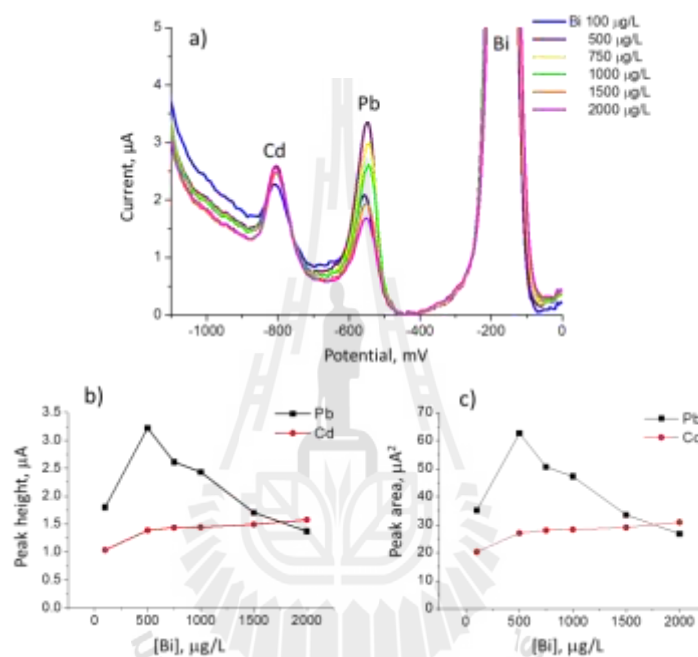


**Figure 4.24** a) Robotic differential pulse stripping voltammetry. The measuring buffer (0.1M acetate buffer pH 4.5 (0.1 M KCl)) had 20 µg/L Pb(II), Cd(II) and Bi(III) levels that varies from 100-2000 µg/L.; deposition time 120s (stirred), and a deposition potential of -1.4 V were used for analyte accumulation onto the working electrode, WE: PLE, CE: Pt spiral and RE: Ag/AgCl b) Peak height and c) Peak area of Pb(II) and Cd(II) as a function of Bi(III) concentration, the curve is associated with the voltammograms shown in a).

The effect of the deposition (accumulation) time on the anodic stripping peak currents of Pb(II) and Cd(II) was studied in the range of 60-900 s. The results from the robotic differential pulse stripping voltammetry trial and plots of the obtained peak current for both heavy metals as a function of deposition time are shown in Figure 4.25. As expected, the peak currents increase with analyte accumulation time. This happened over the entire range of deposition time from 60-900 s. For Cd(II), on the other hand, the stripping currents increased up to the deposition times of 600 s and then stayed fairly constant.

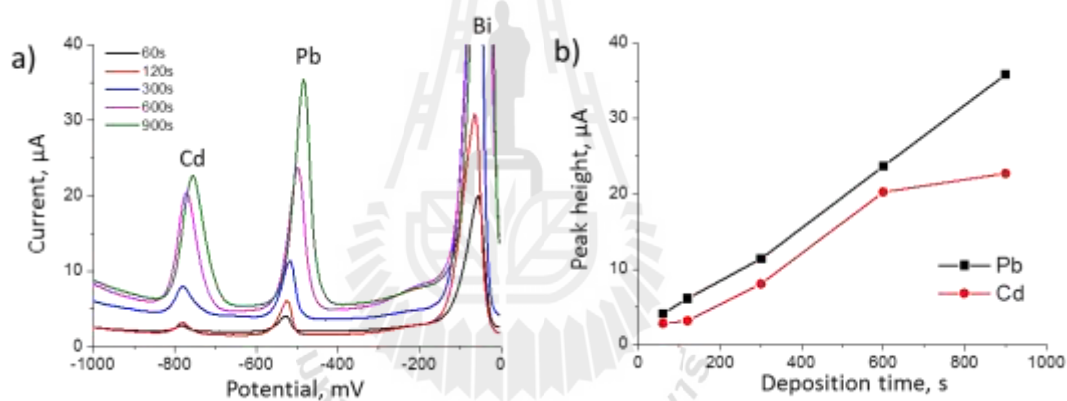


**Figure 4.25** a) Robotic Differential pulse stripping voltammetry of 40 µg/L Pb(II) and Cd(II) under the condition of different deposition (accumulation) time. b) Peak heights increase with increasing deposition time. Experimental condition; Bi(III) 500 µg/L, 0.1 M acetate buffer pH 4.5 (0.1M KCl), under stirring solution, deposition potential -1.4 V, WE: PLE, CE: Pt spiral and RE: Ag/AgCl.

#### **4.4.2 Data of Pb(II) and Cd(II) calibration trials via robotic differential pulse anodic stripping in 24-well microtiterplate**

For Pb(II) and Cd(II) robotic stripping voltammetry, the optimum conditions were obtained in the previous section. Best supporting electrolyte was 0.1 M acetate buffer at pH 4.5. Optimized Bi(III) concentration in the buffer was 500 ppb. And the deposition potential and time analytical assessment via DPV were optimum at -1.4V and 600s, respectively. The voltammetric stripping peak current as a function of concentration of Pb(II) and Cd(II) was investigated using calibration run in the robotic electrochemical system as shown in Figure 4.26. Figure 4.26 a) is another simple schematic of the robotic system displaying the 24-well microtiter plate for standard and sample solutions in Figure 4.26 b) the three-electrod assembly with PLE as working (WE), a pseudo Ag/AgCl as reference (RE) and a platinum spiral as counter electrode (CE), all as mentioned earlier, fitting to a specific holder and connected to the potentiostat. The well load with 0.1 M acetate buffer (pH 4.5), plus Bi(III), Pb(II) and Cd(II) is in Figure 4.26 d). The PLE working electrode was cleaned by repetitive dipping in DI water and then electrochemically cleaned in 1% HNO<sub>3</sub> via potential step treatment. Before the stripping analysis was carried out the electrode was dipped again in DI water. The sequence of well so far was A1, A2 then A3 well. Automated stripping measurement started in the A4 well in which a differential pulse voltammogram was automatically recorded and saved in identified folder. Subsequently, the electrode assembly was brought back to well A1, A2 and A3 for removing residual metal at its surface. Next was stripping voltammetry and so on. In well A4 and A5 the voltammogram of the bare buffer and Bi(III) containing buffer without any Pb/Cd analyte were recorded and the measured traces provided the

background signal. The cycle to address well sample in the 24-well microtiter plate went to the “B1 (measurement) well → A1-A3 wells” then “B2 (measurement) well → A1-A3 wells”. This sequence was repeated until finally well “D5(measurement) well → A1-A3 wells” was reached. Typically, a complete analytical run though on loaded microtiter plate with 15 samples took about 4 hour and 20 minutes.

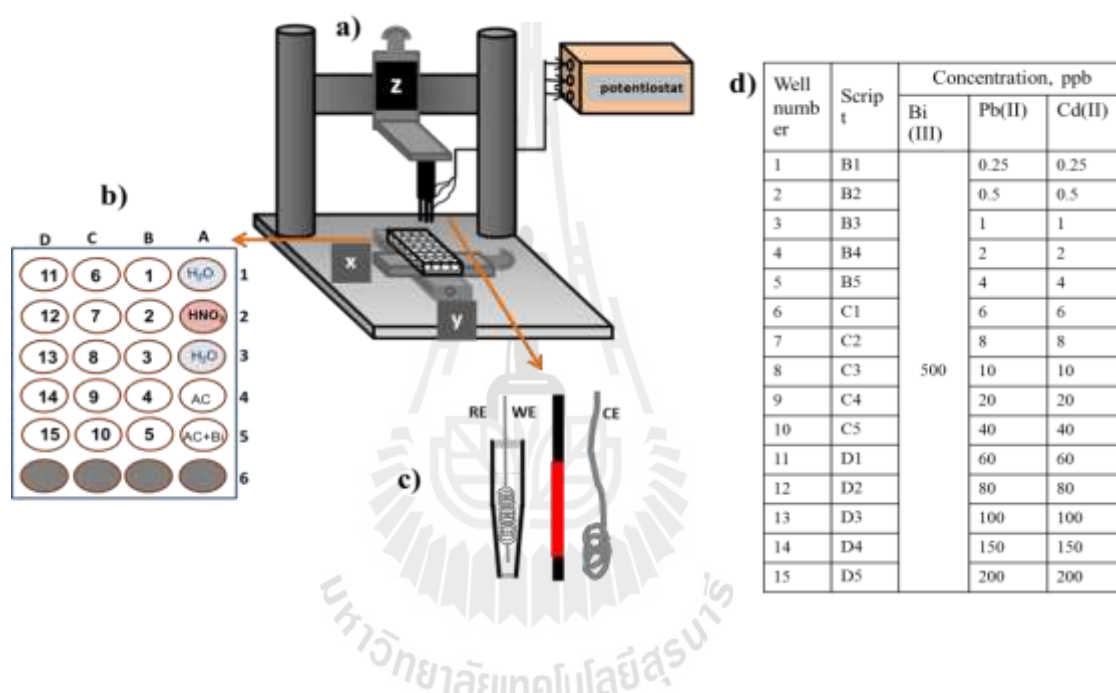


**Figure 4.26** a) Schematic of the robotic electrochemical instrument for automated heavy metal anodic stripping voltammetry, b) Numbering of the 24 well microtiter plate; AC is 0.1 M acetate buffer, Bi is Bi(III), c) Drawing of three electrodes assembly consist of a PLE working (WE), pseudo Ag/AgCl reference (RE) and platinum spiral counter electrode (CE). d) The design of the microtiter plate for automated Pb(II) and Cd(II) calibration measurement.



The calibration curves for the simultaneous voltammetric determination of Cd(II) and Pb(II) in 24-well microtiter plate was achieved without manual interaction via differential pulse stripping voltammetry under optimal conditions. The DPSV for different concentrations of Cd(II) and Pb(II) are illustrated in Figure 4.27. The derived calibration plots were linear over the range from 2-100 and 20-100  $\mu\text{g/L}$  for Pb(II) and Cd(II), respectively. However, the concentrations over than 100  $\mu\text{g/L}$  linearity was lost. The analytical performance of robotic electrochemical method with Bi plate PLE for the determination of Pb(II) and Cd(II) is summarized in Table 4.7. The limit of detection (LOD) was calculated from  $3S_{bl}/S$  where  $S_{bl}$  is the standard deviation of blank measurement ( $n=5$ ) and average  $S$  is sensitivity of the method or the slope of the regression linear curve (Skoog, West, Holler and Crouch, 2004) average over five measurements in five microtiter plate. The relative standard deviation or % RSD was calculated by expressing the standard deviation for a data set as a percentage of the mean data set as a percentage of the mean. For the measurements here, the low relative of standard deviation (% RSD lower than 10 %,  $n=3$  in three microtiter plates) were the routine for robotic Pb(II) and Cd(II) analysis which compares well with the quantity of published of the options of Pb/Cd stripping voltammetry. The results thus gave indication about the usefulness of the established assay for the simultaneous determination of Pb(II) and Cd(II) in real sample. In the next section, the application of the vary type of heavy metal anodic stripping voltammetry for Pb/Cd determination in water and soil sample will be obtained.

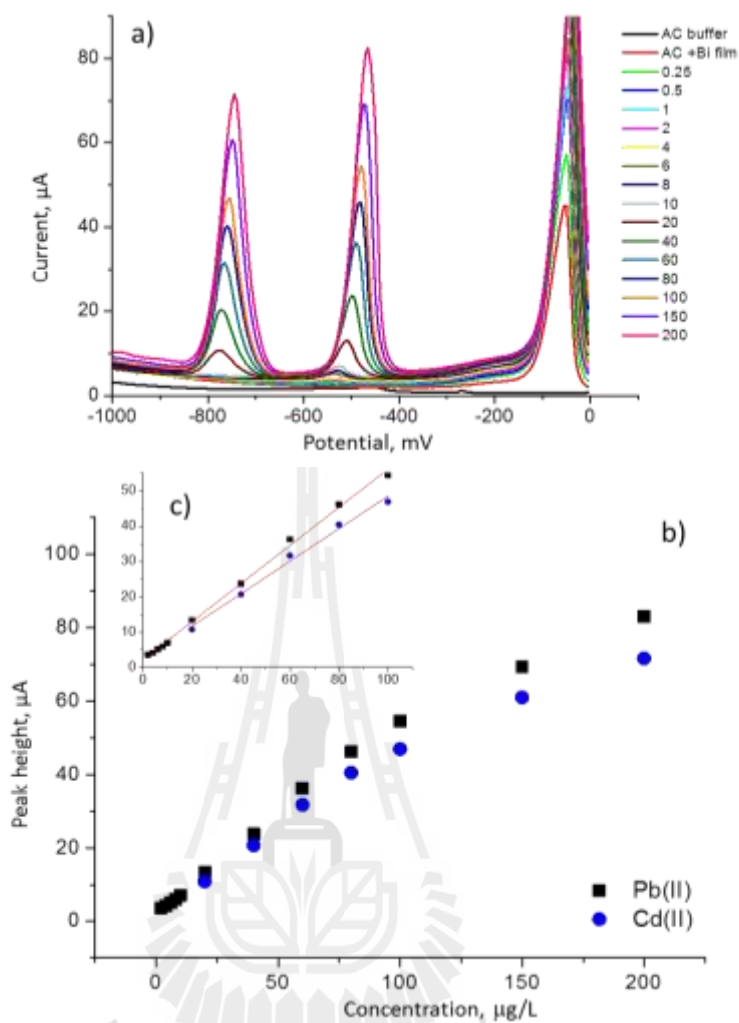


**Figure 4.27** a) Robotic differential pulse stripping voltammetry of Pb(II) and Cd(II) with increasing analyte concentrations from 0 to 200 µg/L (the microtiter plate and sequence of actions followed Figure 4.26). The calibration graphs of Pb(II) and Cd(II) as extracted from a). Experimental condition; Bi(III) 500 µg/L, 0.1 M acetate buffer pH 4.5 (0.1M KCl), under stirring solution, deposition potential -1.4 V for 600 s, WE: PLE, CE: Pt spiral and RE: Ag/AgCl.

**Table 4.7** Robotic Pb(II) and Cd(II) anodic stripping voltammetry in microtiter plate: summary of calibration trials.

<b>Information</b>	<b>Pb(II)</b>	<b>Cd(II)</b>
Detection range	2-100 $\mu\text{g/L}$	20-100 $\mu\text{g/L}$
Correlation coefficient ( $R^2$ )	0.9988	0.9957
Limit of detection (LOD) ( $n=5$ )	2.86	9.54
Relative standard deviation for 20 $\mu\text{g/L}$ Pb(II) and Cd(II) ( $n=3$ )	9.16	2.13

#### **4.4.3 The application of robotic differential pulse stripping voltammetry for Pb(II) and Cd(II) measurements in real samples**

Robotic DPSV in 24-well microtiter plate with bismuth film electrodes in change as sensor was applied to the determination of Pb(II), and Cd(II) in real samples including bottled mineral drinking and tap water from source in Bochum, Germany, Certified reference material (CRM) wastewater, and an aqueous solution from a soil extraction on a sample collected near a battery factory in Nakhon Ratchasima, Thailand. In all cases, the standard addition method was chosen for quantification because matrix effects have a lower influence with this procedure and it compensates for proportional systematic errors.

#### **4.4.3.1 The analysis Pb(II) and Cd(II) in bottled mineral drinking and tap water**

In order to evaluate the proposed method, three replicate determinations ( $n=3$ ) of Pb(II) and Cd(II) in a microtiter plate loaded with drinking water sample, as shown Table 4.8 were carried out. The samples related to the bottle mineral drinking water were in wells B1, C1 and D1 and measured under the optimum condition by standard addition method. The well B2, C2, D2 had the solution of the sample wells in first row but spiked with 20  $\mu\text{g/L}$  Pb(II) and Cd(II). Row 3, 4 and 5 followed this arrangement but with 40, 60 and 80  $\mu\text{g/L}$  heavy metals supplementation.

A representative example of robotically acquired set of DPSVs for trial with bottled mineral drinking water is shown in Figure 4.28 the black line is the line corresponding to the unspiked Pb/Cd to sample. Unobserved were the Pb(II) and Cd(II) peak. The addition standard of solution of Pb(II) and Cd(II) into the drinking water produces clear increase in their respective current peaks. The voltammograms also indicated that the effect of the cation and anion as present in bottled water was practically negligible at concentration in ppm range.

**Table 4.8** The loads solution into 24-well microtiter plate for analysis Pb(II), and Cd(II) in bottle mineral drinking water using robotic DPSV.

24-well microtiter plate				Solution			
D	C	B	A	Drinking Water $\mu\text{L}$	[Pb] $\mu\text{g/L}$	[Cd] $\mu\text{g/L}$	[Bi] $\mu\text{g/L}$
1	2	3	4	5			
$n=3$	$n=2$	$n=1$					
Labeling well							
B1,C1,D1					-	-	
B2,C2,D2					20	20	
B3,C3,D3				1000	40	40	500
B4,C4,D4					60	60	
B5,C5,D5					80	80	

Note: all wells were adjust volumn to 2.0 mL by 0.1 M acetate buffer pH 4.5

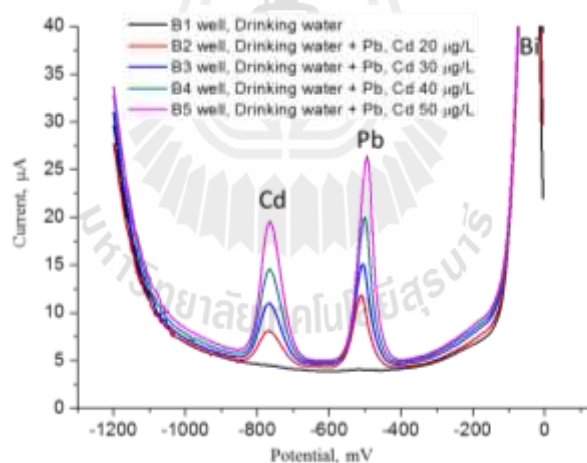


**Figure 4.28** Robotic differential pulse stripping voltammetry of bottled mineral drinking water without and with spike Pb(II) and Cd(II) supplement of 20, 30, 40, and 50  $\mu\text{g/L}$ . The experimental conditions for measurement are the same as Figure 4.27.

In case of the tap water, actually collected an outlet in the laboratory from Elektroanalytik & Sensorik group, NC04, Ruhr-Universität Bochum, Germany, the microtiter plate load for the Pb(II) and Cd(II) analysis was similar to the one in Table 4.8, but instead of the drinking water tap water was used as sample. Figure 4.29 presents the robotic DPSV of tap water without and with Pb(II) and Cd(II) supplementation 20, 30, 40, 50  $\mu\text{g/L}$ . As expected Pb(II) and Cd(II) peak did not show in tap water sample. The reason obviously is the strict regulation for the contamination of draining water and the high quality standard in Germany.

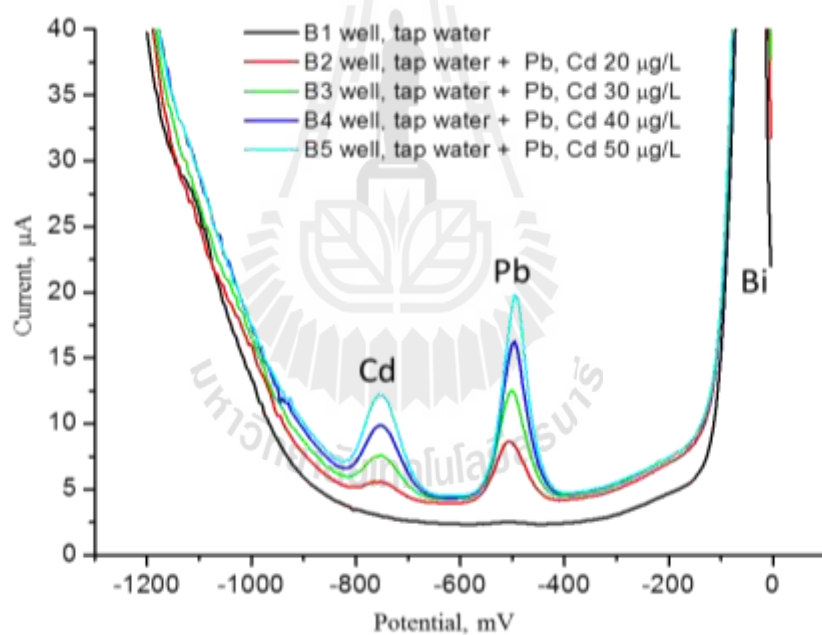


**Figure 4.29** Robotic differential pulse stripping voltammetry of tap water without and with spike Pb(II), and Cd(II) supplement of 20, 30, 40 and 50  $\mu\text{g/L}$ . The experimental conditions for measurement are the same as Figure 4.27.

Figure 4.30 a) shows four DPVs from a voltammetric microtiter plate run: one for the water that was spiked with 20  $\mu\text{g/L}$  Pb/Cd to generate a “contaminated” water sample and then three for this sample but additionally spiked with 30, 40, 50  $\mu\text{g/L}$  Pb/Cd to allow quantifications via the standard addition method. Figure 4.30 b) is the analysis of the movement in a). Two linear regression were drawn through the original data points in the plot of the peak currents vs. concentration of added analyte. The extrapolation of the regression line towards the x-axes and the measure of the x-interception gave the level of Pb/Cd in the sample. In the particular case shown, the values are 20.4 and 22  $\mu\text{g/L}$  for Pb(II) and Cd(II) which compared reasonably well with the adjusted concentration the recovery rate was 102% (for Pb(II)) and 110% (for Cd(II)).

The accuracy in term of % recovery of this proposed automate Pb(II) and Cd(II) analysis was measured for bottled mineral drinking water and tap water that were with spiked standard solution of Pb(II) and Cd(II) and exposed to quantification with the standard addition method.

Apart from a graphical analysis of the results of the standard addition method for quantification of Pb(II), and Cd(II), the linear equations derived from the linear regression plots of Pb(II), and Cd(II) were also used for analyzing the concentration of the two metal ions in the bottled mineral water sample. Table 4.9 summarized all the recovery rates that were revealed in the robotic voltammetric method microtiter plate runs on bottled mineral drinking water and tap water. In average the recovery rate for Pb(II), and Cd(II) were in range of 94-110%. This is about equal to what is the known performance level of voltammetry assessment of heavy metal and a good sign of the functionality of the developed scheme for the target applications.

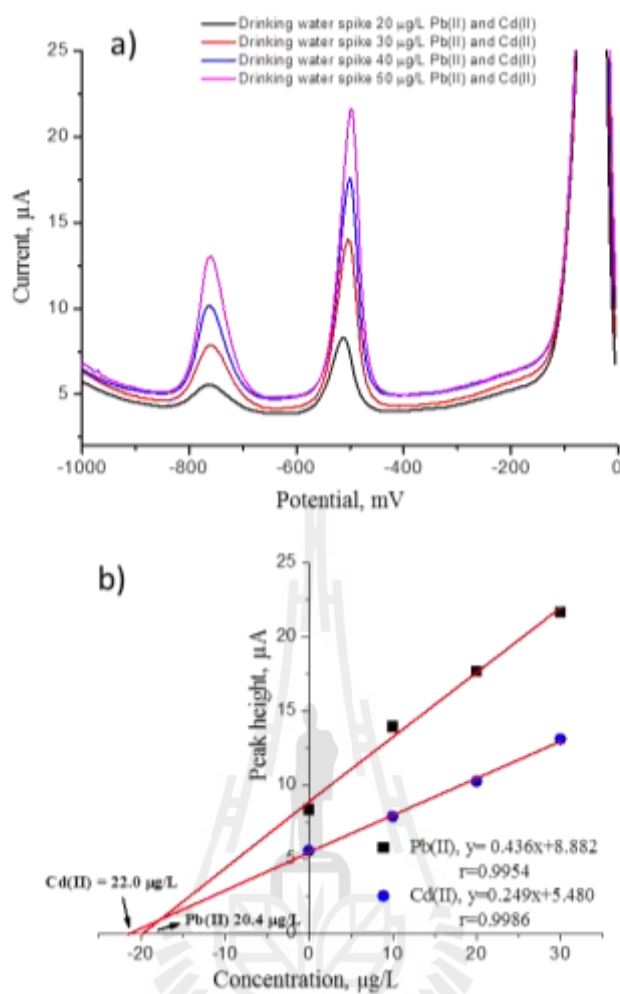


**Figure 4.30** a) Robotic differential pulse stripping voltammetry of bottled mineral drinking water that with a 20  $\mu\text{g/L}$  supplementation of Pb/Cd. b) Standard addition plot used for the determination of Pb(II), and Cd(II) content in the spike bottled mineral drinking water sample. The experimental conditions for the measurement were the same as Figure 4.27.



**Table 4.9** Robotic stripping voltammetry on spiked bottled mineral drinking water and tap water; summary of the determined Pb/Cd contents and the corresponding % recovery rates.

Analyte	Supplementation	Concentration	% Recovery
	$\mu\text{g/L}$	Robotic DPSV, $\mu\text{g/L}$	
Bottled mineral drinking water	Pb 20	$21.28 \pm 1.3$	$106.4 \pm 6.6$
	30	$28.59 \pm 1.8$	$95.3 \pm 5.9$
	Cd 20	$21.10 \pm 0.9$	$105.5 \pm 4.5$
	30	$28.92 \pm 1.5$	$96.4 \pm 5.1$
Tap water	Pb 20	$22.05 \pm 1.1$	$110.2 \pm 5.6$
	30	$29.54 \pm 1.8$	$98.5 \pm 5.2$
	Cd 20	$21.10 \pm 2.3$	$105.5 \pm 9.3$
	30	$28.10 \pm 2.9$	$93.7 \pm 8.0$

Values are the mean of three measurement  $\pm$  standard deviation.

#### 4.4.3.2 Analysis of Pb(II) and Cd(II) in wastewater certified reference material (CRM713)

For control measurements in laboratories dealing with environmental monitoring and testing, the European Union has established a library of waste sample material with a certified content of particular contaminations. One of the certified water reference material has been analyzed with the robotic voltammetry assay of this thesis. It was actually the certified reference material BCR® – 713. The content of specified of BCR® – 713 are listed in Table 4.10, and it can be seen that the Pb/Cd levels were 47, and 5.1 µg/L, respectively. For the load into the wells of the microtiter plate, the water reference material was diluted five-fold and the actual well levels was thus 9.4 µg/L for Pb(II) and 1.02 µg/L for Cd(II).

**Table 4.10** The elements content in certified reference material (CRM) BCR® – 713.

EFFLUENT WASTEWATER			
	Mass concentration		Number of accepted sets of data p
	Certified value <sup>1)</sup>	Uncertainty <sup>2)</sup>	
As	9.7 µg/L	1.1 µg/L	11
Cd	5.1 µg/L	0.6 µg/L	17
Cr	21.9 µg/L	2.4 µg/L	14
Cu	69 µg/L	4 µg/L	16
Fe	0.40 mg/L	0.04 mg/L	13
Mn	43.4 µg/L	3.0 µg/L	16
Ni	30 µg/L	5 µg/L	11
Pb	47 µg/L	4 µg/L	16
Se	5.6 µg/L	1.0 µg/L	10

1) Unweighted mean value of the means of p accepted sets of data, each set being obtained in a different laboratory and/or with a different method of determination. The value is traceable to the International System of Units (SI).

2) The certified uncertainty is the expanded uncertainty estimated in accordance with the Guide to the Expression on Uncertainty in Measurements (GUM) with a coverage factor  $k = 2$ , corresponding to a level of confidence of about 95 %.

Figure 4.31 a) shows a robotic differential pulse stripping voltammogram for wastewater certificated reference material (CRM713) overlaid with the curves valid for supplementation with Pb(II) and Cd(II) at equal concentrations of 20, 40, 60 and 80  $\mu\text{g/L}$ , respectively. A tiny stripping peaks for Pb(II) is present in the bare CRM sample at expected potential of about -500 mV but no visible Cd(II) peak turned up at about -750 mV. Reason is that the well level of about 1  $\mu\text{g/L}$  was below the earlier reported limit of detection for Cd(II) analysis in the robotic electrochemical apparatus.

The concentration of Pb(II) was determined through an analysis the standard addition method (see in Figure 4.31 b)). A good linearity was observed for the linear regression with a correlation coefficient of 0.991. The concentration of the Pb(II) was found from the intercept on the negative  $x$ -axis, which in this individual case 9.71 $\mu\text{g/L}$ , or taking the dilution factor into account, 48.55  $\mu\text{g/L}$  for the original sample. The calculation of the % recovery rate for this example was 103.3%. Table 4.11 is a summary of all measurement in the waste water reference material. The average percentage of recovery rate was about 90-111 % and the certified content was reasonably well compared.

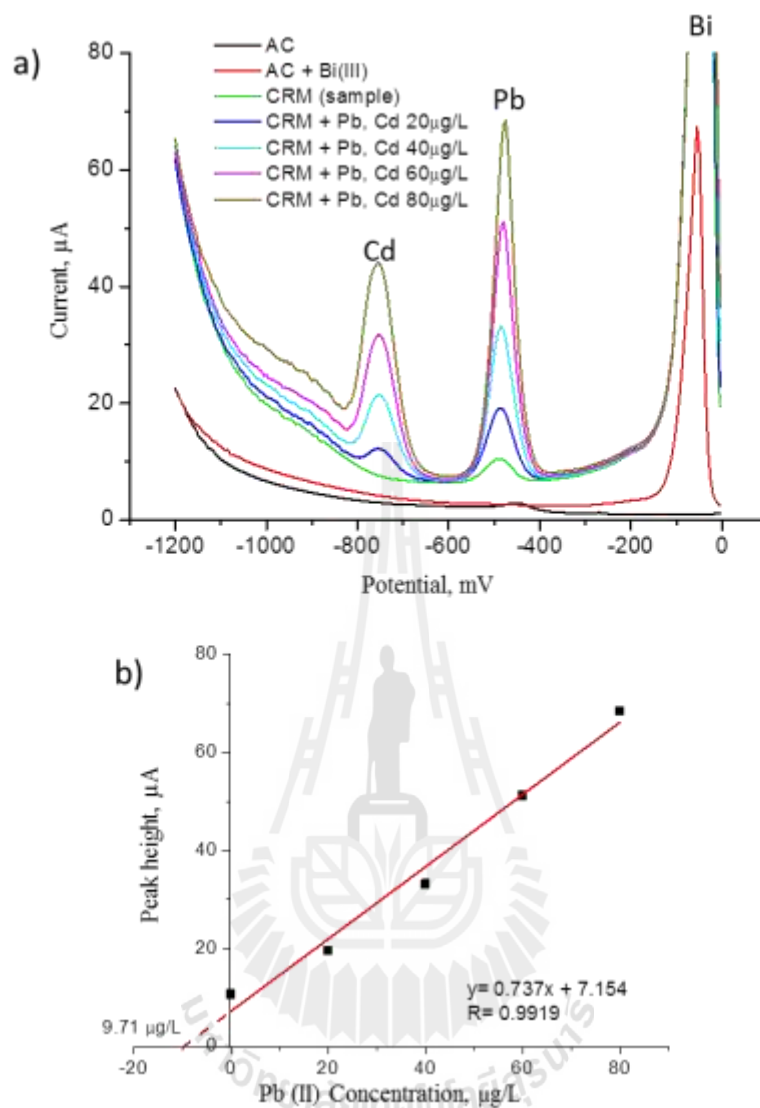


**Figure 4.31** a) Robotic differential pulse stripping voltammetry for certified wastewater reference material, (CRM 713). Show the sample trace and the trace heavy metal after addition of Pb/Cd solution. b) Standard addition plot for the determination Pb(II). The experimental conditions for the measurement were the same as Figure 4.27.

**Table 4.11** Automated stripping voltammetry determination of Pb/Cd in certified waste water reference material: Summary of measure Pb/Cd analyte and of recovery rate (n=6).

Elements	Concentration, $\mu\text{g/L}$		% relative
	Robotic-DPSV	CRM reported	
Pb	42.6 $\pm$ 3	47 $\pm$ 4 <sup>a</sup>	90.6 $\pm$ 6.6
spike 20 $\mu\text{g/L}$	74.5 $\pm$ 1.9	67 <sup>b</sup>	111.2 $\pm$ 4.4
Cd	-	5.1 $\pm$ 0.6 <sup>a</sup>	-
spike 20 $\mu\text{g/L}$	22.6 $\pm$ 0.9	25.1 <sup>b</sup>	90.0 $\pm$ 3.5

<sup>a</sup> Certificated reported  
<sup>b</sup> Certificated reported with spike standard solution

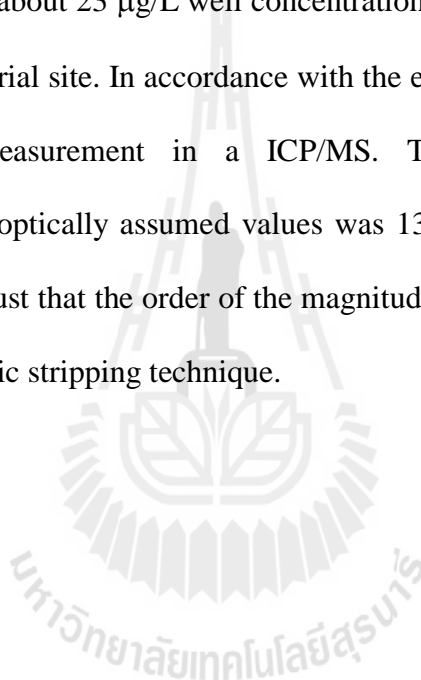
#### 4.4.3.3 The evaluation of Pb(II) and Cd(II) contamination in a soil sample from an industrial zone

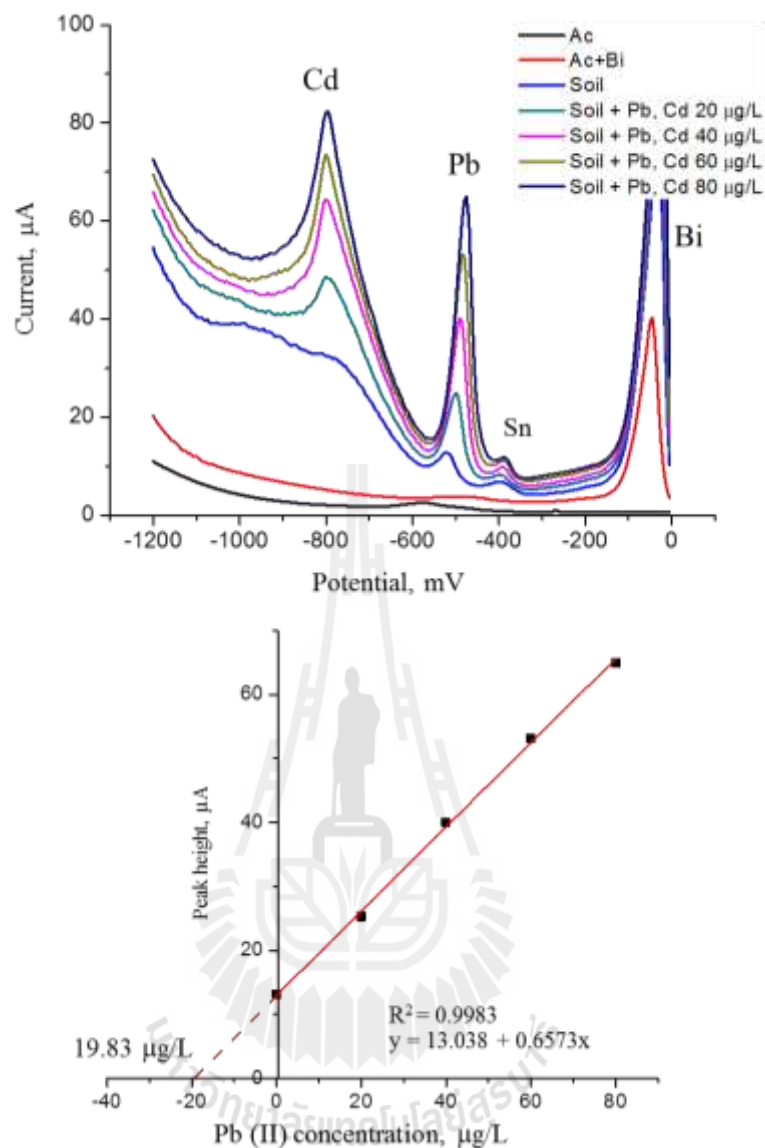
The final application of robotic-DPSV in the 24-well microtiter plate format was aiming of Pb(II) and Cd(II) quantification in a contaminated soil sample collected from a location near industrial site in Nakhon Ratchasima.

Figure 4.32 a) shows the set of automatically recorded DPSV for an acidified microwave extract of a contaminated soil sample, as well as the curves of the addition of standard solution of Pb(II) and Cd(II) at level of 20, 40, 60, 80  $\mu\text{g/L}$ . Apparently no Cd(II) was detected present in the soil sample as a Cd(II) peak was absent. Figure 4.32 b) reveals that the soil is indeed contaminated with Pb(II) as the typical peak of this heavy metal appeared at correct potential of -550 mV vs. RE. Figure 4.32 a) is the

analysis and displays the standard addition plot that allowed the determination of Pb(II) in the soil sample. The outcome of standard addition analysis reveals a cell concentration of 19.83  $\mu\text{g/L}$  which taking dilution into account, corresponding to about 790 mg/kg Pb(II) in the originally collected sample.

Results obtained by the robotic-DPSV method of this thesis were compared with those obtained by ICP/MS. As can be seen in Table 4.12, the spectroscopic measurement revealed about 23  $\mu\text{g/L}$  well concentration equal to about 900 mg/kg soil sample from the industrial site. In accordance with the electroanalysis, Cd(II) was also not seen in the measurement in a ICP/MS. The difference between the electrochemically and optically assumed values was 13% which is not ideal but still good enough to give trust that the order of the magnitude of concentration for assessed properly with the robotic stripping technique.





**Figure 4.32** a) Robotic differential pulse stripping voltammetry for a contaminated soil sample. Shown the current traces reveals for the soil sample together with the one for the sample that was spiked with increasing levels of Pb/Cd standard, b) Standard addition plot for the determination of Pb(II). The experimental conditions for the measurement were the same as Figure 4.27.

As mentioned earlier the Pb(II) level in the soil sample was calculated as 789.6mg/kg. Environmental regulations by the Pollution Control Department; Ministry of Natural Resources and Environment, Thailand and also by U.S. Environmental Protection Agency, U.S.A. set the limit for Habitat and Agriculture areas and for residential area to a maximum of allowed Pb(II) of 400 and 750 mg/kg, respectively. The soil sample expected here was with 790 mg/kg just above the limit for the two regulations. On the other hand, the sample came for a site close to a factory dealing with lead acid batteries and an evaluated level was expected 790 mg/kg, however, the value is still within the limits that have been set by the government agencies for Pb(II) in soil in industrial site.

**Table 4.12** Robotic stripping voltammetry of Pb(II), and Cd(II) in a soul sample by the standard addition method comparison between the electrochemically to a spectroscopic measurement.

Element	Concentration, $\mu\text{g/L}$	
	Robotic DPSV	ICP/MS*
Pb(II)	$19.74 \pm 1.24$	23.3
Cd(II)	ND	ND

\*The center of scientific and technological equipment, Suranaree University of technology, Thailand; Data from dilute soil extract 20 folds; ND = non-detection



## CHAPTER V

### CONCLUSION AND OUTLOOK

In this dissertation, the development of a microtiter plate base robotic electrochemical system for the quantification of a variety of the target analyte was aimed at. The automated voltammetric system used a suitably sized movable three-electrode assembly with a carbon pencil lead working electrode, a Ag/AgCl reference and a Pt counter electrode. Tailored software of the computer control unit of the specially-designed apparatus allowed non-manual electrode (z), and microtiter plate (x, y) micropositioning, and timed potentiostat operation. Specific software scripts facilitated a sequential analytical run through the plate wells and the timer execution of either electrode pretreatment and cleaning procedures or analyte quantification via the appropriate voltammetric technique. The system was adapted for three major applications, namely: (1) automated quantification of ascorbic acid in food samples and vitamin C tablet, (2) automated screening of total capacity antioxidant capacity in fruit juice, herbal tea extracts and vegetable and (3) automated heavy metals analysis in environmental sample.

#### **5.1 The ascorbic acid part**

A sensitive voltammetric assay for AA has been successfully incorporated into a microtiter plate-based robotic electrochemical workstation. With properly adjusted parameters sets for the analytical microtiter plate run, robotic AA differential pulse voltammetry achieved a linear response between 0.1 and 8.0 mM, a sensitivity of

about  $1 \mu\text{A mM}^{-1}$ , and a detection limit of  $0.05 \text{ mM AA}$ . The calibration curve and the standard addition methods worked equally well for the automated voltammetric AA quantification and their % recovery rates for spiked samples was about  $\pm 6\%$ . The developed methodology produced accurate assessment of the AA content of commercial vitamin C tablets, fruit juices and herbal tea extracts. The good performance of the robotic electrochemical AA assay was demonstrated by a reasonable agreement both with data from classical volumetric chemical analysis and with data found in the literature. A manuscript on the theme got published as “Feature article” in the renowned journal *Analytica Chimica Acta*.

## **5.2 The total antioxidant capacity part**

The well-known amperometric free radical DPPH assay for total antioxidant capacity evolution has been established in sample solutions in the 24 well microtiter plate format. The functionality of the method was proved by test runs on samples that had synthetic model antioxidant molecules in them. Applied to total antioxidant capacity measurements of synthetic gallic acid, ascorbic acid and  $\alpha$  tocopherol, the robotic amperometric DPPH• assay in microtiter plates produced data that was well in accordance with literature values and data from spectroscopic reference measurements. Tea, fruit and vegetable extract were inspected with the novel assay and the obtained results continued with acceptable standard deviations for replicate measurements the published values for the specific antioxidant levels (if available). And again, a good agreement was observed between the outcome of comparative and the voltammetric spectroscopic analysis of the some samples. For this part, a publication in *Analytical Chemistry* is available as source for comprehensive information and as overview.

### 5.3 The heavy metal part

Here the robotic electrochemical workstation was adapted for non-manual Pb(II) and Cd(II) measurements using integrated differential pulse stripping voltammetry at bismuth film modified pencil lead working electrode in the three electrode assembly. The Pb/Cd stripping peak current was found to be affected by the spiked Bi(III) concentrations in the measuring buffer and 500 ppb Bi(III) was identified as best for the simultaneous determination of the two trace heavy metals. The accuracy of the assay was demonstrate via good percentage of recovery rates were achieved for the analysis of trace Pb and Cd in spiked mineral drinking and tap water. And the novel non-manual anodic stripping voltammetry scheme worked well for the quantification of the Pb(II) and Cd(II) contamination in a soil sample that was collected from a location close to a lead/acid battery recycling factory. According to official regulation, the measured value was too high to be acceptable for residential area but within the limits set for industrial zones, and thus reasonable for the site of collection.

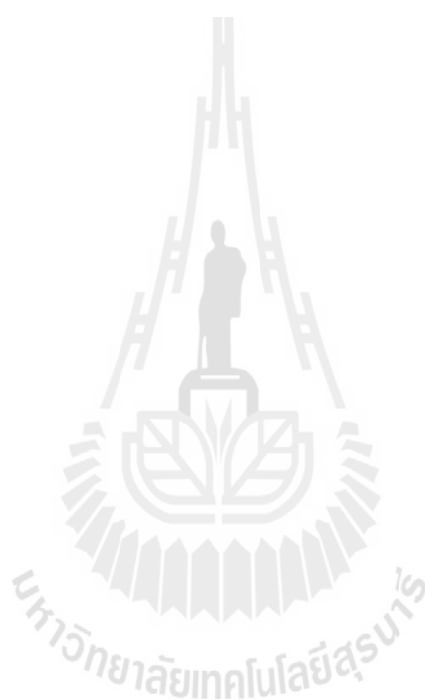
With the established methodology of automated voltammetry in microtiter plates multiple sample can be measured non-manually in a single sequential run through the individual wells. This offers convenience over a manual analysis of the samples loaded into the microtiter plate. Another advantage of microtiter plate based voltammetry is the minimization of manual error. Time saving in terms of the analysis time for the assessment of data on the sample collection is not so much an advantage, as a full plate run takes about the same time as would be needed by the operator to performed the measurement by hand. However, the person operating the sample analysis via robotic electroanalysis is free for other duties as soon as the system was

started and runs while for the manual case is engaged during the entire analysis. This is of course an advantage as precious since expensive labor time can be used more efficiently for other than repetitive execution of analytical procedures. Robotic microtiter plate-based voltammetry is for above reason recommended as an attractive alternative assay for large collections of samples. Potential is seemed for applications in the quality control units of the food, agricultural, cosmetic, health care and pharmaceutical industry. Also, environmental monitoring and testing laboratories may have an interest to use robotic voltammetry for convenient and efficient heavy metal analysis in their many samples.

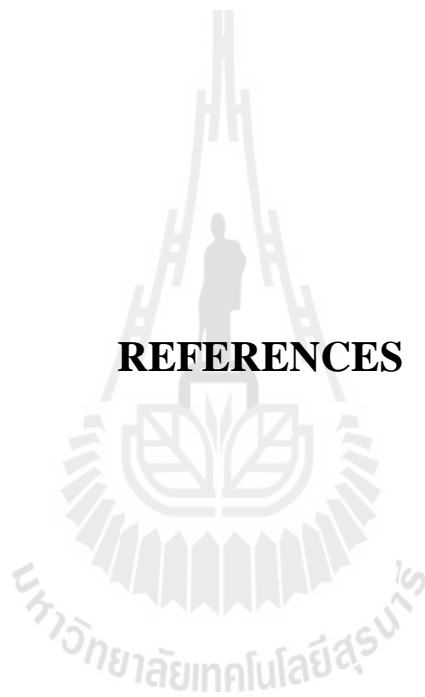
#### **5.4 Outlook**

The robotic electroanalysis for antioxidant and Pb(II), and Cd(II) quantification was established. The robotic electrochemical workstation can of course be applied to other target analytes as well. Necessary would be the identification of the optimum parameters for the particular analyte of interest, e.g., the optimal microtiter plate layout, the script settings for the voltammetry scheme chosen, etc. This adaptation work would be task of future studies with the robotic electroanalysis device as established in this thesis. Another an interesting task for further development of the system is the issue of bringing the employed voltammetry in microtiter plate wells to the highest sensitivity and best detection in limits. This would call for variation of the working electrode material, working electrode modification could lead to signal-enhancement and working with micro- instead of macroelectrode for the well voltammetry would bring lower detection limit and high signal-to-noise ratios. And last but not least a transfer of the methodology from the 24 well microtiter plate format

to higher version, e.g., the 96 well layout, would be an as challenging as promising task for increasing the throughput capability of robotic electroanalysis in plate wells.



## REFERENCES



## REFERENCES

- Achterberg, E. P. and Braungardt, C. (1999). Stripping voltammetry for the determination of trace metal speciation and in-situ measurements of trace metal distributions in marine waters. **Anal. Chim. Acta.** 400: 381.
- Amatatongchai, M., Laosing, S., Chailapakul, O., and Nacapricha, D. (2012) Simple flow injection for screening of total antioxidant capacity by amperometric detection of DPPH radical on carbon nanotube modified-glassy carbon electrode. **Talanta** 95: 267.
- AOAC international (2000). **Official methods of analysis of AOAC International** 17<sup>th</sup>, Arlington, Va:AOAC.
- Atoui, A.I., Mansouri, A., Boskou, G., and Kefalas, P., (2005) Tea and herbal infusions: Their antioxidant activity and phenolic profile. **Food Chem.** 89:27.
- Bagotsky, V. S (2005). **Fundamentals of electrochemistry**. 2<sup>nd</sup> Edition, John Wiley & Son Inc., New Jersey, USA.
- Bancirava, M. (2010) Comparison of the antioxidant capacity and the antimicrobial activity of black and green tea. **Food Research Inter.** 43:1379.
- Bernhoft, A. B. (2012) Mercury Toxicity and Treatment: A Review of the Literature **J. Environ. Public Health** 2012: 1.
- Birlouez-Aragon, I., and Tessier, F.J. (2003) Antioxidant vitamins and degenerative pathologies. A review of vitamin C. **J. Nutr. Health Aging** 7(2): 103.
- Blois, M. (1958) Antioxidant Determinations by the Use of a Stable Free Radical. **Nature** 181: 1199.

- Bond, A.M., Mahon, P.J., Schiewe, J., and Vicente-Beckett, V. (1997). An inexpensive and renewable pencil electrode for use in field-based stripping voltammetry **Anal. Chim. Acta.** 345: 67.
- Bondet, V., Brand-Williams, W., and Berset, C. (1997). Kinetic and Mechanisms of antioxidant activity using the DPPH· free radical method. **Lebensm. Wiss. U. Technol.** 30: 609.
- Borgmann, S., Radtke, I., Erichsen, T., Bloechl, A., Heumann, R., and Schuhmann, W. (2006). Electrochemical high-content screening of nitric oxide release from endothelial cells. **ChemBioChem** 7: 669.
- Brand-Williams, W., Curerlier, M. E., and Berset, C. (1995). Use of a free radical method to evaluate antioxidant activity. **Lebensm. Wiss. U. Technol.** 28: 25.
- Burini, G. (2007). Development of a quantitative method for the analysis of total l-ascorbic acid in foods by high-performance liquid chromatography. **J. Chromatogr., B.** 1154:7.
- Cao, L., Jia, and J., Wang, Z. (2008) Sensitive determination of Cd and Pb by differential pulse stripping voltammetry with in situ-modified zeplite doped carbon paste electrode. **Electrochimi. Acta.** 53: 2177.
- Chan-Eama, S., Teerasong, S., Damwan, K., Nacapricha, D., and Chaisuksant, R. (2011) Sequential injection analysis with electrochemical detection as a tool for economic and rapid evaluation of total antioxidant capacity. **Talanta** 24(5): 1350.
- Chanwitheesuk, A., Teerawutgulrag, A., and Rakariyatham, N. (2005). Screening of antioxidant activity and antioxidant compounds of some edible plants of Thailand. **Food Chem.** 92: 491.



- Chen, J., Lin, A., and Chen, G. (2007). Enhancement of electrochemiluminescence of lucigenin by ascorbic acid at single-wall carbon nanotube film-modified glassy carbon electrode. **Electrochim. Acta.** 52: 4457.
- Chergi, M. and Danet, A.F. (1997). Flow injection determination of L-ascorbic acid in natural juice with biamperometric detection **Anal. Lett.** 30: 2625.
- Chevion, S., Berry, E. M., Kitrossky, M., and Kohen, R. (1997) Evaluation of Plasma Low Molecular Weight Antioxidant Capacity by Cyclic Voltammetry. **Free Radical Biol. Med.** 22: 411.
- Chuanuwatanakul, S., Dungchai, W., Chailapakul, O., and Motomizu, S. (2008) Determination of trace heavy metals by sequential injection-anodic stripping voltammetry using bismuth film screen-printed carbon electrode **Anal. Sci.** 24: 589.
- Civit, L. Nassef, H.M., Fragoso, A., and Sullivan, C.K. (2008). Amperometric determination of ascorbic acid in real samples using a disposable screen-printed electrode modified with electrografted o-aminophenol film. **J. Agric. Food. Chem.** 56: 10452.
- Correa, P., Malcom, G., Schmidt, B., Fonham, E., Ruiz, B., Bravo, J.C., Bravo, L.E., Zarama, G., and Realpe, J.L. (1998). Review article: Antioxidant micronutrients and gastric cancer. **Aliment. Pharmacol. Ther.** 1: 73.
- Cosio, M. S., Buratti, S., Mannino, S., and Benedetti, S. (2007) Use of an electrochemical method to evaluate the antioxidant activity of herb extracts from the Labiatae family. **Food Chem.** 97: 725.

- Crowley, K., and Cassidy, J., (2002) Trace Analysis of Lead at a Nafion-Modified Electrode Using Square-Wave Anodic Stripping Voltammetry. **Electroanalysis** 14: 1077.
- Dayan, D. A., and Paine, A. J. (2001) Mechanisms of chromium toxicity, carcinogenicity and allergenicity: Review of the literature from 1985 to 2000 **Hum. Exp. Toxicol.** 20(9): 439.
- Dechakiatkrai, C., Chen, J., Lynam, C., Shin, K.M., Phanichphant, S., and Wallace, G.G. (2008). Direct ascorbic acid detection with ferritin immobilized on single-walled carbon nanotubes. **Electrochem. Solid-State Lett.** 11: K4.
- Demetrides, D., Economou, A., and Voulgaropoulos, A. (2004). A study of pencil-lead bismuth-film electrodes for the determination of trace metals by anodic stripping voltammetry. **Anal. Chim. Acta.** 519: 167.
- Dilgin, Y., Kızılkaya, K., Ertek1, B., Işık, F., and Dilgin, D. G. (2012) Electrocatalytic oxidation of sulphide using a pencil graphite electrode modified with hematoxylin. **Sens. Actuators, B** Accepted Manuscript.
- Economou, A. (1997) Applications, potentialities and limitations of adsorptive stripping analysis on mercury film electrodes. **Trends Anal. Chem.** 16(5): 286.
- Economou, A. (2005). Bismuth-film electrode: recent developments and potentialities for electroanalysis. **Trends Anal. Chem.** 24: 334.
- Ensafi, A. A. and Zarei, K. (2000). Simultaneous determination of trace amounts of cadmium, nickel and cobalt in water samples by adsorptive voltammetry using ammonium 2-amino-cyclopentene dithiocarboxylate as a chelating agent. **Talanta** 52(3): 435.

- Ensafi, A. A., Rezaei, B., Amini, M., and Heydari-Bafrooei, E. (2012) A novel sensitive DNA–biosensor for detection of a carcinogen, Sudan II, using electrochemically treated pencil graphite electrode by voltammetric methods. **Talanta** 88: 244.
- Erdurak-Kilic, C.S., Uslu, B., Dogan, U., Ozkan, S.A., and Coskun, M. (2006). Anodic voltammetry behavior of ascorbic acid and its determination in pharmaceutical dosage forms and some *Rosa* species of Turkey. **J. Anal. Chem.** 61: 1113.
- Erichsen, T., Reiter, S., Ryabova, V., Bonsen, E.M., Schuhmann, W., Maerkle, W., Tittel, C., Jung, C., and Speiser, B. (2005). Combinatorial microelectrochemistry: Development and evaluation of an electrochemical robotic system. **Rev. Sci. Instrum.** 76: 062204.
- Ernst, H., and Knoll, A. (2001). Electrochemical characterisation of uric acid and ascorbic acid at a platinum electrode. **Anal. Chim. Acta.** 449: 129.
- Eshaghi, Z., Khalili, M., Khazaeifar, A., and Rounaghi, G. H. (2011) Simultaneous extraction and determination of lead, cadmium and copper in rice samples by a new pre-concentration technique: Hollow fiber solid phase microextraction combined with differential pulse anodic stripping. **Electrochim. Acta** 56:3139.
- Ferreira, S.L.C., Bandeira, M.L.S., Lemos, V.A., Santos, H.C., Costa, A.C.S., and Jesus, D.S., (1997) Sensitive spectrophotometric determination of ascorbic acid in fruit juices and pharmaceutical formulations using 2-(5-bromo-2-pyridylazo)-5-diethylaminophenol (Br-PADAP). **Fresenius J. Anal. Chem.** 357: 1174.

- Fifield, F.W. and Kealey, D. (2000) **Principles and Practice of Analytical Chemistry**. Fifth Edition. Blackwell Science Ltd, United kingdom.
- Forgacs, Z., Massányi, P., Lukac, N., and Somosy, Z. (2012) Reproductive toxicology of nickel – review **J. Environ. Sci. Health A Tox. Hazard Subst. Environ. Eng.** 47(9): 1249.
- Fu, F., and Wang, Q. (2011) Removal of heavy metal ions from wastewaters: A review. **J. Environ. Manage.** 92: 407.
- Gao, W., Song, J., and Wu, N. (2005). Voltammetric behavior and square-wave voltammetric determination of trepibutone at a pencil graphite electrode. **J. Electroanal. Chem.** 576: 1.
- Giacomelli, C., Giacomelli, F. C., Alves, L.O., Timbola, A. K., and Spinelli, A. (2004). Electrochemistry of vitamin E hydro-alcoholic solution. **J. Braz. Chem.Soc.** 15: 748.
- Goh, J.K., Tan, W.T., Lim, F.T., and Maamon, N.A.M. (2008). Electrochemical oxidation of ascorbic acid mediated by carbon nanotubed/Li<sup>+</sup>/carbon paste modified solid electrode. **The Malaysian J. Anal. Sci.** 12: 480.
- Gopalan, A. I., Lee, K., Manesh, K. M., Santhosh, P., Kima, J. K., and Kang, J. S. (2007) Electrochemical determination of dopamine and ascorbic acid at a novel gold nanoparticles distributed poly(4-aminothiophenol) modified electrode. **Talanta** 71: 1774.
- Guan, Y., Chu, Q., Fu, L., Wu, T., and Ye, J. (2006). Determination of phenolic antioxidants by micellar electrokinetic capillary chromatography with electrochemical detection. **Food Chem.** 94: 157.

- Güçlü, K., Sözgen, K., Tütem, E., Özyürek, M., and Apak, R. (2005). Spectrophotometric determination of ascorbic acid using copper(II)-neocuproine reagent in beverages and pharmaceuticals. **Talanta** 65(5): 1226.
- Guschin, D. A., Shkil, H., and Schuhmann, W. (2009). Electrodeposition polymers as immobilization matrices in amperometric biosensors: improved polymer synthesis and biosensor fabrication. **Anal. Bioanal Chem.** 395: 1693.
- Henning, S. M., Fajardo-Lira, C., Lee, H. W., and Youssefian, A. A. (2003). Catechin content of 18 teas and a green tea extract supplement correlates with the antioxidant capacity. **Nutrit. Cancer.** 44(2):226
- Hintsche, R., Albers, J., Bernt, H., and Eder, A. (2000). Multiplexing of Microelectrode Arrays in Voltammetric Measurements. **Electroanalysis** 12: 660.
- Hočevar, S. B., Ogorevc, B., Wang, J., and Pihlar, B. (2002). A study on operational parameters for advanced used of bismuth film electrode in anodic stripping voltammetry. **Electroanalysis** 14: 1707.
- Injang, U., Noyrod, P., Siangproh, W., Duangchai, W., Motomizu, S., and Chailapakul, O. (2010). Determination of trace heavy metals in herbs by sequential injection analysis-anodic stripping voltammetry using screen-printed carbon nanotubes electrode. **Anal. Chim. Acta.** 668(1): 54.
- Kadara, R. O. and Tohill, I. (2008) Development of disposable bulk-modified screen-printed electrode based on bismuth oxide for stripping chronopotentiometric analysis of lead(II) and cadmium(II) in soil and water sample **Anal. Chim. Acta** 623: 76.

- Karara, R. and Tothill, I., E. (2004) Stripping chronopotentiometric measurements of lead(II) and cadmium(II) in soils extracts and wastewaters using a bismuth film screen-printed electrode assembly **Anal. Bioanal. Chem.** 378: 770.
- Karara, R. and Tothill, I., E. (2005) Resolving the copper interference effect on the stripping chronopotentiometric response of lead(II) obtained at bismuth film screen printed electrode. **Talanta** 66: 1089.
- Kefala, G., Economou, A., Voulgaropoulos, A., and Sofoniou, M. (2003). A study of bismuth-film electrodes for the detection of trace metal by anodic stripping voltammetry and their application to the determination of Pb and Zn in tap water and human hair. **Talanta**. 61: 603.
- Kefala, G., Economou, A., and Voulgaropoulos, A. (2004) A study of Nafion-coated bismuth-film electrodes for the determination of trace metals by anodic stripping voltammetry **Analyst** 129: 1082.
- Khairy, M., Kadara, R. O., Kampouris, D. K., and Banks, C. E. (2010) In situ Bismuth film modified screen printed electrodes for the bio-monitoring of cadmium in oral (saliva) fluid **Anal. Methods** 2: 645.
- Kilmartin, P.A., Honglei, Z., and Waterhouse, A.L. (2001). A cyclic voltammetry method suitable for characterizing antioxidant properties of wine and wine phenolic. **J.Agric. Food Chem** 49: 1957
- King, D., Friend, j., and Kariuki, J. (2010). Measuring Vitamin C content of commercial orange juice using a pencil lead electrode. **J. Chem. Edu.** 87: 507.
- Kokkinos, C., Economou, A., Raptis, I., and Efstathiou, C. E. (2008) Lithographically fabricated disposable bismuth-film electrodes for the trace determination of

- Pb(II) and Cd(II) by anodic stripping voltammetry **Electrochim. Acta** 53: 5294.
- Krings, U., and Berger, R.G. Antioxidant activity of some roasted foods (2001) **Food Chem.** 72: 223.
- Lai, J., Moxey, A., Nowak, G., Vashum, K., Bailey, K., and McEvoy, M. (2012) The efficacy of zinc supplementation in depression: Systematic review of randomised controlled trials. **J. Affect. Disord.** 136(1-2): e31.
- Lalor, G. C. (2008) Review of cadmium transfers from soil to humans and its health effects in the Jamaican environment **Sci. Total Environ.** 400: 162.
- Landrigan, P.J, Boffetta, P., and Apostoli, P. (2000) The reproductive toxicity and carcinogenicity of lead: a critical review. **Am. J. Ind. Med.** 38(3): 23.
- Lavrich, C., and Kissinger, P.T. (1985). Liquid Chromatography – Electrochemistry: Potential Utility for Therapeutic Drug Monitoring. In: Therapeutic drug monitoring and Toxicology by Liquid Chromatography. S.H.Y. Wong (Ed.), Marcell Dekker Inc. New York, USA, 191.
- Leong, L. P. and Shui, G. (2002) An investigation of antioxidant capacity of fruits in Singapore market. **Food. Chem.** 76: 69.
- Liebert, M., Licht, U., and Böhm, V., (1999) Antioxidant properties and total phenolics content of green and black tea under different brewing condition. **Z Lebensm Unters.forsch A.** 208: 217.
- Lim, Y. Y., Lim, T. T., and Tee, J. J. (2007) Antioxidant properties of several fruits: A comparative study. **Food Chem.** 103: 1003
- Lindner, E., Lu, Z., Mayer, H. A., Speiser, B., Titel, C., and Warad, I. (2005). Combinatorial micro electrochemistry. Part 4: Cyclic voltammetric redox

screening of homogeneous ruthenium(II) hydrogenation catalysts. **Electrochem. Commun.** 7: 1013.

Long, G., Peng, Y., and Bradshaw, D. (2012). A review of copper–arsenic mineral removal from copper concentrates. **Miner. Eng.** 36-38: 179.

Ly, S. Y., Chae, J. K., Jung, Y. S., Jung, W. W., Lee, h. J., and Lee, S. H. (2004). Electrochemical detection of ascorbic acid (vitamin C) using a glassy carbon electrode. **Nahrung/Food** 48: 201.

Magalhaes, L.M., Segundo, M.A., Reis, S., and Lima, J.L.F.C. (2006). Automatic method for determination of total antioxidant capacity using 2,2-diphenyl-1-picrylhydrazyl assay. **Anal. Chim. Acta.** 558: 310.

Mahadik, S.P. and Mukherjee S. (1996) Free radical pathology and antioxidant defense in schizophrenia: a review. **Schizophrenia Research** 19: 1.

Maisuthisakul, P., Pasuk, S., and Ritthiruangdej, P. (2008). Relationship between antioxidant properties and chemical composition of some Thai plants. **J. Food Comp. and Anal.** 21: 229.

Maisuthisakul, P., Pongsawatmanit, R., and Gordon, M.H. (2007). Characterization of the phytochemical and antioxidant properties of extract from Teaw (*Cratoxylum formosum* Dyer). **Food Chem.** 100: 1620.

Märkle, W., Speiser, B., Titel, C. and Vollmer, M. (2004). Combinatorial micro electrochemistry Part 1. Automated micro electrosynthesis of iminoquinol ether and [1,2,4]triazolo[4,3-a]pyridinium perchlorate collections in the wells of microtiter plates. **Electrochim. Acta** 50: 2753.

Marsh, D.G., Jacobs, D.L., and Veening, H. (1973). Analysis of Commercial Vitamin C Tablets by Iodometric and Coulometric. **J. Chem. Edu.** 50: 626.



- Mehlhorn, R. J. and Cole G. (1985) The Free Radical Theory of Aging: A Critical Review. **Adv. Free Radical Bio. Med.** 1: 165.
- Melo, E.A. (2006). Polyphenol, ascorbic acid and total carotenoid contents in common fruits and vegetables. **Braz. J. Food Technol.** 2: 89.
- Milardovic, S., Iveković, D., Rumenjak, V., and Grabarić, B.S. (2005). Use of DPPH| DPPH redox couple for biamperometric determination of antioxidant activity. **Electroanalysis.** 17(20): 1847.
- Molyneux, P. (2004). The use of the stable free radical diphenylpicryl-hydrazyl (DPPH) for estimating antioxidant activity. **Songkhanakar J. Sci. Technol.** 26: 212.
- Monk, P. (2001). **Fundamentals of Electroanalytical Chemistry.** Wiley & Son Inc., West Sussex, England.
- Nanasombat, S. And Teckchuen, N. (2009). Antimicrobial, antioxidant and anticancer activities of Thai local vegetables. **J. Med. Plant. Res.** 3(5): 443.
- Neugebauer, S., Isik, S., Schulte, and A., Schuhmann, W. (2003). Acrylic acid-based copolymers as immobilization matrix for amperometric biosensors. **Anal. Lett.** 36: 2005.
- Ngounou, B., Neugebauer, S., Frodl, A., Reiter, S., and Schuhmann, W. (2004). Combinatorial synthesis of a library of acrylic acid-based polymers and their evaluation as immobilisation matrix for amperometric biosensors. **Electrochim. Acta** 49: 3855.
- Okiei, W., Ogunlesi, M., Azeez, L., Obakachi, V., Osunsanmi, M., and Nkenchor, G. (2009). The voltammetric and titrimetric determination of ascorbic acid levels in tropical fruit sample. **Int. J. Electrochem. Sci.** 4: 276.

- Özcan, A. and Şahin, Y. (2010). Preparation of selective and sensitive electrochemically treated pencil graphite electrode for the determination of uric acid in urine and blood serum. **Biosens. Bioelectron.** 25: 2497.
- Özyürek, M., Güçlü, K., Bektaşoğlu, B., and Apak, A. (2007) Spectrophotometric determination of ascorbic acid by the modified CUPRAC method with extractive separation of flavonoids–La(III) complexes. **Anal. Chim. Acta** 588(1): 88.
- Ping, J., Wu, J., Ying, Y., Wang, M., Liu, G., and Zhang, M. (2011) Evaluation of Trace Heavy Metal Levels in Soil Samples Using an Ionic Liquid Modified Carbon Paste Electrode. **Agri. Food Chem.** 59: 4418.
- Pisoschi, A.M., Cheregi M.C., and Danet, A.F. (2009). Total Antioxidant Capacity of Some Commercial Fruit Juices: Electrochemical and Spectrophotometrical Approaches. **Molecules** 14: 480.
- Pisoschi, A.M., Danet, A.F., and Kalinowski, S. (2008). Ascorbic Acid Determination in Commercial Fruit Juice Samples by Cyclic Voltammetry. **J. Autom. Methods Manage. Chem.** 2008: 1.
- Pournaghi-Azar, M.H., Razmi-Nerbin, H., and Hafezi, B. (2002). Amperometric determination of ascorbic acid in real samples using an aluminium electrode, modified with nickel hexacyanoferrate film by simple electroless dipping method. **Electroanalysis.** 14: 206.
- Ramsey, J.B., and Colichman, E.L. (1942). Potentiometric Determination of Vitamin C. **Ind. Eng. Chem.** 14: 319.

- Reiter, S., Eckhard, K., Blöchl, K., and Schuhmann, W. (2001) Redox modification of proteins using sequential-parallel electrochemistry in microtiter plates. **Analyst** 126: 1912
- Reiter, S., Ruhlig, D., Ngounou, B., Neugebauer, S., Janiak, S., Vilkanauskyte, A., Erichsen, T., and Schuhmann, W. *Macromol.* (2004). An electrochemical robotic system for the optimization of amperometric glucose biosensors based on a library of cathodic electrodeposition paints. **Macromol. Rapid Commun.** 25: 348.
- Roy, P. R., Saha, M. S., Okajima, T., and Ohsaka, T. (2004) Electrooxidation and Amperometric Detection of Ascorbic Acid at GC Electrode Modified by Electropolymerization of *N,N* Dimethylaniline. **Electroanalysis.** 16: 289.
- Rubianes, M.D., and Rivas, G.A. (2003). Carbon nanotubes paste electrode. **Electrochem. Commun.** 5: 689.
- Rueda, M., Aldaz1, A., and Sanchez-Burgos, F. (1978) Oxidation of L-ascorbic acid on a gold electrode. **Electro. Chim. Acta** 23: 419.
- Ruhlig, D., Schulte, A., and Schuhmann, W. (2006). Electrochemical Robotics: Automatic detection of Ni<sup>2+</sup>-ion release from corroding NiTi shape memory alloys using adsorptive stripping voltammetry. **Electroanalysis.** 18: 53.
- Ryabova, V., Schulte, A., Erichsen, T., and Schuhmann, W. (2005). Combinatorial screening of a library of metalloporphyrins for electrochemical nitric oxide sensors. **Analyst.** 130: 1245.
- Sanchez-Moreno, C. (2002). Review: methods used to evaluate the free radical scavenging activity in foods and biological systems. **Food Sci. Technol. Int.** 8: 121.

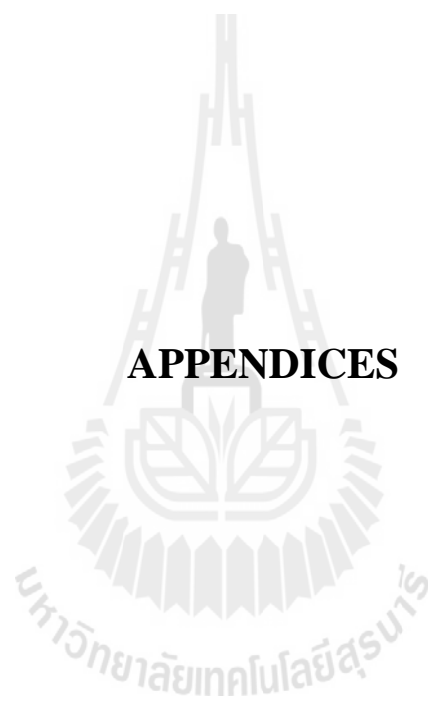
- Serrano, N., Alberich A., Diaz-Cruz, J.M., Arino, C., and Esteban, M. (2008). Signal splitting in the stripping analysis of heavy metal using bismuth film electrodes: Influence of concentration range and deposition parameter. **Electrochim Acta.** 53: 6616.
- Serrano, N., Díaz-Cruz, J. M., Ariño, C., and Esteban, M. (2010) Stripping analysis of heavy metals in tap water using the bismuth film electrode. **Anal. Bioanal. Chem.** 396: 1365.
- Siddhuraju, P. and Becker, K. (2003) Antioxidant Properties of Various Solvent Extracts of Total Phenolic Constituents from Three Different Agroclimatic Origins of Drumstick Tree (*Moringa oleifera* Lam.) Leaves. **J. Agric. Food Chem.** 51: 2144.
- Silva, C. R., Simoni, J. A., Collins, C. H., and Volpe, P. L. O. (1999). Ascorbic acid as a standard for Iodometric titrations an analytical for general chemistry. **J. Chem. Educ.** 76: 1421.
- Siriangkhawut, W., Pencharee, S., Grudpana, K., and Jakmune, J. (2009). Sequential injection monosegmented flow voltammetric determination of cadmium and lead using a bismuth film working electrode. **Talanta** 79: 1118.
- Skoog, D. A., West, D. M., Holler, F. J., and Crouch, S.R. (2004). **Fundamentals of analytical chemistry.** 8<sup>th</sup> Edition, (Ed.), Thomson Learning, Cannada.
- Sonthalia, P., McGaw, E., Show, Y., and Swain, G.M. (2004). Metal ion analysis in contaminated water samples using anodic stripping voltammetry and a monocrySTALLINE diamond thin-film electrode. **Anal. Chim. Acta.** 522: 35.

- Sreelatha, S. and Padma, P. R. (2009) Antioxidant activity and total phenolic content of *Moringa oleifera* leaves in two stages of maturity. **Plant Foods Hum. Nutr.** 64: 303.
- Sud, D., Mahajan, G., and Kaur, M. P. (2008) Agricultural waste material as potential adsorbent for sequestering heavy metal ions from aqueous solutions – A review. **Bioresour. Technol.** 99: 6017.
- Suntornsuk, L., Gritsanapun, W., Nikamhank, S., and Paochom, A. (2002). Quantitation of vitamin C content in herbal juice using direct titration. **J. Pharm. Biomed. Anal.** 28: 849.
- Tang, T.C., Deng A., and Huang, J. (2002). Immunoassay with a Microtiter Plate Incorporated Multichannel Electrochemical Detection System. **Anal. Chem.** 74 (11): 2617.
- Tang, Y. Z. and Liu, A.Q. (2007). Free-radical-scavenging effect of carbazole derivatives on DPPH and ABTS radical. **J. Am. Oil Chem. Soc.** 84: 1095.
- Tercier, M. L., Buffle, J., and Graziottin, F., (1998). A Novel Voltammetric In-Situ Profiling System for Continuous Real-Time Monitoring of Trace Elements in Natural Waters. **Electroanalysis** 10(6): 355.
- Thiago, R. L. C., Denise, P., Lowinsohn, D., and Bertotti, M. (2006) Use of an Electrochemically Etched Platinum Microelectrode for Ascorbic Acid Mapping in Oranges. **J. Agric. Food Chem.** 54(8): 3072.
- Toit, R. d., Volstedt, Y., and Apostolides, Z. (2001) Comparison of the antioxidant content of fruits, vegetables and teas measured as vitamin C equivalents. **Toxicology.** 116: 63.

- VanderJagt, T.J., Ghattas, R., VanderJagt, D.J., Crossey, M., and Glew, R.H. (2002) Comparison of the total antioxidant content of 30 widely used medicinal plants of New Mexico. **Life Sci.** 70: 1035.
- Vinokur, Y., Rodov, V., Reznick, N., Goldman, G., Horev, B., Umiel, N., and Friedman, H. (2006) Rose Petal Tea as an Antioxidant-rich Beverage: Cultivar Effects. **J. Food. Tech.** 71: s42.
- Wang, X., Amatatongchai, M., Nacapricha, D., Hofmann, O., Mello, J. C., Bradley, D. D. C., and Mello, A., J. (2009) Thin-film organic photodiodes for integrated on-chip chemiluminescence detection – application to antioxidant capacity screening. **Sens. Actuators, B.** 140: 643.
- Wang, J. (2001). **Analytical Electrochemistry** 2<sup>nd</sup> Edition, (Ed.), John Wiley & Son Inc., New York, USA.
- Wang, J. (2005). Stripping analysis at bismuth electrode: A review. **Electroanalysis.** 17: 1341.
- Wang, J. and Kawde, A. (2001). Pencil-based renewable biosensor for label-free electrochemical detection of DNA hybridization. **Anal. Chim. Acta.** 431: 219.
- Wang, J., Lu, J., Hocevar, S.B., and Farias, P.A.M. (2000). Bismuth-coated carbon electrodes for anodic stripping voltammetry. **Anal. Chem.** 72: 3218.
- Xu, H., Zeng, L., Huang, D., Xian, Y., and Jin, L. (2008) A nafion-coated bismuth film electrode for the determination of heavy metals in vegetable using differential pulse anodic stripping voltammetry: An alternative to mercury-based electrode. **Food Chem.** 109: 834.
- Yan, L., Teng, Y., and Jhi, T. J. (2006) Antioxidant properties of guava fruit: comparison with some local fruits. **Sunway Acad. J.** 3: 9.

- Youwei, Z., Jinlian, Z., and Yonghong, P. (2008) A comparative study on the free radical scavenging activities of some fresh flowers in southern China. **Food Sci. Tech.** 41: 1586.
- Zielinska, D., Nowax, D.S., and Zielinski, H. (2007). Comparison of Spectrophotometric and Electrochemical Methods for the Evaluation of the Antioxidant Capacity of Buckwheat Products after Hydrothermal Treatment. **J. Agric. Food Chem.** 55: 6124.
- Zoski, C. G. (2007). **Handbook of Electrochemistry**. Elsevier, Amsterdam, The Netherlands.





**APPENDICES**



**APPENDIX A**

**DESIGN OF SOFTWARE FOR THE EXECUTION OF**

**ROBOTIC ELECTROCHEMICAL ANALYSIS IN**

**24-WELL MICROTITER PLATES**

มหาวิทยาลัยเทคโนโลยีสุรนารี

## A.1 Robotic electrochemical parameter for robotic script writing to execute robotic electrochemical system using microtiter plate format

A description of the software and abbreviations used for script design for voltammetry and the command of x, y and z micro-positioning system control robotic software are provided in Table A.1. In the software script for cyclic, differential pulse voltammetry and amperometry for electrode movement were written in Notepad (see Table A.2).

**Table A.1** Listed parameters and abbreviations of voltammetric techniques used in software script of the robotic electrochemical device.

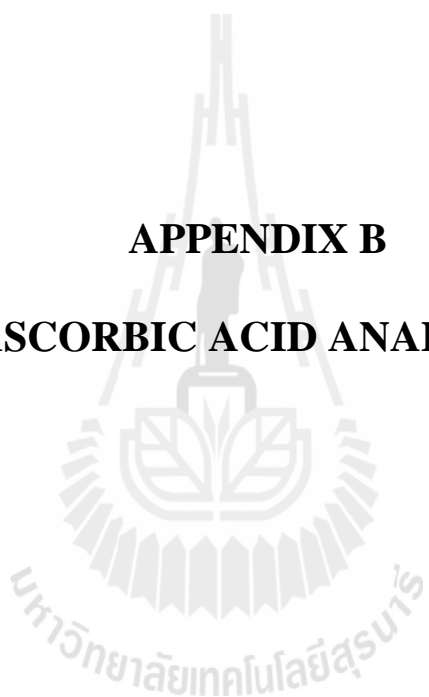
Abbreviation	Implication
E begin	Potential where a scan starts. The applicable range of the potential is -2V to +2V.
E start	Potential where a CV scan started. This value must be between E vtx1 and E vtx2.
E vtx1	Potential where a scan direction is reversed (CV only) The applicable range of the potential is -2 V to +2 V.
E end	Potential where a measurement stops.
E vtx2	Potential where a scan direction is reversed (CV only). The applicable range of the potential is -2 V to +2 V.
E step	Step potential (not for CP)

**Table A.1** Listed parameters and abbreviations of voltammetric techniques used in software script of the robotic electrochemical device (Continued)

Abbreviation	Implication
E pulse	Pulse potential (DPV only)
E amp	Amplitude (of square wave pulse (SWV) and sine wave (acV)). Values are half peak-to-peak (SWV) or rms (acV).
E cond	Potential applied before the deposition stage is started. Is only relevant when $t_{cond} > 0$ s.
E dep	Potential applied during the deposition stage. Is only relevant when $t_{dep} > 0$ s.
E stby	Potential applied after the measurement is finished.
I strip	Stripping current (CP only). If specified as 0, the method is called chemical stripping otherwise it is constant current stripping. The applicable range is $\pm 0.001 \mu\text{A}$ to $\pm 2 \text{ mA}$ . The applicable range of the potential is $-2 \text{ V}$ to $+2 \text{ V}$ .
scan rate	The applied scan rate. The applicable range depends on the value of E step. In case the scan rate is so low that the time between two measured points is longer than approx. 0.05 s, the measured data points are displayed during the measurement.  In other cases the measurement is completed before the points are shown
t pulse	The pulse time in DPV and NPV
Freq	The frequency of the square wave or ac signal.



**APPENDIX B**  
**ASCORBIC ACID ANALYSIS**





## B.2 Selected some examples of data from robotic DPV of fresh guava fruit juice related to Figure 4.13

An extract of voltammetric data, namely the peak current,  $I_p$ , AA evaluation in fresh guava fruit juice is available in Table B.2. A weighed amount of the edible portion of the guava 156.03 g was minced, blended with 300 mL DI water and filtered, 1.0 mL of the filtrate was mixed with 1.0 mL 0.1M KCl and, placed in well of microtiter plate, subjected to robotic DPV analysis.

**Table B.2** The voltammetric peak height ( $I_p$ ) of Guava juice with added AA standard solution as used for evaluation of AA content in Guava juice via robotic DPV in the standard addition method.

Sample	$I_p$ ( $\mu\text{A}$ )			Note
	1	2	3	
Guava	0.149	0.110	0.108	Raw data
Guava + 1mM AA	0.240	0.178	0.167	
Guava + 2mM AA	0.323	0.248	0.224	
Guava + 3mM AA	0.412	0.314	0.283	From linear equation
$R^2$	0.9997	0.9999	1.0000	
Slope	0.0872	0.0682	0.0582	
Intercept at y axis	0.1502	0.1102	0.1082	Average
Intercept at x axis, mM (for standard addition)	1.722	1.620	1.859	<b>1.730</b>
AA, mg/300mL	91.00	85.60	98.20	<b>91.20</b>
AA, mg/100g Guava	58.32	54.86	62.94	<b>58.71</b>

## B.4 The quantification AA in real samples via titration method

### 1.1 The titration AA in vitamin C tablet and guava fresh fruit juice using

#### DCIP method

##### 1.1.1 Standardization of DCIP

Following the equation in Figure 3.12, 1 mole AA reacted with 1 mole DCIP. 0.1002 g AA in 250 mL buffer was titrated with the DCIP standard of get known exact concentration. Table B.3 is the used volume for end point establishment and the calculated DCIP concentration.

**Table B.3** The data for the DCIP standardization.

No.	Volume DCIP (mL)	Calculation [DCIP] (Molar)
1	15.70	7.233x10 <sup>-4</sup>
2	15.80	
3	15.70	
average	15.73	

Involved calculation;

The mole of AA 0.1002 g 250 mL (molecular weight AA are 176.13 g/mole)

$$n = \frac{g}{mw} = \frac{0.1002 \text{ g} \times 1000}{176.13 \times 250} = 2.276 \times 10^{-3} \text{ M, AA} = 2.276 \text{ mM}$$

Therefore, the concentration of DCIP is:

$$C_1 V_1 = C_2 V_2,$$

$$C_1 = \text{AA concentration, M,}$$



$V_1 = \text{AA volume, mL,}$

$C_2 = \text{DCIP concentration, M,}$

$V_2 = \text{DCIP volume, mL,}$

$2.276 \times 10^{-3} \times 5 = C_2 \times 15.73, \text{and}$

$C_2 = 7.233 \times 10^{-4} \text{ M.}$

### 1.1.2 The calculation of AA in Vitamin C tablet (Ja trademark)

As studied in Figure 3.11 b), 0.10 g of the powder of a vitamin C tablet was dissolved in 100 mL DI water and 20 mL were used for multiple titration with standardized DCIP.

**Table B.4** The volume of DCIP used for endpoint in titration of dissolved AA from vitamin C tablets.

No.	Volume DCIP (mL)	Calculation [AA], mg/Tablet
1	3.40	129.7
2	3.40	
3	3.40	
average	3.40	

Calculation, see below:

mole DCIP = mole AA,

$$n = \frac{CV}{1000} = \frac{7.233 \times 10^{-4}}{1000} = 2.459 \times 10^{-6} \text{ mol} = 4.33 \times 10^{-4} \text{ g,}$$

20 mL have AA  $4.33 \times 10^{-4} \text{ g,}$

100 mL have AA  $2.165 \times 10^{-3}$  g,

0.1 g of vitamin C tablet have AA  $2.165 \times 10^{-3}$  g,

1 tablet weighs 6 g,

Therefore 6 g of vitamin C tablet have AA 129.7 mg.

### 1.1.3 The calculation AA in guava fresh fruit

As started in figure 3.11 b), a amount of the edible portion of the fruit ,were 156.03 g, was minced, blended with 300 mL DI water and filtrated. 10 mL adjusted were injected via titration with DCIP

**Table B.5** The volume of DCIP from titration for evaluation AA in guava.

No.	Volume DCIP (mL)	Calculation [AA], mg/100g fruit
1	21.20	51.93
2	21.10	
3	21.30	
average	21.20	

Calculation as before for the Vitamin C tablet sample.

## 1.2 The titration of AA in Moringa tea using iodine black titration

### 1.2.1 Standardization of the 0.2 M Na<sub>2</sub>S<sub>2</sub>O<sub>3</sub> solution

**Table B.6** The volumes of Na<sub>2</sub>S<sub>2</sub>O<sub>3</sub> and KIO<sub>3</sub>, as derived in a standardization trial for Na<sub>2</sub>S<sub>2</sub>O<sub>3</sub>.

No.	Volume Na <sub>2</sub> S <sub>2</sub> O <sub>3</sub> (mL)	Volume 0.05 M KIO <sub>3</sub> (mL)	[S <sub>2</sub> O <sub>3</sub> <sup>2-</sup> ]
1	15.50	10.0	0.1967
2	15.00	10.0	
3	15.25	10.0	
average	15.25	10.0	

In accordance to Figure 3.12 a) and following equation:

$$M_{\text{S}_2\text{O}_3^{2-}} = \frac{6M_{\text{IO}_3} V_{\text{IO}_3}}{V_{\text{S}_2\text{O}_3^{2-}}} = \frac{6 \times 10.0 \times 0.0500}{15.25} = 0.1967\text{M}$$

### 1.2.2 The calculation AA in Moringa tea

The Moringa tea was prepared as Chapter 3.8.7 and titrated following Chapter 3.8.8.

**Table B.7** The volume of  $\text{Na}_2\text{S}_2\text{O}_3$  and  $\text{KIO}_3$  related to an evaluation of AA in Moringa tea.

No.	Volume $\text{Na}_2\text{S}_2\text{O}_3$ (mL)	Volume 0.05 M $\text{KIO}_3$ (mL)	Calculation AA (mg/1g tea)
1	14.70	10.0	4.17
2	14.90	10.0	
3	14.80	10.0	
average	14.777	10.0	

Calculation provided below based on Figure 3.12 b) and equation:

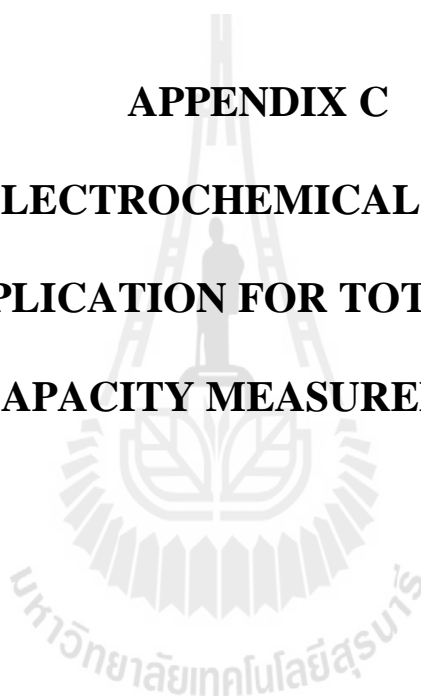
$$\begin{aligned}
 \text{Mole AA} &= (3M_{\text{IO}_3^-} V_{\text{IO}_3^-}) - \left(\frac{1}{2}M_{\text{S}_2\text{O}_3^{2-}} V_{\text{S}_2\text{O}_3^{2-}}\right), \\
 &= 3 \times 0.05 \times 10.0 \times 10^{-3} - (1/2) \times 0.1967 \times 14.77 \times 10^{-3}, \\
 &= 0.0474 \times 10^{-3} = 8.35 \times 10^{-3} \text{ g/2g tea} = 4.17 \text{ mg/1g tea.}
 \end{aligned}$$

**APPENDIX C**

**ROBOTIC ELECTROCHEMICAL DPPH RADICAL**

**METHOD: APPLICATION FOR TOTAL ANTIOXIDANT**

**CAPACITY MEASUREMENT**







## C.2 The spectrophotometric control measurement of the reaction between DPPH• and Trolox

### 1.1 The UV-Visible spectrum of 0.1mM DPPH•

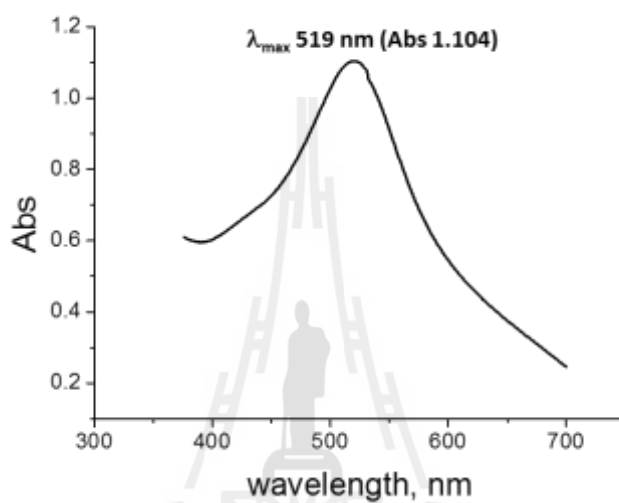


Figure C.2 The UV-Visible spectrum of 0.1mM DPPH•



## 1.2 The color of the reaction between DPPH and Trolox for spectrophotometric measurement

**Table C.3** The volume of 1 mM Trolox added into 0.1mM DPPH•.

Tube number	Added 1 mM Trolox into 0.1 mM 500 $\mu$ L DPPH•, $\mu$ L
1	0
2	10
3	15
4	20
5	30
6	40
7	50
8	60
9	80
10	100
11	120
12	140



**Figure C.2** The color of reaction mixtures containing DPPH• and Trolox at related to Table C.3.

### C.3 The calculation the Trolox equivalent (TE) of standard antioxidant (gallic acid, ascorbic acid and $\alpha$ -tocopherol)

#### 1.1 The calculation of TE for GA via robotic amp erometry; a representation example

Following equations were used calculation TE of GA, AA, Tocopherol.

$$1) \quad \Delta I_{AH} = \frac{[(I_{\text{Well \#12}} - I_{\text{Well \#13}}) + (I_{\text{Well \#13}} - I_{\text{Well \#14}}) + (I_{\text{Well \#14}} - I_{\text{Well \#15}})]}{3},$$

$$2) \quad \Delta I_{\text{Trolox}} = \frac{[(I_{\text{Well \#15}} - I_{\text{Well \#16}}) + (I_{\text{Well \#16}} - I_{\text{Well \#17}})]}{2},$$

$$3) \quad TE_{AH} = \frac{\Delta I_{AH}}{\Delta I_{\text{Trolox}}},$$

AH is GA, AA or  $\alpha$ -Tocopherol,

where;

Well#12 = DPPH• standard solution,

Well#13 = added 1 mM antioxidant standard solution, AH, 10  $\mu$ L,

Well#14 = added 1 mM antioxidant standard solution, AH, 20  $\mu$ L,

Well#15 = added 1 mM antioxidant standard solution, AH, 30  $\mu$ L,

Well#16 = added 1 mM Trolox 10  $\mu$ L, and

Well#17 = added 1 mM Trolox 20  $\mu$ L.

Following Figure 4.22, the calculation TE of GA used as the following:

$$\Delta I_{AH} = \frac{[(0.239 - 0.191) + (0.191 - 0.143) + (0.143 - 0.108)]}{3},$$

$$\Delta I_{\text{Trolox}} = \frac{[(0.108 - 0.085) + (0.085 - 0.067)]}{2},$$

$$TE_{AH} = \frac{\Delta I_{AH}}{\Delta I_{\text{Trolox}}} = \frac{0.0437}{0.0205} = \mathbf{2.13}.$$

TE of GA average in one microtiter plate (n=3) :  $(2.13+2.01+2.37)/3 = 2.2\pm 0.2$ .

### 1.2 The example calculation TE of GA via spectrophotometry

Calibration plots obtained for this assessments followed the equation:

$$y = -0.0063x + 0.703, R^2 = 0.9903 \text{ (see Figure 4.22),}$$

where y axis presented absorbance (Abs) of solution,

x axis presented volume of Trolox (or standard antioxidant).

$$TE = \frac{\text{volume Trolox at Abs Trolox}}{\text{volume Trolox at Abs Gallic}}$$

The 30  $\mu$ L volume of Trolox was represented 0.514 Abs that was calculated from linear equation. From Experiment, the same volume of gallic acid 1mM and trolox 1 mM (30  $\mu$ L ) was displayed 0.211 Abs. The volume Trolox at gallic absorbance was calculated (y) by linear equation then, the volume of gallic acid (x) are 12.32  $\mu$ L. The trolox equivalent of gallic acid is following;

$$TE = \frac{\text{Trolox}}{\text{Gallic acid}} = \frac{30}{12.32} = 2.435,$$

TE of GA average in (n=3) =  $(2.44+2.17+2.55)/3 = 2.4\pm 0.2$ .

## C.4 The calculation of the Trolox equivalent (TE) of a real sample

### 1.1 The calculation TE of orange juice via robotic amperometry

These equations were used calculation TE a real sample, here orange juice:

$$1) \quad \Delta I_{\text{sample}} = \frac{[(I_{\text{Well \#5}} - I_{\text{Well \#6}}) + (I_{\text{Well \#6}} - I_{\text{Well \#7}}) + (I_{\text{Well \#7}} - I_{\text{Well \#8}})]}{3},$$

$$2) \quad \Delta I_{\text{Trolox}} = \frac{[(I_{\text{Well \#8}} - I_{\text{Well \#9}}) + (I_{\text{Well \#9}} - I_{\text{Well \#10}})]}{2},$$

$$3) \quad TE_{\text{sample}} = \frac{\Delta I_{\text{sample}}}{\Delta I_{\text{Trolox}}},$$

where;

- Well#5 = DPPH• standard solution,
- Well#6 = added real sample, orange juice, 10  $\mu\text{L}$ ,
- Well#7 = added real sample, orange juice, 20  $\mu\text{L}$ ,
- Well#8 = added real sample, orange juice, 30  $\mu\text{L}$ ,
- Well#9 = added 1 mM Trolox 10  $\mu\text{L}$ , and
- Well#10 = added 1 mM Trolox 20  $\mu\text{L}$ .

Following Figure 4.24, the calculation TE of orange juice:

$$\Delta I_{\text{orange}} = \frac{[(0.192-0.168) + (0.168-0.144) + (0.144-0.128)]}{3} = 0.215 \mu\text{A},$$

$$\Delta I_{\text{Trolox}} = \frac{[(0.128-0.091) + (0.091-0.059)]}{2} = 3.44 \mu\text{A},$$

Means of 10  $\mu\text{L}$  1mM Trolox are,

1000 mL have Trolox  $1 \times 10^{-3}$  mole,

Thus; 10  $\mu\text{L}$  have Trolox =  $10 \times 10^{-9}$  mole or 10 nmole,

From robotic amperometry;

Trolox  $3.44 \mu\text{A} = 10 \times 10^{-9}$  mole Trolox.

$$\text{Orange } 2.15 \mu\text{A} = \frac{10 \times 10^{-9} \times 2.15}{3.44} = 6.25 \times 10^{-9} \text{ mole},$$

Added orange 10  $\mu\text{L}$  have TE  $6.25 \times 10^{-9}$  mole,

Thus, an orange juice 1mL has 0.62  $\mu\text{mole}$  Trolox equivalent.

The easy alternative way for TE calculation;

$$TE_{\text{sample}} = \frac{\Delta I_{\text{sample}}}{\Delta I_{\text{Trolox}}},$$

$$TE_{\text{orange}} = \frac{\Delta I_{\text{orange}}}{\Delta I_{\text{Trolox}}} = \frac{2.15}{3.44} = \mathbf{0.62} \text{ } \mu\text{mole Trolox equivalent.}$$

### C.5 The % yield of the vegetable plant extraction

**Table C.3** The % yield of plant extraction

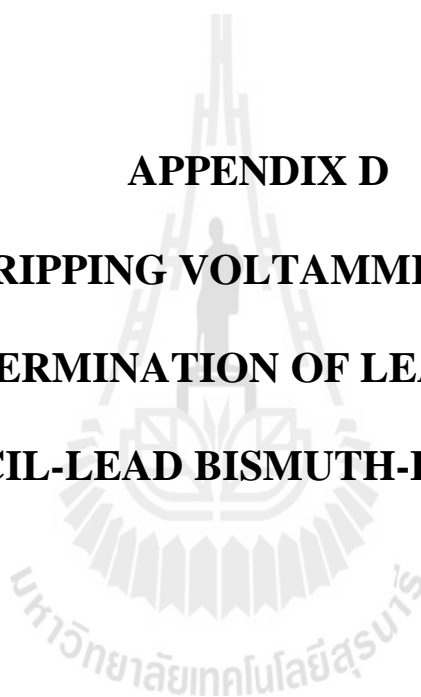
Plants	Leaf dried (g)	Extracted (g)	%yield
Teaw ( <i>Cratoxylum formosum</i> Dyer)	50.00	4.5148	9.03
Phak Paew ( <i>Polygonum odoratum</i> Lour.)	50.04	2.9801	5.96
Kri-Leck ( <i>Cassia siamea</i> )	50.08	5.6029	11.21

**APPENDIX D**

**ROBOTIC STRIPPING VOLTAMMETRY AS APPLIED**

**FOR THE DETERMINATION OF LEAD AND CADMIUM**

**WITH A PENCIL-LEAD BISMUTH-FILM ELECTRODE**















## D.2 The evaluation Pb(II) in soil extraction

The amount Pb(II) in soil sample by standard addition method from Table 4.12. 19.74 ppb lead was determined in the soil extract sample, which however, was 20 fold diluted. Accordingly, 394.8 ppb, Pb was in the original extract. The weight of soil providing the extract was 0.5 g. There the soil was contaminated with Pb at 789.6  $((394.8 \times 1000) / 0.5)$  mg/kg.

## D.3 Soil quality standard from Pollution Control Department; Ministry of natural Resources and Environment, Thailand

**Table D.6** Soil quality standard for habitat and agriculture, and for other purpose.

Soil Quality Standard for purpose	Heavy metals	Standard Value	Analytical Methods
Soil Quality Standards for Habitat and Agriculture	Cadmium and compounds	Not exceed 37 mg/kg	Inductively Coupled Plasma-Atomic Emission Spectrometry or Inductively Coupled Plasma-Mass Spectrometry or Atomic Absorption, Direct Aspiration or Atomic Absorption, Furnace Technique or other Methods Approved by Pollution Control Department
	Lead	Not exceed 400 mg/kg	
Soil Quality Standard for Other Purposes	Cadmium and compounds	Not exceed 810 mg/kg	Inductively Coupled Plasma-Atomic Emission Spectrometry or Inductively Coupled Plasma-Mass Spectrometry or Atomic Absorption, Direct Aspiration or Atomic Absorption, Furnace Technique or other Methods Approved by Pollution Control Department
	Lead	Not exceed 750 mg/kg	

Reference: 1) Pollution Control Department; Ministry of natural Resources and Environment, Thailand

2) U.S. Environmental Protection Agency, U.S.A.

# CURRICULUM VITAE

**SIREERAT INTARAKAMHANG:** Born: July 27, 1981, Thailand

## Education:

1999–2003: B.Sc. Chemistry, Khon Kaen University, Khon Kaen, Thailand

2003-2005: M.Sc. Chemistry, Suranaree University of Technology, Thailand

## Experience:

2006: Lecturer, Nakhon Ratchasima Rajabhat University, Thailand

2007: Lecturer, Rajamangala University of Technology Isan, Thailand

2009, September-November and 2011, August - 2012, January: Research stay abroad at Analytische Chemie, Electroanalytik & Sensorik in Professor Dr. Wolfgang Schuhmann's group, Department of Chemistry and Biochemistry, Ruhr University Bochum, Germany

## Publications:

1) Intarakamhang, S., Leson, C., Schuhmann, W., Schulte, A. (2011) A novel automated electrochemical ascorbic acid assay in the 24-well microtiter plate format.

**Anal. Chim. Acta** 687:1. (IF 2012: 4.555)

2) Intarakamhang, S., Schulte, A. (2012) Automated Electrochemical Free Radical Scavenger Screening in Dietary Samples. **Anal. Chem.** 84(15):6767. (IF 2011: 5.856)

3) Intarakamhang, S., Schuhmann, W., Schulte, A. (2012) Robotic Heavy Metal Anodic Stripping Voltammetry: Ease and Efficacy for Trace Lead and Cadmium Electroanalysis. **J. Solid State Electrochem.** (published online on 26 February 2013, IF 2011: 2.131)